EXPLORING THE ROLE OF MECHANICAL CUES IN T CELL FUNCTION

A Thesis Submitted to

Academic Faculty

Department of Life Science and Biotechnology

Completed under the guidance of

Dr. Dipyaman Ganguly, CSIR-IICB

By

Chinky Shiu Chen Liu

Index No.- 43/17/Life Sc./25

For the degree of Doctor of Philosophy (Science) from the

Department of Life Science and Biotechnology, Jadavpur University

भारतीय रासायनिक जीवविज्ञान संस्थान
INDIAN INSTITUTE OF CHEMICAL BIOLOGY
A Unit of Council of Scientific & Industrial Research
An Autonomous Body, under Ministry of Science & Technology
Government of India
4, राजा एस. सी. मल्लिक रोड, यादवपुर, कोलकाता 700 032
4, Raja S. C. Mullick Road, Jadavpur, Kolkata-700 032

Dipyaman Ganguly MBBS PhD PhD
Principal Scientist & Swarnajayanti Fellow
Cancer Biology & Inflammatory Disorders
IICB-Translational Research Unit of Excellence

CERTIFICATE FROM THE SUPERVISOR

This is to certify that the thesis entitled "Exploring the role of mechanical cues in T cell function" submitted by Smt. Chinky Shiu Chen Liu who got her name registered on 19.05.2017 for the award of Ph.D. (Science) degree of Jadavpur University, is absolutely based upon her own work under the supervision of Dr. Dipyaman Ganguly and that neither this thesis nor any part of it has been submitted for either any degree/diploma or any other academic award anywhere before.

Dipyaman Ganguly

Dated: 12·03·2021

Dr. Dipyaman Ganguly

Principal Scientist

CSIR-IICB, Kolkata

Dr. Dipyaman Ganguly MBBS PhD PhD
Principal Scientist, Associate Professor (AcSIR)
Swarnajayanti Fellow, DST, Govt. of India
IICB-Translational Research Unit of Excellence
CSIR-Indian Institute of Chemical Biology, Kolkata
Email: dipyaman@iicb.res.in

INDEX NO. 43/17/Life Sc./25

ABSTRACT

TITLE: Exploring the role of mechanical cues in T cell function

Submitted by: Chinky Shiu Chen Liu

T lymphocytes are constantly subjected to mechanical cues from their microenvironment. The past few decades have seen a significant development in scientific research concerning the crucial role of biophysical forces in governing various T lymphocyte-mediated processes. Mounting research have confirmed that T lymphocyte activation is critically dependent on its capacity to sense and respond to mechanical forces which are generated during its interaction with cellular partners and with its microenvironment. Despite extensive research on the role of mechanical forces on T lymphocyte biology, no dedicated T lymphocyte-intrinsic mechanosensory module was identified until recently. In the following thesis, I have described the role of Piezo1 mechanosensors in T lymphocyte function, particularly in the contexts of T lymphocyte activation and migration. Upon interaction with cognate antigen presenting cells (APCs), T lymphocytes experience significant mechanical force which activates Piezo1 channels. Activated Piezo1 allows influx of extracellular calcium which triggers calpain-dependent polymerisation and remodelling of the actin cytoskeletal scaffold. This event is crucial for formation and stabilisation of the T cell-APC immunological synapse, thereby facilitating optimal T lymphocyte activation. Moreover, Piezo1-mediated mechanotransduction also plays a critical role in T lymphocyte chemotactic migration. Downregulation of Piezo1 resulted in dramatically impaired motility of T lymphocytes in

response to stimulus. Thus, we have identified a previously unknown pathway of Piezo1-mediated mechanoregulation of T lymphocyte function.

Table of Contents

Acknowledgements

I would like to sincerely thank my mentor, Dr. Dipyaman Ganguly, for his constant guidance and support. His knowledge and expertise were invaluable through the course of my pre-doctoral training. His insights and feedback were instrumental in shaping my research. He always encouraged me to present my work at conferences and get valuable feedback, that helped me build my confidence. He is highly accomplished in his field and works meticulously to secure funds for his lab, while constantly guiding his students.

Words are not enough to thank my current and past lab members – Dr. Amrit Raj Ghosh, Dr. Oindrila Rahaman, Dr. Shamik Bhattacharya, Dr. Subhasis Barik, Roopkatha Bhattacharya, Dr. Beera Shankar Anand, Dr. Deblina Raychaudhuri, Purbita Bandopadhyay, Jafar Sarif, Ranit D'Rozario, Dr. Bishnu Prasad Sinha, Asmaul Hoque and Dr. Jayasree Roy Mondol. They have been remarkable lab mates who never hesitated to help me out with my experiments. I could not have gotten a better team. Their support and company have made this journey into a memorable one. I also have to thank all our trainees during my time in this lab – Shounak Roy, Raghumay Ghosh, Swarnasree Ghosh, Sanjali Mitra, Shreya Bhattacharya, Swapnonil Banerji, Siddharta Ghosh, Suparna Datta, Sampurna Pal, Saptashwa Chakraborty. I am especially grateful to Dr. Dibyanti Mukherjee. She helped me with all my bacterial cultures and DNA construct expansion whenever I needed them. Considering I had little experience in that arena, she turned out to be a saviour of many experiments.

I am very grateful to all my collaborators - Dr. Arindam Talukdar (IICB, Medicinal and Organic Chemistry) and his students, Dr. Barnali Pal and Sunny Goon; Dr. Bidisha Sinha (IISER-Kolkata) and her students, Dr. Arikta Biswas and Tithi Mandal. I am sincerely grateful that they agreed to devote time and conscious effort for my projects. Dr. Deepak Kumar Sinha and his student,

Parijat Biswas from Indian Association of Cultivation of Sciences, and Dr. Prafullakumar Tailor and his team from National Institute of Immunology, have also been immensely helpful when I was starting out my projects. I am also thankful to Dr. Santu Bandopadhyay for helping our lab during the initial phases with reagents and flow cytometer.

I am extremely thankful to IICB technicians – Mr. Tanmoy Dalui, Mrs. Payel Karmakar Haldar (flow cytometry) and Mr. Binayak Pal and Mr. Sounak Bhattacharya (confocal imaging) for helping me out with experiments requiring these instruments. I am also immensely grateful to my all my neighbouring labs for always helping me out as much as possible. Sudipto Da has also been very helpful maintaining lab purchase records and administrative work.

My parents (Dr. Liu Yung Kang and Mrs. Nilima Liu) have been my strongest source of inspiration in every aspect of my life. Their hard work and unwavering perseverance despite all odds, have always motivated me to work harder. I owe my achievements to their love, support and enormous sacrifice. They have always set strong examples of persons with indomitable personality and dogged attitude towards every setback. They have moulded me into a person with a strong mind and they inspire me to fight every challenge. My sisters (Pinky Liu and Liu Chuen Chen) have been my confidantes. Their accomplishments in their individual careers never cease to inspire and motivate me to aim higher. Growing up with them has blessed me with tons of extraordinary memories that have made me who I am.

I owe a lot to my best friend and partner, Amrit. He is my stronghold and has stood by me through my toughest career moments. He inspires me to never give up. The kind of faith he has shown in my abilities has been my strongest source of encouragement. He is also my strongest critic which helps me work towards improvement.

As known to many, the road to getting a Ph.D. isn't an easy one. Of course, there are families, friends, colleagues and mentors to help you out and support you. But it is also necessary to have some form of diversion if the journey becomes too much to bear. For me, it was my dog, Bontu – the pug. Calling Bontu just a form of diversion wouldn't do justice to her importance in my life. She is my family. Be it a bad day at work, a failed experiment or the pressure of unfinished assignment, she always comes to greet me at the door with a kind of excitement and energy that melts your worries away. Of course, she refuses to let me study or work on the laptop by sitting on it. But she is one of my greatest sources of comfort and happiness, and I owe a lot to her presence in my life.

Finally, I would like to apologise if I have failed to specifically mention anyone. I am thankful to everyone who have tried to helped me in my journey till here. I would not have reached this milestone in my career had it not been due to the support of people around me.

List of Figures

List of Abbreviations

A

ADAP	Adhesion and degranulation-promoting adapter protein
ADCC	Antibody-dependent cell cytotoxicity
AFM	Atomic force microscopy
AGM	Aorta-gonads-mesonephros
AIRE	Autoimmune regulator
ALR	Absent in melanoma 2 (AIM2)-like receptor
AMPK	Adenosine monophosphate (AMP)-activated protein kinase
AP-1	Activator protein 1
APC	Antigen presenting cell
Arp 2/3	Actin-related protein 2/3
ATP	Adenosine triphosphate
αCD3/CD28	anti-CD3 and anti-CD28 antibody

B

Bcl-6	B cell lymphoma 6
BCR	B cell receptor
BFP	Biomembrane force probe
BMP2	Bone morphogenetic protein 2

C

CAR	Chimeric antigen receptor
CCR	Chemokine receptor

cDC	Classical dendritic cell
CDR	Complementarity determining region
CE	Corneal epithelium
CED	C-terminal extracellular domain
CESC	Corneal epithelial stem cell
CFSE	Carboxyfluorescein succinimidyl
cGAS	cyclic GMP-AMP
ChIP	Chromatin immunoprecipitation
CHS	Contact hypersensitivity
CLR	C-type lectin receptor
CpG	Cytosine-guanosine oligodeoxynucleotides with phosphodiester bonds
CRAC	Calcium release-activated calcium channel
CsA	Cyclosporin A
CSCM	Corneal squamous cell metaplasia
cSMAC	Central supermolecular activation cluster
CTL	Cytotoxic T lymphocyte
CTLA-4	Cytotoxic T-lymphocyte-associated protein 4
CTV	Cell trace violet

D

DAG	Diacyl glycerol
DAMP	Danger-associated molecular pattern
DAP10	DNAX activation protein 10
DAPI	2-(4-Amidinophenyl)-6-indolecarbamidine dihydrochloride

DC	Dendritic cell
DHFR	Dihydrofolate reductase
DHS	Dehydrated hereditary stomatocytosis
DMSO	Dimethyl sulfoxide
DN	Double-negative (for thymocytes)
DNA	Deoxy-ribonucleic acid
DOCK2	Dedicator of cytokinesis 2
DP	Double-positive (for thymocytes)
DPM	Diffraction phase microscopy
dSMAC	Distal supramolecular activation cluster
dSTORM	Direct stochastic optical-reconstruction microscopy

E

ECM	Extracellular matrix
EDN 1	Endothelin 1
EE	Enteroendocrine
ER	Endoplasmic reticulum
ERK	Extracellular-signal-regulated kinase

F

FACS	Fluorescence-activated cell sorting
FAK	Focal adhesion kinase
F_C	Fragment crystallizable region of antibody
FDC	Follicular dendritic cell
FLIC	Fluorescence interference contrast microscopy

FP	Fusion peptide
FRET	Fluorescence resonance energy transfer
FS	Flicker spectroscopy

G

GBM	Glioblastoma multiforme
GCX	Glycocalyx
GM-CSF	Granulocyte-macrophage colony-stimulating factor
GP	Glycoprotein
GPCR	G protein-coupled receptors
GRB2	Growth factor receptor-bound protein 2

H

H3K27me3	Histone 3-lysine 27-trimethylation
HDAC3	Histone deacetylase 3
HEV	High endothelial venule
HFU	Highly focussed ultrasound
HIF1α	Hypoxia-inducible factor 1 alpha
hNSPC	Human neural stem/progenitor cells
HSC	Hematopoietic stem cell

I

ICAM-1	Intercellular Adhesion Molecule 1
ILC	Innate lymphoid cell
Ig	Immunoglobulin
IKK	IκB kinase

IL	Interleukin
ILP	Invadosome-like protusion
IP_3	Inositol 1,4,5-triphosphate
IS	Immunological synapse
ITAM	Immunoreceptor tyrosine-based activation motif
ITIM	Immunoreceptor tyrosine-based inhibitory motif
IU	International unit

J

JAK	Janus kinase

K

K_D	Dissociation constant

L

LAT	Linker for activated T cells
Lck	Lymphocyte-specific protein tyrosine kinase
LFA-1	Lymphocyte function-associated antigen 1
LINC	Linker of nucleoskeleton and cytoskeleton complex
LN	Lymph node
LPS	Lipopolysaccharide
LTMR	Low-threshold mechanoreceptors

M

MA	Mechanically activated
MACS	Magnetically activated cell sorting

MAPK	Mitogen-activated protein kinase
MHC	Major Histocompatibility Complex
moDC	monocyte-derived dendritic cell
MRTF	Myocardin-related transcription factor
MSC	Mesenchymal stem cell
MSD	Mean-squared displacement
MscL	Large-conductance mechanosensitive channel
MscS	Small-conductance mechanosensitive channel

N

Nck	Non-catalytic region of tyrosine kinase adaptor protein 1
NFAT	Nuclear factor of activated T cells
NFκB	Nuclear factor kappa-light-chain-enhancer of activated B cells
NK	Natural killer cells
NLR	Nucleotide-binding oligomerisation domain (NOD)-like receptor
NLRP3	NLR family pyrin domain containing 3
NO	Nitric oxide
NOMPC	No mechanoreceptor potential C
NOS 2	Nitric oxide synthase 2
NPSC	Neural progenitor stem cells
NSCL	Non-small cell lung carcinoma

P

PA	Polyacrylamide
PA/FCS	Photon arrival time analysis with fluorescence correlation spectroscopy

PALM	Photoactivated localisation microscopy
PAMP	Pathogen-associated molecular patterns
PBMC	Peripheral blood mononuclear cell
PBS	Phosphate-buffered saline
pDC	Plasmacytoid dendritic cell
PD-1	Programmed cell death protein 1
PDMS	Polydimethoxysilane
PEG	Polyethylene glycol
PFA	Paraformaldehyde
PfEMP-1	*Plasmodium falciparum* virulence protein-1
PI3-K	Phosphoinositide 3-kinase
PIP2	Phosphatidylinositol-4, 5-bisphosphate {also abbreviated as PI(4,5)P2}
PIP3	Phosphatidylinositol-3, 4, 5-triphosphate
PKC	Protein kinase C
PLC-γ	Phospholipase C gamma
pMHC	peptide-MHC complex
PRR	Pathogen recognition receptor
PRS	Proline-rich sequence
pSMAC	Peripheral supramolecular activation cluster
PSGL-1	P-selectin-glycoprotein-ligand-1
PTEN	Phosphatase and tensin homolog
pZAP70	phosphorylated ZAP70
P2RX	Purinergic ionotropic receptors

R

RA	Rapidly activating
RAG	Recombination-activating gene
RBC	Red blood cell
ReCOM	Remote-controlled mechanogenetics
RHR	REL-homology region
RICM	Reflection interference contrast microscopy
RLR	Retinoic acid inducible gene 1-(RIG-1)-like receptors
ROCK	Rho-associated protein kinase
RORγt	Retinoic acid receptor (RAR)-related orphan receptor gamma t
ROS	Reactive oxygen species
ROI	Region-of-interest
RUNX1	Runt-related transcription factor 1

S

SCF	Stromal cell factor
SDF1α	Stromal cell-derived factor alpha
SH2	Src Homology 2 domain
SHP-1	SH2-domain-containing protein tyrosine phosphatase-1
SLAP	Src-like adaptor protein
SLP-76	SH2 domain containing leukocyte phosphoprotein 76
SMAC	Supramolecular activation cluster
smFlnA	Smooth muscle actin crosslinking filamin A
SMLM	Single-molecule-localisation microscopy

ssRNA/DNA	single-stranded RNA/DNA
SOCE	Store-operated calcium entry
SRF	Serum response factor
S1PR	Sphingosine-1-phosphate receptor
STAT	Signal transducer and activator of transcription
STIM	Stromal interaction molecule
STOML3	Stomatin-like protein 3

T

T_{CM}	Central memory T cell
T_{EM}	Effector memory T cell
T_{RM}	Tissue resident memory T cell
TAZ	Transcriptional coactivator with PDZ-binding motif
TCR	T cell receptor
TFM	Traction force microscopy
TGF-β	Transforming growth factor beta
TGT	Tension gauge tether
T_H1	T-helper type 1 cell
T_H2	T-helper type 2 cell
T_H17	T-helper type 17 cell
T_{FH}	T follicular helper cell
TG	Transglutaminase
TIRFM	Total internal reflection microscopy
TLR	Toll-like receptor

TNFα	Tumor necrosis factor alpha
TOCCSL	Thinning out clusters while conserving stoichiometry of labelling
T_{reg}	Regulatory T lymphocytes
TRP	Transient receptor potential
TRPC	Transient receptor potential channel
TRPV	Transient receptor potential vanilloid
T_{tol}	Tension tolerance

V

VEC	Vascular endothelial cells
VEGF	Vascular endothelial growth factor
VWF	von Willebrand's Factor

W

WASp	Wiskott- Aldrich syndrome protein

Y

YAP	Yes-associated protein

Chapter 1. Introduction

1.1 Evolution of multicellularity, immune response and mechanical adaptations

The immune system forms our primary defence against pathogen invasion and aberrations from normal systemic homeostasis. The major part of the history of immunology was governed by the idea that discrimination between self and non-self, drives immune response [(1)]. Mounting evidence forced people to adopt a fresher perspective, which led to the development of the idea that immune response is driven by danger signals [(2)]. These danger signals could be of foreign origin (pathogens) or could be self-derived. The latter theory, despite its flaws, can be used to explain immune responses in conditions of disrupted homeostasis like cancer and autoimmunity [(3)]. Maintenance of tissue homeostasis and integrity is the primary objective of an organism. It is however, an intensive process in multicellular organisms composed of cells and tissue structures of vastly different phenotype and function. This intensely heterogenous population of cells must form intricate associations and interactions, so as to establish constant harmony and co-ordination, while maintaining tissue integrity and normalcy. It is, therefore crucial to recognise and eliminate 'rogue' self-cells that may pose significant danger to normal homeostasis in multicellular organisms. Evolution of the immune system from unicellular to multicellular organisms is closely associated with parallel development of the immune system arsenal [(3,4)]. Increasing complexity of the immune system with evolution of multicellularity, enabled establishment of integrity of complex multicellular tissue systems. Advanced immune system components facilitated close surveillance of multicellular systems from foreign attacks and self-derived anomalies [(4,5)].

Interestingly, evolution of multicellularity also correlated with diversification of cellular mechanical properties [6]. It has been proposed that mechanical adaptations co-evolved with multicellularity so as to facilitate close interactions between cells during formation of organs and tissue structures that form the organism [7]. Evolution of multicellularity is associated with development of complex tissue microenvironments as well as interactions with complex external surroundings. In order to maintain system integrity, cells and organs must have the capacity to show relentless resistance, adaptability and survivability to constant mechanical stress from their internal and external surroundings [6,7]. Constant cross-talk between cells of different mechanical, phenotypic and functional properties in the context of different tissue microenvironments, involves close regulation by mechanical forces and properties.

With parallel evolution of multicellularity and the immune response, in concordance with variations of cellular mechanical adaptations; it is not implausible to conceive that mechanical interactions played a crucial role during development of complex immune response. Indeed, a large reserve of existing and on-going research has found intricate regulation of the immune response by mechanical forces. Immune cells including, monocytes, dendritic cells, neutrophils, natural killer cells, T and B lymphocytes have all shown characteristic mechanoresponsiveness during trafficking and cellular interactions [8]. Leukocytes encounter diverse mechanical environment during their lifetime from peripheral circulation to lymphoid organs and peripheral tissues. The mechanical properties vary immensely depending on location and state of inflammation. Indeed, studies have shown that diseased states like cancer and autoimmunity are associated with changes in tissue mechanical properties that affect immune cell function and fate. Mechanical forces encountered either in the form of shear stress in circulation or during cellular interactions with the ECM or other immune cell partners, play a crucial role in determining immune cell functional outcomes [8]. Details of

mechanoregulation of immune cell function will be described in detail in the latter chapters (Chapter 3).

1.2 Mechanoregulation of T lymphocytes

T lymphocytes are highly responsive to mechanical cues [9,10]. Interaction between T lymphocytes and cognate antigen-presenting cells are typified by generation of strong tensile forces at the interacting interface. The origin these forces can be attributed to apposing membrane dynamics at the interface along with cytoskeletal-adhesion interactions [9, 10]. Mechanotransduction at the immune synapse is critical in regulating T lymphocyte activation and effector functions. Abolishment of force generation by pharmacological interventions, result in severe loss of T cell activation and impaired effector functions. Mechanotransduction has also been shown to play an invaluable role in T cell thymic selection during development. Mechanical forces regulate T cell specificity to antigens by enhancing the TCR discriminatory capacity between various antigens [9,10]. T lymphocyte trafficking and migration to specific sites is a crucial process of maintaining tight immunosurveillance. T lymphocytes are also sensitive to substrate rigidity and hence, modulate their behaviour according to surrounding tissue mechanical properties [9, 10]. Mechanical cues are intricately associated with efficient T cell trafficking and migration [10]. The role of mechanical forces in T lymphocyte biology has been described in detail in the latter chapters (Chapter 3).

1.3 Thesis summary

Although numerous studies have elucidated the role of mechanical cues in T lymphocyte biology in great detail, a dedicated T lymphocyte mechanosensor was not identified until recently. Piezo1 channels belong to a class of evolutionarily conserved mechanosensors [10]. They're triggered in response to changes in membrane tension upon application of force. Upon activation, they allow influx of extracellular cations which regulate downstream signalling [10]. In the following thesis, I have attempted to form a model describing the process of Piezo1-mediated mechanotransduction in T lymphocyte function [10,11]. We found that Piezo1 channels are highly expressed in human and mouse T lymphocytes. Upon T cell binding to cognate APCs, changes in surface membrane tension due to force, are sensed by T cell-specific Piezo1 channels. Triggered channels allow influx of extracellular Ca^{2+} which triggers calpain-dependent remodelling of the actin cytoskeleton scaffold. As described later, polymerisation and reorganisation of the actin cytoskeleton is crucial during formation and maintenance of a stable immunological synapse that facilitates optimal T cell activation and signalling. Loss of Piezo1 by siRNA-mediated downregulation abolished T cell activation in response to TCR crosslinking and also impaired T cell priming by APCs [10,11]. Moreover, we went on to find out that Piezo1 also plays an invaluable role in efficient T cell migration. Piezo1 downregulation impaired T cell motility in response to chemokine. Cells moved with lower speed and covered lesser distances. Loss of Piezo1 also abolished 2D and 3D chemotactic migration. Effective recruitment of T lymphocytes to lymph nodes or peripheral inflamed sites requires directed migration of T lymphocytes in response to chemokine gradients. In-vivo mouse models of site-specific inflammation showed loss of Piezo1, dramatically reduced the ability of T lymphocytes to migrate towards inflammatory cues, thus attenuating immune

response. Thus, Piezo1 mechanosensors play an active role to regulate and effective T lymphocyte activity, both in terms of activation and migration. Piezo1 was shown to undergo active repatterning of their cellular localisation, by preferentially migrating to cellular regions that encounter mechanical cues. Piezo1, thus enables effective scanning of the surroundings for mechanical cues that is necessary for optimal T lymphocyte function. This finding of a committed T lymphocyte mechanosensor, greatly improves our understanding of T lymphocyte function during an immune response.

T lymphocytes are widely used in adoptive immunotherapy where they are engineered to express specific receptors that recognise and kill target cells [(10)]. These cells are activated and expanded ex-vivo before transferring into affected individuals. By delving deeper into Piezo1-mediated mechanotransduction in T lymphocytes, one can develop effective strategies to design T lymphocytes that can function optimally during immunotherapy against cancer or infectious diseases.

1.4 References

1. Burnet FM. Immunological Recognition of Self. Science. 1961 Feb 3; 133(3449):307-311.
2. Matzinger P. The danger model: a renewed sense of self. Science. 2002 Apr 12;296(5566):301-5.
3. Pradeu T, Cooper EL. The danger theory: 20 years later. Front Immunol. 2012 Sep 17; 3:287.
4. Danilova N. The evolution of immune mechanisms. J Exp Zool B Mol Dev Evol. 2006 Nov 15;306(6):496-520.
5. Houghton AN, Guevara-Patiño JA. Immune recognition of self in immunity against cancer. J Clin Invest. 2004 Aug;114(4):468-71.
6. Chen J, Wang N. Tissue cell differentiation and multicellular evolution via cytoskeletal stiffening in mechanically stressed microenvironments. Acta Mech Sin. 2019; 35(2):270-274.
7. Jacobeen S, Pentz JT, Graba EC, Brandys CG, Ratcliff WC, Yunker PJ. Cellular packing, mechanical stress and the evolution of multicellularity. Nat Phys. 2018 Mar; 14:286-290.
8. Huse M. Mechanical forces in the immune system. Nat Rev Immunol. 2017 Nov;17(11):679-690.
9. Harrison DL, Fang Y, Huang J. T-Cell Mechanobiology: Force Sensation, Potentiation, and Translation. Front Phys. 2019 Apr; 7:45.
10. Liu CSC, Ganguly D. Mechanical Cues for T Cell Activation: Role of Piezo1 Mechanosensors. Crit Rev Immunol. 2019;39(1):15-38.

11. Liu CSC, Raychaudhuri D, Paul B, Chakrabarty Y, Ghosh AR, Rahaman O, Talukdar A, Ganguly D. Cutting Edge: Piezo1 Mechanosensors Optimize Human T Cell Activation. J Immunol. 2018 Feb 15;200(4):1255-1260.

Chapter 2: Overview of the Immune System

The immune system constitutes our primary defense against invading pathogens and infections [(1)]. The immune system is an intricate network comprising of multiple cellular players, that are involved in complex relationships and cross-talks, that function together to actively maintain host defense. The immune system is conventionally characterised as having two arms – the innate immunity and the adaptive immunity [(1)]. The innate immune branch comprises the first line of protection against foreign pathogenic attack and is characterised by prompt response time and broad specificity. The adaptive immune response, however is triggered in the latter phases of infection and is typified by specificity and generation of long-term memory response. These two branches are closely connected and heavily dependent on one each other.

2.1 Innate Immunity

The innate immune response focuses on providing immediate protection against foreign attacks and hence, is designed to recognise and react to a broad range of pathogens [(1)]. The components of the innate immunity range from antimicrobial peptides produced by non-immune cells like epithelial cells that maintain barrier integrity to diverse immune cells that rely on pathogen recognition receptors (PRRs) to recognise foreign microbes [(1)]. The skin and the mucosal layer act as a formidable barrier to pathogen attack by secreting antimicrobial components like defensins and cathelicidin [(2)]. They also counter pathogen attack by forming impenetrable physical structures like tight junctions, or creating conditions that are non-permissive for microbial growth (low pH for example) [(3)]. Innate immune responses are orchestrated by a diverse range of cellular players that express PRRs, which enable them to

bind to pathogen-associated molecular patterns (PAMPs), expressed on invading microbes [4]. PRR-expressing immune cells like dendritic cells, macrophages and neutrophils also respond to cell-intrinsic danger molecules that are produced by dying or damaged cells. These endogenous toxic components are known as damage-associated molecular patterns (DAMPs), and their recognition can sometimes trigger exacerbated immune reaction leading to autoimmunity [4]. PRRs include C-type lectin receptors (CLRs), expressed mainly on macrophages and dendritic cells that recognise carbohydrate moieties on bacterial and fungal wall. The major class of PRRs include Toll-like receptors (TLRs) that recognise broad range of DAMPs, expressed both by invading pathogens and host-derived damaged components (Fig. 2-1) [4,5]. TLR1, TLR2, TLR6, TLR4 and TLR5 are among the surface-expressing receptors that bind to bacterial surface components like the peptidoglycan wall, lipopolysaccharide (LPS) layer and flagellin [4,5]. TLR3, TLR7, TLR8 and TLR9 are intracellular PRRs that recognise foreign or host-intrinsic nucleic acids like single stranded RNA (ssRNA), single or double stranded DNA (ss/ds DNA). TLR7 and TLR9 are mostly expressed on plasmacytoid dendritic cells (pDCs) and recognise viral ssRNA or DNA rich in CpG motifs [4,5,6]. Abnormal recognition of host-derived nucleic acids by these TLRs in the context of endogenous alarmins tigger dysregulated autoimmune response. The TLR-mediated signalling pathway mostly involves MyD88-dependent type I Interferon (IFN) signalling cascade [6]. It also leads to activation of transcription factors like NFκB and AP-1 that upregulates production of proinflammatory cytokines. Other PRRs include Nod-like receptors (NLRs), RIG-I-like receptors (RLRs), AIM2-like receptors (ALRs) [4-6] and cGAS [7] which upon activation trigger a complex cascade of pathways involving mitogen activated protein kinase (MAPK), nuclear factor kappa B (NF-κB) and Type I IFN pathway that drive pathogen control [4-7] (Fig. 1). The Inflammasome pathway employs diverse PRRs for protection against foreign microbes as well as host-derived danger

signals (DAMPs) [8,9]. They include NLRs (nucleotide-binding oligomerization domain (NOD), leucine-rich repeat (LRR)-containing protein), AIM2 (absent in melanoma 2) and pyrin (Fig. 2-1). Upon activation, they induce activation of caspases and proteases that enable downstream production of functional IL-1β and IL-18; and subsequent cell lysis by pyroptosis. The canonical inflammasome pathway acts through activation of caspase 1 while the non-canonical pathway employs caspases 4, 5 and 11 [8,9].

The complement system also forms an essential part of innate immunity and involves plasma proteins that bind to target pathogens [10]. The classical pathway of complement relies on the formation of a membrane attack complex that initiates lysis of target pathogen or infected cell. The alternative pathway of complement activation involves marking an infected cell or pathogen through opsonisation for antibody-mediated destruction. Neutrophils are among the first responders to pathogen attack. They act by phagocytosing the invading microbe and killing them through NAPDH oxidase-dependent respiratory burst, that produces toxic oxygen radicals [11]. Complement-mediated opsonisation of attacking microbe facilitates enhanced neutrophil killing mediated through F_C receptor binding on the neutrophil surface. Basophils and mast cells respond to intracellular pathogens like helminths. They express high-affinity IgE receptor (FcЄRI), that upon crosslinking trigger cell degranulation and release inflammatory mediators like heparin, histamine, prostaglandins, leukotrienes and TNFα [10]. Natural killer (NK) cells form a crucial part of the innate immune response. Despite being conventionally categorised as the third lymphocyte subset, they form a primary element of innate immunity by driving non-specific killing of virus-infected cells [12]. They express T lymphocyte-specific CD3 molecule but lack antigen-specific TCRs. They are also designed to kill tumor cells. NK cells have the ability to gauge imbalance in the expression of activating and inhibitory receptors on the host cell which is usually triggered in infected or damaged

host cells. For example, virus-infected host cells or tumor cells generally downregulate their expression of class I MHC molecules which signals the NK cells to lose their inhibitory state and kill the target cell [11,12]. NK cells produce IFN-γ that control viral replication and activate dendritic cells and macrophages. NK cells express Fc receptors like FcγIIIR (CD16) that facilitates binding to antibody-coated pathogen or infected cells subsequently killing them in a process known as antibody-dependent cell cytotoxicity (ADCC) [11,12].

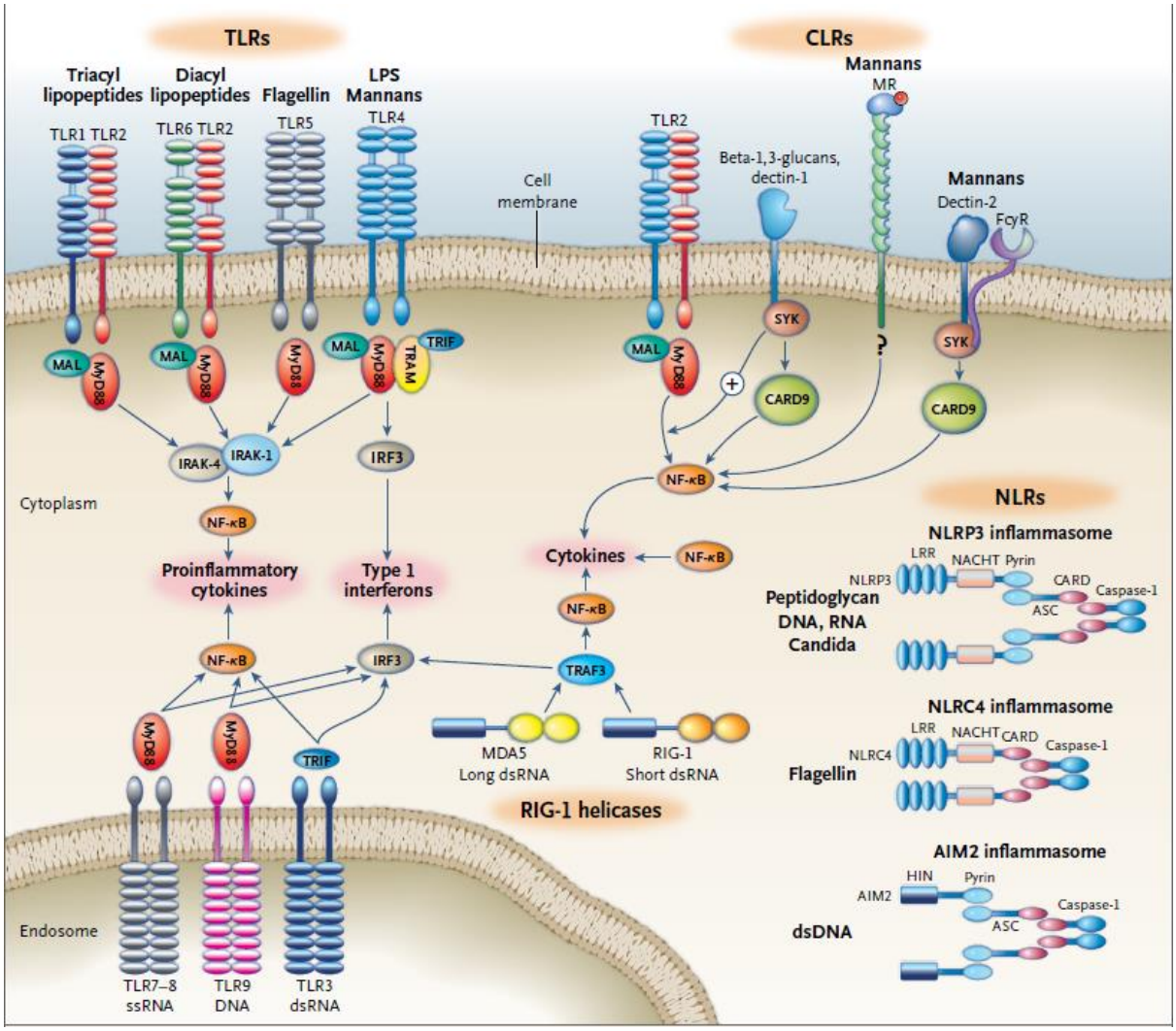

Figure 2-1. Types of pathogen recognition receptors involved in innate immune response.

Pathogen recognition receptors can be classified into 4 broad categories that include Toll-like receptors (TLRs), C-type lectin receptors (CLRs), retinoic acid–inducible gene I protein (RIG-I) helicase and nucleotide-binding oligomerization domain (NOD) leucine rich- repeat (LRR)–containing receptors (NLRs). Surface and intracellular TLRs bind to microbial ligands and signal through MyD88-dependent and independent pathways to trigger NFκB-mediated production of proinflammatory cytokines or IRF-mediated Type I IFN secretion. CLRs and RIG-1 recognise microbe-associated sugar moieties and DNA molecules which induces NFκB activation and cytokine production. NLRs include a wide range of cytosolic receptors that bind to various microbial ligands and form inflammasome complexes that signal to activate caspase-dependent production proinflammatory cytokines like IL-18 and IL-1β. (*Figure adapted from Netea et.al, N Engl J Med 2011* [9])

2.2 Adaptive Immunity

The initial innate immune response paves way for the more robust and specific adaptive immune response. The two main components of the adaptive immune response involve B lymphocytes and T lymphocytes [13]. Activation of these subsets depend on cellular interactions and molecular mediators produced during the innate immune phase. When microbes breach the epithelial barrier and take up residence in surrounding tissues, they are promptly taken up by tissue-resident phagocytes [14]. Macrophages which are tissue-resident monocytes are among the major class of phagocytes [14]. They inhabit various epithelial barrier regions, ranging from the submucosal layer of the gastrointestinal tract and the lung alveoli to neural and liver tissues, where they are identified as microglial cells and Kupffer cells. Circulating monocytes act as peripheral sentinels and migrate into tissues where they differentiate into macrophages upon antigen encounter. Granulocytes like neutrophils, eosinophils and basophils also form a major class of phagocytic cells [13,14]. These phagocytes can recognise and destroy pathogens without any assistance from the adaptive component of the immune response. Dendritic cells form the third and the most important category of phagocytes. Dendritic cells form the primary link between the innate and the adaptive arms of any immune response [13,14]. There are two types of dendritic cells – classical dendritic cells (cDCs) and plasmacytoid dendritic cells (pDCs) [15]. cDCs majorly function to recognise and phagocytose foreign microbes. Upon recognition, microbes undergo phagocytosis and are subsequently processed by DCs into small peptide antigens which are expressed on the DC surface bound to class II MHC molecules [15]. DCs act as professional antigen presenting cells (APCs). They present microbial antigens to T lymphocytes bearing antigen-specific TCRs triggering their activation, clonal expansion and effector functions [16]. They also present

specific antigens to B lymphocytes and facilitate production of antigen-specific antibodies with the help of T lymphocytes [16]. T and B lymphocytes organise what is recognised as cell-mediated immunity and humoral immunity, respectively. Activated T cells can either directly kill target pathogens or infected host cells (For e.g.: Cytotoxic T cells) or can differentiate into helper T lymphocytes that produce effector cytokines that regulate function of other immune cells [13,16]. Helper-T lymphocytes also interact and regulate B lymphocyte activation (Details in the following chapter). Antibodies mediate pathogen control in several ways. They bind to target microbes (For e.g.: Viruses) and their products (For e.g.: Bacterial toxins) and prevent them from infecting host cells in a process known as neutralisation. Antibody-bound microbes can also bind to phagocytes bearing receptors for the antibody Fc region, which facilitate their phagocytosis and destruction. This process of antibody coating is known as opsonisation. Antibodies also act by activating the complement system that trigger destruction of pathogen or infected cell [13,16].

Both T lymphocytes and B lymphocytes bear antigen-specific receptors in the form of T cell receptors (TCRs) or surface Immunoglobulins (Ig) [16]. Upon activation by cognate antigens, they undergo clonal expansion which allow increased production of antigen-specific effector T and B cells. Moreover, this expansion is simultaneously supported by a dynamic process known as somatic hypermutation which actively produces and selects for cells that express receptors which have higher affinity (yet specificity) for target antigens [17]. This process facilitates enhanced recognition and killing of target pathogens. The T lymphocyte-specific cell-mediated immunity and B lymphocyte-specific humoral immunity is characterised by generation of long-term memory response [18,19]. Formation of long-lived memory T and B lymphocytes as well as long-lived antibodies facilitate prompt and effective immune response

to secondary infections [18,19]. This property of the adaptive immune response has enabled development of successful vaccines against numerous diseases over decades [20].

2.3 The biology of T lymphocytes

T lymphocytes form the primary component of cell-mediated adaptive immunity [21]. They express antigen-specific surface receptors known as the T cell receptor (TCR). TCRs recognise antigens-bound to major histocompatibility molecules (MHCs) on antigen presenting cells (APCs) or target cells. The TCR consists of a heavy chain and light chain each of which possess variable domains (V-region) and constant domains (C-region) [21,22]. The V-region of the TCR binds to antigens. TCRs cannot bind to antigens itself. They recognise antigens in the context of short self-peptides known as MHC (major histocompatibility complex) molecules expressed on host cells [23]. MHC molecules are transmembrane glycoproteins coded by a cluster of genes and they show high polymorphism among individuals with most individuals being heterozygous for the MHC genes [24]. This is considered to be an important evolutionary mechanism that increases the breadth of pathogen specificity that can be recognised by the TCR. TCR binding not only depends on antigen specificity but also depend on the properties of bound MHC molecule. This property of antigen recognition by TCR is known as MHC restriction [25] which was discovered by Peter Doherty and Rolf Zinkernagel in 1970s [26]. T cells can be divided into two types depending on the TCR type they express. T cells expressing the α:β TCR (αβ T cells) are more abundant than γ:δ TCR expressing T cells [27]. The TCR specificity is regulated by complementarity determining regions (CDR) which are hypervariable loops of the variable region of the TCR [28].

2.3.1 Generation of the T lymphocyte receptor (TCR)

The T lymphocytes population is characterised by having a wide repertoire of TCRs which enable recognition of a diverse range of antigens. This extensive TCR repertoire is generated by DNA recombination in the gene segments coding for the antigen-binding variable region

of the TCR. DNA coding for TCR variable region is formed of multiple gene segments, which undergo recombination and rearrangement to produce TCRs of varying specificities [29,30]. TCR light chain or TCRα variable region is coded by two gene segments – V (variable, V_α) and J (joining, J_α) gene segments [29]. The TCR heavy chain or TCRβ variable region (V_β) comprises of a third gene segment called the D (diversity) region in addition to V and J segments. Multiple alleles of each gene segment exists and their alternate combinations generate germline TCR diversity (Fig. 2-2). This V(D)J recombination is carried out by V(D)J recombinases called RAG1 and RAG2 (RAG – recombination activating gene 1) [29-31]. Additional germline diversity is also generated by addition of varying combinations of P and N nucleotides between the V, D and J segments [29-31]. T cell clones with different TCR specificities that are generated subsequently go through a rigorous process of selection where self-reactive clones are eliminated [32].

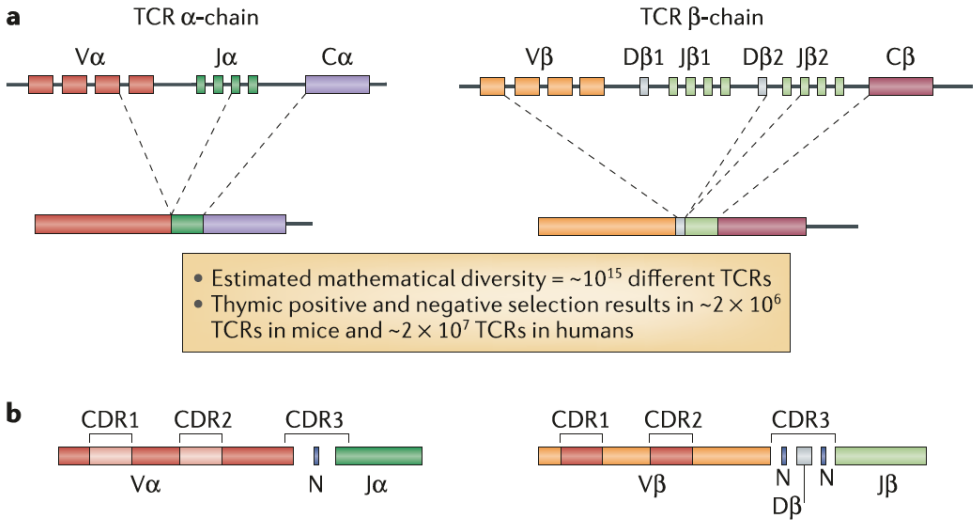

Figure 2-2. Generation of T cell receptor diversity. The diverse TCR repertoire is generated as a result of somatic recombination between V-J and V-D-J gene segments coding for TCR α and β chain respectively. Productive recombination forms complementarity determining regions (CDRs) of hypervariability in the V regions that determine antigen specificity of the TCR. CDR1 and CDR2 are formed by somatic recombination of different V-region gene segments while CDR3 is determined by somatic recombination in addition to non-template-

nucleotide (N) addition at the V(D)J junction. *(Adapted from Turner et.al., Nat Rev Immunol., 2006* [33]*)*

2.3.2 Development of T lymphocytes

Lymphocyte development begins in the fetal bone marrow where hematopoietic stem cells (HSCs) give rise to common lymphoid progenitor cells [34]. Common lymphoid progenitor [35] cells give rise to B lymphocytes, T lymphocytes and innate lymphoid cells (ILCs). Some lymphoid progenitor cells migrate to the thymus where they develop into thymocytes and eventually mature into T lymphocytes. Activation of the Notch signalling pathway commits development of thymocytes to the T lymphocyte lineage [35,36]. The thymus is the primary source of T lymphocytes till before puberty after which T lymphocyte production decreases substantially [37]. The thymic stromal cells play an indispensable role in T lymphocyte development and shaping of the T lymphocyte population. Majority of thymocytes develop into αβ T lymphocytes. γδ T lymphocytes form only 5% of the T lymphocyte population. Development of T lymphocyte occurs in a series of stages (Fig. 2-3) [38-40]. The earliest stage consists of thymocytes that lack both CD4 and CD8 co-receptors and hence are called double-negative (DN) thymocytes. DN thymocytes lack surface expression of TCR-CD3 complex. DN thymocytes progress through 4 stages depending on expression of CD25 (IL-2 receptor α chain), CD44 (adhesion molecule) and c-kit (receptor for stromal cell factor, SCF). The first DN1 stage is characterised by expression of c-kit and CD44 and lack of expression of CD25. This is followed by gradual CD25 expression upregulation (DN2) and subsequently upregulated CD25 while downregulation of CD44 and c-kit (DN3). The DN1 stage lack rearranged genes coding for a mature TCR. The β chain of the TCR first begins to form in the DN2 stage and DN3 stage through VDJ recombination. Thymocytes that have been unable to

produce a functional β chain rearrangement die by apoptosis. The rest undergo proliferation while downregulating CD25 expression (DN4 stage). In DN3 thymocytes, the rearranged β chain forms a complex with a surrogate α chain forming a pre-TCR. The pre-TCR interacts with CD3 complex and forms a signalling-proficient pre-TCR complex that facilitates cell survival and proliferation in the DN4 stage. Further pre-TCR β chain recombination is arrested in this stage. The DN4 stage proceeds to the double positive (DP) stage where thymocytes acquire expression of CD4 and CD8 co-receptor. DP cells subsequently cease cell proliferation and undergo recombination in the TCR α chain coding loci to produce a functional αβ TCR [38-40].

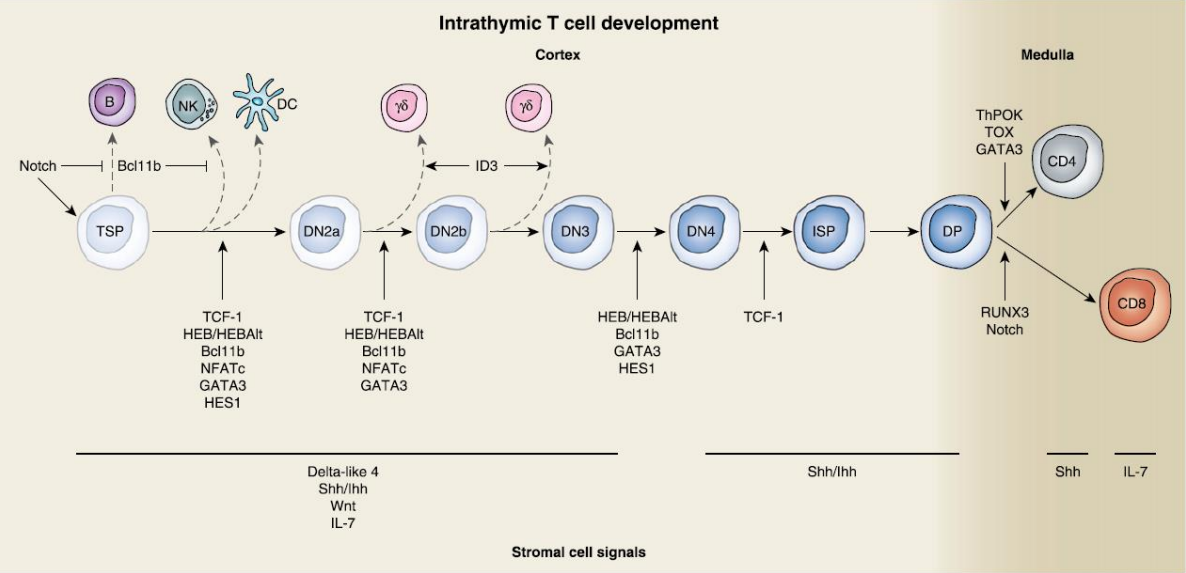

Figure 2-3. Thymic development of T cell lymphocytes. Notch-Dll4 signalling commits thymic progenitor cells to the T lymphocyte lineage. T lymphocyte development consists of a series of stages - CD4/CD8-negative, DN1 to DN4, to CD4/CD8-expressing double positive (DP) to CD4 or CD8-expressing T lymphocytes. Transition between these stages is regulated by upregulation or downregulation of various transcription factors and surface receptors. *(Adapted from Shah et.al., J Immunol., 2014 [40])*

2.3.3 T lymphocyte selection

Mature T lymphocytes bearing developed TCR complexes are subjected to a rigorous process of positive and negative selection [41]. Positive selection involves selection of those cells whose TCRs can recognise self-peptide and self-MHC complexes thus generating self-MHC restricted TCR repertoire [41,42]. Majority of the rearranged TCRs fail to interact with self-peptides and MHCs expressed on thymic stromal cells. T lymphocytes bearing such TCRs fail to receive any survival signals and consequently die by apoptosis. During the process of positive selection, DP lymphocytes also lose expression of one of the co-receptors, thus becoming CD4 or CD8-expressing, single positive T lymphocytes [42]. Positive selection occurs in the thymic cortex and migrate as single positive T lymphocytes to the thymic medulla where negative selection takes place. T lymphocytes that show high affinity for self-antigens are eliminated so as to maintain T cell tolerance to self-antigen [41,42]. The thymic medulla provides a rich environment with self-antigen cues that help selecting for non-self-reactive T lymphocytes. Expression of host-specific self-antigens by the thymic medulla is controlled in part by AIRE (autoimmune regulator) which is expressed by thymic stromal cells [44,45]. Mutations in AIRE produce devastating autoimmune conditions [45] thus, underlining its importance in establishment of thymic central tolerance. While it is not possible for the thymus to express every host-specific tissue antigen, it is likely that some self-reactive clones do escape thymic negative selection and reach peripheral circulation. There are however, several mechanisms of peripheral tolerance that prevent activation and or survival of such T lymphocytes [47]. According to the affinity hypothesis [48] of T cell selection, threshold TCR affinity for self-antigens must differ between positive and negative selection (Fig. 2-4). If a T lymphocyte bearing TCRs fails to show any affinity for self-peptide/MHC complexes they die as a result of

neglect. Low affinity interactions allow T lymphocyte survival while ensuring no self-reactivity, thereby leading to positive selection. High affinity interactions between TCR and self-antigens is a strong indicator of self-reactivity, thus triggering negative selection [48]. There have been exceptions to this theory. For example, a subset of T lymphocytes known as T regulatory (T_{reg}) cells have been shown to play a central role in establishing peripheral tolerance. These cells, however possess TCRs that have high affinity for self-antigens and have yet managed to undergo positive selection [48,49].

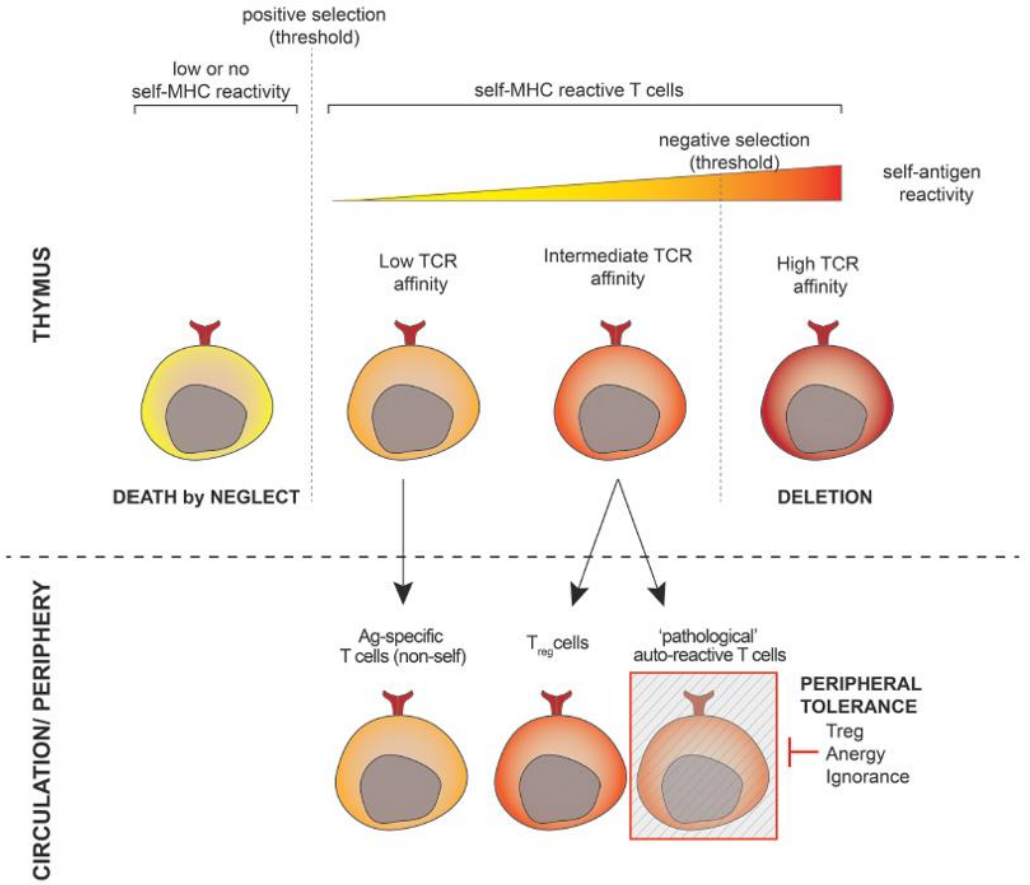

Figure 2-4. The process of T lymphocyte positive and negative selection. T lymphocyte positive selection consists of allowing survival of T cells bearing TCRs bearing low affinity for self-peptide/self-MHC complexes expressed on thymic stromal cells. This ensures self-MHC restriction of T lymphocytes and TCRs that fail to bind to self pMHCs die by apoptosis. In order to eliminate autoreactive T cells, T cells bearing TCRs that show high affinity for self pMHCs

are also eliminated by apoptosis. Those T cells having high/intermediate affinity for self pMHCs and escape clonal deletion in the thymus, form T regulatory cells or autoreactivity is prevented through various mechanisms of peripheral tolerance. *(Adapted from Boehncke et.al., Front Immunol., 2019* [50]*)*

2.3.4 T lymphocyte signalling

The TCR heterodimer possesses short intracellular cytosolic tail which makes them incompetent to trigger downstream signalling by itself upon antigen recognition [51]. The TCR heterodimer associates with the CD3 complex to form a signalling-proficient TCR complex [51]. The CD3 complex consists of Ɛδ and γƐ heterodimers, and ζζ homodimer. The cytosolic tails of the CD3 complex contains immunoreceptor tyrosine-based activation motifs (ITAMs) [51,52]. Upon TCR crosslinking, tyrosine residues in ITAMs get phosphorylated by Lck kinases and these serve as docking sites for SH2-containing signalling proteins like ZAP-70 (Fig. 2-5). Lck activity is counteracted by CD45 phosphatases. Recruitment and phosphorylation of ZAP-70 by phosphorylated ITAMs triggers downstream recruitment and phosphorylation of SLP-76 and LAT that create a scaffold for binding of multiple adaptors and signalling protein complexes [51-53]. Phosphorylated ZAP-70 also recruit and activate PI-3 kinase which generates PIP3 (phosphatidylinositol-3, 4, 5-triphosphate) from PIP2 (phosphatidylinositol-4, 5-bisphosphate). Membrane PIP3 and SLP-76/LAT recruit major signalling components that each trigger activation of distinct pathways. These include activation of the serine/threonine kinase (Akt), PLC-γ (Phospholipase C), Vav and adaptor protein, ADAP (adhesion and degranulation-promoting adapter protein). Akt activation is required for regulation of T lymphocyte metabolism like increasing glucose uptake and glycolysis. Akt signalling also

activates the mTOR pathway which is required for protein biosynthesis by increasing ribosome production and mRNA synthesis and enhanced lipid production [51-53] (Fig. 2-5).

Activation of the PLC-γ pathway generates cytosolic second messengers like diacylglycerol (DAG) and inositol 1,4,5-triphosphate (IP_3) [52-53]. They trigger mobilisation of Ca^{2+} from endoplasmic reticulum (ER) into the cytosol. Depletion of ER calcium triggers formation of STIM1 clusters on the ER and their binding to CRAC (calcium release-activated calcium channel) channels on the plasma membrane. This facilitates entry of extracellular calcium into the cell and calcium reloading of depleted ER stores. Increase in cytosolic Ca^{2+} triggers calmodulin-dependent activation of NFAT (nuclear factor of activated T cells) family of transcription factors [52-53]. PLC-γ signalling also activates Ras which subsequently triggers the MAPK (mitogen-activated protein kinase) pathway. The MAPK pathway results in activation of the AP-1 transcription factor. The third branch of the PLC-γ signalling pathway involves the activation of PKC-Θ (protein kinase C) which is required for activation of AP-1 and NF-κB [52-54] (Fig. 2-5). All these signalling pathways act together to induce and regulate expression of genes required for activation and proliferation of T cells, as well as their effector functions.

Vav activation, in response to TCR stimulation is required for efficient cytoskeletal remodelling during formation of a stable immune synapse. Activated Vav recruits Rho GTPases like Cdc42. Activated Cdc42 induces a conformational change in WASp (Wiskott-Aldrich syndrome protein) which eventually recruits Arp2/3. This triggers actin polymerisation and formation of the immunological synapse [52-54] (Fig. 2-5).

ADAP is an adaptor protein that is activated downstream of TCR crosslinking [52-54]. It enhances integrin-mediated adhesion to cognate APCs. T cell adhesion to cognate APCs is mediated by LFA-1 and ICAM-1 interactions. LFA-1 is usually present in a weak affinity state in non-

stimulated T cells. Recruitment and activation of ADAP after TCR stimulation results in subsequent recruitment and activation of small GTPase, Rap1 at the membrane. Rap1 induces LFA-1 clustering on the T cell membrane and its conversion to high-affinity state that promotes ICAM-1 binding on APCs. This, in conjunction with Vav signalling allows formation of a stable immunological synapse where efficient T cell signalling occurs [52-54] (Fig. 2-5).

Naïve T lymphocytes require additional co-stimulation to achieve optimal activation [55]. CD28 is among the most important T cell co-stimulatory molecule. It interacts with CD80 (B7.1) and CD86 (B7.2) expressed on APCs. CD28-mediated signalling is required for T cell survival, proliferation and production of cytokines [55]. T lymphocytes also express inhibitory receptors like CTLA-4 and PD-1 which attenuate T cell response to prevent uncontrolled T cell activation [55,56]. Activated T lymphocytes express CTLA-4 on the cell surface that compete with CD28 for binding to CD80 and CD86 on APCs. CTLA-4 has much higher avidity for B7 costimulatory molecules as compared to CD28, thereby effectively blocking T cell activation. PD-1 is another such inhibitory receptor expressed on activated T lymphocytes. PD-1 contains ITIM (immunoreceptor tyrosine-based inhibitory motifs) on its cytoplasmic region. ITIMs recruit inhibitory phosphatases that dephosphorylate tyrosine groups on signalling proteins leading to their inactivation. PD-1 binds to ligands, PD-L1 and PD-L2. Inhibitory receptors function to control uninhibited T cell responses. Diseased conditions like cancer are often characterised by upregulation of inhibitory receptors which result in dysfunctional or exhausted T lymphocytes. These inhibitory receptors are therefore, often targeted during immunotherapy to overcome T cell inactivation [56,57].

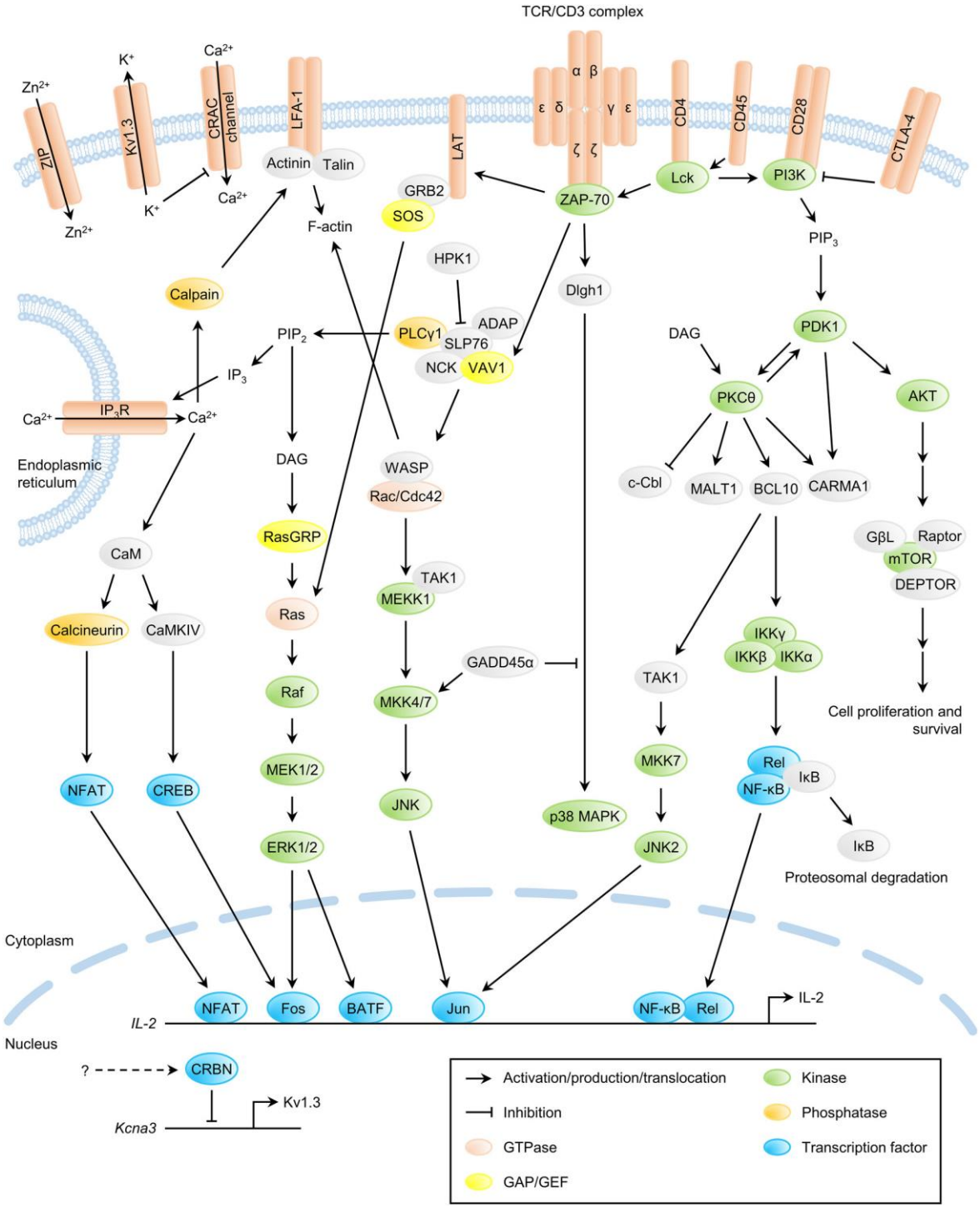

Figure 2-5. T lymphocyte signalling pathways. TCR binding to cognate peptide-MHCs on antigen presenting cells triggers ITAM phosphorylation on CD3 signalling domains that recruits and activates tyrosine kinases – Lck and ZAP70. These kinases phosphorylate various adaptor proteins that trigger a cascade of signalling pathways which can be broadly classified into 4 categories. They include Rho-GTPase-dependent actin polymerisation, Akt-mTOR regulation of T lymphocyte metabolism, Rap1-dependent T lymphocyte adhesion and

migration, and PLC-γ-dependent of activation of NF-κB, AP-1 and MAPK signalling cascade. (*Adapted from Hwang et.al., Exp Mol Med., 2020* [58]*)*

2.3.5 Subsets of T lymphocytes

T lymphocytes can be broadly divided into two major, $CD4^+$ and $CD8^+$ subsets [59], each of which can be further differentiated into multiple types depending on function.

$CD8^+$ T lymphocytes

$CD8^+$ T lymphocytes are cytotoxic T cells that kill target cells [60]. They recognise microbial antigens bound to class I MHC molecules expressed on infected host cells. They form an elementary part of host defense against intracellular pathogens like viruses and intracellular bacteria. Virus-infected cells express viral proteins bound to MHC I molecules on host cells which allow $CD8^+$ T lymphocyte recognition of infected cell [60]. $CD8^+$ T lymphocyte cytotoxic activity may require additional priming by dendritic cells and $CD4^+$ T effector cells. $CD8^+$ T cell-mediated killing involves binding of cytotoxic cells with the target cell and formation of a synapse. $CD8^+$ T cells then secrete cell-lysing components like perforins into the synapse that punches holes into the target cell membrane. Cell-lysing granzymes are subsequently released into the target cell through these holes where cells undergo caspase-dependent or independent apoptosis [60]. Activated $CD8^+$ T lymphocytes also mediate target cell apoptosis through activation of FasL and Fas signalling pathway [60]. Activated cytotoxic $CD8^+$ T lymphocytes produce IFN-γ and TNF-α. IFN-γ inhibits viral replication. IFN-γ and TNF-α act to activate macrophages to enhance pathogen uptake [60]. $CD8^+$ T lymphocytes also play a primary role in tumor control and usually undergo exhaustion during cancer progression.

$CD8^+$ T lymphocytes are primarily targeted for PDL1-PD1 and CTLA-4 therapy to overcome immune cell exhaustion in cancer immunotherapy [61].

$CD4^+$ T lymphocytes

Activated $CD4^+$ T lymphocytes differentiate to effector T cells which are helper T (T_h) cells that mainly act by producing cytokines that regulate function of other immune cells [62]. The respond to foreign antigens bound to class II MHC molecules on APCs [63]. Upon antigen recognition and subsequent activation, naïve $CD4^+$ T lymphocytes undergo proliferation and differentiation to various effector cell types. The main $CD4^+$ T lymphocyte effector subset include T_H1 (T helper 1 subset), T_H2, T_H17, T_{FH} (T follicular helper cells) and T_{reg} (Regulatory T cells) [64,65]. T_H1 cells mainly produce IFN-γ that induce macrophage activation during elimination of intracellular pathogens. T_H2 cells produce IL-4 that activate mast cells and basophils. They also produce IL-5 which recruit and activate eosinophils and IL-13 which protect mucosal surfaces against helminth infections. T_H17 cells are characterised by production of IL-17 and IL-22 that trigger downstream recruitment of neutrophils and production of antimicrobial peptides, respectively [64,65]. T_{FH} are predominantly found in secondary lymphoid organs where they make antigen-dependent interactions with naïve B cells and induce germinal centre formation [66]. T_{FH} cells activate naive B cells to produce, high-affinity, class-switched immunoglobulins with different effector functions like opsonising IgG antibodies or IgE antibodies that trigger degranulation of mast cells and basophils in allergic responses. T_{reg} cells help in immune response suppression by production of anti-inflammatory IL-10 and promote central or peripheral tolerance to self-antigens. Each of these T_H subsets can be identified on the basis of expression of fate-determining transcription factor which is induced in response to specific cytokines [66]. Distinct cytokines induce differentiation of

specific T_H subset mediated through activation of different STAT family of transcription factors (Fig. 2-6). IFN-γ and IL-12 trigger activation of STAT1 and STAT4 which induces T-bet expression and differentiation to the T_H1 type. IL-4 signalling induces STAT6-mediated upregulation of GATA-3 which induces differentiation to the T_H2 pathway. TGF-β, IL-6 and IL-23 induces STAT3 activation that subsequently triggers upregulation of RORγT which commits programming to the T_H17 pathway. T_{FH} cells are induced and maintained by IL-6 signalling-dependent activation of STAT3/Bcl-6 pathway [66,67]. Induction of T_{reg} cells requires IL-2 and TGF-β signalling in the absence of pro-inflammatory cytokines like IL-6. This cytokine milieu induces STAT5 activation and downstream upregulation of FoxP3 which determines T_{reg} differentiation [66,67].

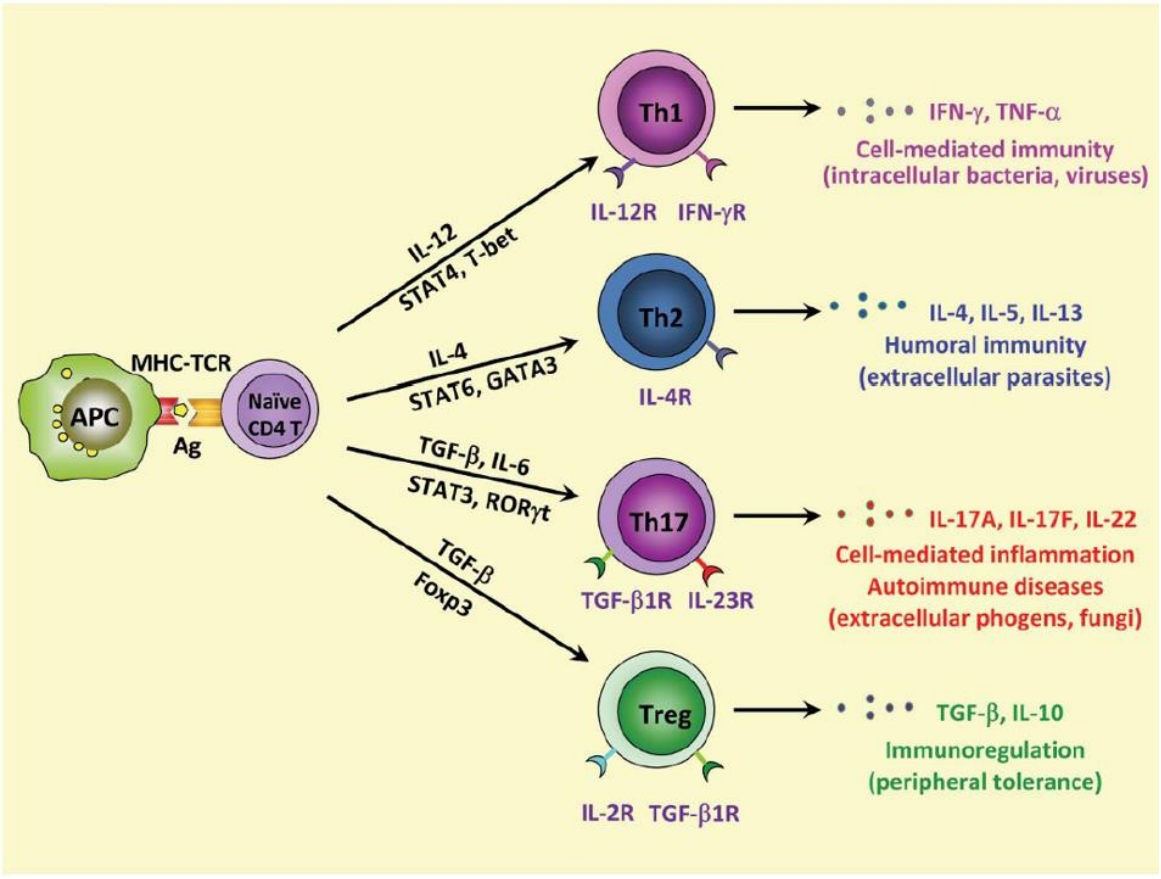

Figure 2-6. Differentiation of CD4⁺ T lymphocyte effector subsets. Naïve CD4⁺ T lymphocytes, upon activation, differentiate to effector subsets, each with its own function. Effector CD4⁺ T

lymphocytes can be broadly classified into 4 subsets that include IFN-γ producing Th1, IL-4 and IL-13 producing Th2, IL-17 producing Th17 and IL-10 producing immunosuppressive T regulatory (T_{reg}). Each of these subsets are induced in response to distinct cytokine milieu and can be identified by a lineage-determining transcription factor – T-bet for Th1, GATA3 for Th2, RORγt for Th17 and FoxP3 for T_{reg}. Each of these subsets function in specific aspects of immune response depending on type of infection as described in the figure. *(Adapted from Leung et.al., Cell Mol Immunol., 2010* [67]*)*

2.3.6 T lymphocyte memory response

Effector T cells show rapid activation in the absence of any co-stimulation [64]. Hence, they play an active role along with the components of the innate immune response during secondary re-infections [68]. Their diverse functional phenotype and plasticity allows them to adapt and respond to diverse pathogenic challenges. After a successful immune response, the pool of effector T cells undergo significant reduction by apoptosis while allowing only a small population of memory T cells to survive and maintain long-lasting immunity [68]. Memory T cells differ from naïve T cells by upregulating CD44 and downregulating CD62L (L-selectin) expression [69]. This enables selective trafficking of these cells from blood to peripheral tissues unlike naïve T cells which home towards secondary lymphoid organs. Memory T cells also express CD45RO. Unlike naïve T cells, memory T cells do not undergo homeostatic interactions with self-MHC/self-peptide complexes for survival in the periphery. Instead, they rely on IL-7 and IL-15 for survival [69,70]. Memory T cells fall under 3 categories – central memory (T_{CM}), effector memory (T_{EM}) and tissue-resident memory T cells (T_{RM}) [71] (Fig. 2-7). T_{CM} cells are characterised by surface expression of CCR7 and they home to peripheral lymphoid tissues like naïve T cells. T_{EM} lack CCR7 expression while expressing high levels of β-

integrins that facilitate their rapid entry into peripheral inflamed tissues. Upon antigen stimulation, they get rapidly activated (unlike T_{CM}) to produce inflammatory cytokines like IFN-γ, IL-4 and IL-5. T_{RM} occupy peripheral tissue regions like epithelial dermis or intestinal lamina propria, and do not undergo trafficking. They express high levels of tissue-homing chemokine receptors like CCR9 and CXCR3 while lacking CCR7. Tissue-residence of T_{RM} is enabled by CD69-mediated induction of S1PR (sphingosine-1-phosphate receptor) expression. Generation of CD8 memory T cells require CD4 T cell help since mice lacking MHC II failed to maintain its CD8 T cell memory pool [71]. Memory T cells provide long-term protection to many pathogenic infections and play an important role in vaccine responses [72].

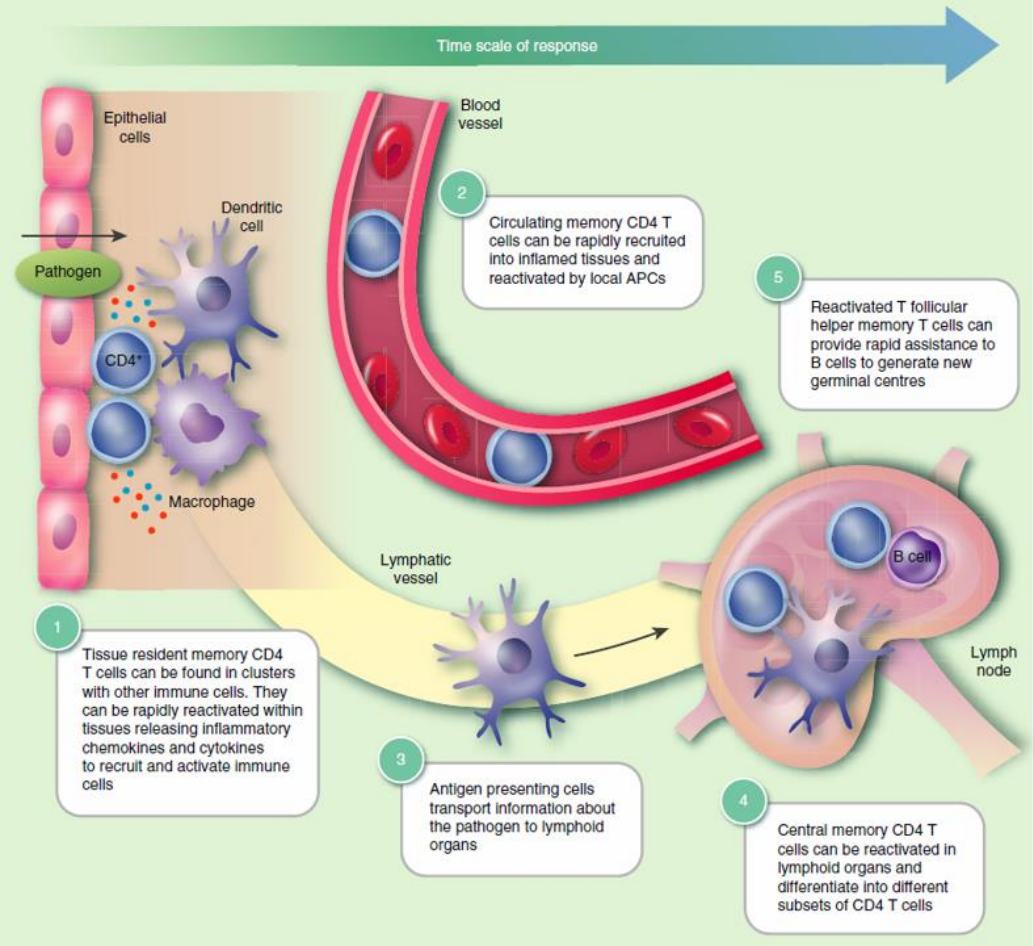

Figure 2-7. Function of memory T lymphocyte subsets in response to pathogen re-infection.

Upon pathogen re-encounter in peripheral tissue sites, tissue-resident (T_{RM}) memory cells are

activated where they produce inflammatory cytokines and chemokines which recruits circulating effector memory T cells (T_{EM}) to the infected site. Central memory T cells (T_{CM}) are activated by APCs at secondary lymphoid organs and subsequently undergo clonal expansion and differentiation to effector T lymphocytes which enter peripheral circulation and provide systemic protection. Activation of memory T follicular cells (T_{FH}) enable activation of B cell-mediated responses in the germinal centres. *(Adapted from Gray et.al., Immunology, 2018* [72]*.)*

Chapter 3. Mechanical Forces in Biology

The domain of biology was largely driven by the notion that physiological and cellular processes are ultimately governed by genetic and epigenetic factors [73]. A large part of research in this field is dedicated to finding cell-intrinsic molecular and signalling players that affect these factors and determine cellular or physiological outcomes. It is however, becoming increasingly evident that the physical environment of cells and tissues contribute majorly towards their function and fate [74]. Cells and tissues have constant dynamic crosstalk with their physical surroundings. They respond and adapt to the mechanical properties of their environment. Researchers have begun to acknowledge that biology as a singular domain cannot yield a holistic insight into physiological processes. Studies that adopt an integrated multidisciplinary approach, involving explanation of biological phenomena using laws and principles of physics are now being undertaken to study cellular processes in disease and development.

The field of mechanobiology involves study of interactions between the cells and tissues with the physical properties of their surroundings in various biological processes [74]. Interest in mechanobiology emerged in the early parts of the 20th century when observations were made that cells modify their behaviour according to the stiffness properties of their substrate [75]. The study found that rat epithelial and fibroblast cells tend to spread less and show improved lamellipodia-based motility on stiffer substrates (above a threshold of ~5kPa). This change in motile behaviour and morphology can be triggered simply by modifying the mechanical properties of the substrate without changing the chemical environment. Cell attachment to the substrate via focal adhesion complexes was also affected significantly by substrate rigidity. This was one of the pioneering discoveries in the biophysical domain which revealed

an unexplored, yet crucial aspect in physiological processes. Since then, numerous studies have shown that mechanotransduction is an integral process of cell and tissue biology [75].

3.1 Mechanotransduction

Mechanotransduction is the process of sensing cell or environment-specific mechanical stimuli like substrate stiffness, shear stress or membrane stretching, and converting them into molecular and chemical signals which govern cellular function and fate [77]. Processes like cellular proliferation, migration, cell shape, cellular differentiation and fate determination, tissue regeneration and repair are all dependent on complex interactions between cells and their 3D mechanical environment [77]. Interactions involving the extracellular matrix (ECM), cytoskeletal components, membrane dynamics are subjected to regulation by mechanical forces, that are generated either from the external environment or from within the cell [77]. The dynamics of these mechanical interactions have been shown to undergo significant dysregulation in diseased states like cancer and inflammation thus, confirming their importance in normal cellular physiology [78].

An interesting proposition was put forward by Chen and Wang, [79] who suggested that evolution of multicellularity from unicellular organisms could have been regulated by the development of cellular ability to sense surrounding stiffness. The study proposes that single-celled prokaryotes underwent rigidification and toughening of their cytoskeleton, which enabled them to maintain their shape and form as well protect their structural integrity from external mechanical stress (Fig. 3-1). Cells of different origin show a wide range of stiffness which can be explained on the basis of their function. Embryonic stem cells and neural cells fall have lower stiffness in the range from 0.1kPa to 0.5kPa [80,81]. Smooth muscle cells, endothelial cells and fibroblasts have higher stiffness ranging from 1-5kPa [82]. Skeletal muscle cells on the other hand show stiffness in the range of 12kPa which can be explained by the fact that it is subjected to constant mechanical stress, and therefore should have the capacity

withstand any tissue damage [83]. Similarly, the primary function of fibroblast cells is to produce ECM proteins that function in tissue remodelling [84] which necessitates the higher stiffness property of the cells. Stiffness properties of a cell is determined by organisation of cytoskeletal components and membrane proteins. Clustered organisation of transmembrane adhesion proteins that form attachments with the ECM like integrins, adhesion proteins that form cell-cell attachments like cadherins, cytoskeletal scaffold including actin and myosin bundles, and the nuclear lamina all act together to maintain a cell in a quasi-steady state of tension that determine cell stiffness and shape [79,85,86].

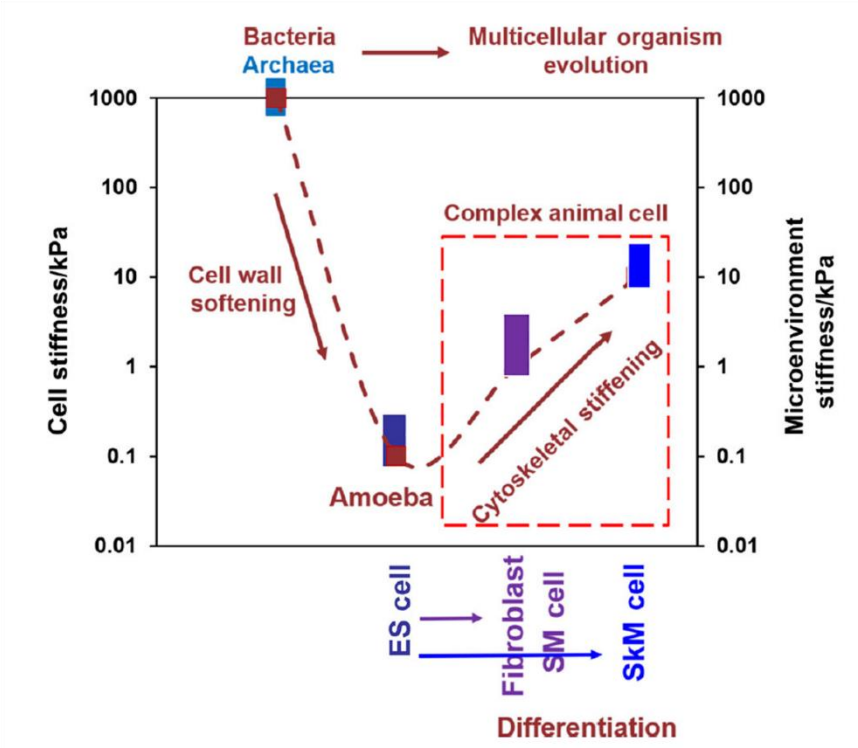

Figure 3-1. Correlation between evolution of multicellularity and changes in cell stiffness.
Evolution from single-celled prokaryotes to multicellular organisms is associated with changes in cytoskeletal stiffness which facilitates coping with complex microenvironment rich in mechanical stress. It has been hypothesised that embryo development and differentiation to multiple tissue cells mimics evolution of multicellularity. Differentiation of an embryonic stem (ES) cell from the inner cell mass of a blastocyst to fibroblasts or smooth muscle cells (SM) or skeletal muscle cells (SKM) is accompanied by dramatic increase of cell stiffness from 0.1kPa

to 12kPa. With increasing degree of tissue differentiation, cell stiffness is seen to increase which allows the tissues to adapt to mechanically stressful microenvironments. *(Adapted from Chen and Wang. Acta Mech Sin., 2019* [79]*.)*

3.2 Mechanotransduction in physiological processes

In the following section, I will briefly explain the role of mechanical forces in various cellular processes, thus, describing its ubiquity and indispensability.

3.2.1 Cell migration

Proper cell movement is a fundamental event in all physiological processes like morphogenesis, tissue regeneration and maintenance as well as immune response [87]. Aberrant cell motility is associated with many diseases like cancer and unregulated inflammation [87]. Moving cells constantly sense and adapt to mechanical cues from their surroundings [88]. They respond to tissue topography, confinement and also actively induce changes in the tissue and ECM structure during migration. These changes provide local directional and migration cues that guide the moving cell [89]. Helvert et.al., [90] in his review aptly describes the mechanoreciprocity between a moving cell and its environment (Fig. 3-2). Moving cells undergo changes in cell shape and also produce local deformations in the surrounding environment [91]. These local tissue deformations cause accumulation of mechanical stress that impedes cell movement. To ensure unimpeded movement, the cells must generate mechanical forces call traction forces that will overcome this resistance. The magnitude of driving and resistive forces depends on the mechanical properties of the moving cell and surrounding tissue environment. Depending on the physical cues moving cells alter their modes of migration [91]. Switching of migration modes depending on mechanical cues will be discussed in greater detail in the latter sections.

Mechanochemical feedback regulation of cellular migration has been found to play a significant role in cancer metastasis [92]. The tumour microenvironment is characterised by

inflammation, fibrosis, angiogenesis, cell proliferation and death [93]. There is extensive ECM remodelling induced by invading cancer cells like collagen deposition and crosslinking. The tumour milieu therefore, shows extensive tissue remodelling and increased tissue stiffness [94]. The tumour microenvironment is therefore a hotspot for mechanical stimuli originating from intercellular interactions or cell-ECM interaction, shear stress, interstitial hydrostatic pressure and membrane tension stemming from tumour cell contractility. The altered mechanical properties of the tumour microenvironment favour tumour cell survival, growth and migration by activating mechanoresponsive signalling pathways [94,95]. Metastatic tumour cells undergo epithelial to mesenchymal transitions, which is characterised by alterations in their cytoskeletal composition and organisation [96]. Structural transition of tumour cells produces a change in their mechanical properties which include changes in shape, cell contractility and amount of tension they exert on the ECM and other cells. These changes substantially enhance their invasive and migratory capacity [97]. Drugs that inhibit changes in the mechanical attributes of tumour progression are being explored to treat cancer. Ruxolitinib is an inhibitor of the JAK-STAT signalling pathway and has been shown to reduce tumour microenvironment stiffening by collagen deposition. Its currently under clinical trials to treat breast cancer and leukemia [98-100]. Drugs targeting ROCK [101] and FAK [102] that determine cell contractility and consequent cell motility resulting from stiffness are also being tried in combinatorial immunotherapy against cancer.

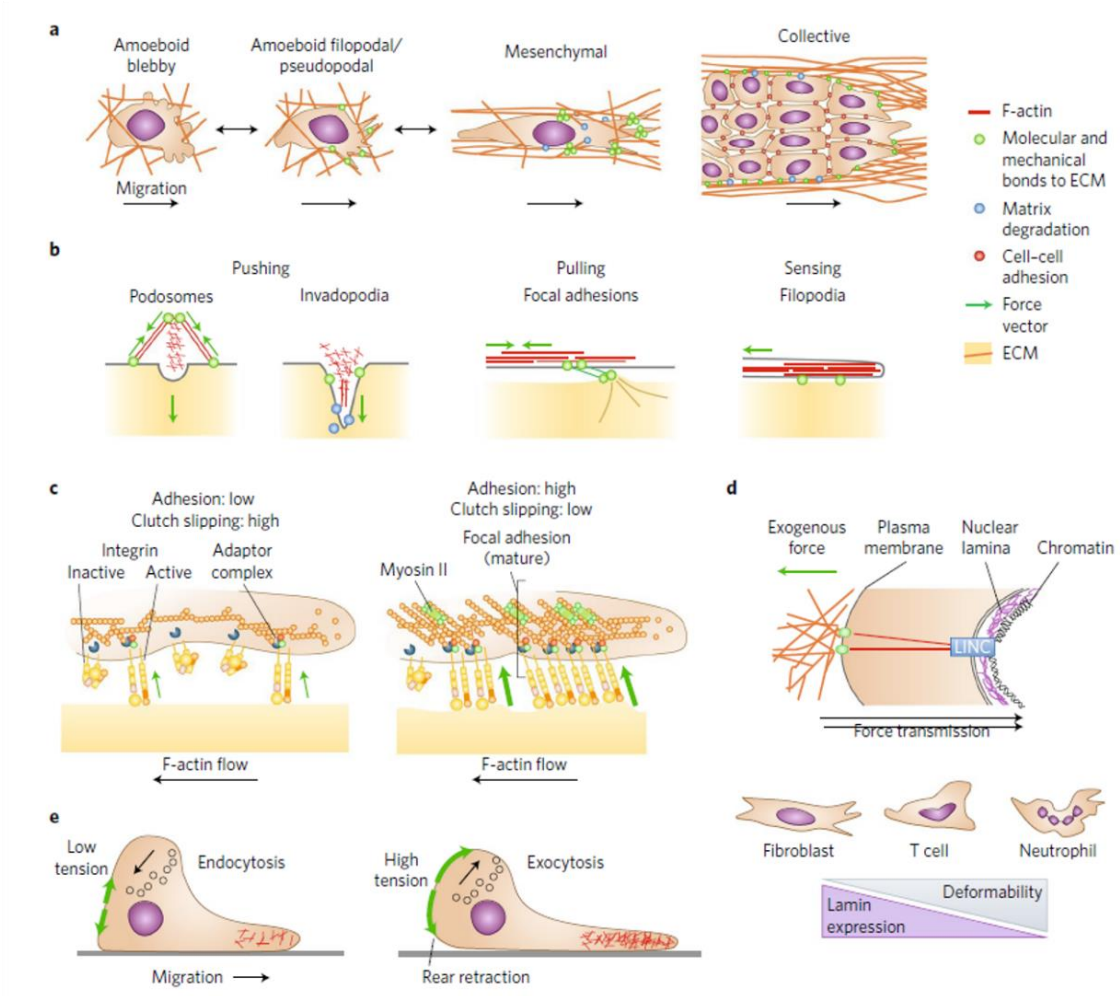

Figure 3-2. Mechanoregulation of cell migration. 3D cell migration involves either single cell or collective migration. Single cell migration may be divided into ameboid or membrane-bled based movement and filipodia or pseudopodia-based movement. Collective migration requires establishment of a leading cell that drives collective movement of the remaining population. This kind of migration is usually seen during development and morphogenesis (a). Cell movement requires formation of various actin-based membrane extensions including podosomes and invadopodia which apply pushing forces against the membrane. Focal adhesion-based extensions and filopodia generate pulling and traction forces against the substrate that helps cell propulsion (b). Adhesion-based migration requires force-driven strengthening of binding to the substrate which is generated from actin polymerisation and myosin-based contractions of actin fibres (c). Frontal or distal nuclear positioning is very essential during 3D migration of cells especially through tissue pores. The cell nucleus acts as a mechanical gauge and provides cues for guided migration along the path of least resistance

(d). F-actin polymerisation drives formation of cell leading edge. Tension build-up at the leading edge prevents further actin polymerisation and allows contraction at the trailing edge while balancing membrane components through the process of endocytosis/exocytosis. This allows propulsion of the cell in the forward direction (e). *(Adapted from Helvert et.al., Nat Cell Biol., 2018* [90]*.)*

3.2.2 Cell proliferation

Numerous studies have shown that substrate stiffness regulates the cell's capacity to proliferate. Using ECM protein-coated polyacrylamide hydrogels of varying stiffness, it was found that increasing substrate stiffness increases the proliferation rate of mesenchymal stem cells [103]. Constant replacement of dying differentiated cells in the epidermal cell layer necessitates these cells to have a high turnover rate. The basal stem/progenitor cell layer must achieve a proper balance between cell proliferation and differentiation so as to maintain homeostasis. In a study by Miroshnikova et.al. [104], the authors propose that dividing epithelial cells causes redistribution of local force generation patterns, that signals the cells to differentiate while stopping proliferation. A steady state epithelial cell monolayer corresponds to a 'solid-like jammed state'. Proliferation in this state causes 'over-crowding' and produces local cell deformation and consequent change in the local stress. This leads to reduction in cortical tension which weakens cell-substrate interaction, while increasing adhesion to neighbouring cells. These changes prompt the cells to undergo differentiation and detachment from the basal layer and movement to upper higher differentiated layers. This mechanism ensures regulation of proper cell density. Differentiated cells on having lost substrate contacts switches to E-cadherin-based adhesion and this restores the cortical

tension state of the cell. This ensures proper positioning of differentiated epithelia in the upper layers [104].

Maintaining constant cell density in epithelial barriers is essential because unchecked growth might lead to formation of tumours, while slow growth will destroy the integrity of the epithelial barrier. Studies have shown that mechanically-induced signalling pathways are triggered in response to cell density, that may promote differentiation or apoptosis on overcrowding [105]. Studies have shown that epithelial cell overcrowding changes cell geometry and consequent changes in the local stress patterns. Stress anisotropy thus induces mechanosensitive signalling pathways that promote cell extrusion and apoptosis [106]. Mechanosensitive YAP (Yes-associated protein)/TAZ (transcriptional coactivator with PDZ-binding motif) pathway has been shown to be induced in response to ECM stiffness and distortion in cell shape in mesenchymal stem cells and endothelial cells [107]. YAP/TAZ transcription factors sense cytoskeletal tension resulting from stress fibre formation due to interactions with a rigid ECM and distortions in cell shape.

Extensive studies have directly linked mechanical forces to mitotic capacity of cells. Assembly and orientation of mitotic spindle, segregation of daughter chromosomes and cytokinesis have been shown to be driven by physical forces [108]. Using micropatterned adhesive substrates, it was shown that the mitotic spindle assembly aligns with the mechanical force distribution exerted on the cell [109,110]. Orientation of the mitotic spindle determines symmetry and direction of cell division [110]. By analysing changes in cell shape in space and time, computational studies can predict patterns of force generation and subsequent cell division [111-114]. A study by Itabashi et.al. [115] showed that external application of force to dividing HeLa cells alters the force patterns within the mitotic spindle. Application of force to

metaphasic cells mounts tension in the mitotic spindles which accelerates progression to anaphase and facilitates chromosomal segregation. Reduction in spindle fibre tension causes failure of chromosomal segregation. Thus, local mechanical environment of the cell can produce significant effects on its proliferative fate. During the cytokinesis phase of cell division, there is formation of a contractile ring which causes localised ingression of the dividing cell along with the cell membrane of the adjoining cells. There is accumulation of non-muscle myoII contractile protein around the contracting region which mediates cytokinesis. Study by Pinheiro D. et.al. [116] found that generation of mechanical forces due to formation of this contractile ring regulates MyoII-mediated actomyosin dynamics and cytokinesis.

Studies have proposed that mechanical forces in the tissue environment might be one of the driving factors in cell competition, that is, expansion of a particular cell population at the expense of neighbouring cell populations [117]. This has important implications in cancer pathogenesis. Altered mechanical milieu in the tumour microenvironment has shown to activated mechanosensitive signalling pathways like the YAP/TAZ nuclear localisation and downstream signalling that promote cancer cell proliferation [118,119]. These findings provide strong validation for the role of physical cues in regulation of cell proliferation.

3.2.3 Chromatin regulation

Mechanotransduction has been shown to play a pivotal role in regulating gene expression [120]. Cells can undergo alterations in their transcriptional programming depending on surrounding mechanical cues. Nuclear mechanotransduction plays a significant role in regulation of transcriptional programming [121]. Mechanical cues sensed at the plasma membrane is propagated to the nucleus through various cellular components including the

cytoskeletal system and LINC (linkers of nucleoskeleton and cytoskeleton) complexes. Nesprin proteins form physical connections between the cytosolic cytoskeleton with nuclear proteins and have been shown to be crucial for nuclear mechanotransduction [122]. Application of localised forces using magnetic twisting cytometry has successfully induced expression of a GFP-tagged bacterial-chromosome dihydrofolate reductase (DHFR) transgene in cells [123]. Transcriptional upregulation strongly correlated with force-induced transcriptional upregulation. Disruption of the force-propagating actin cytoskeletal network abolished force-induced transcription activation. Mutations in the genes coding for nuclear lamina proteins like lamin A and C primarily affect tissues that subjected to active mechanical cues like the skeletal and cardiac muscles causing muscular dystrophy and cardiomyopathy [124,125]. This provides strong suggestions that these nuclear proteins are essential for mechanotransduction in these regions.

Mechanical forces alter chromatin organisation and also affects its epigenetic state through changes in the polymerisation state nuclear actin [126]. Nuclear actin polymerisation triggers recruitment of specific transcription factors into the nucleus, where they trigger transcription of specific gene modules. Fibroblasts cultured on substrates with symmetric geometries or anisotropic geometries show differential transcriptional patterns [127]. Cells grown on isotropic substrates upregulate expression of genes specific to cytoskeletal components and extracellular matrix components due to activation of the serum response factor (SRF) pathway. Cells grown on polarised substrates on the other hand show preferential expression of genes involved in cellular contacts and those involved in the cell cycle due to activation of the NFκB pathway. Altered substrate geometries provide distinct mechanical cues that triggers differential nuclear actomyosin dynamics and chromatin histone acetylation and subsequent recruitment of different transcription factors, myocardin-related transcription

factor (MRTF) and p65 transcription factors. Cell binding to anisotropic substrates will cause the cells to polarise and trigger mechanical force-induced actin polymerisation. F-actin formation will release MRTF bound to monomeric globular actin, and cause its subsequent import to the nucleus where it can bind to the SRF promoter and induce signalling. MRTF is a negative regulator of the NFκB pathway hence, the switch in transcriptional upregulation depending on substrate and cell geometry [127]. Force-driven actomyosin contractility also releases HDAC3 from the cytoplasm and enables its recruitment into the nucleus, where it alters chromatin organisation and transcriptional regulation [127]. Similarly, mechanotransduction through the YAP/TAZ pathway requires Rho-GTPase-mediated actomyosin reorganisation for its nuclear import [118].

In addition to mechanical force-driven transcription factor recruitment, studies have also found force-induced nuclear structure alterations can trigger transcription [128,129]. Altered chromatin organisation allows access to RNA polymerase II and other transcriptional regulators [128] as well as histone methylases/demethylases, acetylase/deacetylases that induce chromatin silencing/de-silencing [129]. Mechanical force has been shown to induce ATP-dependent heterochromatin formation in differentiated mesenchymal stem cells, which triggers localised gene silencing [130]. Progenitor epithelial stem cells show mechanical force-mediated induction of H3K27me3 characteristic of heterochromatin gene induction (Figure 3-3). Disruption of mechanoregulation through loss of mechanoresponsive elements – emerin, MyoIIA and actin results in abnormal differentiation and apoptosis [131,132]. Nuclear mechanotransduction not only regulates chromosomal organisation but also affects spatial clustering of genes which is essential for their activation [126]. Using chromatin conformation capture (3C) technique along with ChIP-seq analysis, it was observed that TNFα stimulation causes spatial clustering of responsive genes that facilitate their transcriptional regulation

[133]. Spatial reorientation allows co-regulation of genes involved in a specific pathway. Spatial and temporal gene clustering are driven by force-generating nuclear actomyosin dynamics [134].

Diseased phenotypes leading to modifications in mechanical cues can induce transcriptional reprogramming in cells, that could drive disease pathogenesis. Epithelial-to-mesenchymal transitions is characteristic of cancer and has been shown to be driven by dysregulated mechanochemical feedback in transcriptional machinery [135,136]. Force-driven alterations in chromatin organisation and its subsequent impact on global gene transcription has to be elucidated. But current data provides strong evidence that mechanical strain can trigger distinct transcriptional fates depending on their duration and context. Disruption in the mechanochemical feedback process can alter tissue homeostasis producing diseased phenotypes [137].

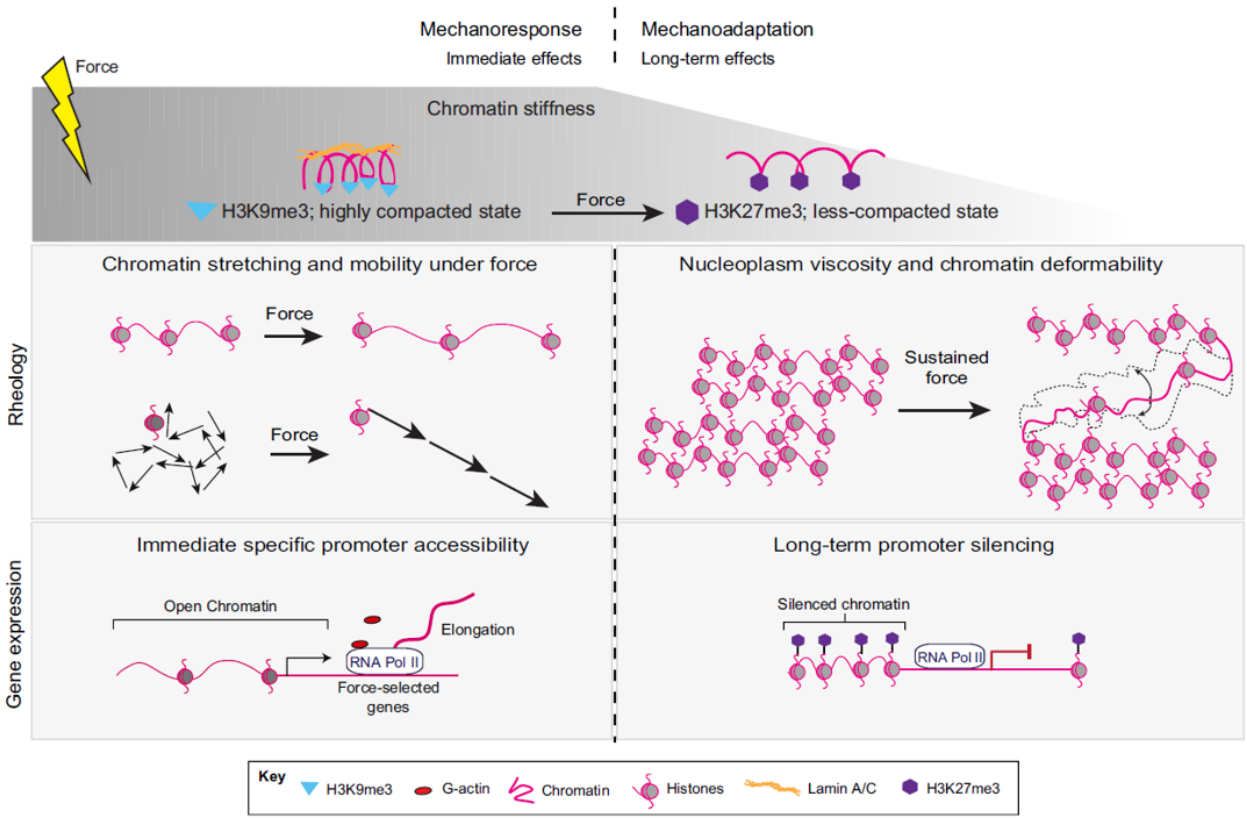

Figure 3-3. Mechanoregulation of chromatin architecture. High mechanical stress drives chromatin decondensation which is characterised by a transition of H3K9me3-tagged, nuclear-laminin-associated condensed chromatin, to H3K27me3-tagged decondensed chromatin. Chromatin decondensation allows absorption and dissipation of stress which results in increased chromatin accessibility to transcription-promoting factors. Prolonged mechanical stress, however, leads to chromatin deformation and global silencing. *(Adapted from Miroshnikova et.al. J Cell Sci., 2017* [131]*.)*

3.2.4 Cell differentiation and fate determination

Mechanical cues guide differentiation patterns of proliferating stem cells and also allow temporal and spatial regulation of fate specification [138]. Mesenchymal stem cells (MSC) can be effectively directed to differentiate into chondrocyte, neuroblast or osteoblasts by varying stiffness properties of substrates [139]. Soft substrates with stiffness ranging from 0.1-1kPa facilitate MSC differentiation to the neuroblast lineage. Substrates of moderate stiffness (20-25kPa) allow differentiation to chondrocyte fate and those of high stiffness (30-45kPa) allow MSC differentiation to the osteocyte fate. The stem cell microenvironment is replete with changing mechanical cues hence, the term 'mechano-niche' is used to describe it [140]. The stem cell mechano-niche is a dominant factor in the maintenance and differentiation of the stem cell population. Atomic force microscopy studies have been used to analyse the distinct mechanical states of differentiated and progenitor cells. MSCs tend to differentiate towards cell lineages whose mechanical attributes reflect those of the substrate on which they are growing [139,140]. Hence, softer substrates as those found in the brain microenvironment induce preferential commitment of MSCs to cells of the neurogenic lineage, while harder substrates like the bone or cartilage matrix favours differentiation towards the osteogenic or chondrocyte lineage [139,140]. Similarly, neural stem cell and progenitor differentiation to the

neuron versus astrocyte fate is also regulated by physical cues [141]. Softer substrates favour neuronal differentiation while stiffer substrates trigger formation of astrocytes [141,142]. Studies have shown that mechanical stretch significantly affects NPSC (neural progenitor stem cells) differentiation [143]. Development of the central nervous system is closely accompanied with mass cell movement and tissue structural remodelling, all of which act together to produce regional mechanical stress on NPSCs [143,144]. Application of external mechanical strain of physiological magnitudes to NPSCs, it was found that its differentiation to oligodendrocytes was significantly paired while neuronal or astrocyte differentiation remained unaffected [145]. This regulation is mediated through mechanosensitive interactions between α6 integrin with the ECM component laminin. This finding is particularly interesting because laminin is abundant in the developing brain and also in NPSCs-populated regions of the adult brain [145]. This ensures a sustained mechanotransduction signalling mechanism that regulates proper cell differentiation.

Pathological conditions that trigger modification of the mechanical milieu causes abnormal differentiation patterns [146]. Chronic inflammation is associated with numerous diseases like autoimmunity, cancer, impaired tissue restoration during wound healing [147]. One of the main attributes of chronic inflammation is fibrosis where there is overt deposition of ECM components [148,149]. This leads to extensive modifications of the ECM stiffness properties and tissue mechanics [148-150]. The corneal epithelial (CE) layer is maintained by constantly dividing corneal epithelial stem cells (CESCs). Chronic inflammation is associated with corneal squamous cell metaplasia (CSCM) where CESCs undergo keratinisation and adopt skin-like phenotype [151]. Study by Nowell CS et.al. [152] showed that altered mechanical microenvironment in chronic inflammation triggers aberrant mechanotransduction which activates YAP/TAZ-dependent β-catenin signalling pathway which causes ectopic epidermal

differentiation in the corneal surface. These studies therefore, provide ample evidence of how mechanotransduction is integral to cell differentiation and tissue homeostasis.

3.2.5 Development and morphogenesis

Cell fate determination during organogenesis is also regulated by mechanical forces [153]. Organ formation and maintenance not only requires cellular differentiation to the appropriate lineage but also proper positioning of differentiated cells to maintain organ integrity and function [154]. Formation of blastocyst during development of the mammalian embryo entails efficient sorting of cells into domains where they adopt specific fate [154]. A study showed Yap transcription factor-mediated mechanosensing plays a crucial in cellular positioning and fate determination during development of the mammalian embryo [155]. Cell-intrinsic forces stemming from cell-cell adhesive interactions, and actomyosin contractile network confer a certain degree of asymmetry to development of embryonic tissues [156]. Anisotropic biophysical forces regulate the crucial events of morphogenesis like epithelial invagination during gastrulation and differentiation of germ layers [156]. External mechanical cues also impact morphogenesis. Shear stress generated from fluid-filled tissue environment has been shown to determine polarity axis in mouse embryo [157]. The mouse embryo contains cilia on its ventral surface which undergoes rotational movement in a specific direction, that subsequently produces directional environmental fluid flow known as the nodal flow. Disrupting nodal flow hampers development of the polarity axis by interfering with gradient-dependent sonic hedgehog and retinoic acid-dependent signalling thus, alluding towards the importance of shear forces during development [157]. Interaction between embryonic cells and the components of the ECM also provide mechanical cues. ECM remodelling during morphogenesis provides altered biophysical cues depending on ECM stiffness, that are sensed

through fibronectin-integrin interaction rich-focal regions [158]. Germinal stratification entails epithelial cell stretching and division that generate tensile forces, which regulate tissue formation. Fetal haematopoiesis have been shown to be governed by shear forces originating from maternal blood circulation [159]. Shear forces regulate expression of RUNX1, the master regulator of fetal haematopoiesis. Formation of hematopoietic stem cells (HSCs) in one of the earliest regions of haematopoiesis, namely, the aorta-gonads-mesonephros (AGM) region have also been shown to be crucially dependent on blood flow through nitric oxide (NO)-dependent signalling [160]. In addition to driving haematopoiesis, shear stress also regulates formation and organisation of cardiac muscles during morphogenesis [161]. Bone formation is also regulated by hydrostatic forces along with cellular stress and strain [162-164]. Branching of vessels during endothelial angiogenesis can be manipulated by modifying membrane curvature, that is dependent on varying membrane stiffness through the course of embryonic development [165,166].

The above findings strongly suggest the significance of cellular intrinsic and extrinsic mechanical forces in embryonic development and fate mapping. Detailed mechanistic insights into the mechanotransductory pathways involved in tissue morphogenesis is however, needed so that mechanical properties of biological tissues and cellular interactions can be exploited in tissue regeneration and repair. Microfabrication techniques enable synthesis of artificial matrices of specific mechanical properties that can define stem cell fate and proper sorting during transplantation or tissue remodelling [167,168]. Diseased conditions like cancer and fibrosis that alter the biophysical properties of the tissue environment is associated with dysregulated cellular growth and tissue formation. Further elucidation of this complex mechanosensory network can aid in advancement of therapeutic and curative strategies [169].

3.4. Measuring mechanical properties and cellular forces

The domain of mechanobiology employs a wide range of techniques that enable quantification of cellular or external forces as well as mechanical properties of cells and their surroundings [170]. As Cusachs et.al. [171] rightly pointed out, direct measurement of mechanical forces is not feasible, rather force measurement can be derived from other measurable parameters that are affected by mechanical force. Consequently, modern techniques that quantify forces generally measure other force-associated mechanical quantities and extrapolate the data to obtain force measurements [171]. As previously discussed, cells have the machinery to generate mechanical forces during various processes [82]. Cellular force quantification methods can be broadly classified into two categories based on the underlying assumptions about the mechanical properties of the interacting substrate. Under these categories, they can be further distinguished based on the usage of external manipulations during measurement [171]. These techniques, in addition to quantifying cell-generated forces can also measure the biophysical properties like cell/tissue stiffness, cellular stress or strain, viscosity, elasticity, tension, etc (Box 1).

Traction force microscopy (TFM): Cells exert force against their local surroundings. These cell-generated traction forces originate from contractile actomyosin networks and are transmitted to the extracellular environment through cell-ECM adhesion interactions [172]. These forces are hard to quantify since their magnitude and the distance across which they act are small, typically in the range of nN to pN [172]. Culturing cells on soft synthetic matrices that are linearly elastic and isotropic allows measurement of its traction force-induced uniform deformation. Cellular traction forces can be resolved into two components: one which acts parallel to the surface of the substrate or in-plane tractions, and one which acts

normally to the substrate [172]. These forces can be quantified using 2D and 3D TFM methods respectively. TFM calculates stress maps of the cell surface by quantifying force-induced substrate deformation. Synthetic matrices like polyacrylamide, polydimethoxysilane (PDMS) [173] are generally embedded with uniformly distributed fluorescent particles less than 1µm in size. These particles can be tracked in space and time with the help of imaging techniques. Positions of these particles in substrates in the presence and absence of cell attachment can be used to measuring particle displacement which can be subsequently used to quantify traction force resulting in substrate deformation. Since particle size is much smaller than cell size, traction force maps can show subcellular origin of forces (Fig. 3-4-A). They have been crucial in defining activity of mechanical forces in cellular events like migration, adhesion, proliferation [173], etc.

Recent study by Uroz et.al. [174], showed the involvement of cellular traction forces during migration and cytokinesis in zebrafish cardiomyocytes. Zebrafish cardiomyocytes shows tremendous regeneration capacity involved in tissue repair [175]. They exhibit the unique property of collective migration which is strongly regulated by mechanical forces [175]. Myocardial cells were cultured on collagen-coated polyacrylamide (PA) gels of stiffness around 14kPa which closely mimics heart tissue stiffness [174]. 200nm-sized fluorescent beads were embedded in the PA gels. TFM revealed higher traction forces was exerted against the substrate at the leading edge of migrating cells. Force generation precisely localised with myosin stress fibre formation at the leading edge. These forces showed tangential orientation with respect the substrate. The study further revealed that cells migrate in a monolayer form where inward pulling forces generated by the leading cell is transmitted to the remaining following cells thereby resulting in collective movement [174].

It is crucial to critically consider mechanical parameters while adopting force-measuring techniques. This technique uses artificial substrates which are linearly elastic as well as isotropic (change in mechanical properties are uniform in all directions). So, deformation changes (strain) can be directly used to calculate cellular stress (force). This technique however, does not take substrate geometries into consideration because it assumes that substrate area is much larger than cell size [174]. The ECM, however comprises of a multitude of protein complexes whose mechanical properties are considerably different [176]. Moreover, mechanical properties are not uniform throughout the ECM, and traction forces generated by cells shows regional variations. Measuring traction forces on linearly elastic substrates also amounts to gross oversimplification, since many matrix fibrous proteins shows nonlinear elastic properties including anisotropism [177]. Physiological accuracy of traction force measurements on such synthetic matrices, thus, requires further validation [178]. 3D traction force measurements show remarkable differences with 2D measurements where studies have shown that substrate mechanical properties are actively modified by interacting cells [179-181]. These findings require further elucidation and fine-tuning before they can be accurately applied to physiological systems.

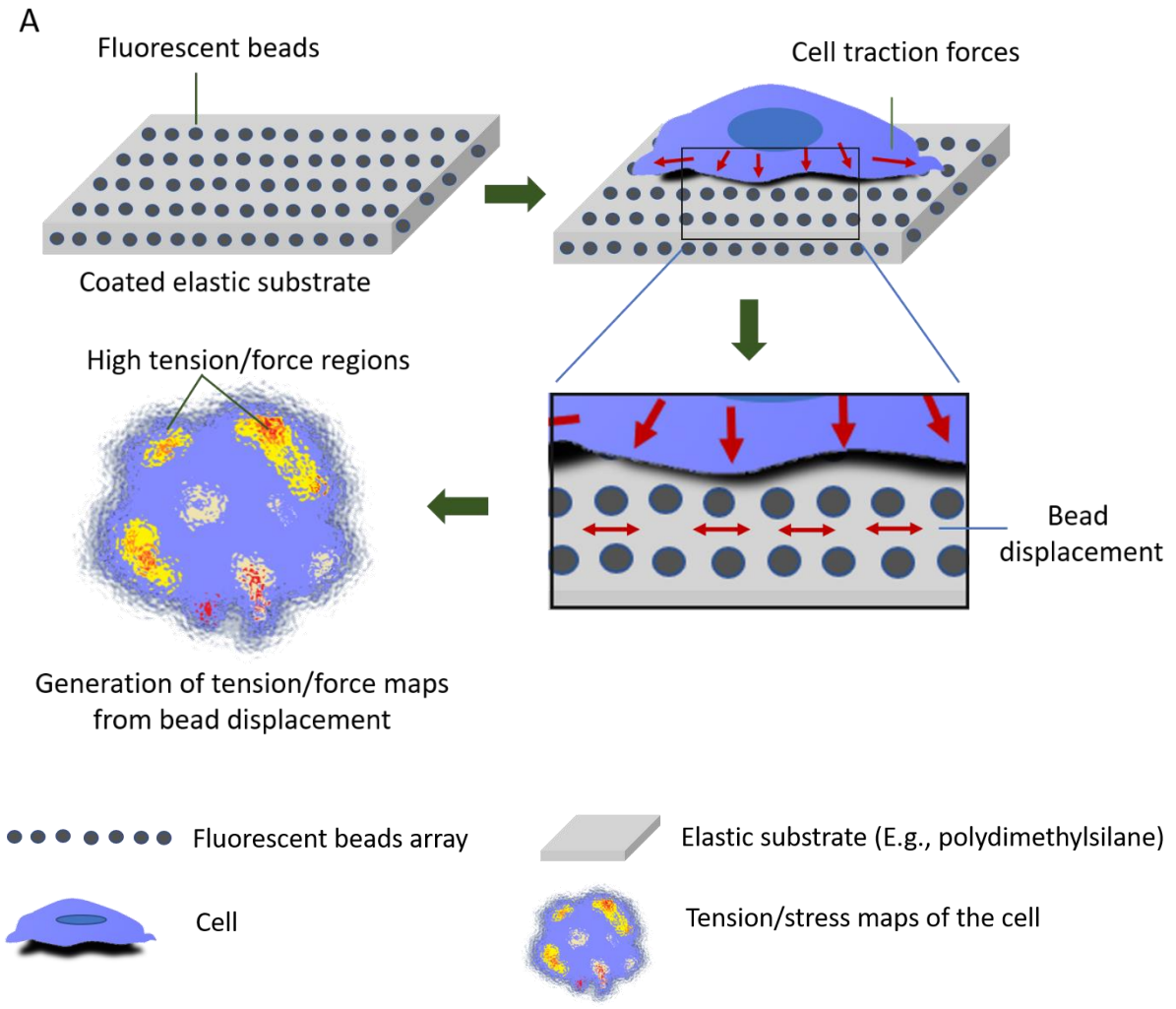

Figure 3-4-A. Traction force microscopy. Traction force microscopy is used to measure forces generated by moving cells or traction forces exerted during adhesion interactions. This technique involves using an elastic matrix embedded with an array of fluorescent particles. Forces exerted by the cell on the substrate will result in bead displacement which can be tracked over time. Displacement-time curve of the beads and the Young's modulus (indicator of substrate elasticity) of the matrix can be used to calculate force exerted by the cells. This can be represented in the form of stress/tension maps that can define force gradients in specific regions of the cells.

Cantilever-based contact measurements: Using an elastic probe (cantilever) of defined stiffness, one can apply defined external pulling or pushing forces to the to the cell, which can help quantify the mechanical behaviour of the cells like its stiffness and membrane tension, etc [182,183]. Typically, the cantilever probe is allowed to make contact with the substrate/cell of interest at constant low forces (in the range of >100pN) [182,183]. Force-associated interactions between the probe and cell/substrate will cause deflection or bending of the cantilever, that can be quantified through optical imaging. Atomic force microscopy allows measurement of spatially localised mechanical interactions. The cantilever-attached AFM tip is of <10nm radius which allows spatially precise contact with cell or substrate of interest [182,183]. The position of the cantilever probe can be accurately manoeuvred using a piezo-electric stage. Forces generated on contact with the cell or substrate produce cantilever deflection which is quantified in terms of position of laser reflecting off the cantilever detected by a photodiode [182,183] (Fig. 3-4-B). AFM techniques allows real-time measurement of force dynamics in cells. This form of AFM imaging is known as the contact-mode force measurements [182]. In the 'tapping mode' [182] of AFM, the cantilever probe is made to vibrate at a particular frequency. When the probe makes contact with the cell or substrate, its oscillation amplitude and hence, frequency changes depending on forces generated during interaction [182].

AFM can also be used to measure mechanical properties like stiffness [184]. The AFM probe is used to apply defined pN forces to the sample, which produces deformations during which the cantilever experiences force-dependent bending or displacement [184]. The AFM tip is gradually brought close to the sample of interest during which it experiences zero force since its distance from the biological sample is large. This phase is known as 'approach' and is observed as a flat line in the force curve map (force versus displacement curve). As the probe

approaches closer to the sample, it begins to experience attractive forces. The probe is said to have achieved contact with the sample when first repulsive forces in the form of positive cantilever deflection is observed. During the ramp phase, the probe is made to gradually approach deeper into the substrate till it reaches maximum force following which its withdrawn. Cantilever displacement as a result of cellular forces during this process is measured and is used to obtain force maps. Force maps are then used to calculate force generation using known cantilever stiffness. The shape of force curve during ramp phase and retraction phase can help determine the mechanical behaviour of cellular and/or substrate interactions [182,183].

The AFM tip can also be coupled with specific molecules or antibodies that interact with specific proteins on the cell surface [185]. Using a similar strategy of approach, ramp and retraction, the mechanical nature of surface protein interactions can be quantified. Thus, AFM-based techniques can be used to study mechanical behaviour of cells and tissues including cellular and molecular interactions in their environment.

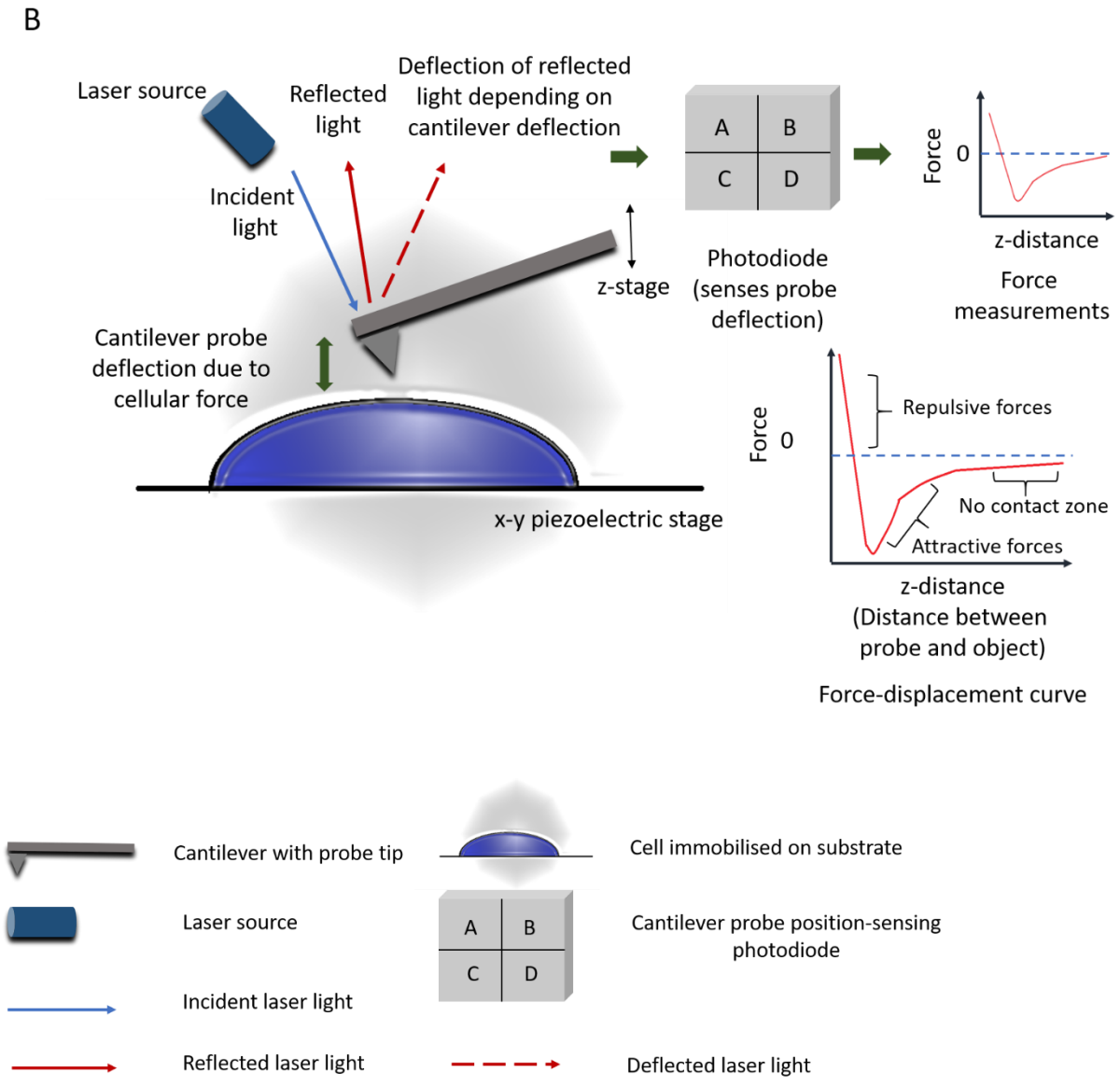

Figure 3-4-B. Atomic force microscopy. Atomic force microscopy can be used to measure forces at the single cell/molecule level. The set-up consists of a cantilever attached to a probe at its end. The probe can be coated with specific ligands. Ligand-coated probe is brought close to a cell bearing specific receptor and contact between ligand and receptor is established with minimal force. The cantilever is then subjected incident to laser beams. Light that reflects off the cantilever is detected by a photodiode which calculates the cantilever position. If ligand-receptor interaction is characterised by generation of additional forces, this will produce deflections in cantilever position and consequently deflections in reflected laser which can be detected by the photodiode sensor. The amount of force generated and the nature of force

are determined by force-displacement curves. The cantilever position is predetermined and fixed using xyz piezoelectric stage.

Molecular sensors: A wide range of force quantifying techniques rely on the use of molecular sensors like fluorescence-based tension linkers to quantify forces during cellular interactions [(186)]. Force-sensitive molecular sensors of predefined tension values can be used to quantify forces generated during molecular interactions. The mechanical properties of these sensors are initially calibrated by using single molecular force spectroscopy techniques. The sensors are then subsequently attached to protein/molecule whose force-dependent interactions are to be analysed. These methods typically use fluorescent probes attached to force sensors and relative changes in fluorescence, due to structural changes in the probe-attached sensors during the course of mechanical interaction enable measurement of mechanical forces [(187)].

Measuring tension during mechanical interactions between cell surface bound proteins can be measured using tension gauge tethers (TGT) [(188)]. TGT consists of a flexible biopolymer chain (tether) that is immobilised on the cell surface/artificial substrate and a covalently bound ligand molecule on one end that can interact with protein of interest on a neighbouring cell. The tethers are designed with defined tension values which allows them to withstand mechanical tension till it reaches a rupturing critical force value known as tension tolerance (T_{tol}). Briefly, surface/cell-anchored mechanical tethers of varying T_{tol} values are allowed to interact with specific cell surface-bound molecule of interest. If the tension generated across the ligand-receptor interaction is lower that tether-specific T_{tol} value, the tether will remain intact and consequently signalling downstream of ligand-receptor interaction will be maintained. If mechanical tension across membrane interaction increases beyond the critical force value (T_{tol}), the tether will rupture and downstream signalling will be impaired. Using

mechanical tethers of serially increasing T_{tol} values, one can determine the range of tension generated across interacting membranes as the highest critical force that it can endure without rupturing [188]. TGTs can analyse force kinetics at the single molecular level and measurement is independent on ligand/receptor densities. Double stranded DNA molecule is frequently used as tethers in TGTs. A 21 bp DNA double stranded helix has been shown to undergo unwinding or rupturing at critical force of about 12pN [188]. This value can be modified by applying forces at different regions of the DNA molecule. Tension generated across integrin-ECM interaction was studied using TGTs [189,190]. Briefly, DNA tethers covalently bound to integrin-binding peptide molecule was immobilised on a surface through biotin-streptavidin interactions. Ligand bound tethers with increasing T_{tol} values were used. Cells were then seeded on tether-coated plates and cell adhesion was quantified. Cell adhesion was dramatically diminished on plates coated with tethers of T_{tol} values of 33pN and below. Cell adhesion was significant on plates coated with tethers of T_{tol} values of 43pN, mostly remaining constant above this value thus quantifying that tension generated across ECM-ligand bond lies in the range of 40pN [190,191].

Many TGTs also employ the use of easy-to-detect fluorescent signals during measurement of membrane tension [192] (Fig. 3-4-C). The DNA molecule to be used as a tension probe is structurally modified to consist of surface anchor region on one end and a ligand bound region on the other end. The two regions are linked with a short double stranded hairpin region that can undergo tension-dependent unfolding. The surface-anchored strand is end-coupled with a fluorophore probe and the ligand-bound strand on the other end is coupled with a quencher probe. In a relaxed DNA tether, the fluorophore-bound end and the ligand-bound end are in close proximity with each other resulting in reduced fluorescence due to FRET. If tension is generated on ligand-receptor binding, the DNA tether will undergo tension-dependent

conformational change by unwinding and stretching of the DNA hairpin region. This increase the distance between fluorophore and quencher molecule that can be observed as increase in fluorescence intensity. By using DNA tethers of different GC content, lengths and hairpin size, one can modify the tension value at which it unfolds, thus enabling measurement of different membrane-associated molecular interactions [192]. Other molecular tethers based on biocompatible flexible biopolymers like polyethylene glycol (PEG) have also been used to measure tension and mechanical forces across membrane interactions [192].

C

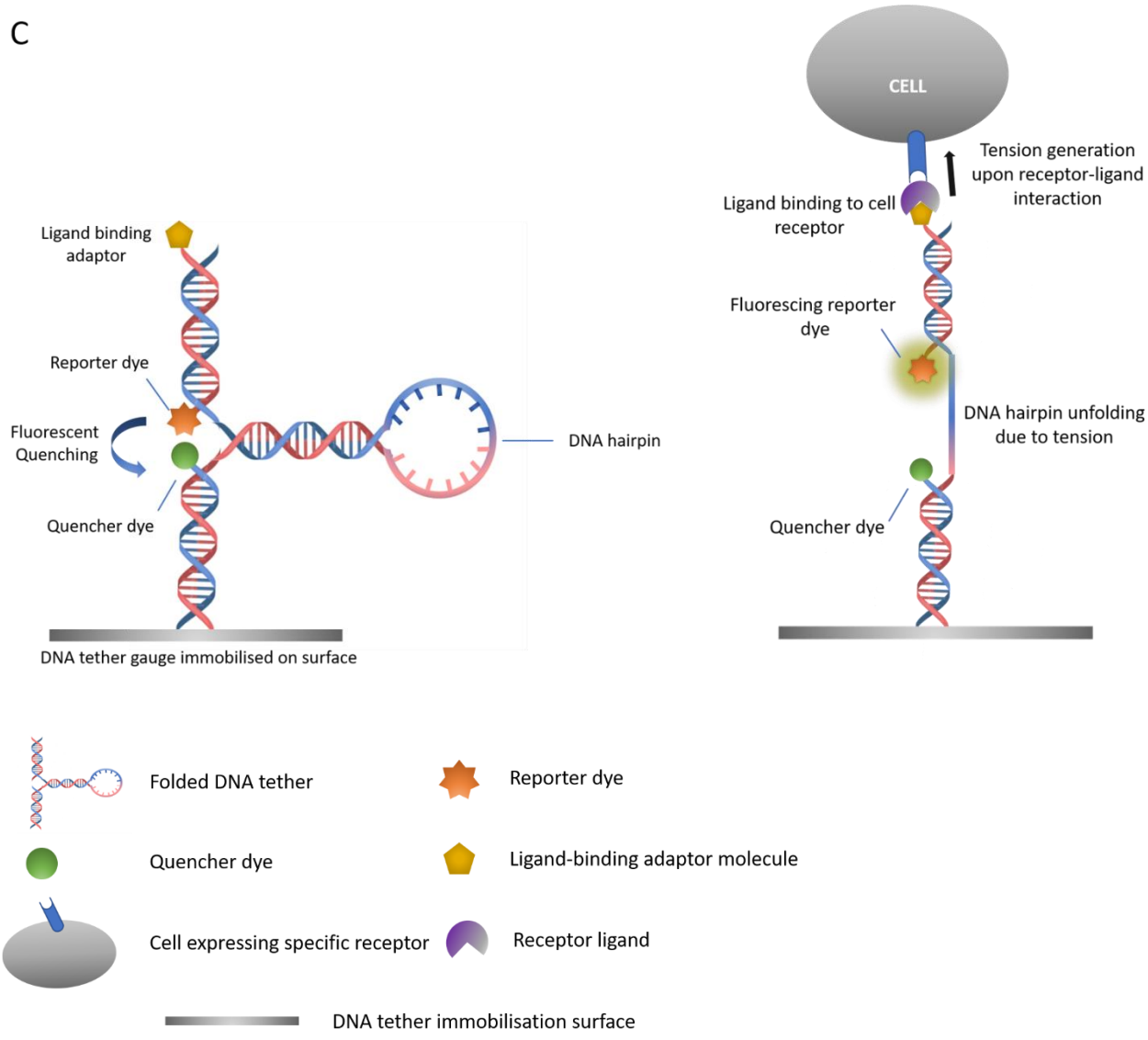

Figure 3-4-C. Tension-gauge DNA tethers. DNA tethers are molecular sensors and can be used to estimate force generation during single molecular interactions. Each DNA tether contains a hairpin region with attached reporter and quencher dyes. In its unfolded state, no fluorescence is observed because of close proximity between reporter and quencher dyes. DNA unfolding in response to force result in separation of the two dyes and increase in fluorescence. DNA tethers are synthesised as such that each of them has predefined unfolding tension values. The DNA unfolding tension value can be manipulated by regulating the length and nucleotide content of the hairpin region. Thus, by using DNA tethers of multiple tension values, one can examine a particular receptor-ligand interaction and estimate the amount of force generated at the single molecule level. One end of the DNA tension tether is anchored to a substrate. The other end is attached to an adaptor coated with ligand that facilitates receptor binding.

Micropipette aspiration technique: Use of micropipette aspiration technique dates back to 1970s, when it was developed to examine the mechanical properties of cells [(193)]. The technique studies cellular mechanical behaviour by measuring changes in cell shape in response to suction pressure [(193)]. The technique uses a glass micropipette that can be precisely positioned on the cell surface with the of micromanipulators to apply highly regulated suction pressure on the cell surface. The suction pressure is generated and regulated by controlling hydrostatic pressure originating from attached water reservoirs. An optical imaging system attached to the device that will enable observation and calculation of cellular deformation in response to suction pressure (Fig. 3-4-D). Cellular deformation depends on the cells mechanical properties including membrane elasticity, viscoelastic properties, cell stiffness, etc. Using this technique, it was found that neutrophils tend to show fluid-like properties while endothelial cells and chondrocytes tend to act as elastic solids [(194)]. It has been shown that HIV entry into cells is associated with dynamic changes in the membrane mechanical behaviour [(195)]. HIV entry into cell is facilitated by interaction between the viral envelope protein, gp41 and target receptors on T cells. Initial binding triggers a

conformation change in the glycoprotein which causes exposure of a fusion peptide (FP) and enables its insertion into the target T cell membrane. Micropipette aspiration studies have shown that insertion of HIV-specific FP into the T cell membrane reduces its membrane stiffness and enhances its stretching elasticity. This greatly facilitates HIV fusion and entry into target cells and thus, seems to be crucial for the process of HIV infection [195]. Micropipette aspiration was also used to apply a pulling force on drosophila embryonic cells to study cell fusion [196]. During cell fusion one cell partner extends membrane protrusions on the receiving cell partner which in turn accumulate myosin at the fusing synapse. Myosin recruitment at the synapse facilitates membrane fusion. Myosin was shown to have a mechanosensory role, and its accumulation was dependent on its ability to sense cortical tension and mechanical force. Micropipette aspiration of fusing cells measured increase in cortical tension of fusing cells which promoted fusion in drosophila embryos [196].

Micropipette aspiration systems are complicated, and requires acute precision in terms of size and geometry of the micropipette-suction end, since measurements thus obtained are critically dependent on those parameters [197]. Although this technique allows study of cell mechanics at the single cell level, the technique is time-consuming and consequent time-dependent variations in results may be observed. Researchers, therefore sought to develop systems that enabled simultaneous quantification for a large number of cells. So, they developed combined the basic principle of micropipette aspiration with microfluidics to develop a more high-throughput technology to this end [198]. Traditional glass micropipettes have been replaced with microfluidic channels composed of synthetic elastomers [198,199]. Microfluidic channels are constricted in size and their width varies along the length of the channel. They can also be constructed to form capillary networks through which cells are allowed to move and time taken for cells is used to calculate mechanical properties like

stiffness. Serial deformation of cells moving through differently constricted conduits allows robust measurement of the cells' mechanical behaviour under different conditions [198-200].

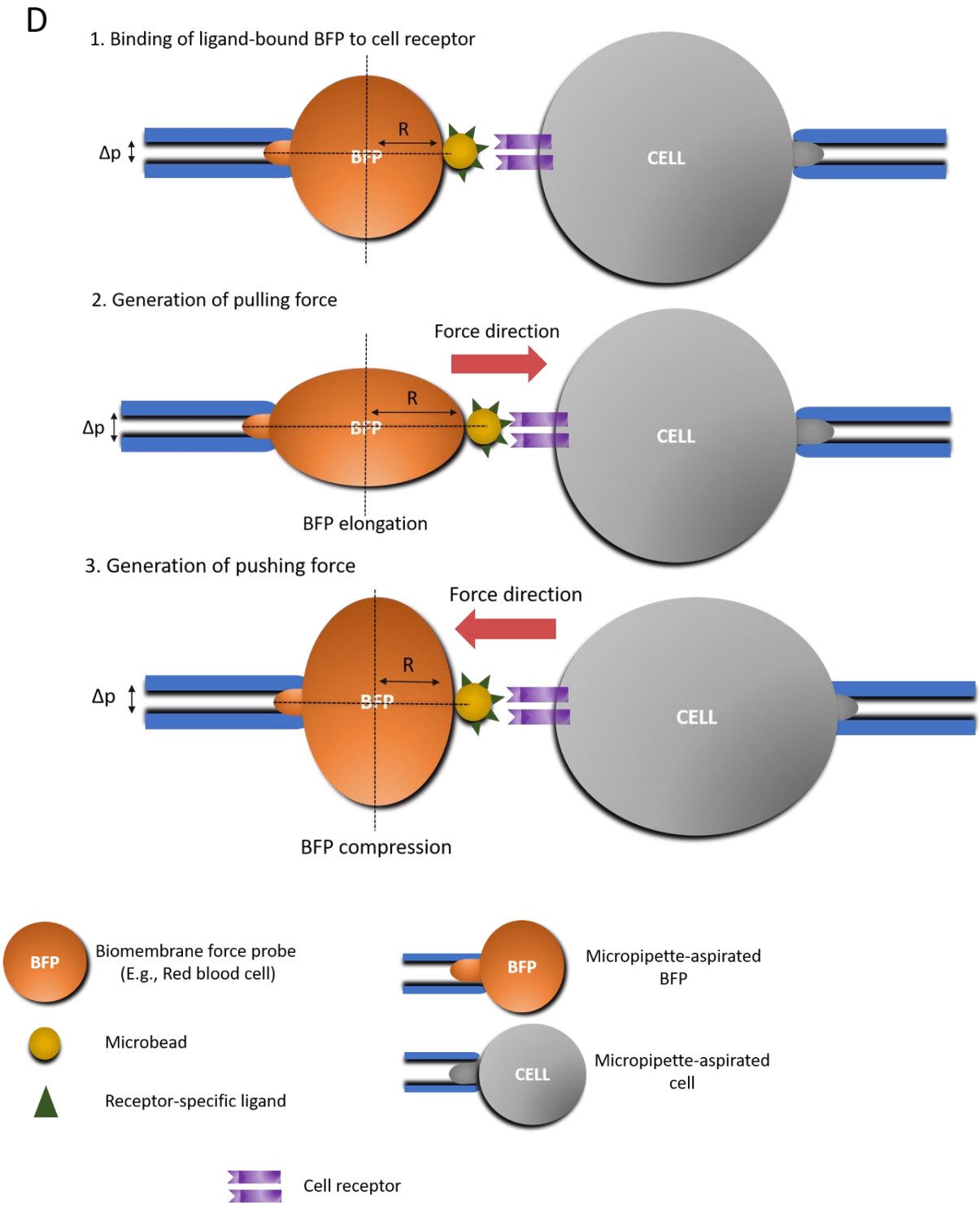

Figure 3-4-D. Micropipette aspiration technique. This technique requires an elastic biomembrane force probe (BFP) which is typically a red blood cell held in position with the

help of micropipette aspiration at a predefine pressure (Δp). The other end of the BFP is coupled to a bead coated with specific ligand. The cell to be probed is held in position with the help of micropipette aspiration. The cell expressing ligand-specific receptor is brought into close proximity with the ligand-attached BFP and contact is allowed to form. Changes in BFP shape (axial compression or elongation) will allow one to determine the nature and magnitude of forces generated during receptor-ligand interaction. The degree of RBC deformation is used to calculate force generated. Pulling forces exerted by the cell, will result in BFP elongation while pushing forces will cause the BFP to contract.

Optical trapping: This technique was developed by Arthur Ashkin in 1970 [201]. He proposed that light photons carry momentum, due to which focussed light can be used to apply piconewton range force to microparticles through momentum transfer. He observed that when microbeads are placed in the path of a highly focussed laser beam, the microbead showed linear movement at a constant acceleration. By using two opposing beams, he was able to capture or 'trap' the particle in the beam, thus creating an optical trap [201]. Any object subjected to a highly focussed laser experiences two opposing forces from scattered light known as scattering force, and from refracted light known as gradient force. Any object positioned in the centre of the optical trap is subjected to these two equal opposing forces which balances out thus, causing the net force on the object to amount to zero. Any external influence that causes the object to displace from the trap centre, triggers restoring forces to act on the object that attempt to push it back to the trap centre. Optically trapped beads coupled with ligands that bind to membrane-bound receptors can be made to interact with the cell surface. Any mechanical force generated during the course of interaction will cause displacement of the trapped bead from the trap centre. Displacement of the trapped bead will be proportional to the pulling force generated during ligand-receptor binding [201] (Fig. 4-E). This technique has been used to study the mechanical properties of cells like red blood

cells, synthetic lipid vesicles, mechanical force generation during surface receptor binding and adhesion [202]. Forces generated during fibronectin-integrin binding was quantified by using fibronectin-coated beads positioned precisely near the leading edge of a moving cell by means of an optical trap [203]. Pulling forces generated during movement produced bead displacement from the trap focus centre which was used to calculate mechanical force produced during cell movement. Similarly, mechanical behaviour of cells during movement or binding was analysed [203].

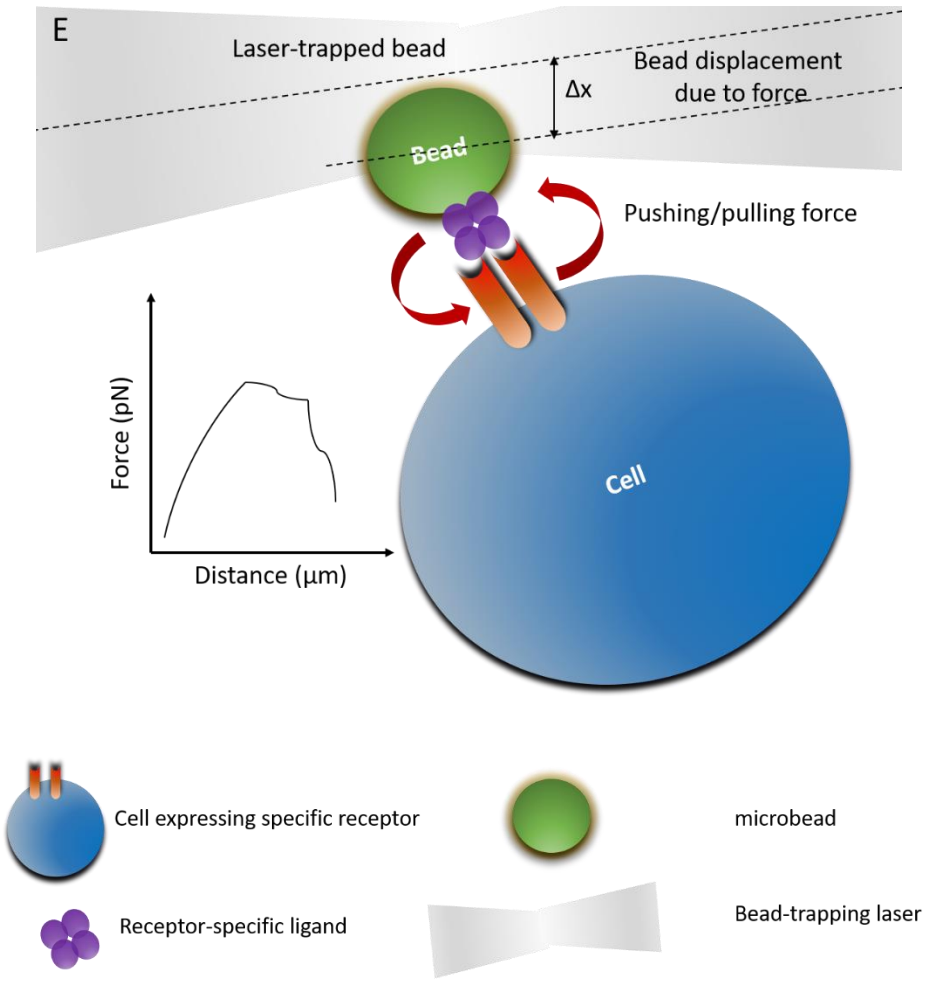

Figure 3-4-E. Optical Trapping. This technique also allows one to probe mechanical interactions at the single molecular level. A microbead (of predetermined stiffness) coated with specific ligands is placed under the control of focussed laser beams (laser trapping). Laser-trapped bead is allowed to make contact with cell expressing specific receptor. The

position of the bead is fixed with the help of laser trapping. Upon exposure to mechanical forces generated during receptor-ligand interaction, the bead undergoes displacement from its original position. This bead displacement is calculated with the help of sensors and is subsequently used to estimate the amount of force generated from the force-distance curve.

Measuring membrane fluctuations: Live cell membranes show continuous membrane fluctuations, which are observed as constant dynamic undulations on the surface [(204)]. These fluctuations are either thermal in origin (passive fluctuations) or actively generated through metabolic processes (active fluctuations) [(205)]. Extensive work has shown that the cell membrane and membranes enclosing cell organelles undergo continuous fluctuations that are affected by cellular processes like cell migration, cell adhesion and division [(204)]. Measuring frequency and amplitude of fluctuations will provide information about the mechanical properties of cells as well as their mechanical interactions with the surroundings. Studies have shown that membrane fluctuations are strongly affected by membrane rigidity or stiffness [(205)]. Measuring membrane fluctuations can be particularly challenging because membrane displacements in the undulations are very small and extremely fast. Moreover, any invasive technique that requires physical probing of the cell is not feasible since membrane fluctuations are acutely sensitive to minute external forces [(206)]. A number of techniques have been developed for imaging and quantification of membrane fluctuations. One of the earliest techniques used was flicker spectroscopy (FS) [(206)] in which time-dependent phase contrast images of the membrane was obtained where fluctuations were observed as cell thickness-dependent variations in intensity. Phase contrast due to intensity variations was linearly dependent on cell thickness variations due to membrane fluctuations. The RBC membrane mechanics was first probed using this technique [(207)]. ATP-dependent RBC membrane fluctuations or 'RBC flickering' was discovered using this technique. Membrane bending

modulus or rigidity or membrane curvature during cellular interaction and movement showed strong inter-dependence with membrane fluctuations. Limitations such as low intensity difference between membrane edge and surroundings, and camera specifications-limited time and spatial resolution could complicate precise and localised membrane measurements. Dynamic optical displacement spectroscopy overcomes some of the FS-associated limitations [208]. It exploits the basics of fluorescence correlation spectroscopy in which detection of membrane fluctuations is limited to a small detection volume. The membrane under study is loaded with a fluorescent dye, and changes in fluorescent intensity as a result of membrane fluctuations in the detection volume are measured. Since intensity changes are recorded for a highly diminished localised region of the membrane, membrane curvature and consequent fluorescence variations in this region is negligible and intensity variations will be linearly dependent on membrane displacement due to fluctuations [208]. This technique has higher spatiotemporal resolution and can be used to probe localised regions of the membrane. This technique has been adopted to measure membrane fluctuations and mechanical properties of the leading lamellipodium during cell movement. Fluctuation spectroscopy has also been used in combination with optical tweezers [209]. A low power laser beam is applied to the cell surface ensuring no external force is applied in the process, which may affect fluctuation frequency. Fluctuations will cause membrane displacement-dependent light scattering off the cell surface, that can be subsequently detected and quantified by photodetectors. This technique enables measurement over a larger cell area. Techniques that exploit the interference property of reflected light have also been used to quantify fluctuations [210]. When substrate-adhered cells are subjected to incident light, light reflected off the substrate and that off the cell base create a reflection interference pattern that is determined by the distance between cell base and substrate/surface. This distance is highly variable depending

on the fluctuating membrane. Fluctuating membrane height is observed as time-dependent variations in intensity. Reflection interference contrast microscopy [210,211] (RICM) requires prior calibration with media of specified volume and substrates in order to determine refractive indices and depth using which intensities can be obtained from membrane height [210-212]. One of the major limitations of RICM is that it requires cell contact with the substrate, which makes analysis of suspension cells difficult. Moreover, mechanical behaviour of cells can be significantly modified depending on substrate/surface physical properties [214]. Fluorescence interference contrast microscopy (FLIC) is based on similar principle except that it measures variations in fluorescence intensity emanated from membrane bound probes to measure cell membrane-surface height [213]. Other interference-based techniques that can be used to ascertain membrane mechanical dynamics include diffraction phase microscopy (DPM) which measures phase shift as a result of fluctuating membrane [215]. Studies have shown that membrane properties like membrane tension can reciprocally influence membrane fluctuations [216,217]. Contractile forces generated from actin-myosin activity also influences membrane fluctuations [218]. Hence, measurement of membrane fluctuations can yield useful information about membrane mechanics.

Box 1. Mechanical properties of cells

The mechanical properties of any cell/substrate can be described in terms of their ability to deform under mechanical force. The following parameters can be used to describe the mechanical behaviour of cells and their surroundings:

Tension: It is used to describe outward-stretching forces.

Compression: It is used to describe inward-directed forces.

Stress: This can be used to describe the effect of deformation-producing force per unit area of force applied. Its unit is pascals or Nm^{-2}.

Strain: It is used to describe the deformation produced in terms of relative change in length, area or volume on application of stress.

Shear Stress: It is calculated as force applied parallelly to the object per unit area.

Shear Strain: Strain produced as a result of shear stress.

Elasticity: It is calculated in terms of the Young's modulus (E) which characterises the relationship between applied stress and resultant strain. In linear materials the strain produced is directly proportional to the applied stress. Hence, E is constant for a specific type of material. In non-linear materials, however E is dependent on the amplitude of strain. This parameter essentially defines the ability of materials to undergo deformation under the influence of force and the capacity to revert to its original form in the absence of force.

Stiffness: It is used to define the resistance of a solid body to deformation in response to force.

Viscosity: It is used to describe a fluid's resistance to deformation/flow as a result of shear stress.

3.5. Mechanical forces in the immune system

Immune cell functions have been shown to be critically regulated by mechanical forces [219]. A triggered immune response to any pathogenic or non-pathogenic insult requires immune cells to be subjected to diverse mechanical cues during the course of immune reaction [219,220]. An effective response involves recruitment of innate immune cells like neutrophils, monocytes and dendritic cells to the site of insult. The latter stages of immune response include the active participation of the adaptive arm of immunity, that requires migration of T and B lymphocytes to peripheral lymphoid organs where they are activated to develop long-term immunological memory. These events require immune cells traversing through extensive tissue barriers with varying mechanical properties that affect their function [220]. The physical properties of these tissues change during the course of inflammation and pathogenesis [221]. Interacting immune cell partners also undergo mechanical force-dependent regulation of function and phenotype [219,220]. Mechano-regulation of the immune response can broadly be categorised into the following events:

Migration: Immune cells migrate from the circulating blood stream to peripheral tissues during inflammation, which involves a dramatic change in their mechanical environment [219]. Leukocyte extravasation occurs through post-capillary venules draining through the inflamed tissue. Trans-endothelial migration occurs through of series of events like tissue-rolling, adhesion and diapedesis. Upon chemotactic recruitment to the site of inflammation, leukocytes bind to selectin molecules on activated vascular endothelial cells (VEC) which enable leukocyte rolling and arrest. Leukocytes experience strong mechanical forces during the process [220] (Fig. 3-5-1). A leukocyte rolling along the blood vessel also experiences hydrodynamic shear forces due to circulating blood [221]. Shear forces acting in the direction

of blood flow guide the rolling leukocyte forward along the blood vessel. Leukocytes also experience a shear torque which exerts forces on the bonds between the leukocytes and VECs [223]. As cells move forward along the endothelium, forces exerted on the adhesion bonds to the endothelium increases causing them to ultimately rupture and release the leukocyte which enables the cell to roll in the direction of blood flow. The microvilli tips in the frontal end of the cells subsequently form adhesion bonds with the endothelium again which facilitate rolling forward followed by retraction of rear membrane tethers. Efficient movement along the blood vessel thus requires a temporal balance between hydrodynamic shear forces and torque, which regulate rear membrane bond dissociation and frontal microvilli formation [223]. Atomic force microscopy measurements have calculated that a tensile force of up to 165pN is experienced by P-selectin and P-selectin-glycoprotein-ligand-1 (PSGL-1) bond in rolling neutrophils [224]. Selectin-mediated adhesion in this scenario show characteristics of slip bonds which dissociate under influence of increasing force thus enabling guided movement. Transendothelial migration occurs through vascular endothelial junctions (paracellular) mostly and sometimes through individual endothelial cells (transcellular). Inflamed post-capillary venules show higher permeability to leukocytes because of loosened intercellular junctions [225]. Studies have shown that integrin-mediated binding of leukocytes to ICAM-1 expressing endothelial cells triggers downstream activation of the myosin light chain kinase and consequent heightened myosin-actin contractions [226]. Transendothelial diapedesis is characterised for formation of ICAM-1 clusters beneath the adhered leukocyte, which have been shown to anchor the adhered leukocyte. These ICAM-1-rich docking clusters are rich in actin and have been shown to generate contractile forces that open the endothelial junctions and physically pull the adhered leukocytes across the endothelium [227,228]. Moreover, 3D traction force microscopy results revealed that transmigrating leukocytes exert

strong traction forces against the VEC, which produces a local change in the endothelial layer tension that facilitates opens up the endothelial junctions, enabling transendothelial movement of leukocytes [229].

Studies have revealed that integrin-dependent 2D migration of immune cells is subjected to mechanical regulation. Migrating neutrophils and lymphocytes extend actin-rich frontal-end lamellipodia and rear-ended uropod [219]. Integrin adhesion at the leading lamellipodia triggers actin polymerisation, which exerts an inward pulling force on the integrin subunits and strengthens integrin binding by inducing a ligand binding favourable conformational change [219,230]. Strong integrin binding triggers rapid and extensive polymerisation at the leading edge, which applies force against the plasma membrane. Actin polymerisation-coupled with myosin II-based contractility produces retrograde flow of actin and forward cell propulsion [219,230]. Migration requires dynamic integrin binding and retrograde actin flow to allow movement. Depending on the mechanical properties of substrates, coupling between integrin binding a F-actin flow may vary causing the cells to switch from non-adhesion-based movement to adhesion-based movement [231]. Thus, integrins seem to serve as a mechanical force sensor, that guide immune cell migration and determine their modes of migration. Traction force microscopy have shown that immune cells adopt different mechanical modes of migration, with lymphocytes and neutrophils generating forces at the rear end of the cell, while macrophages and dendritic cells generating forces at the frontal end [219, 231]. Migrating immune cells maintain polarity that determine direction of movement. Polarity of migrating cells have also been shown to be regulated by cytoskeletal force-dependent changes in membrane mechanical tension [232].

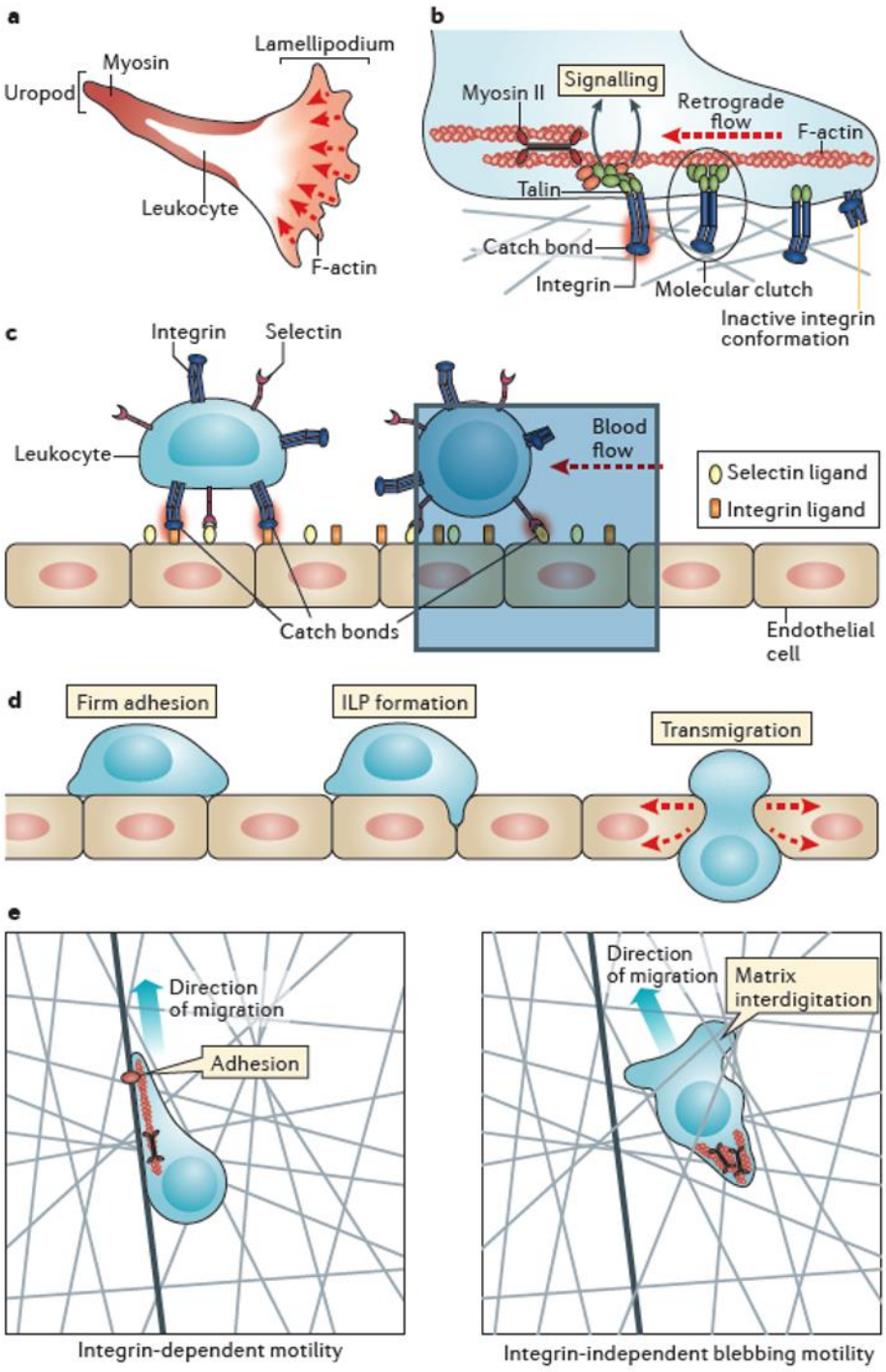

Figure 3-5-1. Mechanoregulation of immune cell migration. Immune cell migration is characterised by generation of cell polarity which includes formation of leading-edge membrane extensions called lamellipodia and trailing-end retracting uropod. These cytoplasmic-membrane extensions are generated due to actin polymerisation at the leading edge and its retrograde flow as a result of myosin contraction at the rear end (a). Immune

cell migration is also partly dependent on integrin-based adhesions with the tissue microenvironment. Integrin adhesion shows characteristics of catch bonds. It usually remains in an inactive conformation in unstimulated cells. Upon cell stimulation, there is cytoskeletal rearrangement which triggers integrin activation through inside-out signalling. Activated integrin binds to ECM components with much stronger affinity (b). Similarly, leukocyte rolling on the endothelial blood vessel requires firm but dynamic interactions that are mediated by integrin-selectin binding. Integrin binding in this context also shows greater affinity in the presence of shear stress produced by blood flow (c). Leukocyte diapedesis across the endothelial wall involves formation of membrane protrusions called invadosome-like protusion (ILPs). ILPs scan for specific regions of the endothelial layer and choose to transmigrate across regions which provide least resistive forces (d). Immune cells do not necessarily confine themselves to adhesion-based migration which requires formation of cytoskeletal-based membrane lamellipodia. They also adopt adhesion-independent mode of migration which is facilitated by membrane blebbing. *(Adapted from Huse M. Nat Rev Immunol. 2017 [(219)].)*

Immune cell function and cellular interactions: Immune cell effector response is triggered by interactions with other immune cells. This interaction is characterised by active changes in cell mechanics. Generation of mechanical forces at the cellular synapse and alterations in interacting membrane mechanical properties have been shown to govern effector responses [(233)].

Studies have shown that B cell maturation and antibody-mediated effector response requires efficient extraction of presented antigens from the surface of APCs [(234)]. Naïve B cells bind foreign antigens on APCs which triggers BCR clustering, synapse formation followed by rapid internalisation of antigens from the APC surface [(234)]. These internalised antigens are processed and presented by the B cells on their surface to T cells in germinal centres, where they go through essential processes like affinity maturation and class switching. Mounting

experimental evidence have shown that B cells tend to physically extract the APC surface-bound antigen by exerting substantial mechanical force on the synapse [234]. DNA-based molecular force sensors have shown that antigen extraction was crucially dependent on the substrate mechanical properties [235]. Follicular dendritic cells (FDCs) were found to be mechanically stiffer than other APCs and hence, presented a better surface for efficient antigen extraction by B cells [235,236]. Synthetic substrates that were stiffer allowed better force generation through myosin-mediated contractions at the synapse and hence, allowed better antigen extraction by B cells. Interestingly, substrate stiffness also regulates efficient antigen discrimination by B cells [237] (Fig. 3-5-2). Generation of antigen-specific high affinity antibodies requires B cell interaction with high affinity antigens presented on APCs. Only interactions between high affinity foreign antigens on APCs and BCR clusters on B cells enough generate contractile forces high enough to facilitate antigen extraction from the APC membrane, and subsequent internalisation by B cells. Thus, mechanical forces generated at B cell-APC synapse enables affinity-based screening of antigens and downstream clonal B cell effector response [237,238]. Origin of these contractile forces were found to be attributed to F-actin and myosin IIa foci generated at sites of antigen-BCR clusters [238].

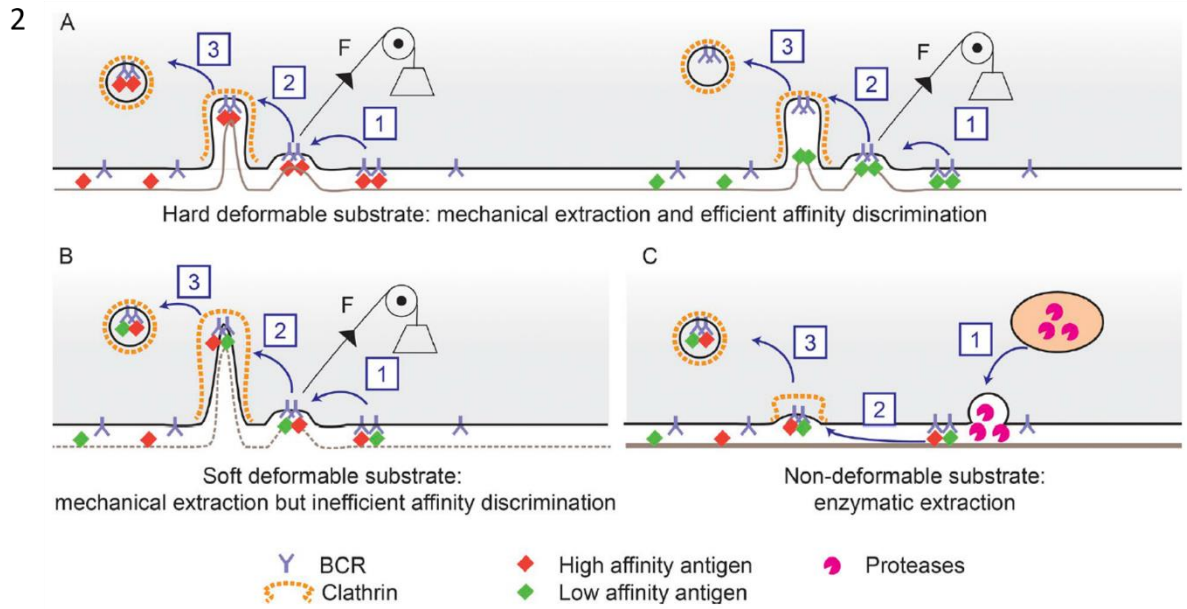

Figure 3-5-2. Mechanoregulation of B lymphocyte function. Mechanical tension facilitates antigen discrimination by B lymphocyte. Varying substrate stiffness provides altered mechanical cues for B cell antigen extraction. Upon antigen binding, B cell receptors (BCRs) form microclusters which are subjected to mechanical tension generated from myosin-mediated contractile forces on stiff but elastic substrates. High affinity antigen-BCR interactions survive external force and are successfully endocytosed (B Lymphocytes, A). Softer substrates do not exert considerable force. Hence, selection on the basis of antigen affinity is less rigorous (B Lymphocytes, B). On rigid substrates, antigen extraction and subsequent endocytosis is not driven by mechanical forces, but rather through enzymatic reactions (B Lymphocytes, C) *(Adapted from Pierobon et.al. J Cell Biol. 2017. [237])*

Similar observations were found when antigen presentation to T cells by DCs and B cells were studied. Single force spectroscopy measurements found that forces generated at T cell-DC synapse were higher as compared to T cell-B cell synapse, which could account for DCs greater capacity to activate T cells compared to B cells [233]. Forces generated at the T cell-DC synapse peaked at ≈1.5nN while those at T cell-B cell synapse plateaued at ≈0.3nN [239]. Using DCs that express range of peptides of varying affinities for transgenic TCRs expressed on $CD8^+$ T cells,

it was observed that only DCs expressing antigens of highest affinity produced forces on T cell contact that were sufficient to induce T cell activation [240]. Atomic force microscopy was used to determine affinity-dependent force generation between T cells and DCs loaded with varying peptides. DC properties have been shown to be modulated by application of external mechanical strain [241]. DCs subjected to a cyclic strain of a certain magnitude showed heightened expression of MHC II molecules and costimulatory molecules like CD86 and CD40 consistent with DC maturation. Moreover, mechanically strained DCs were more adept at allo-stimulation of T cells thus, confirming their mechanoresponsive property. It has been recently shown that DC activation is strongly correlated with tissue stiffness [242]. DCs grown on stiffer substrates show enhanced activation and metabolism favouring glycolytic pathways (Fig. 3-5-3). Bone-marrow derived DCs grown under high mechanical stress produce higher amounts of inflammatory cytokines and were more adept at priming anti-tumor response in mice.

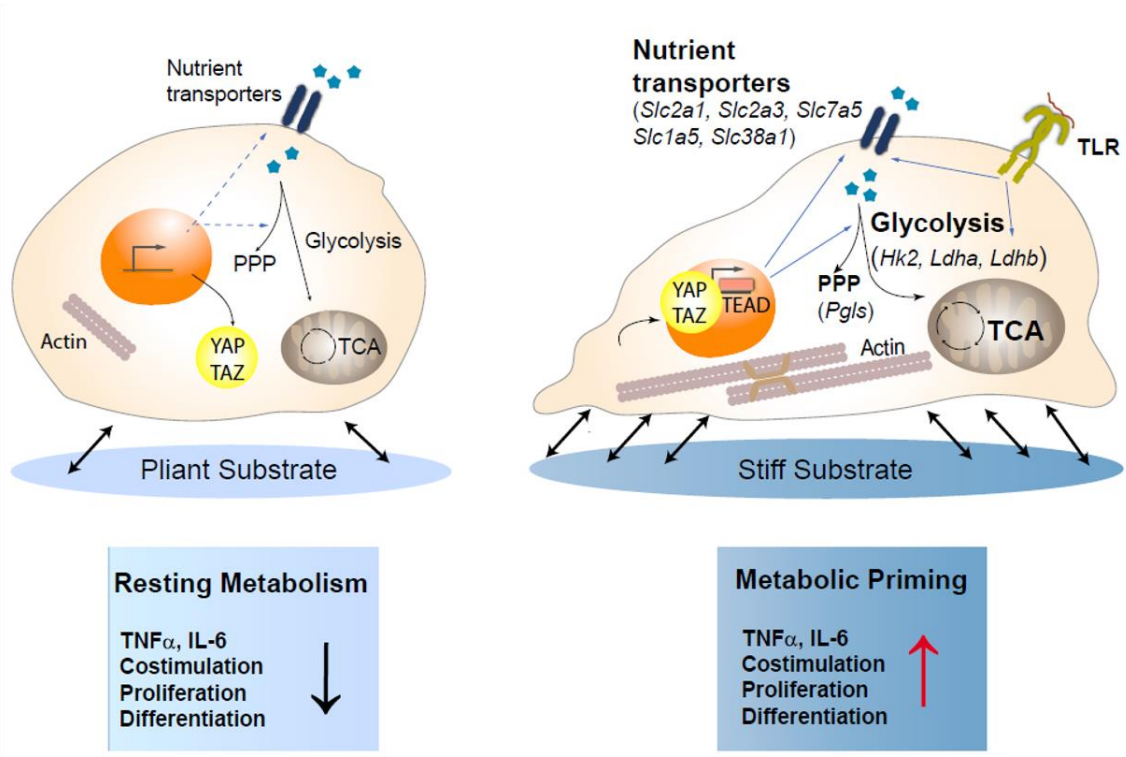

Figure 3-5-3. Mechanoregulation of dendritic cell function. Dendritic cells undergo enhanced metabolism in the presence of mechanical cues provided by stiffer substrates. Mechanical force drives upregulation of dendritic cell proinflammatory activity like secretion of IL-6 and TNFα. Dendritic cells undergo increased proliferation while preferentially switching to glucose-dependent metabolic pathways on stiffer tissue environments. Mechanotransduction in dendritic cells is mediated through YAP/TAZ transcriptional signalling. *(Adapted from Chakraborty et. al. Cel Rep. 2021 [242].)*

Tissue infiltrating monocytes and macrophages have been shown to exhibit a certain degree of mechanosensitivity in some studies (Fig. 3-5-4). Tissue infiltration of monocytes involves various degrees of monocyte mechanical deformation through attachments and movement through the extracellular matrix [243]. Studies have shown that tissue-infiltrating macrophages or monocytes show differential transcriptional upregulation when subjected to cyclical mechanical strain, which includes activation of tissue matrix metalloproteinases in the presence of phorbol myristate acetate [243]. Deformation triggered activation of early transcription factors like c-jun and c-fos as well as activation factors that induce monocyte differentiation [243]. Thus, environmental mechanical cues trigger transcriptional programming of monocytes that facilitate their tissue infiltrating capacity as well their differentiation. This finding had interesting implications in the study of the role of macrophages in atherosclerosis. Hypertension is one of the significant risk factors associated with atherosclerosis. Macrophages show active tissue infiltration and accumulation in coronary artery plaques [244]. A study has shown that macrophages are subjected to considerable mechanical strain in these hypertensive conditions which triggers expression of a particular scavenger receptor, cytokines and other ECM-degrading proteins that enhance tissue degradation, monocyte infiltration/differentiation, plaque formation and rupture

during atherogenesis [244]. Monocytes have also shown to be responsive to mechanical shear stress. Mechanical compression triggers them to adopt a more proinflammatory phenotype through differential regulation of nitric oxide synthase 2 (NOS 2) and IL12B-mediated signalling [245]. Another study shows cyclical force-mediated induction proinflammatory programming in monocytes occurs through activation of c-Jun and Endothelin 1 (EDN1), that trigger HIF1α-mediated downstream transcriptional reprogramming [246]. Pulmonary infections produce significant changes in the lungs' hydrostatic pressure. This triggers proinflammatory activity of monocytes and downstream neutrophil recruitment, thereby facilitating a robust immune response against invading pathogens [246]. Mechanosensitivity might also play a crucial role in the exacerbated activity of these cells in diseases, that involve active remodelling of the surrounding lung tissue environment like in pulmonary cystic fibrosis.

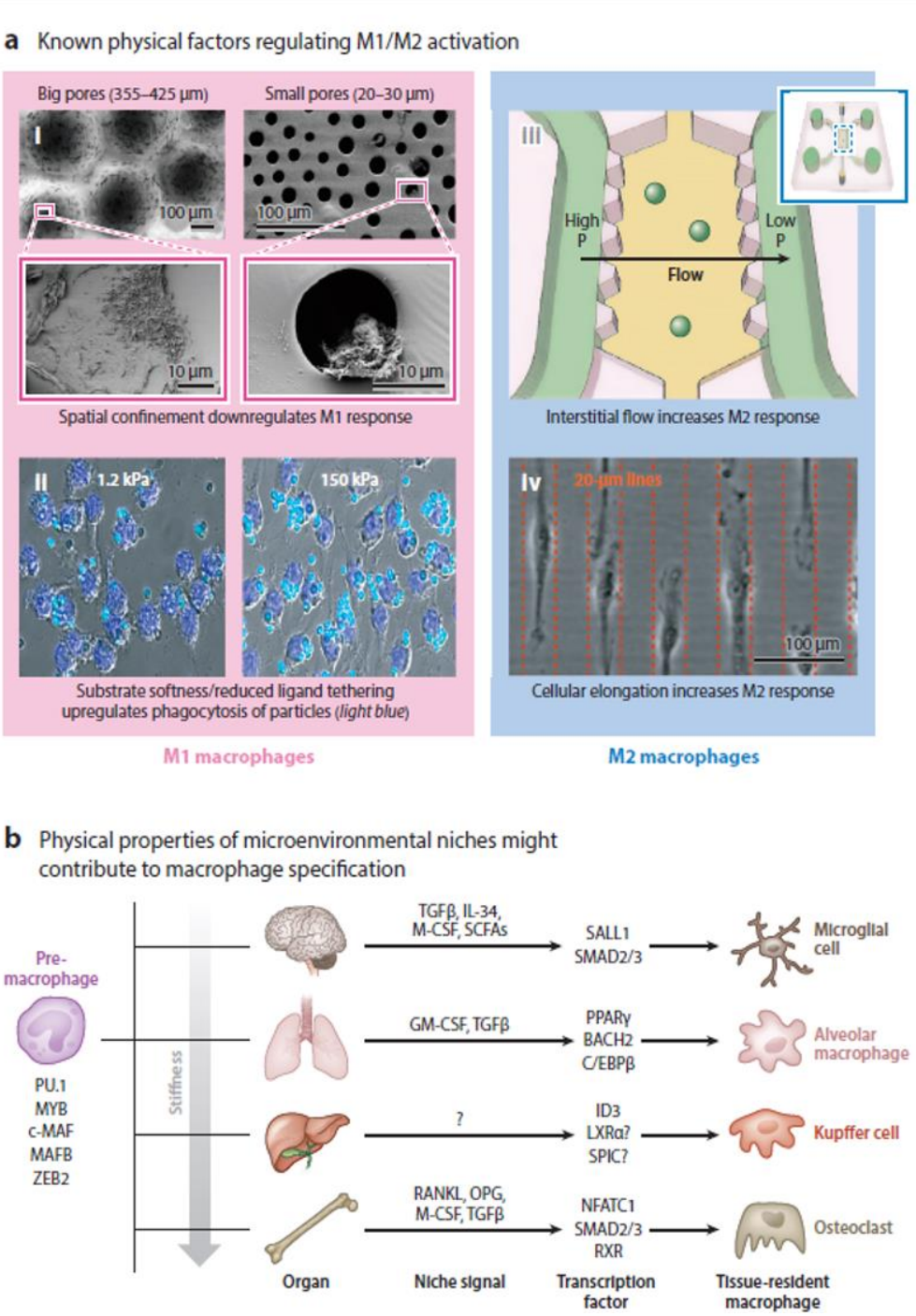

Figure 3-5-4. Mechanoregulation of macrophage function. Macrophage M1/M2 polarisation is regulated by physical properties of the environment. When cultured on substrates with smaller pore size, that provides spatially confined environment, macrophages preferentially adopt anti-inflammatory M2 phenotype. Shear stress and cell stretching, on the other hand, enhances proinflammatory M2 response of macrophages. Macrophages grown on less stiffer substrates also show enhanced phagocytic activity (a). Varying stiffness of different tissue

microenvironments provide altered mechanical cues which drive activation of alternate signalling pathways and consequent macrophage phenotype (b). *(Adapted from Jain et.al. Annu Rev Biomed Eng. 2019 [247].)*

Reports have also shown that neutrophil function is affected by biophysical cues. An effective and controlled neutrophil response requires active transitions between quiescent and active states, a process which is dependent on its ability to sensing mechanical signals [248]. It has been reported that neutrophil priming is dependent on mechanical perturbations in the cell during adhesion and extravasation, while constant physical cues tend to downregulate neutrophil activity so as to maintain homeostasis. This is crucial in order to achieve efficient neutrophil recruitment and function in damaged sites, while at the same time preventing exaggerated uncontrolled response [248].

Immune receptor activity: Numerous studies have shown that immune receptors like the T cell receptor, B cell receptor, innate immune receptors like Toll-like receptors and C-type Lectin receptors are responsive to mechanical cues.

B cell activation requires efficient recognition of antigens by the BCR. BCR recognition and downstream signalling is dependent of a number of antigenic parameters like antigen density, affinity as well as the mechanical stiffness of the antigen-presenting substrate [235,236]. Thus, BCRs actively tune their activation and response to both physical and chemical properties of the antigen. DNA-based tension guage tether techniques have shown that different BCRs show unique sensitivity to mechanical cues [249]. BCRs of the IgM type show acute sensitivity to a wide range of magnitude of mechanical forces while those of the IgG and IgE isotypes show a lower threshold force for their activation, thus enabling their rapid response to

antigenic cues. While lower forces ranging between 12-43pN triggered weak to moderate IgM activation, forces >50pN triggered strong IgM-BCR response. Low forces seem to act through integrin-mediated signalling, while high magnitude forces seemed to act through myosin IIA or focal adhesion kinase (FAK) -mediated downstream mechanism to tune B cell responses [249]. Lower mechanical force activation thresholds for IgE or IgG BCRs that are usually highly expressed on plasma cells or memory cells might account for their ability to respond rapidly to antigen recall stimulus. The varying threshold for force-based activation was attributed to levels of phosphatidylinositol (PI) (4,5)-biphosphate (PI(4,5)P2) in the cytoplasmic tails of BCRs [250]. The cytoplasmic tail of the IgG heavy chain is highly rich in PI(4,5)P2 which lowers mechanical force threshold of BCR activation. PI(4,5)P2 enriched microdomains may facilitate efficient BCR clustering in the immune synapse in response to low forces and also increase recruitment of PI(4,5)P2-binding signalling proteins. Altering PI(4,5)P2 content of the BCR cytoplasmic tail resulted in modification of threshold force sensitivity [250].

Immature DCs grown on synthetic substrates of varying stiffness show altered expression of C-type lectin receptors which result in their altered ability to internalise antigens and differentiate into mature phenotypes [251]. Substrate stiffness also affects integrin-mediate adhesive behaviour of DCs and CCR7-dependent motility [251]. A recent study has delved into the role of mechanical forces in natural killer cell activity. They found that a small population of natural killer cells are responsive to mechanical cues from their environment and this small group of mechanosensitive cells accounts for significant activation of NK cell response [252,253]. NK cell activity is affected by substrate stiffness where peak activity is achieved at an optimal substrate stiffness beyond which activity is impaired [252]. Clustering of NK cell receptor, NKG2D and costimulatory adaptor protein, DAP10, and downstream cytotoxic activity also showed similar bell-shaped dependence on substrate stiffness. Using ligand-coated

nanowires, it was observed that NK cells exert centripetal forces to nanowires thus alluding to their ability to probe its microenvironment through force-sensing mechanisms [253]. NK cell cytotoxic activity was also found to be dependent on forces generated from actomyosin flow through modulation of interaction between actin and SHP-1 (SH2-domain-containing protein tyrosine phosphatase-1) [253]. Detailed studies are however, required to elucidate mechanisms of mechanotransduction in these cells.

A recent study has shown that mechanical forces aid in Dectin-1-mediated phagocytosis of fungal pathogens [254]. Dectin-1 is an innate immune receptor (PRR, pathogen recognition receptor) expressed on a variety of innate cells like neutrophils, macrophages and DCs [255]. Its stimulation with glycan polymers leads to generation of mechanical force through Rho-ROCK mediated stress fibre formation. Generated forces greatly enable phagocytosis of fungal pathogens. Interestingly, few reports have also studied the influence of mechanical forces in the inflammasome pathway [254]. One study has reported that cyclical forces activate the NLRP3 inflammasome through ROS generation in mouse alveolar macrophages, which could account for lung inflammation during mechanical ventilation [256]. Other reports have found that while cyclical forces increase NLRP3 and capsae-1 expression, it may also act to inhibit IL-1β production through inhibition of the AMPK pathway [257]. Further studies should be conducted to resolve these conflicting findings. Nevertheless, these studies show that mechanical forces have a ubiquitous importance in immunity.

The T cell receptor activity has also shown to be critically affected by mechanical forces in numerous studies [258]. T cell function is widely governed by external mechanical forces and mechanical properties of its microenvironment. Many studies have established the TCR complex as the mechanosensor that senses mechanical cues, and transduces them into

phenotypic or functional changes. We will delve into the mechanobiology of T cells in the following chapter.

Chapter 3.6. Mechanobiology of T lymphocytes

Role of mechanical forces in T cell function and phenotype has been an area of active research since the last decade. There are abundant reports that inarguably validate the central role of mechanotransduction in this immune cell subset. Based on the functional and physiological aspects, role of mechanotransduction in T cells can be studied into the following categories- TCR triggering, T cell antigen recognition, T cell thymic selection and T cell effector functions. The following section will also describe the evolution of studies in the area of T cell mechanobiology and development of the T cell mechanosensor model.

3.6.1 Development of the T cell mechanosensing model of TCR triggering

For many decades, researchers have tried to resolve the events that lead to TCR triggering downstream of peptide-MHC and TCR complex binding. Binding of specific peptide-MHC complexes on APCs to TCRs lead to downstream signal transduction through modifications in the cytoplasmic domains of the CD3 complex, that ultimately result in T cell activation [(259)]. TCR triggering can broadly be defined as the molecular events underlying the passage from the initial TCR-pMHC recognition to signal transduction through biochemical changes in the TCR-CD3 cytoplasmic regions that result in T cell activation. There are certain attributes of TCR-pMHC recognition event that may pose as a considerable challenge while forming a precise model for TCR triggering [(259)].

a. Sensitivity: Each T cell expresses a specific repertoire of TCRs that is capable of binding foreign pMHC molecules limited by a confined range of specificities and affinities [(259)]. APCs however, express pMHC complexes of varying affinities and specificities for the TCRs. For

efficient TCR triggering, each T cell expressing a specific TCR must respond to even a single molecule of agonist peptide-MHC complex on the interacting APC among a sea of non-stimulatory peptide-MHC complexes [259,260].

b. Self versus non-self discrimination: APCs and target cells abundantly express self pMHC complexes as compared to scarce expression of agonist foreign pMHC complexes [259]. During T cell development, T cells expressing TCRs capable of binding self-pMHC complexes with low/moderate affinity are positively selected [32]. So, all T cells are capable of binding self-pMHC complexes. Continued interaction with low affinity self-pMHC is also required for generation of survival signals for peripheral T cells [261]. T cells with very high affinity for self-pMHC complexes are removed by a process termed as negative selection so as to prevent autoreactivity [32]. Since TCRs can bind both to self and foreign pMHCs, how do T cells discriminate between the two so that they can efficiently act against foreign pMHCs while preserving tolerance towards self-antigens? Varying ligand affinities for TCRs may not serve as a sound parameter that will ensure T cells' selective response towards foreign peptides. Studies with transgenic mice have shown that increasing a ligand's affinity for a specific TCR by a very small margin results in its negative selection instead of positive selection [259,262]. This shows that the threshold affinity of ligands that will define its status as 'foreign' or 'self' is extremely narrow. Also, the far greater abundance of self-pMHCs on the APC or target cell makes it even more difficult for the rarer foreign pMHCs to be recognised by the TCRs [259].

c. Versatility and Diversity: Efficient TCR triggering also necessitates the ability of TCRs to recognise multiple ligands of varying affinities and respond differentially to each of them. For example, mature peripheral T cells need constant interaction with low-affinity self pMHCs to generate survival signals, whereas high-affinity foreign pMHCs should result in their activation

[261]. Moreover, it has been seen that the TCR-pMHC interacting interface shows immense structural diversity despite presence of considerable conserved residues [262]. This feature allows mounting of efficient T cell response against a wide spectrum of foreign agents. Hence, the TCR triggering process must also account for this structural diversity.

The TCR complex displays very high specificity towards foreign antigens and is capable of distinguishing between peptides differing in as much as a single amino acid [263]. How the TCR complex is able to achieve such a remarkable degree of specificity has been the subject of intense research.

Interestingly, it has been shown that binding affinity between a TCR and a cognate pMHC is very weak lying within the range of 1-5µM [265]. TCR-pMHC interactions of dissociation constant (K_D, measure of TCR affinity for specific ligand) within this range produced optimal T cell activation, as measured by magnitude of Ca^{2+} influx, secretion of cytokines and T cell cytotoxicity. Using engineered TCRs that show varying affinities for their cognate ligands (as measured by their respective K_D), it was found that beyond a certain threshold, increasing TCR-peptide ligand affinity strongly attenuates signalling [265]. This is contradictory to what is expected of an efficient TCR triggering mechanism in response to scarce foreign antigens on APC or target cells. Moreover, TCR binding to cognate pMHCs also displays a high dissociation rate as measured by 3D measurements using surface plasmon resonance in free solutions [266]. The weak affinity of TCR-pMHC binding can thus, be attributed to a slow association rate along with faster dissociation rate. This was contrary to the TCR occupancy model of T cell activation which proposed that magnitude of TCR triggering was dependent on the duration of TCR occupancy [266]. pMHCs that were capable of binding to TCRs for sufficiently longer durations were capable of inducing downstream signalling that led to T cell activation.

Hence, the TCR triggering model must encompass these seemingly conflicting attributes of TCR-pMHC recognition and must account for the highly sensitive yet specific nature of TCR activation in response to foreign ligands. A number of models have been proposed over the past few decades that sought to explain the high efficiency of TCR triggering and downstream T cell activation which will be briefly discussed below.

Models of TCR Triggering

A. The Serial Triggering model: As explained before, APCs and target cells express very low amounts of foreign pMHCs in comparison to hugely abundant self-pMHCs [260]. In order to account for efficient yet specific TCR triggering in response to rare agonist foreign pMHCs, the serial triggering model proposes that a single agonist pMHC molecule on an APC or target cell is reused through multiple cycles of binding and engaging different TCRs on the antigen-specific T cells [267]. TCR activation is known to be associated with endocytosis of activated TCRs, resulting in its downregulation. Using different peptide concentrations, they measured the stoichiometry of TCR and pMHC interactions. They used radioactively labelled peptides that enabled quantification of the number of peptide-MHC complexes on APCs at each peptide dose. Using fluorescently labelled antibodies against TCR-CD3 complex, the extent of TCR downregulation at various pMHC concentrations was measured. It was found that few pMHC complexes on APCs triggered downregulation of a substantially large population of cognate TCRs on the T cell surface. In order to ensure that pMHCs binding to TCRs triggered downregulation of cognate TCRs only, T cell clones bearing αβ receptors of dual specificity were designed. These T cell clones were incubated with peptides that bound to either of those αβ receptors and it was found that specific TCRs were downregulated only when they interacted with cognate peptide-MHC complexes while the other αβ receptor remained

unaffected. Also, the extent of cytokine production by T cells showed significant correlation with the extent of TCR downregulation [267]. Thus, this study concluded each pMHC complex on the APC must engage and trigger multiple cognate TCRs, whose cumulative effect will cause significant signal amplification and result in optimal T cell activation [267,268] (Fig. 3-6-1).

Advantages: The serial triggering model seemed to provide logical explanations for certain features of TCR-pMHC triggering. For example, for a single pMHC complex to bind to a number of cognate TCRs, it would be necessary that the TCR-pMHC interaction should have a higher dissociation rate and lower affinity, and TCR-pMHC binding will have fast kinetics all of which had substantial experimental evidence as described before. This model also explains how a few cognate pMHC complex on the APC or target cell can trigger productive interactions with cognate TCRs that will result in optimal T cell activation.

Disadvantages: There are however, a number of caveats in this model. This model did not measure TCR-pMHC interaction by direct visualisation methods or in a time kinetics dependent manner. Instead, they assumed that the extent of TCR downregulation can be used as an index for TCR-pMHC binding stoichiometry. Studies have shown that TCR downregulation can occur as a bystander effect, with non-engaged TCRs also undergoing concomitant internalisation [269]. According to this study, TCR downregulation can occur by two mechanisms: i. by direct TCR-pMHC binding leading to downregulation of engaged TCRs ii. Intracellular signalling involving tyrosine kinases that lead to downregulation of unbound bystander TCRs. Thus, one cannot accurately measure TCR engagement as extent of TCR downregulation. Another drawback of this model is that it failed to consider the possibility of TCR crosslinking or physical association and co-regulation of bound and unbound TCRs. The

authors suggest that at low cognate peptide densities, co-regulation of non-engaged TCRs can enable 'signal spreading' and amplification [269].

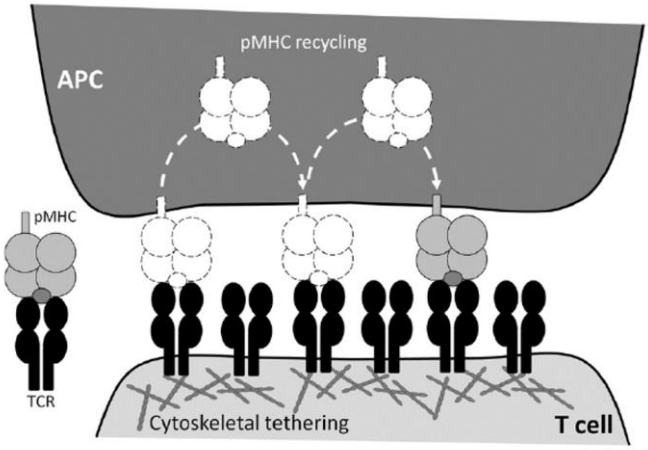

Figure 3-6-1. The serial triggering model of TCR activation. This model proposes an explanation for optimal TCR activation in response few TCR-specific cognate antigens on APCs. The model proposes that a single peptide-MHC (pMHC) complex is goes through multiple cycles of reuse, thereby binding to and triggering multiple TCRs simultaneously. *(Adapted from Liu & Ganguly. Crit Rev Immunol. 2019.)*

B. The Kinetic Segregation Model: This model proposes that efficient TCR triggering requires close and stable interaction of the TCR-pMHC complex. This is facilitated by redistribution of membrane components when cells interact with each other [270]. It was observed that efficient binding of cell surface receptors with their ligands was associated with spatial segregation of bulky membrane components like carbohydrate-rich domains, so as to enable formation of small signalling domains containing interacting receptors and other signalling proteins [270]. This model postulates that when T cells interact with APCs or target cells, there is a size-dependent segregation of large membrane molecules, particularly tyrosine phosphatase

CD45 from the zone of TCR-pMHC interaction [270,271]. This allows enhanced tyrosine kinase-dependent downstream signalling and TCR activation.

Surface proteins in resting T cells transiently and randomly associate with one another as a result of membrane diffusion [271]. Randomly diffusing tyrosine phosphatases interact with and activate Src kinases. These kinases further phosphorylate tyrosine residues on ITAM motifs on the cytoplasmic domains of the TCR-CD3 complex. Phosphorylated ITAMs are in turn subjected to dephosphorylation by tyrosine phosphatases in the vicinity. Combined activities of phosphatases and kinases result in basal phosphorylation state of T cells that maintain its resting state [271]. When T cells interact with APC, close apposition of the interacting membranes cause membrane proteins to spatially segregate because of steric hinderance. Bulky molecules like CD45, CD148, LFA-1 and CD43 are excluded from regions of contact [270,271]. This enables formation of close and stable bonds between T cells and APCs (Fig. 3-6-2). Close proximation of T cell and APC membrane is also facilitated by other interacting surface proteins like CD2 [272]. This enables efficient scanning of TCRs for specific pMHC complexes on APCs. Moreover, exclusion of phosphatases from the contact zone shifts the equilibrium towards higher phosphorylated ITAM levels that result in TCR triggering and activation. Even unbound TCRs diffusing into the zone of interaction can eventually get phosphorylated resulting in signal amplification. Binding of TCRs to their cognate pMHC prevent their diffusion out of the contact region, thereby increasing the half-lives of their phosphorylated states. So even a small region of contact (≈300nm) can potentially result in physiological T cell activation [271,272]. Since the phosphorylated state of the TCR is stabilised by TCR-cognate pMHC interaction in contact zones, specificity of TCR triggering is maintained. The TCR-pMHC bond half-life will determine the stability of the phosphorylated TCRs and

consequent downstream signalling. This ensures that only specific antigens that will form stable bonds with cognate TCRs can result in TCR triggering.

Advantages: A couple of evidence supports this model. It has been seen that CD45 is mostly excluded from the zone of TCR microclusters which act as hubs of T cell signalling [(273)]. It was initially thought that the large extracellular domain of CD45 sterically hinders close apposition of T cell and APC membrane thereby affecting TCR triggering. Complete removal of CD45 was not feasible because its phosphatase activity is initially needed to remove the inhibitory phosphate residues from T cell-activating tyrosine kinases. It was thought that removal of the extracellular domain from CD45 should restore signalling capacity of CD45-deficient T cells by allowing productive interactions, while preserving its activity at the same time [(274)]. It was however, seen that replacement of the large extracellular domain by a smaller extracellular domain of protein Thy-1 did not restore signalling capacity. This is could be due to the reason that the extracellular domain of CD45 is needed for its enzymatic activity [(274)]. According to this model, decreasing the intermembrane distance between T cells and APC will result in productive interaction. So, any changes to the dimensions of the TCR-CD3 complex should affect TCR triggering. Although any structural changes in the TCR-CD3 complex severely affects its association with each other and also binding to the pMHC complex, it has been shown that addition of extra immunoglobulin superfamily domains in the MHC molecule led to severe disruption of TCR signalling without hampering TCR-pMHC binding [(275)]. Further supporting evidence finds that membrane-associated TCR ligands are more efficient at TCR triggering as compared to their soluble counterparts [(276)].

Disadvantages: The kinetic-segregation model states that TCR-triggering involves spatial resolution of inhibitory and activating molecules on the cell surface. But no conclusive report

has shown that spatial exclusion of CD45 alone is sufficient to trigger T cells. Moreover, it dismisses the role of other events like TCR conformational change in response to antigen binding or receptor clustering since it attributes TCR triggering almost exclusively to kinetic segregation of phosphatases. Evidences supporting this model cannot exclude other mechanisms. Active membrane dynamics in this model strongly points towards the role of biophysical forces in TCR triggering. This model also does not provide any explanation for TCR triggering in light of their binding affinities and kinetics.

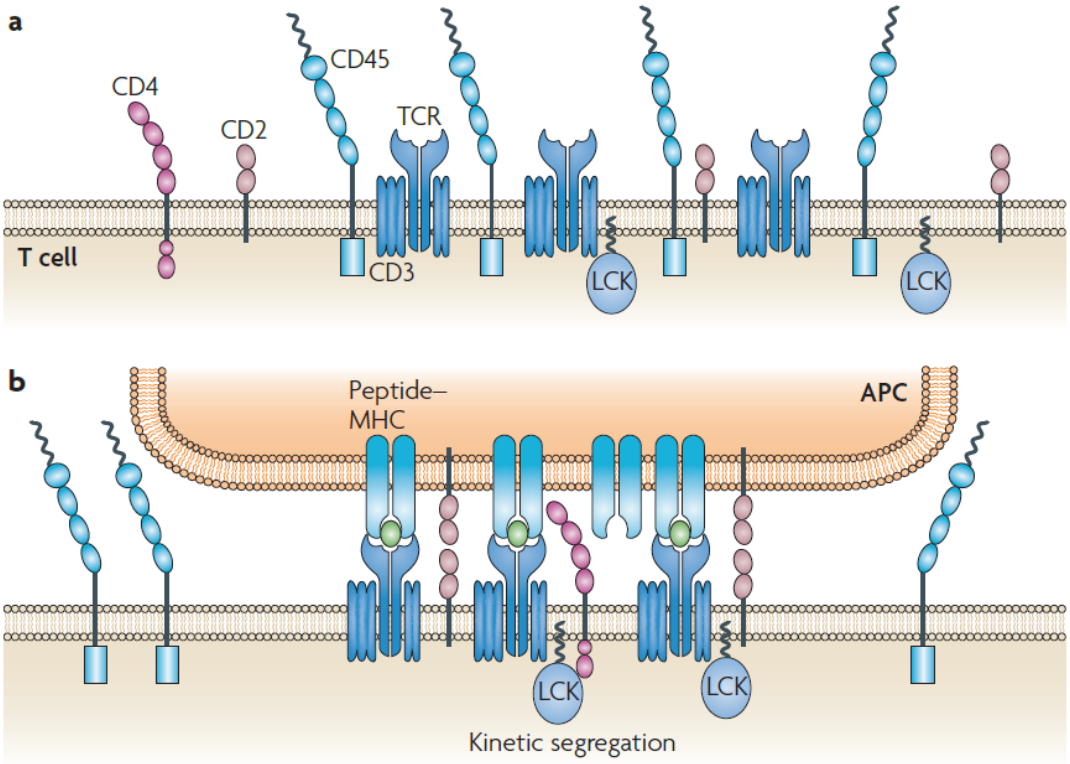

Figure 3-6-2. The kinetic segregation model of TCR triggering. In resting T lymphocytes, the ITAM motifs of the TCR complex are constantly phosphorylated and dephosphorylated by Lck kinases and CD45 phosphatases located in close proximity with the TCR complex. These two opposing activities maintain the TCR in an unstimulated, resting state. Upon antigen binding on APCs, these TCR-associated signalling domains undergo a spatial reconfiguration. This involves exclusion of large proteins like CD45 phosphates from the signalling synapse (kinetic segregation) to facilitate close interaction between TCR and pMHC on APCs. This favours

uninhibited Lck activity and phosphorylation of TCR signalling domains, triggering TCR activation. *(Adapted from Chakraborty AK et.al. Nat Rev Immunol. 2010 [277])*

C. The Receptor Aggregation Model: This model postulates that physical aggregation of TCR-CD3 complexes on the T cell surface is required or TCR triggering and activation [272]. Aggregation of TCRs increases proximity of Lck kinases associated with the TCR-CD3 complexes. This facilitates trans-autophosphorylation of tyrosine residues in adjacent TCR-CD3 complexes and triggers downstream signalling and activation [272]. It is difficult to conceive of TCR aggregation considering the rare abundance of specific pMHC ligand on APC. Moreover, TCR can be triggered even in the presence of a single pMHC molecule. Following extensions to the model have been proposed to explain this conflict.

i. Co-receptor heterodimerisation: According to this model, a single pMHC complex is capable of binding both TCR as well as CD4 or CD8 co-receptor [278]. This brings Lck kinases associated with the CD4 or CD8 co-receptor in close proximity to the ITAM motifs of the TCR-CD3 complex thus inducing its trans-phosphorylation and activation [278] (Fig. 3-6-3a). The major drawback of this hypothesis is that TCR triggering occurs even in the absence of co-receptors [278].

ii. Pseudodimer formation: The model proposes that adjacent TCRs bind to TCR-specific foreign pMHC and self pMHC [278]. Co-receptor associated with TCR bound to self pMHC simultaneously engages the foreign pMHC bound to adjacent TCR. This facilitates aggregation of adjacent TCRs and induces downstream trans-autophosphorylation and signal transduction. Since there is a far greater abundance of self pMHCs compared to foreign pMHCs, the probability of TCRs binding to self pMHCs is much higher (Fig. 3-6-3b).

Experimental studies have shown significant accumulation of self pMHC complexes at the immunological synapse between an interacting APC and T cell [279]. It was observed that soluble dimers of TCR-specific foreign pMHC and endogenous pMHC were able to activate TCRs much more efficiently as compared to TCR-specific foreign pMHC monomers alone or dimers of self pMHCs [280]. None of the endogenous peptides showed any TCR stimulatory capacity. When APCs designed to express GPI-anchored MHC molecules were used, T cell activation was significantly abolished. GPI-anchored MHC molecules are unable to recycle through endosomal compartments and fail to express surface MHC molecules that are bound to self-peptides [281].

There are however, no studies that conclusively show that self pMHC and foreign pMHC exist as dimers that can simultaneously bind to adjacent TCRs triggering their dimerization [282]. Also, a number of studies have shown that TCRs in resting T cells naturally exist in higher-order multimeric forms in the absence of any antigen binding [283]. There is also a lower probability of encountering spontaneous heterodimers of self and non-self pMHCs on the APC surface as compared to spontaneous TCR dimers. Thus, the possibility of pre-existing TCRs multimers is much higher as compared to the possibility of TCR dimerization in response to antigen binding to cognate TCRs [283].

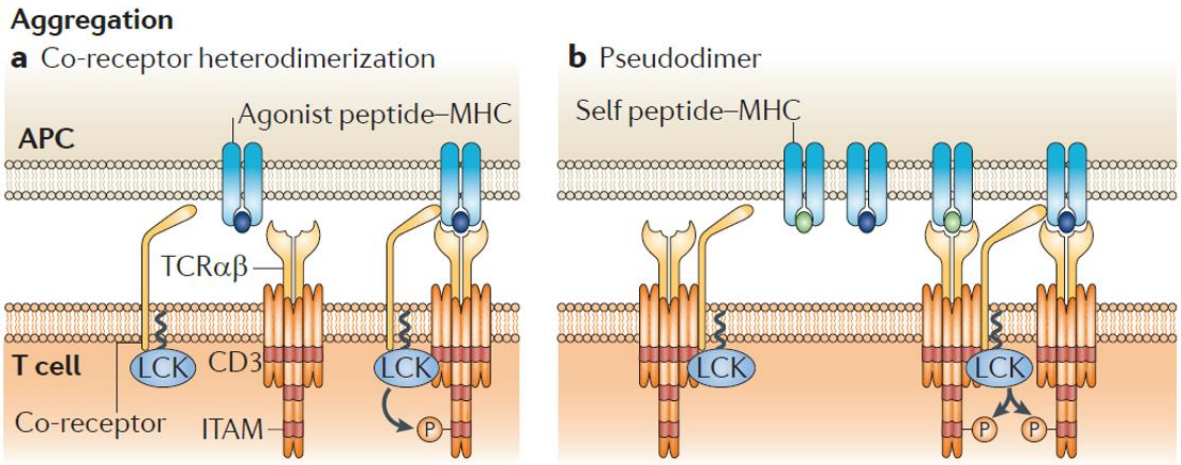

Figure 3-6-3. The receptor aggregation model of TCR triggering. This model proposes that efficient TCR triggering is enabled by formation of TCR aggregates upon antigen binding. This increases proximity of TCR-associated Lck kinases that enhances phosphorylation of TCR-signalling ITAMs and subsequent TCR activation. The co-receptor hetrodimerisation model postulates that foreign peptide-MHCs interact with both TCR and co-receptors (CD4 or CD8) and subsequent co-receptor association produces TCR aggregation (a). The pseudodimer model proposes that aggregation occurs between TCRs bound to self-pMHCs and foreign pMHCs. Since self-peptide MHCs show far greater abundance than foreign pMHCs, probability of TCR aggregation and subsequent activation increases (c). *(Adapted from van der Merwe PA. Nat Rev Immunol. 2011 [260].)*

TCR microclusters in non-activated and activated T cells have been observed through total internal reflection microscopy (TIRFM) imaging [284,285] and have been validated by single-molecule-localisation microscopy (SMLM) [286]. These microclusters have been shown to be necessary for sustained TCR signalling. Recent studies have however, refuted the existence of pre-formed TCR microclusters on resting T cells or that their formation occur as an event leading to TCR triggering. These studies claim that TCR microculsters were observed as imaging artifacts due to limitations of the SMLM technique. Using label-density-variation SMLM technique that overcomes the limitation of conventional SMLM it was observed that

TCRs show random distribution on the membrane of resting T cells [287]. TCRs were labelled using specific fluorescent antibodies and label-density-variation dSTORM (direct stochastic optical-reconstruction microscopy) was performed, which revealed that TCRs are randomly distributed as single molecules on the T cell membrane [287]. Imaging of these cells using the conventional dSTORM method showed non-uniform clustered TCRs on the membrane. This was found to be a result of overcounting artifacts in the conventional SMLM technique. Random organisation of TCRs on the cell membrane was confirmed by using live-cell PALM (photoactivated localisation microscopy) which is more robust and precludes overcounting [287]. The authors further suggest that random TCR distribution might have been evolutionarily more favourable over a clustered distribution in resting T cells. This facilitates rapid sampling of rare cognate antigen by the T cells. Random TCR organisation enables the cell to rapidly sieve out excess non-cognate pMHC interactions while allowing quick selection of rare but specific pMHCs [287].

As mentioned earlier, TCR oligomerisation in response to antigen binding was stipulated to be the deciding event that led to TCR activation on pMHC binding. Cognate antigen-induced TCR clustering was however, never observed within the immunological synapse itself. TOCCSL (Thinning out clusters while conserving stoichiometry of labelling) failed to detect any TCR clustering in the presence or absence of cognate antigens [288]. Latest studies using PA/FCS (photon arrival time analysis with fluorescence correlation spectroscopy) and FRET (fluorescence resonance energy transfer), it was shown that stoichiometry of TCR and ligand binding was 1:1 [288]. Single and dual colour TOCCSL did not show any laterally diffusing TCR oligomers. In order to account for the probable failure of detecting short-lived protein clusters that may disassociate during the recovery phase after photobleaching, PA/FCS (photon antibunching/fluorescence correlation spectroscopy) method was used. This approach

confirmed that mobile TCRs are monomeric [288]. FRET-based approach further confirmed that non-diffusing TCRs also show a non-clustered single molecular arrangement. Using FRET-based approach it was observed that binding of cognate pMHC complexes to TCRs did not induce in TCR organisation into clusters [288].

D. The TCR conformational change model:

Many studies propose that antigen binding to the TCR produces conformational changes in the various domains of the TCR complex [289]. Conformational changes in the TCR complexes enable association of downstream signalling molecules with the TCR complex that result in TCR activation. Following domains of the TCR complex have been shown to undergo changes in conformation on TCR engagement:

TCR-pMHC bond conformation: TCR-pMHC bond conformation was determined by FRET-based measurements [290]. Briefly, site-specific fluorescent labelling of pMHC and TCR molecules with FRET donor and acceptor respectively was performed. pMHC-TCR bond distance was estimated from varying FRET efficiencies on TCR binding with pMHCs of varying affinities. Bond distance measured in real time provided information about dynamic TCR-pMHC bond conformational changes (or compactness). Higher affinity pMHC complexes resulted in greater FRET efficiencies and reduced bond length [290]. Single molecular FRET measured real time conformational changes of a single TCR-pMHC molecular level independent of antigen binding affinities or kinetics. This showed that bond conformational change upon TCR binding is an inherent property of the bound TCR-pMHC complex, and it does not depend on antigen affinity or binding kinetics of the TCR-pMHC complex [291]. This study also showed that TCR-pMHC bond conformational change does not depend on TCR aggregation [290]. More potent TCR ligands formed shorter and compacter bonds with the TCR

that led to greater detachment of the CD3 complex from the plasma membrane resulting in increased exposure and access of the buried ITAM motifs to phosphorylation [291].

TCRαβ ectodomains: Using site-directed fluorescent labelling, Beddoe et.al [292], showed that upon binding of specific antigens to cognate TCRs, the A-B loop of the constant domain of the α chain (Cα) of the TCR complex undergoes a distinct conformation change (Fig. 3-6-4). Impairing this change in conformation by site-directed mutagenesis or using antigens of varying affinities for the TCR complex, resulted in diminished TCR signalling triggering upon antigen binding. The study showed that by altering affinities of ligands for cognate TCRs, their ability to induce a conformational change upon TCR binding and subsequent TCR triggering can be controlled. Ligands possessing higher affinities for the TCR complex induce switching of the aforementioned A-B loop from a 'closed' state to an 'open' state and potent TCR triggering [292]. This study claimed that TCR conformation change occurs independent of TCR clustering and both may act in concert to produce efficient TCR triggering. The structure of the A-B loop in the α chain constant domain has however, not been resolved clearly. It is also not clear how this change in conformation is propagated through other TCRs and the CD3 signalling complex in the cell. Further elucidation of the structural components is essential to understand the mechanism.

CD3 cytoplasmic domains: The TCR molecule forms close non-covalent associations with the CD3 complex [293]. The CD3 subunits are integral to TCR binding-mediated downstream signalling. The CD3 complex is composed of the following subunits: CD3εγ and CD3Ɛδ heterodimers and CD3ζζ homodimers [293]. TCR binding triggers a series of downstream signalling events through the CD3 cytoplasmic domain rich in ITAMs. Since the TCR molecule lacks cytoplasmic tails that can relay downstream signalling, signalling upon TCR ligation is

conveyed through the conformational changes in the CD3 cytoplasmic domains [294]. Gil et.al. [295] described a model to account for TCR triggering in which he described that a conserved proline-rich sequence (PRS) in the cytoplasmic tail of the CD3ε chain is crucial for TCR activation by relaying signal from the TCR molecule to the signalling-efficient CD3 complex upon antigen ligation. The model proposes that binding of specific pMHC complexes or antibodies to the TCR produces a change in the conformation of the TCR-CD3 complex that exposes the otherwise buried PRS motif and makes it accessible to Src-like adaptor proteins like SLAP and Nck. Mutations in the PRS motif prevented binding of the Nck through it Src homology 3.1 domain and thus formation of a stable immune synapse and T cell activation. Mingueneau et.al. [296], however, knock-in deletion of the PRS found that it is not crucial for activation of mature $CD4^+$ or $CD8^+$ T cells in response to pMHCs but rather functions crucially during T cell development.

A study proposed that binding of TCR to its ligand induces a conformational change in the CD3ε cytoplasmic domain, and causes it release itself from plasma membrane binding. This provides ITAMs access to intracellular kinases and adaptor proteins essential for downstream TCR signalling [297]. Xue et al. [298] corroborated this finding by in his study by performing FRET measurements. FRET efficiency was calculated between fluorescently tagged CD3 moiety and plasma membrane. FRET efficiency was higher in wild type cells but reduces dramatically in cells, where the basic residues of the CD3ε cytoplasmic tail that interact with the membrane were modified. This led them to propose that normally the CD3ε cytoplasmic tail forms close interactions with plasma membrane rendering the ITAMs inaccessible to kinases (safety-on state). Upon TCR binding, conformation change in the cytoplasmic domain releases the buried ITAMs allowing their phosphorylation and downstream signalling [299,300]. Characteristic conformation change that can be attributed to TCR triggering has not been resolved.

Moreover, numerous studies have shown that ITAMs in the CD3 cytoplasmic domain are subjected to homeostatic phosphorylation and dephosphorylation under TCR-unbound conditions [301]. Addition of tyrosine phosphatase inhibitors resulted in hyperphosphorylation state of the unbound TCR-CD3 complex, which confirms that the CD3 cytoplasmic domains have access to kinases even in the absence of antigen binding [302,303].

CD3 ectodomains: In attempts to elucidate the mechanisms that contribute to TCR activation, Sun et. al. [304] studied the structure of the CD3 subunits heterodimers. Each CD3 domain comprises of 7 (A-G) β strands that undergo parallel sideward interaction to form two β sheets that are oriented anti-parallelly. The CD3εγ ectodomain possesses two immunoglobulin-like domains and hydrogen-bonded C-terminal β strands that interact hydrophobically. It was found that the hydrogen-bonded G strands of the CD3 ε and γ chains further increases the rigidity and stability of the CD3 complex. This paired G strand is inserted into the plasma membrane via a conserved proximal motif [305]. The authors suggested that the rigid paired G strand may act as a mechanical piston, that could enable relative displacement of the CD3 complex components upon TCR ligation, thereby facilitating exposure and activation of kinase signalling domains in the complex. Disrupting the insertion of the paired G strand into the membrane by mutating the conserved insertion motif resulted in significant abolishment of TCR signalling as well as T cell development [306].

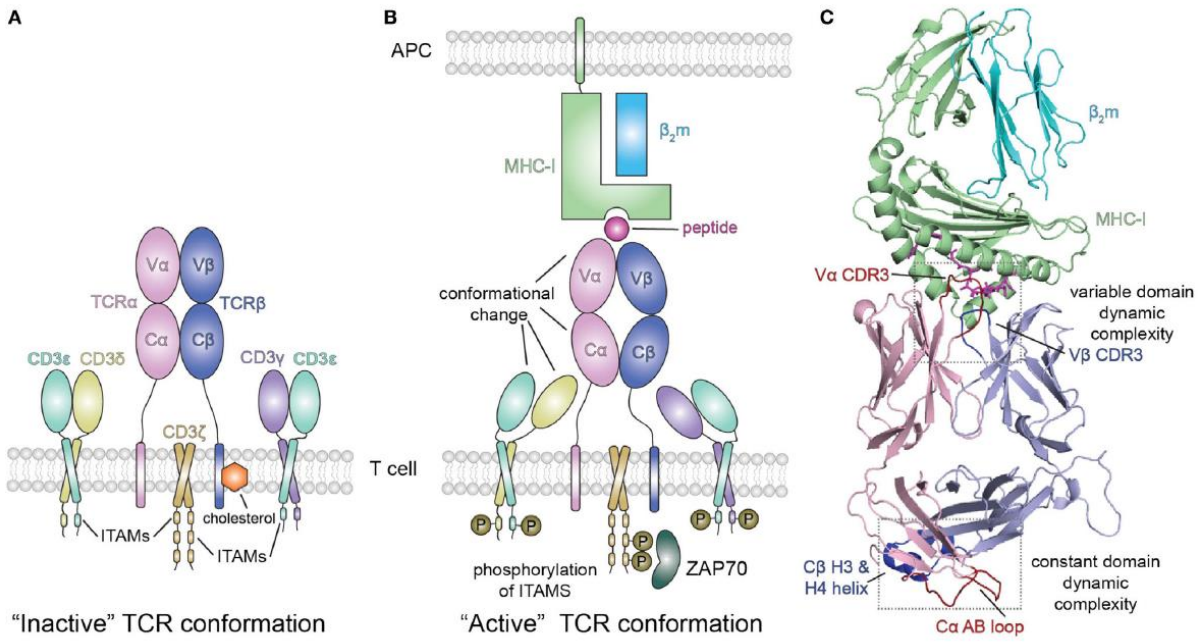

Figure 3-6-4. The conformational change model of TCR triggering. Binding of cognate pMHCs on APCs triggers allosteric changes in conformation of the TCR-CD3 complex. The CD3 domains undergo spatial reorientation relative to one another which allow trans-phosphorylation of ITAMs (A, B). Upon antigen binding the AB loop of the TCR C_α chain changes from a closed, inactive conformation to an open, active conformation (C). The change is propagated through the CD3 signalling subunits that facilitates receptor association and active signalling. (Adapted from Natarajan K. Front Immunol. 2018 [307].)

E. The Receptor Deformation Model: The receptor deformation model of TCR triggering [308] is founded on the serial triggering model. This model proposes that dissociation of the TCR-pMHC is crucial for efficient TCR activation because it will facilitate efficient serial triggering of multiple TCRs with the same agonist pMHC complex. External forces on the TCR-pMHC bond will cause it to dissociate thereby enabling recycling and rebinding of previously bound cognate pMHCs on APCs to multiple TCRs on the T cell while it scans the APC surface for cognate antigens (Fig. 3-6-5). The study hypothesised that the TCR-pMHC bond is subjected to external mechanical forces which they termed as 'rupture forces.' They are generated from

within the T cell cytoskeleton and they tend to produce a pulling effect on the TCR-pMHC bond [308]. These rupture forces also test antigen binding. Since bonds formed between non-agonist (non-specific) antigens and TCRs are weak, they do not withstand these rupture forces and tend to dissociate preventing non-specific TCR triggering. Agonist antigens on the other hand, form strong durable interactions with the TCR complex that lasts long enough to trigger signalling.

The authors explain that force-induced receptor deformation can be propagated through the signalling-competent CD3 subunits or the co-receptors only when TCR-pMHC interaction is rigid. Strong binding of the TCR and agonist pMHC enables it to resist its pre-mature dissociation and facilitate downstream signalling. Post-TCR triggering, release of the pMHC due to these forces will facilitate serial triggering as described before [308].

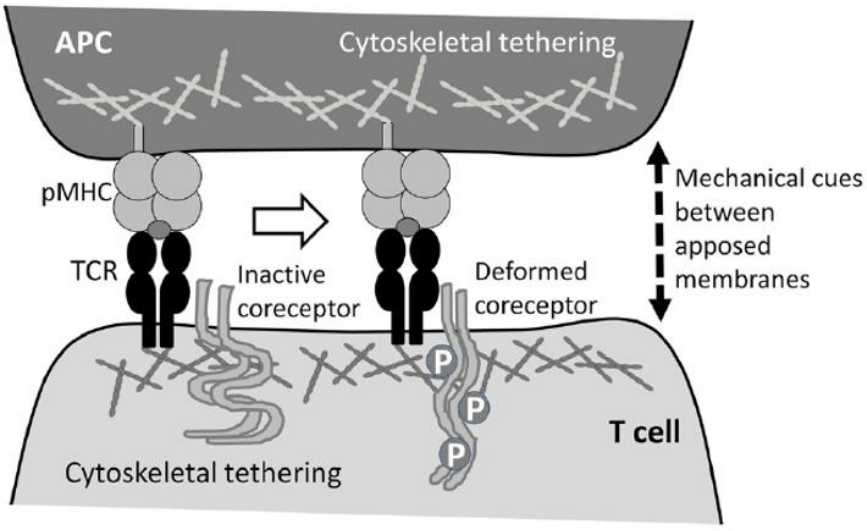

Figure 3-6-5. The receptor deformation model of TCR triggering. The TCR-pMHC bond is subjected to forces generated from cytoskeletal tethering. These forces produce TCR complex deformations that enhances activity of signalling subunits. This model also postulates that

external forces may facilitate pMHC dissociation from the TCR complex, thereby facilitating their recycle (serial triggering). *(Adapted from Liu & Ganguly. Crit. Rev. Immunol. 2019. [311])*

The model seemed to be in conflict with certain aspects of TCR triggering since higher dissociation rate of the TCR-pMHC bond is correlated with weaker TCR signalling [309,310]. Moreover, the author could not successfully describe the origin and nature of the forces. Although they claimed that the forces were generated due to T cell motility while scanning for antigens on the APC surface, whether these forces were enough to produce a subsequent change in the TCR complex conformation was not shown. Definitive structural changes in the TCR-pMHC complex during T cell movement on the APC surface was also not shown.

The receptor deformation model however, introduced a relatively novel concept about the plausible role of mechanical forces in TCR triggering. Ma et.al. [308] were among the first to propose that in addition to structural and molecular events, biophysical forces and membrane dynamics may have a crucial role in TCR activation. Research in the past decade have substantiated this hypothesis with innumerable in-vitro and in-vivo experimental evidence and have thus, provided detailed insights into a relative unchartered domain of mechanical TCR signalling. Mechanical forces in biology have been found to be ubiquitous and indispensable in many physiological processes. In the following section we will delve into the recent findings about the crucial biophysical aspect of TCR triggering and signalling.

3.6.2 Mechanical forces in TCR activation

Evidence of the importance of mechanical force during T cell activation dates back to research led by Li et.al.,2010 [312] who showed that application of external forces to the TCR-pMHC complex can initiate downstream TCR signalling. This group also showed that the TCR-pMHC complex only respond to tangential shear forces, alluding to their ability to selectively respond to directional forces. Reports have shown that T cell activation is dependent on the stiffness properties of antigen presenting substrates [313]. When $CD4^+$ and $CD8^+$ T cells were cultured on TCR-crosslinking CD3 and CD28 antibodies-coated synthetic elastomers of varying stiffness, it was observed that softer substrates (Young's Modulus >100kPa) were more efficient at stimulating IL-2 production and T cell proliferation compared to stiffer substrate (Young's Modulus >2 MPa) [313]. Naïve T cells showed better expansion on softer substrates, while T cells cultured on stiffer substrate showed a higher resemblance towards an effector phenotype [313]. Another contemporary report showed that within a physiological stiffness range of 10kPa-100kPa, activation of naive $CD4^+$ T cells showed increasing activation with increasing substrate rigidity [314]. All these findings generated considerable interest and development of T cell mechanosensing domain in research.

Generation of forces during TCR binding

T cell interaction with cognate APCs generates significant physical forces at the interacting synapse [315]. These forces were quantified by a number of biophysical force measurement techniques. The measurements also enabled identification of phases of force generation during T cell interaction with APCs. The study used a biomembrane force probe (BFP) setup in which a red blood cell (RBC) was used as a force probe [316] (Fig. 3-6-6). The RBC was coupled to a microbead coated with TCR crosslinking antibodies. Antibody-coated microbead acted as

a model antigen. When the BFP was brought close to a $CD4^+$ T lymphocyte, 3 distinct phases of force generation were observed after contact. The first phase was the latent phase which was marked no activity in either interacting partners. This was followed by a pushing phase which was observed as the T cell extending membrane protrusions on the bead-coupled RBC, where force was measured in terms of extent of axial RBC compression. There was peak Ca^{2+} influx during this phase which corresponds to T cell activation. The final phase consisted of active retractions of T cell membrane protrusions (pulling phase) which was measured as RBC elongation, finally culminating into engulfment of microbead by the T cell. The study showed that these phases of active force generation were not observed when BFPs coupled with irrelevant antibodies were used, thus confirming TCR-specific action of forces. Abolishing force generation by disrupting cytoskeletal network impaired T cell signalling [316]. These 3 phases of force generation could possibly conform to the phases observed when T cells interact with DCs [317]. The first latent phase could correspond to the T cells trying to establish contacts with the APCs while scanning for cognate antigens. The second phase could correspond to successful establishment of contact and extension of T cell membrane on APC surface during synapse formation and concomitant T cell signalling. The final phase can be associated with stabilisation of T cell-APC contacts culminating in T cell withdrawal from APC membrane. Atomic force microscopy (AFM) measurements yielded similar results [318] (Fig. 3-6-7). Pulling and pushing forces were measured by quantifying AFM cantilever deflection. These forces were associated with concomitant Ca^{2+} influx in T cells and abrogation of these forces impeded T cell activation. Single spectroscopic force measurement technique was also used to quantify forces generated between interacting T cell and DC presenting a range of altered ligand peptides (APL) [319]. It was found that only those APLs that were able to induce high force generation were efficient at optimal TCR triggering.

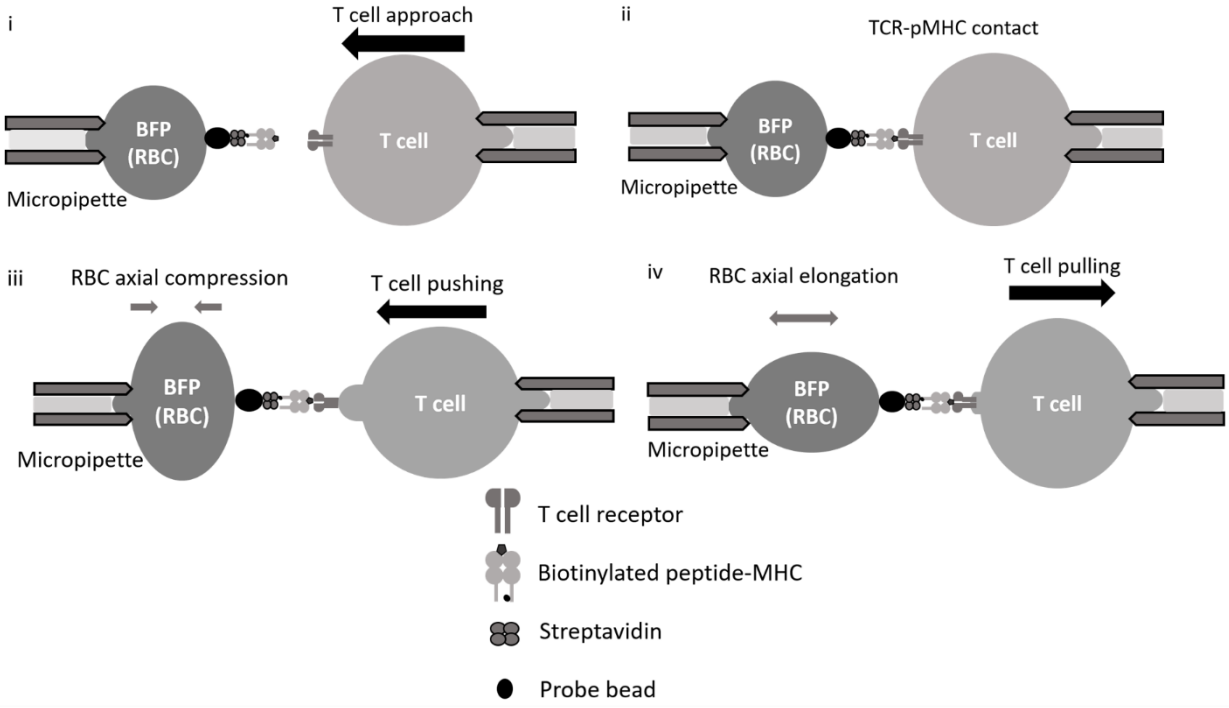

Figure 3-6-6. Measurement of forces during TCR interaction through biomembrane force probe (BFP). This approach uses an RBC probe to study forces generated during T cell interaction. A micropipette-aspirated RBC bound to specific pMHCs is brought into close contact with a specific T cell (i). After establishment of contact (ii), the cells are held in their fixed positions. 3 phases of T cell-APC interaction were observed – a latent phase where no changes were observed followed by a T cell pushing phase as visualised by RBC compression (iii) and a T cell pulling phase which consisted of partial T cell membrane retraction (iv). By measuring the extent of BFP compression/elongation and the probe stiffness value, the magnitude of forces generated were calculated.

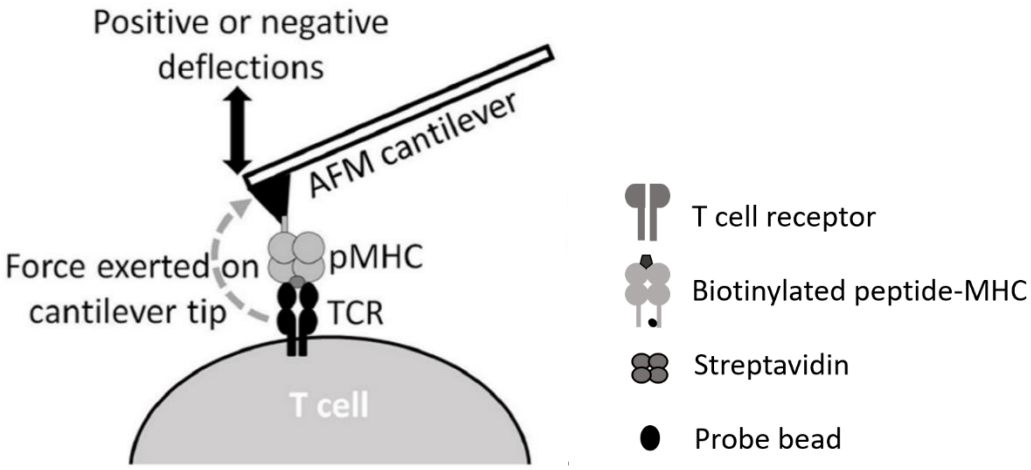

Figure 3-6-7. Measurement of forces during TCR interaction through atomic force microscopy. In this approach, an AFM cantilever tip coated with biotinylated pMHC or anti-CD3 antibodies is made to establish contact with T cells. Depending on the deflection of the cantilever tip, the direction and magnitude of forces generated by TCR binding can be calculated. A positive deflection is indicative of the target cell stiffness properties while an induced negative deflection can be used to estimate the binding strength. *(Adapted from Liu & Ganguly. Crit Rev Immunol. 2019. [311])*

Many initial studies designated the TCR complex as the mechanosensory that senses and transduces mechanical signal signals into chemical outputs. Pioneering studies led by Reinherz et.al. [320], showed that the TCR complex shows acts as an anisotropic mechanosesnor, where it senses mechanical force during its interaction with cognate APCs, and relays the signal to downstream signalling molecules through a change in its quaternary conformation. They theorise that only forces applied in a specific direction to the TCR-pMHC complex can initiate TCR signalling, thus designating it as an anisotropic sensor of mechanical force. Studies have also proposed that mechanical energy driven topological change in the TCR complex might lead to exposure of TCR signalling domains otherwise buried in the plasma

membrane like ITAM motifs [294]. Moreover, it can also facilitate interaction of CD3 subunits with co-receptors and allow access to signalling proteins like Lck kinases (Receptor conformation model) [294]. Moreover, force-dependent structural changes may also allow spatial segregation of signalling and inhibitory domains like exclusion of inhibitory CD45 phosphatase from ITAM motifs and tyrosine kinases thereby facilitating T cell activation (Kinetic Segregation model) [270].

Thus, force generation during T cell-APC interaction is crucial for downstream T cell activation. Abolishment of these forces either through actin-myosin cytoskeletal disruption or alteration of peptide geometry so as to prevent optimal force generation at the interface tend to abrogate T cell activation [315].

3.6.3 Mechanical forces in efficient TCR antigen recognition

T cells encounter a vast sea of antigens on APCs most of which are self-antigens, while the some are of foreign nature. A T cell bears TCRs that shows limited specificity only for a particular antigenic epitope. Therefore, it is crucial that TCRs effectively scan the APC surface for antigens and show specific response to cognate antigens only. Interesting reports have studied the role of mechanical forces in aiding efficient TCR discrimination between non-specific and specific agonist TCR ligands [321]. Mounting evidence shows that TCR-pMHC specificity is imposed by regulation of TCR-pMHC bond lifetimes by mechanical forces [322] (Fig. 3-6-8). Studies involving BFP technique show that bonds formed between TCRs and cognate (agonist) pMHC molecules behave as 'catch bonds' [322]. The lifetimes of these bonds increase in the presence of mechanical forces. On the other hand, bonds between TCRs and non-agonist pMHC molecules characteristically behave as 'slip bonds.' These bonds tend to rupture under increasing mechanical load. A study reported that the lifetime of a bond

between agonist peptide-TCR peaked under application of 10pN external force [323]. During T cell-APC interaction, forces are generated due to interacting apposing membranes. These forces, therefore act to test the fidelity of antigen binding to its TCR. A bond between a TCR and its specific antigen is considerably prolonged under these mechanically loaded conditions. Accumulation of these long-lived TCR-pMHC catch bonds during T cell-APC interaction results in effective TCR triggering and downstream signalling. A non-specific bond between a TCR and non-agonist ligand, however fails to survive under constant mechanical pressure [322]. These transient bonds fail to activate T cells. DNA-based nanoparticle tension sensors were used to create a tension map during TCR interaction [324]. It was found that T cells exert cell-intrinsic forces ranging from 12-19pN to the TCR within immediate binding of pMHC molecule. These forces gauge the stability of the TCR-pMHC bond, allowing only specific bonds to prevail. These cell-intrinsic forces were generated due to LFA-1-mediated adhesion, actin polymerisation and myosin contractile activities [324]. By using DNA tethers that apply below threshold forces or by impairing cell-intrinsic force generation, it was observed that TCRs lose their ability to discriminate between antigens. In attempts to find out about the molecular mechanisms accounting for force-based ligand discrimination, a study reported that physical force produces a structural change in the TCR complex that influences pMHC-TCR bond lifetimes. The Cβ domain of the TCRαβ heterodimer contains an FG loop. Mechanical force induces a structural transition in this particular FG loop, that allosterically affects the TCR-pMHC bond lifetimes at peptide-recognising distal variable domain which in turn determines TCR peptide specificity [325].

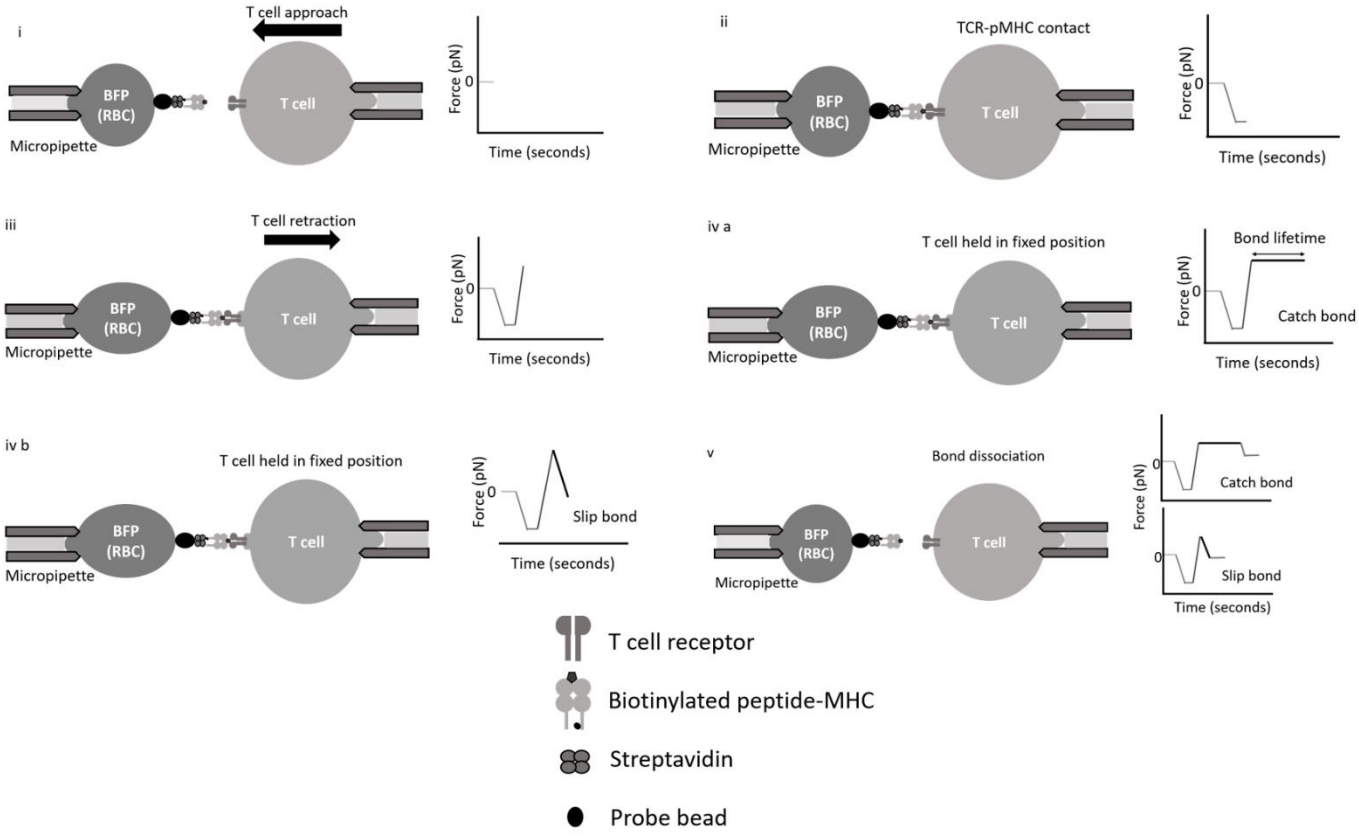

Figure 3-6-8. Measurement of TCR-pMHC bond lifetime using BFP. This approach was used to calculate bond lifetimes between agonist and non-agonist TCR-pMHC interaction. RBC bound to pMHCs is brought into close contact with specific TCR (i). Contact period was kept brief to prevent multiple TCR engagement (ii). After contact establishment, T cells were gradually retracted that generated increasing tensile forces on the TCR-pMHC bond (iii) and then was held in a fixed position till a fixed value of force is reached (clamped force). Agonists pMHCs are able to withstand this force and its bond lifetime is calculated as the period of time between clamped force and bond dissociation (iv a, v). Non-agonists pMHCs, however form slip bonds that rupture before reaching clamped force levels (iv b).

3.6.4 Mechanical forces in T lymphocyte thymic selection

Thymocytes bearing TCRs of a particular antigenic specificity are subjected to a rigorous process of positive and negative selection, which ensure an effective yet specific response to

invading pathogens. Existing models propose that thymic T cell selection is determined by TCR affinity for the pMHC molecule [326]. TCR binding kinetics and affinity regulate stable interactions with self pMHC complexes expressed on thymic stromal cells. Thymocytes expressing TCRs that fail to interact with any self pMHC molecules do not receive survival signals and undergo apoptosis. TCRs that show very strong affinity for self pMHC complexes either undergo receptor editing or apoptosis so as to prevent formation of self-reactive T cells, through a process known as negative selection. Only thymocytes bearing TCRs of moderate affinity for self pMHC complexes undergo positive selection by receiving appropriate survival signals through low affinity interactions with self pMHC molecules on thymic cells [41,326]. These cells form the pool of circulating mature naïve T cells. These processes ensure that the T cell repertoire consists of cells that can effectively respond to pathogenic insult, while maintaining tolerance to self-antigens. Studies based on TCR binding kinetics show that positive selection is a result of dynamic accumulation of moderate affinity interactions whose cumulative effect results in prolonged stable TCR-pMHC interactions, leading to generation of T cell survival signals. Negative selection on the other hand, can be induced even in the presence of few but high affinity strong interactions, thus ensuring tight scrutiny of potential autoreactivity. This model of T cell selection proposes that the selection process is dependent on the formation of stable TCR-pMHC bonds, which in turn, is dependent on accumulation of weak signals or generation of few strong signals. The model, however fails to account for the fact that TCR-pMHC bond lifetimes are not solely dependent on affinity-regulated interaction frequency. As mentioned earlier, TCR-pMHC bonds show distinct behaviour under the influence of physiological levels of mechanical forces. Exertion of physical forces tend to extend lifetimes of bonds between agonist pMHC and its cognate TCR (catch bonds) while causing dissociation of non-agonists pMHC and TCR bonds (slip bonds). A recent study led by

Zhu et.al. [327] described the potential role of physical forces in governing affinity-based TCR-pMHC bond lifetimes and consequent selection. Double-positive (DP) thymocytes were allowed to interact with BFP coated with ligands, that induce either positive or negative selection. It was observed that high-affinity peptides that induce negative selection formed strong TCR-pMHC interactions along with the CD8 co-receptor. Trimolecular interactions involving TCR-pMHC-CD8 behaved as 'catch bonds' in the presence of low forces, generated by thymocytes during interaction with ligand-expressing BFP. On the other hand, TCR binding to low affinity ligands that induce positive selection, triggered generation of low-level forces and behaved characteristically as slip bonds between TCR-pMHC and pMHC-CD8 co-receptor. Force-dependent catch bonds formed due to high affinity pMHC-CD8 interaction with the TCR-CD3 complex, which resulted in a cis heterodimer formation capable of signalling. The ability of a ligand to form CD8-dependent catch bonds with the TCR determines its fate as a negative selection ligand [327]. The study also showed that physical force facilitated thymocytes to efficiently and accurately discriminate between positive and negative-selection ligands. Thus, mechanical forces serve to effectively amplify kinetic differences in affinity-based TCR-pMHC bond lifetimes and facilitate appropriate selection outcomes [327,328]. Further studies are however, needed to elucidate the mechanisms mediating force-dependent T cell selection outcomes.

3.6.5 Mechanical forces in T cell effector functions

Mechanical properties of the T cell microenvironment have a crucial effect on their effector properties. T cells are subjected to an extensive array of physical cues during its lifetime from its development in the thymus, circulation in blood and migration to peripheral lymph nodes and tissues [258]. Each of these locations display characteristically different mechanical

properties (Fig. 3-6-9). Tissues like thymus and bone marrow fall under the category of soft sites, while skeletal tissues are hard sites [329]. It has been shown that mechanical properties of tissues undergo significant changes during inflammation and disease pathogenesis [330]. Inflammation is associated with significant increase in tissue stiffness. These mechanical changes also affect phenotype and function of infiltrating and resident immune cells. It is observed that the mechanical properties of immune cells themselves undergo changes during inflammation [330]. Immune precursor cells have been shown to alter their viscoelastic properties during differentiation so as to adopt mechanical characteristics more suited their function [331]. For example, differentiated myeloid cells show a 50% decrease in their viscosity so as to optimise their migration through small blood vessel pores and tissues [332]. Myeloid antigen presenting cells like monocytes, dendritic cells and macrophages have distinct mechanical stiffness values that undergo changes during inflammation [330]. The mechanical properties of APC were regulated by F-actin content and myosin IIA activity. APC mechanical rigidity values ranges between 0.2 kPa to 1.5 kPa depending on inflammation and differentiation [330]. T cell function show characteristic differences depending on mechanical properties of substrate. T cells showed faster and sustained migration on stiffer substrates (in the range of 100 kPa) as compared to softer ones (0.5 kPa to 6.4 kPa) [329]. Stiffer substrates also induced pronounced T cell membrane protrusions and cell spreading. RNA microanalysis of T cells grown on artificial substrates of varying stiffness revealed activation of distinct gene sets depending on substrate rigidity. Differential transcriptional activation was not achieved in the absence of TCR activation. Expression of cytokines like TNFα, IL17, IFNG, IL22 increased with increasing stiffness. T cell surface markers like ICOS, CD69, CD40LG also showed significant substrate stiffness-dependent changes [329]. Stiffness properties also seemed to have an effect on T cell polarisation as evident by enhanced expression of lineage-specific

transcriptional markers like TBX21 and FOXP3 on stiffer substrates [329]. Other genes that showed enhanced expression in response to stiffness included, proliferation activator Myc and glycolysis inducing factor HIF1α. These results suggest that mechanical stiffness of tissues can cause transcriptional reprogramming of T cells to facilitate certain effector functions. This report showed that genes involved in metabolic regulation in glycolysis, oxidative phosphorylation and mitochondrial biogenesis show selective upregulation in stiffer substrates [329]. Genes involved with T cell activation, differentiation, cell cycle, apoptosis also showed strong associations with substrate stiffness. Gene expression analysis in a murine hypertrophic scar model (HTS) was performed to screen for mechanoresponsive genes during wound formation. The analysis revealed a group of genes associated with T cell signalling. T cells in wounds showed mechanical upregulation of IL4 and IL13-dependent T_H2 pathway and MCP-1 signalling [333]. Mice lacking T cells showed considerable reduction of scar formation and this was attributed to dampened mechanoresponsive T cell-mediated recruitment of inflammatory monocytes and fibroblast precursors [333]. Thus, T cell mechanotransduction plays an important role in wound healing mechanisms.

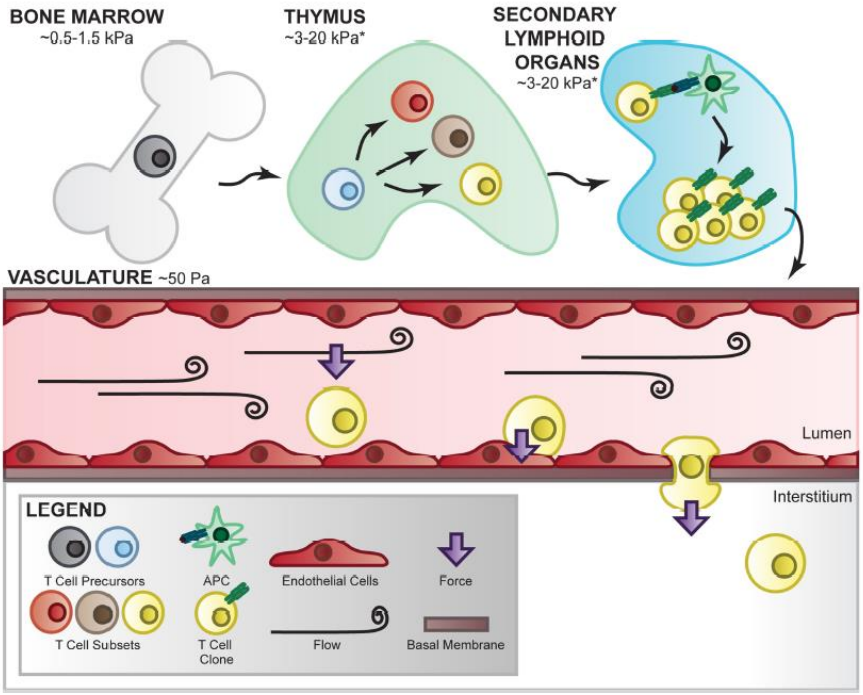

Figure 3-6-9. Mechanical attributes of T lymphocyte tissue microenvironment. T lymphocytes encounter diverse tissue microenvironment with varying mechanical properties during their lifetime. Its development begins in the bone marrow and continues in the thymus after which mature T lymphocytes are released into peripheral blood circulation and lymphoid organs. All these tissue sites vary in their physical properties and ECM composition which affect T lymphocyte phenotype and function. Trafficking through different tissue sites subjects T lymphocytes to shear force, deformations and cell contacts. These events provide vastly different mechanical cues that regulate T cell function and fate. *(Adapted from Harrison et.al. Front Physio. 2019* [315]*.)*

Mechanical cues also play an indispensable role in the function of cytotoxic T lymphocytes (CTLs) [334]. CTLs bind to target cells and locally release perforins and granzymes-containing lytic granules into the synaptic region. Formation of a secure immune synapse is therefore, essential for killing of target cells while reducing bystander damage. Immune synapse formation is driven by PI3K activity-mediated F-actin polymerisation [335]. Disruption of immune synapse formation impairs targeted cytotoxic function of CTLs. PI3K activity is

facilitated by Dedicator of cytokinesis 2 (DOCK2) which recruits DOCK2 to the membrane. PI3K activity is however inhibited by a lipid phosphatase, Phosphatase and tensin homolog (PTEN) [335]. DOCK2-deficient cells were impaired in their cytotoxic ability and measurements showed low force generation at the synapse of these cells with target [334]. Cells lacking PTEN however, showed considerable increase in force generation at the immune synapse. Direct inhibition of PI3K interfered with actin-myosin activity and abrogated force generation at the synapse. Abolishment of forces severely impaired CTL function. By artificially manipulating membrane tension of the target cell, it was observed that increasing target cell membrane tension enhanced formation of perforin pores in the target membrane facilitating its lysis [334]. Thus, mechanical forces at the immune synapse acted to increase membrane tension of the target cell, that potentiated its killing by CTLs (Fig. 3-6-10). This study was validated by recent findings which studied immune synapse formation between CTLs and target cells in three-dimensional culture. CTLs grown on micropillar arrays extend membrane protrusions that exert force as measured by micropillar deflection [336]. Release of lytic granules actively occurred in areas of deflecting micropillars. Detailed analysis found that these force exerting areas were actin-rich membrane protrusions whose formation was driven by cytoskeletal WASp and Arp2/3 actin nucleation proteins [336]. These protrusions were essential for force-mediated target cell killing. Force-mediated deformation of target cells also facilitated deposition of perforins and granzymes and subsequent lysis [336].

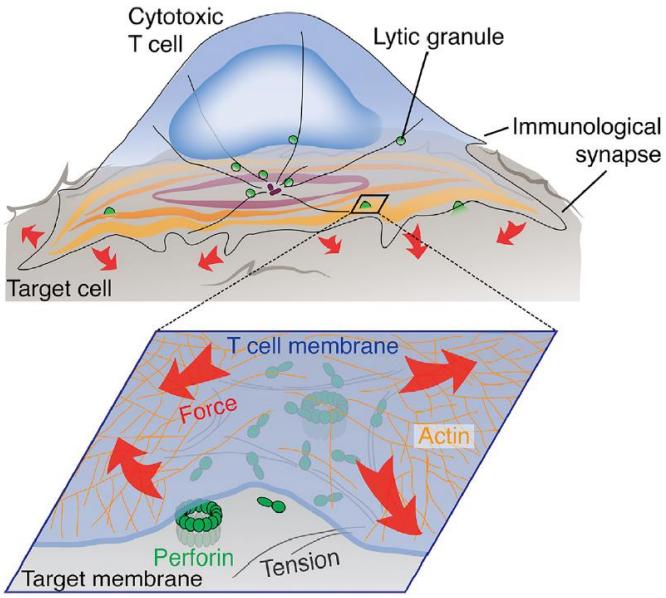

Figure 3-6-10. Mechanoregulation of cytotoxic T lymphocyte (CTL) function. The immunological synapse formed between CTL and target cell is characterised by generation of strong mechanical forces. Force exertion across the synapse is essential for efficient CTL killing. Contractile forces generated due to CTL actin cytoskeletal activity increases membrane tension of the target cell, thereby facilitating deposition of cell-killing machinery (perforins and granzymes). (Adapted from Basu et.al. Cell. 2016 [334].)

T cell function requires active migration from blood to peripheral lymph nodes and inflamed tissues. T cell infiltration to the LN consists of a series of mechanically regulated steps of rolling along the endothelial wall, arrest and adhesion on sites of high endothelial venules (HEVs), followed by their transmigration across these sites to the LN [219,315] (Fig. 3-6-11). Rolling and subsequent arrest on the endothelial wall is mediated by adhesion proteins like selectins and integrins. These proteins respond to mechanical shear stress generated from blood flow [337]. Shear stress induces conformational changes of these selectin and integrin proteins and reinforce their binding to their respective ligands through inside-out signalling [338,339]. Force-driven stable interactions between T lymphocytes and the endothelial wall

facilitates extravasation of these cells to the LN or damaged tissues. In these compartments, T cells migratory behaviour is significantly regulated by the mechanical properties of the tissue. T cells undergo durotaxis where they migrate preferentially to stiffer sites like inflamed tissues [340]. T cells like all immune cells generate forces which aid cell migration. The forces are generated from the actomyosin cytoskeletal network [231,341]. Migrating immune cells extend actin-myosin rich membrane protrusions that exert traction forces against the substrate. Traction forces also serve to locally activate integrins and facilitate ICAM adhesion-based migration through tissues [340]. Chemotaxis is a crucial process which enables directional movement of immune cells along chemokine gradient. Directional movement is maintained by inducing cell polarity [342]. Moving T cells are exposed to various topographical cues and experience significant membrane stress. Membrane stress has been associated with driving F-actin based cell polarity and directional migration [343]. Immune cells have also been shown to sample its 3D environment for mechanical cues. It has been shown that leukocytes use their nucleus to gauge mechanical resistance in 3D environments and actively change their nuclear position in order to adopt the path of least resistance [344]. Mechanotransduction during T cell motility is a developing area and needs further studies to analyse underlying mechanisms.

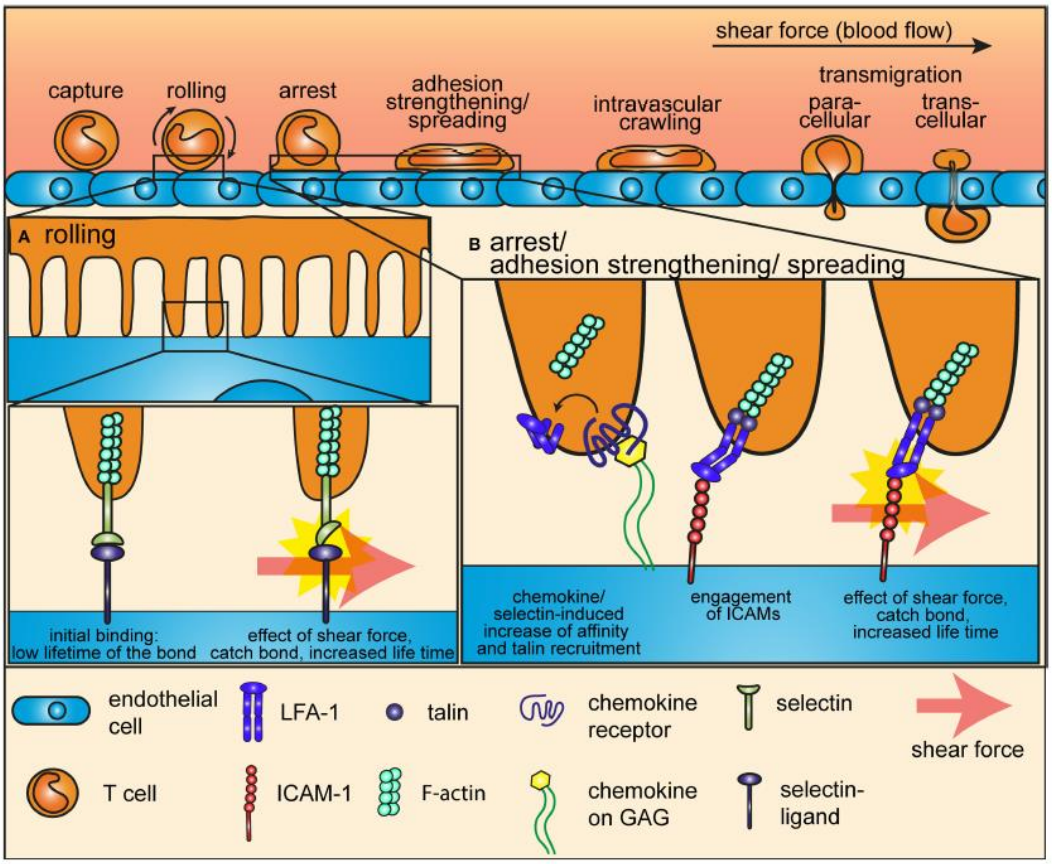

Figure 3-6-11. Mechanoregulation of T lymphocyte motility. Migration of T lymphocytes is a multi-step process involving crawling, rolling and adhesion followed by transmigration across the endothelial wall. Shear stress, generated from blood flow, plays an essential role in mediating T lymphocyte crawling and adhesion to the endothelial layer of blood vessels. Rolling along endothelial layer is driven by selectin-integrin binding. Strength of integrin-selectin binding is enhanced by shear force, thus displaying properties of a 'catch bond' (A). Diapedesis across the endothelial layer requires lymphocyte arrest and firm adhesion to HEV (high endothelial venule) regions. This interaction is facilitated by ICAM-LFA-1 integrin binding which is also regulated by shear forces (B). *(Adapted from Rossy J. et.al. Front. Immuno. 2018.* [340] *.)*

Since mechanotransduction plays such an integral role in T cell physiology and function, numerous attempts have been made to exploit its mechanotransduction property to activate or alter its behaviour in diseased states. Adoptive transfer of in-vitro activated T cells is being

considered as a promising strategy in infectious diseases and cancer [345]. T cells are being engineered so as to enhance its antigen binding ability and responsiveness. T cells expressing chimeric antigen receptors are being developed towards this end [346]. These engineered T cells, however require ex-vivo expansion and activation to its full potential before being adoptively transferred. Since TCRs show considerable mechanosensitivity, activation surfaces with different mechanical properties including stiffness, ligand spatial arrangements are being designed so as to achieve optimal T cell activation [347]. The use of CAR T cells in cancer immunotherapy seems to have promising benefits. A major caveat in this method is its failure to act against soluble tumour antigens. CAR T cells, however show robust response against membrane-bound antigens thus alluding towards a potential role of membrane mechanotransduction in their behaviour [347]. An interesting study reported that soluble immunosuppressive TGFβ can activate anti-TGFβ CAR T cells towards immunostimulatory phenotype. It was shown that TGFβ induced actin-driven TCR clustering of CAR T cells that led to generation of active tensile forces [348]. Dampening force generation in these cells by extending TCR extracellular spacer regions and disrupting mechanical interactions between ligand binding and signalling domains, severely impaired T cell activation in response to appropriate ligands [348]. Exploiting T cell mechanosensitivity in immune therapy, however requires further detailed elucidation of mechanotransduction pathways involved in their phenotype, activation and function. The knowledge will considerably enhance scope for T cell engineering in ways that will allow their selective and optimal activation in mechanically altered inflamed tissue sites.

3.6.6 Identification of potential mechanosensors

The process of mechanotransduction requires candidate proteins that can sense mechanical forces and modulate their activity so as to convert mechanical cues into biochemical signalling. Extensive research in this field has led to the identification of various proteins, that have the ability to respond directly to mechanical cues through either change in conformation or activation status. A review by Chen et.al., (2017) [349], describes that the process of cellular mechanotransduction can be divided into 4 stages. The first stage where the cell is exposed to mechanical cues is known as 'mechanopresentation'. This stage is followed by 'mechanoreception' where the mechanoreceptor senses mechanical cues and undergoes a change in its structural or activation behaviour. The stage of 'mechanotransmission' requires propagation of mechanical signals from the mechanoreceptor to downstream signalling molecules. The final stage, 'mechanotransduction' requires all the above events to culminate into a biochemical signal that affects changes in cell activity. In the following section, I will briefly describe few potential mechanosensors that play crucial roles in a number of cellular processes.

Adhesion proteins: Cells and tissues experience considerable mechanical stress at their interacting surface. Focal adhesion (FA) sites are considered to be the primary hotspot for force generation and sensing as a result of tissue interaction with the ECM [350]. Proteins involved in FA like integrins, focal adhesion kinases (FAKs), etc., display significant attributes of a mechanosensor [351,352]. Integrins form intense connections between the ECM and cell interior. It has been shown that its affinity for ECM ligands is modulated by mechanical cues which can be either external cues or cell-intrinsic. Integrin activity is modulated by ECM composition controlled mechanical stiffness [351]. Moreover, due its strong interactions with

the cell cytoskeletal components, cell-intrinsic force generation as a result of cytoskeletal activity produces a change in integrin conformation and increase in ligand affinity through a mechanism of inside-out signalling [351]. Thus, integrins are highly sensitive to mechanical cues and play a significant role in mechanical force-regulated processes like cellular migration, cancer cell metastasis, surface-receptor-mediated signalling etc. Studies have shown that recruitment of FAKs to FA is dependent on mechanical signals [352]. Its autophosphorylation-dependent activation is regulated by mechanical forces and mechanical manipulation like stretching, increasing rigidity of substrate tends to enhance its activation. FAK activity and cytoskeletal force generation shows strong feedback regulation [352]. Other adaptor proteins like talin, vinculin and paxillin that are involved in establishing cytoskeletal contacts with cell surface receptors also show immense sensitivity to mechanical cues [353]. Their ability to bind to target proteins, undergo conformational changes and activation are strongly regulated through mechanical forces. They play crucial role in mechanotransduction from the cell surface to the cell interior.

Cytoskeletal network: The cell cytoskeleton consists of actin filaments, microtubules, intermediate filaments and their interacting proteins. The cellular cytoskeletal network undergoes dynamic changes depending on cell morphology, movement and activation. Cytoskeletal activity is broadly regulated through transduction of external mechanical cues [354]. Cytoskeletal network also acts as source of contractile force generation [354]. Cytoskeletal tension level serves as a meter that regulates quality of mechanotransduction of external forces while generation of intracellular forces. F-actin polymerisation and their contraction through myosin motor movement determine their tension and contractility. Activity of the actomyosin network is regulated by proteins like Arp2/3 nucleation factor, Rho-ROCK

signalling proteins, etc [354]. Disruption of cytoskeletal network by impairing activity of any one of these components, affects cytoskeletal tension, force propagation and generation.

Nucleus: Recent reports have attempted to study the potential mechanosensing capacity of nucleus in cells. These reports show that the nucleus is highly responsive to mechanical cues [355]. Mechanical forces trigger changes in its membrane and laminar structure and composition, while also affecting chromatin organisation and consequent gene expression patterns. Forces are transmitted from the cytoskeleton to the nucleus through the LINC (linker of nucleoskeleton and cytoskeleton complex) proteins [355]. The nucleus also responds to mechanical forces by spatial reorganisation of its chromatin that can lead to selective activation or silencing of genes [126]. Genes displaced towards the nucleus boundary generally tend to undergo silencing while those centrally placed generally undergo activation. Nuclear deformation due to physical forces produces chromatin decondensation thereby affecting the epigenetic state of chromatin. External force application also produces chromatin stretching and activation of transcription. Certain models also show that the NPC (Nuclear pore complex) undergoes conformation changes in response to external mechanical forces, thereby regulating import and export of transcription activation/inhibitory factors across the nucleus [356]. More studies are needed to decode the process of nucleus mechanosensation.

Cell -surface receptors: Many cells require membrane proteins act as mechanoreceptors by sensing physical cues at the cell surface, like shear stress or forces generated during membrane interactions. Platelet adhesion and aggregation at sites of vascular injury is a process tightly regulated my mechanical forces [357]. Platelet adhesion to the vascular subendothelium occurs through binding of glycoprotein (GP) Ib complex subendothelium via the ligand von Willebrand's Factor (VWF). GPIb-IX binding to VWF is initially weak and is

strengthened by shear-force mediated structural changes in the GPIb-binding A1 domain of VWF [357]. Moreover, the GPIb protein has a mechanosensory domain that unfolds in response to external mechanical force. This causes platelet activation with release of intracellular Ca^{2+}, integrin activation leading to subsequent adhesion and aggregation. Thus, GPIb acts as a mechanoreceptor whose activity triggers platelet-mediated clotting process [357]. The endothelial proteoglycan-glycoprotein layer (glycocalyx; GCX) has been shown to act as mechanosensors that regulate vascular tone and permeability [358]. The GCX primarily composed of glycoproteins that consists of oligosaccharide chains containing salicylic acid residues, and proteoglycans with glycosaminoglycans side chains [358]. It has been shown that mechanical shear stress stemming from circulating blood is responsible for maintaining vascular tone [358]. The GCX components have been implicated in shear stress-mediated release of nitric oxide and subsequent triggering of signalling that causes vasodilation. GCX components, therefore act as mechanosensors that sense and respond to shear stress [358]. Also, endothelial cells tend to align in along the direction of shear stress during angiogenesis, process that is dependent of GCX-mediated mechanotransduction [358]. Transient receptor potential (TRP) channels comprise a group of proteins that respond to mechanical stimuli [359]. They sense mechanical cues including changes in osmotic pressure [360]. These ion channels respond to membrane stretch causing influx of extracellular Ca^{2+} leading to induction of downstream signalling pathways. Their mechanosensation property has been implicated in various physiological processes like, stretch-induced muscle damage, Duchenne muscular dystrophy, regulation of vascular tone in response to blood pressure, etc [359]. The TRPV (transient receptor potential vanilloid) mechanoreceptor family also plays a similar role in regulating cell volume by sensing changes in the osmotic pressure of cells. They are widely expressed in osmosensory neurons, smooth muscle cells of blood vessels and epithelial cells

[359]. This family of mechanoreceptors sense mechanical membrane stretch in response to osmotic swelling or shrinkage and participates in regulation of cell morphology and function.

3.6.7 Putative T cell mechanosensors

Since mechanotransduction is central to T cell function, numerous studies have reported potential mechanoreceptors that can sense and respond to mechanical stimuli (Fig. 3-6-12). As already discussed earlier, the TCR complex has been designated as an anisotropic T cell mechanosensor, due to its ability to functionally respond to mechanical forces [361]. The FG loop in Cβ domain of the TCRαβ has been shown to be the transducer of mechanical forces through changes in its conformation and induction of signalling [361]. Application of external forces of ≈50pN to the TCR complex resulted in downstream TCR triggering induced Ca^{2+} influx. Forces that did not act through the TCR complex failed to induce TCR activation. Directionality of force application also seems relevant since some studies have reported that application of shear-like tangential forces to the TCR complex were more efficient in triggering a TCR response [362]. These reports led to the development of the TCR complex as a highly probable candidate or mechanosensation. Many reports have also considered integrin adhesion receptors as potential mechanosensors in TCR signalling. As aforementioned, integrin activity is strongly regulated by mechanical forces [363]. Their affinity to extracellular ligands and subsequent activation is subjected to a positive feedback loop mechanism of inside-out signalling triggered by mechanical forces. Initial TCR binding to cognate antigens triggers downstream signalling activity which includes local actin cytoskeletal rearrangement at the TCR-APC contact region. Contractile actomyosin activity exerts pulling forces on the LFA-1 integrin molecule tethered to the membrane [364]. These forces induce a conformational change in the LFA-1 molecule which increases its ligand-binding capacity, subsequently strengthening LFA-1 and ICAM-1 adhesion to APCs [363]. This enhances interaction between interacting partners, strengthening TCR triggering and downstream signalling. A recent report

delved into the modes of T cell mechanosensing depending on the choice of mechanoreceptor. When T cells were allowed to adhere to substrates of varying stiffness only by means of TCR-antigen interactions, T cells responded to stiffness in a biphasic manner [365]. It showed peak T cell activity, as measured by extent of cell spreading, only at optimal substrate stiffness below and beyond which T cell spreading was suboptimal. This optimal value of substrate rigidity was comparable to physiological stiffness values of APCs. If T cells were allowed to adhere to substrates by means of more interactions like LFA-1 integrin binding in addition to TCR-mediated binding, this bimodal mechanoresponse was abolished. Instead, cell spreading continued to increase with increasing substrate stiffness till it reached saturation [365]. This differential response is brought into effect through downstream engagement of cytoskeletal actin networks and requires further clarification. T cell binding to cognate antigens on APCs involves extensive cytoskeletal rearrangement at the developing synapse. It involves active movement of TCR microclusters towards the immune synapse which is essential of sustained yet regulated TCR signalling [366]. It has been reported that Cas-L protein is highly expressed in T cells and acts as a mechanosensor during the formation of T cell-APC immune synapse [367]. Cas-L is recruited to developing immune synapse where it senses mechanical force generated from actin polymerisation [368] and myosin-driven contractility, where it subsequently gets activated through Lck-dependent phosphorylation [369]. Activated Cas-L promotes integrin activation through inside-out signalling and facilitates stronger T cell-APC adhesion [370,371]. Activated Cas-L associates with TCR microclusters and signalling proteins while causing stabilisation of the immune synapse between T cells and APCs so as to facilitate sustained TCR signalling [370,371].

While the above findings suggest many probable mechanoreceptor candidates for T cell signalling, it is however, necessary to formulate a T cell mechanotransduction model with an

appropriate mechanosensor protein. A model T cell mechanosensor must have the capacity to sense mechanical cues at surface during the initial preceding stages that lead to TCR triggering. Although these candidate proteins show strong sensitivity to mechanical cues by responding structurally and/or functionally to mechanical forces, none of them show any intrinsic mechanosensitivity. Their activity is not exclusively regulated by mechanical forces and they more than often need to interact with signalling-potent partners to execute their function in response to external forces. For example, while the activity of the TCR complex can be modulated by mechanical forces, it cannot be activated solely by mechanical forces. Numerous studies have shown that the TCR complex cannot be triggered solely by the application of non-specific mechanical forces [361, 362]. TCR crosslinking by TCR-specific antigen-MHC complex is indispensable in the process of T cell activation through mechanotransduction. Other candidates like integrins and Cas-L, show activation downstream of initial TCR activation and hence, cannot serve as the mechanoreceptor that gather initial mechanical cues responsible for TCR activation. This necessitates the identification of other proteins that are dedicated mechanosensors, and are singularly and independently activated in response to mechanical forces that trigger TCR signalling.

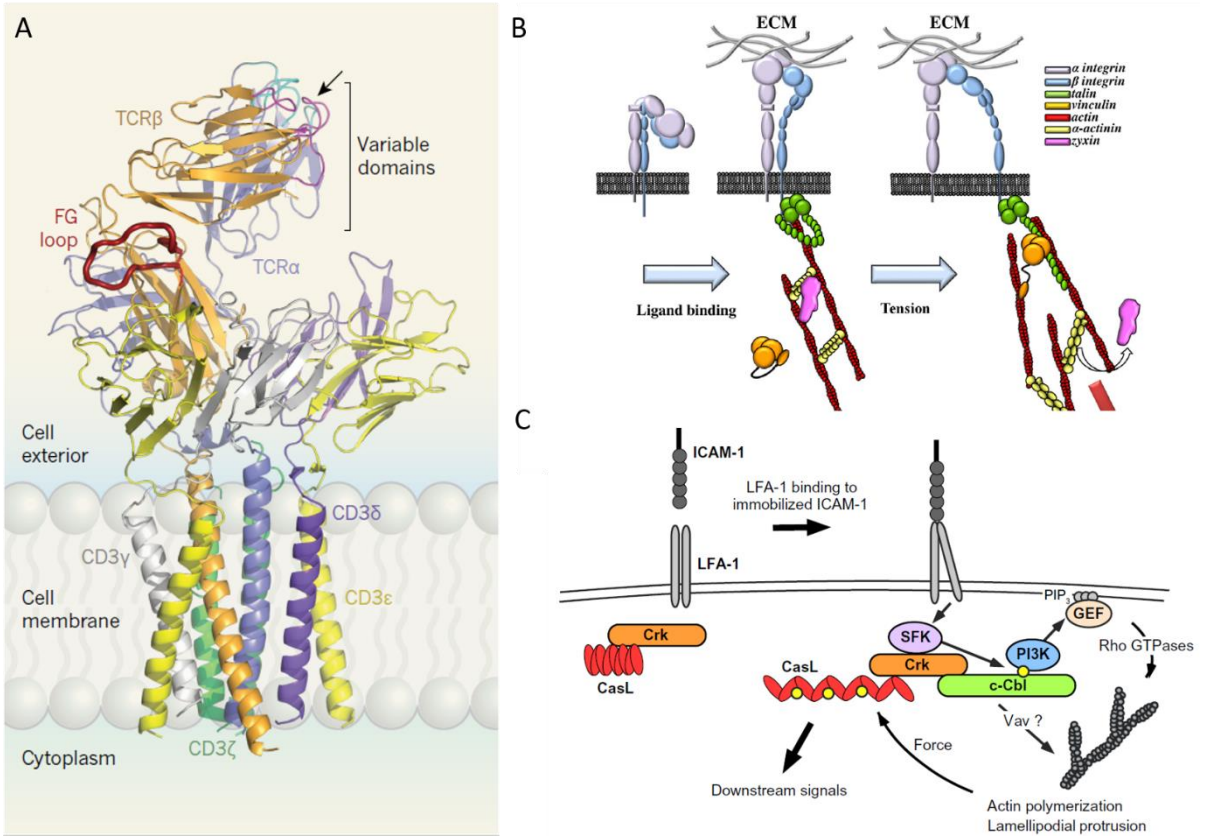

Figure 3-6-12. Putative T cell mechanosensors. The αβ TCR was proposed to be an anisotropic mechanosensor since it was shown to undergo changes in conformation in response to mechanical forces. The FG loop of the Cβ domain was shown to be the transducer of mechanical force to downstream signalling molecules (A). Integrin binding to ECM components is dependent of internal forces. Contractile forces generated by cytoskeletal activity exerts tension on the tethered integrin molecule which undergoes structural change and enhanced binding capacity to ECM components (B). T lymphocyte LFA-1 binding to ICAM triggers activation of Src family kinases (SFK) which promotes phosphorylation of c-Cbl. Phosphorylated c-Cbl recruits PI3K which subsequently activates Rho-GTPase-dependent actin polymerisation. F-actin exerts contractile forces on CasL causing it to transition to an 'open' state where its phosphorylated by Src kinases. Phosphorylated CasL subsequently recruits a number of T cell signalling proteins that determine T cell function in response to force (C). *[Adapted from Reinherz EL. Nature. 2019 (A) [361], Janoštiak R. et.al. Eur J Cell Biol. 2014 (B) [370], Roy NH. Et.al. Sci Signal. 2018 (C) [371].]*

Chapter 4. Piezo mechanosensors

Piezo proteins belong to a class of evolutionarily conserved ion channels that are gated by mechanical force [372]. Their activation by mechanical forces allows passage of extracellular cations like Ca^{2+}, Mg^{2+} and Na^{+} into the cell. Hence, these channels can be effectively blocked by cation channel inhibitors like ruthenium red [373]. There are two homologs of this protein: Piezo1 and Piezo2 coded by FAM38 and FAM38B respectively [373]. Piezo1 proteins are widely expressed in mechanically active tissue compartments like red blood cells, endothelial cells, epithelial lining, skeletal tissues, etc. Piezo2 is primarily associated with tactile sensation in neuronal cells [374]. The identity of a dedicated mechanosensor in vertebrates remained elusive until Coste et.al [373] identified Piezo1 and Piezo2 channels as sensors of mechanical force. They performed a microarray profiling of Neuro 2A mouse cell line that show rapidly adapting mechanically activated (MA) currents when mechanical force was applied externally on the surface by means of piezo-electrically driven probe. Electrical currents were measured by the patch-clamp method. Enriched transcripts that were detected by microarray were the downregulated by siRNAs and their effect was observed on the generation of these MA currents. Downregulation of FAM38A gene (coding of Piezo1) caused a significant reduction of MA currents. Overexpression of Piezo1 and its homolog Piezo2 in other cells led to generation of large currents in response to mechanical stimuli [373].

4.1 Structure of mammalian Piezo channels

The structure of Piezo1 was elucidated through cryo-electron microscopic studies of mouse Piezo1 protein [375,376]. It has a homo trimeric structure consisting of 3 curved blades, arranged in a propeller-like fashion around a central ion-conducting transmembrane pore, that is

attached to a cap-like domain which forms the C-terminal extracellular domain (CED) (Fig. 4-1). Topology modelling through bioinformatics-based predictions claims that each blade possesses 38 transmembrane segments [377,378] (Fig. 4-1-2). Each blade in the trimeric structure consists of 6-9 repeating units of transmembrane helices known as piezo-repeats. The extracellular blades are highly flexible and their position in the plasma membrane induces local membrane curvature [379]. 3D mapping has revealed various motion-based orientations of these blades [380]. Their alignment with respect to the cell membrane and their structural flexibility may enable them to act as effective sensors of mechanical force on the cell surface. Piezo1 proteins also contains 3 rod-like domains that interacts with the intracellular region of each blade and connects to the central pore via an anchor region and also to the C-terminal domain (CTD) [376,378]. Since this intracellular beam region is accurately positioned between the force-sensing extracellular blades and the ion-conducting central pore, it is an ideal structure to transmit mechanically-induced conformational changes of the extracellular and peripheral transmembrane domains to the central pore [377,378]. Thus, it acts as potential transducers of mechanical force and regulates channel activity. The CED which forms a cap-like structure topping the central pore [376]. Experimental evidence shows that this region is likely to determine ion-conducting properties of this channel. Deleting the cap domain that is positioned above the transmembrane core or mutating its acidic residues altered the ion-permeation property of this channel suggesting that it allows selective passage of cations over anions [381]. The C-terminal domain mostly located in the central pore has been found to interfere with channel conductance, ion sensitivity and RR-mediated inhibition. Mutations of the E2133 glutamate residue in this region that neutralised, reduced side chain length or replaced its charge with a positive residue have been shown to affect conductance capacity

and ion preference [377]. The extracellular cap domain also contains 3 subdomains that have been shown to regulate inactivation kinetics of Piezo1 proteins post-stimulation [376].

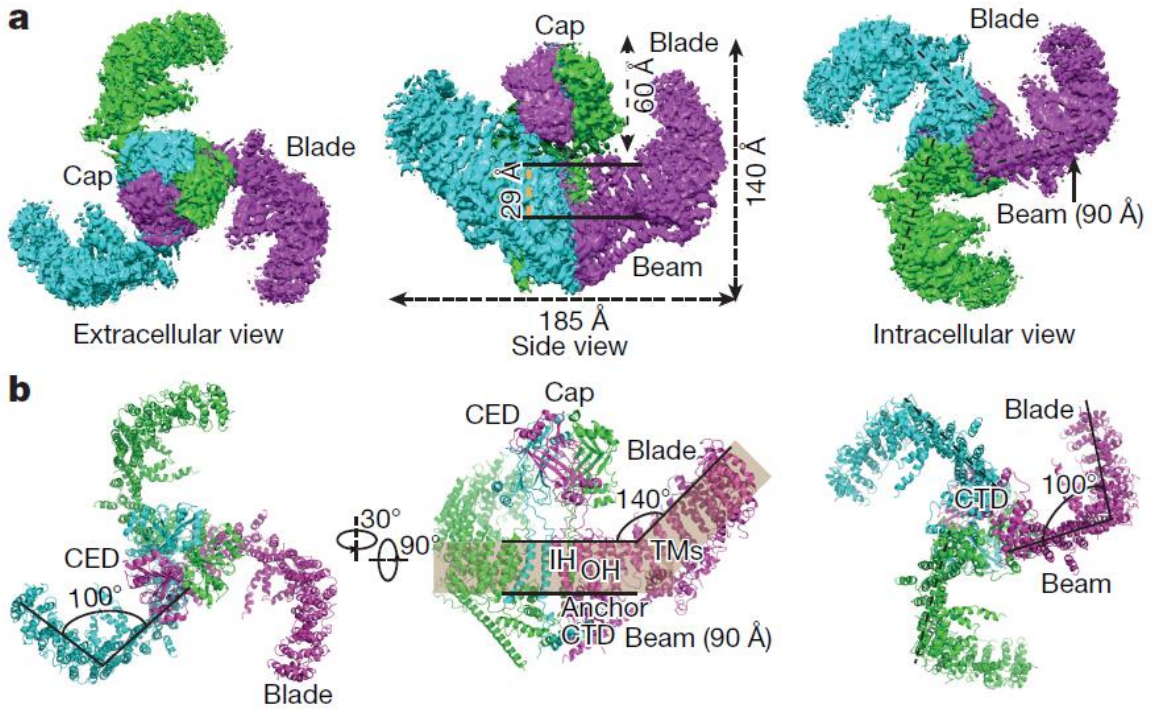

Figure 4-1-1. Architecture of mammalian Piezo1 channel. Piezo1 channel has a trimeric structure. It has a 'cap' domain that covers the central ion-conducting pore. The extracellular domain of the 3 subunits were arranged in a propeller blade-like fashion. The 'beam' domain serves to anchor the extracellular blades with the central pore. The image represents the cryo-electron map at a resolution of 3.97 Å (a). The images are cartoon model representative of the same with the blade regions removed to allow better viewing of the orientation of the transmembrane helices forming the protein subunits (b). *(Adapted from Zhao et.al. Nature. 2018. [380])*

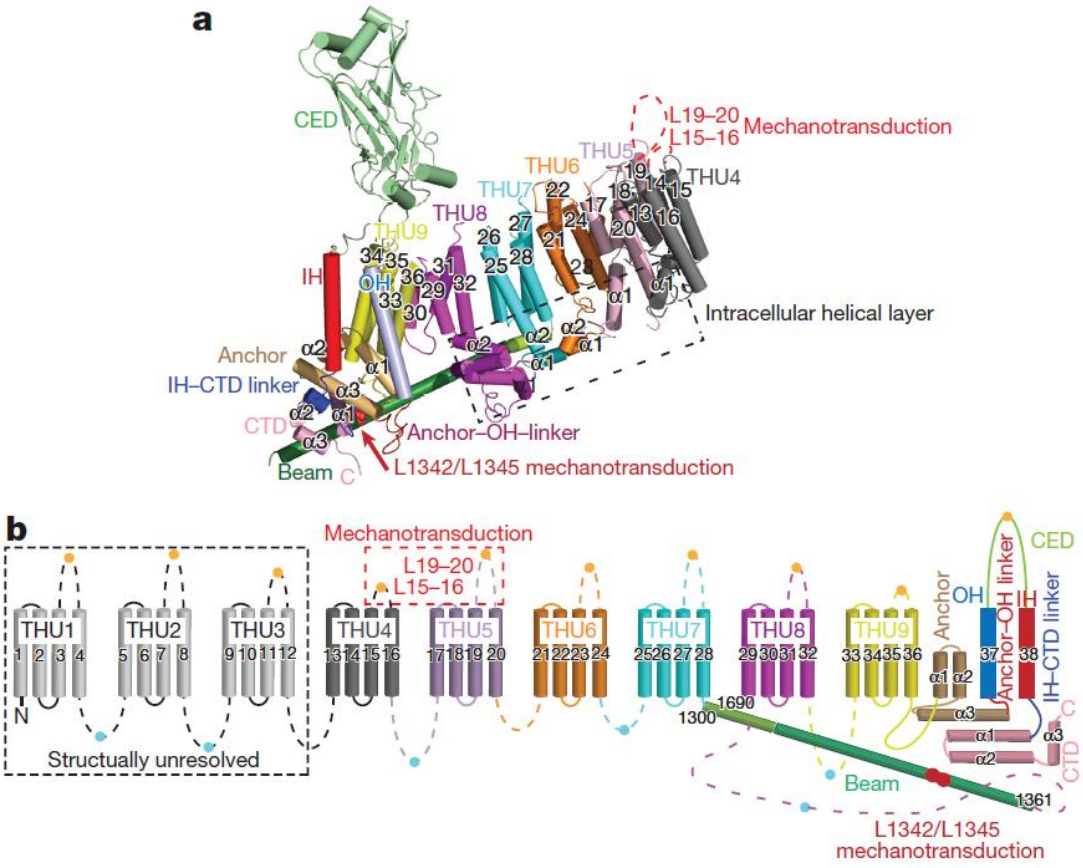

Figure 4-1-2. Configuration of the repetitive transmembrane helical units (THUs) forming the Piezo1 channel. The Piezo1 channel is a homotrimeric protein with each subunit consisting of 38 transmembrane helices ™. Representative cartoon image of the arrangement of THUs forming individual domains of each subunit (a). Resolved 38-TM model with individual THUs attributed to each domain and function (b). *(Adapted from Zhao et.al. FEBS J. 2019.* [(324)]*)*

It was assumed that Piezo2 structure will be highly close to that of Piezo1 due to similarity in pore-domain sequence, overall size and topology modelling. A recent study by Wang et.al., [(383)] resolved the structure of Piezo2 through cyro-electron microscopy. The study revealed a similar trimeric architecture where each blade consists of 38 transmembrane helices. The 3 extracellular blades curve to form a dome-like structure that guards the central ion-conducting pore. The entire structure is capped by a cap-like domain similar to Piezo1. The

ion-conducting pore has transmembrane and cytoplasmic have constriction sites that may regulate its gating mechanism [384]. It has been observed that sensory neurons express a wide range of spliced isoforms of Piezo2, while those non-sensory cells usually express a single spliced variant [385]. By analysing exon sequences frequently subjected to splicing, it was found that certain sequences mapped to the intracellular loop regions of this protein. Cryo-electron microscopic structures did not provide enough resolution to determine loop positions but because it is placed near the C-terminus region it might be involved in interactions with central pore. These spliced variants were cell-specific and show altered mechanical sensitivity, with some showing faster inactivation rates of the channel further supporting the role of these loop domains in tuning channel sensitivity [385].

4.2 Gating of Piezo channels

2 general models have been described to explain the gating mechanism of channels that are activated in response to mechanical force.

The **force-from-lipid** principle [386] of mechanical gating explains that unlike moving soluble molecules that are subjected to uniform forces from interactions with neighbouring molecules, molecules in a lipid bilayer are subjected to constant anisotropic forces. These forces are inherently generated during assembly of the lipid bilayer, and are constantly exerted during maintenance of the lipid bilayer integrity. These forces are analogous to surface tension that is generated in a water-oil interface and are mainly concentrated at polar-nonpolar junctions in the bilayer. Membrane lipid molecules tend to assemble into compact sheet forms in order to reduce surface tension. Surrounding water molecules interact with polar head groups of the lipid layer, while non-polar chains are sequestered. This creates a strong lateral force that is balanced by intermolecular repulsion between

hydrocarbon tails and polar heads. Thus, in equilibrium, force is uniformly distributed throughout the bilayer. Therefore, proteins that are inserted within the lipid bilayer are subjected to directional forces. Application of external force or chemical modifications to the lipid membrane that produce membrane deformations or membrane strain, can alter the direction of these internal forces, causing the inserted protein to change their conformation and consequently affecting their function. A classic example of this gating principle is bacterial mechanosensitive channels MscL and MscS [387]. These channels are gated in response to mechanical forces that produces a change in resting membrane tension. Experiments in which these channels have been reconstituted into artificial lipid bilayers have shown that membrane stretch alone is sufficient to open these channels. Presence of other proteins or cytoskeletal components is not needed for channel activity [387]. Eukaryotic two-pore domain potassium channels (K2p) also fall under this category of mechanical gating [388]. In this model, modification of the resting tension of the lipid bilayer is sufficient to transduce alterations in lipid-protein interaction thereby leading to channel activation (Fig. 4-2-1a.).

The **force-from-filament** or the tether model of mechanical gating proposes that mechanosensitive channels are gated through force-dependent changes in their interaction with other proteins [389] (Fig. 4-2-1b). These mechanosensitive channels are tethered to intracellular cytoskeletal components. Cytoskeletal remodelling or changes in ECM interactions exerts mechanical strain on tethered mechanosensitive channels that might lead to conformation changed-mediated channel activation. The NOMPC channel belonging to the family of transient receptor potential channel (TRPC) protein is a classic example of tether model [390]. The cytoplasmic N terminus region of this protein is enriched in ankyrin repeats (AR) that associate with microtubules. This association is required for gating of the channel. By using deletional mutants of this channel in which AR were sequentially deleted, it was

shown that these repeats are essential for mechanical gating of these channels [390]. Amplitude of current generated from wild type and mutated channels were compared and it was observed that deletional mutants were impaired in their ability to respond to mechanical force. By inducing microtubule-depolymerising, similar impairment in mechanogating was observed thus providing evidence that force for gating is generated from cytoskeletal filaments [390]. This study, however, did not delve into the possibility of this mechanoreceptor interacting with adjacent lipid bilayer or whether any force is transduced through it. Integrin adhesion receptors are examples of this mechanism of mechanical gating. As discussed before, changes in cytoskeletal generated forces induces activation of tethered integrins through structural changes [363,364].

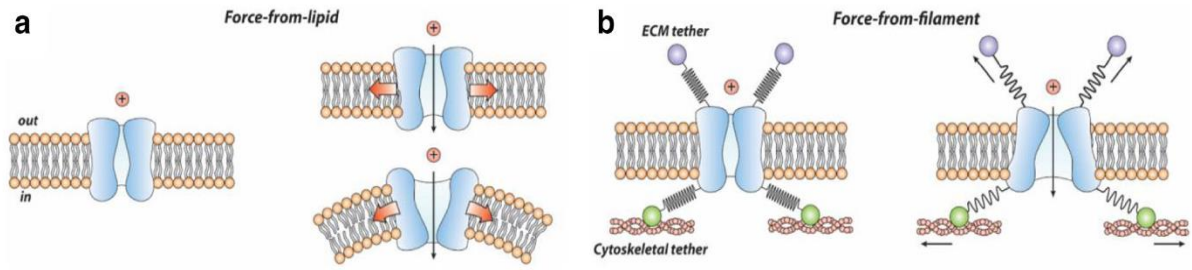

Figure 4-2-1. Gating strategies of mechanosensors. Two main models have been proposed to explain the gating mechanism of mechanosensitive channel. The force-from-lipid model postulates that changes in the lipid bilayer resting tension triggers opening of the channel (a). The force-from filament model states that external forces originating due to interaction with the ECM components or cell-intrinsic forces generated due to cytoskeletal tethering causes gating of the mechanosensitive channel (b). (Adapted from Ridone P. et.al. Biophys Rev. 2019 [378].)

4.2.1 Gating of Piezo channels through lipid bilayer tension

A report by Syeda et.al. [391] showed that Piezo1 channels are inherently mechanosensitive. They can be activated by changes in lateral membrane tension only and do not require any additional cellular components for gating. Purified Piezo1 proteins were reconstituted in artificial lipid bilayers and channel activity was recorded in response to mechanical stimuli generated by subjecting the lipid vesicle to an osmotic gradient. An osmotic gradient will produce changes in the droplet volume and concomitant asymmetric changes in membrane tension across the lipid bilayer. Since these lipid droplets were devoid of any cytoskeletal components or membrane proteins, this study proves that Piezo1 channels are gated through sensing of lateral membrane tension only. Disrupting cytoskeletal network through impairing actin or microtubule polymerisation did not impede Piezo1 activation. Piezo1 was also stimulated when cell membranes were mechanically stretched through patch clamping techniques. Piezo1 activity is measured by measuring Piezo1-activated currents, that are generated due to ion passage across the channel on activation. Application of positive and negative pressure to cell membrane patches induced local membrane curvature. Negative pressure applied to cell-attached patches produced convex curvature of the membrane, while positive pressure produced concave curvature. Membrane curvature induced Piezo1 activation and generation of Piezo1 currents [392,393]. Application of increasing positive pressure to the membrane patch generated Piezo1 currents of increasing amplitude. According to Laplace's law, pressure-induced changes in surface curvature is directly related to lateral tension ($T = R.\Delta p/2$; where T is the lateral tension; Δp is changes in applied pressure; R is the radius of curvature of the surface) [394]. Hence, pressure-induced changes in membrane curvature produces changes in the lateral membrane that leads to activation of Piezo1.

Gating of mechanosensitive MscL channel involves in-plane expansion of pore area [395]. Piezo channels, however, have low ion conductivity (100 times lesser than MscL) and are cation-selective [396]. Both these properties are inconsistent with a large pore diameter. It has been observed that Piezo1 reconstitution into lipid droplets induces a local membrane curvature [397]. Any lateral membrane tension that will trigger membrane flattening will lead to channel opening with expansion of the channel-membrane system, without actually increasing pore diameter [397]. This model is primarily based on the fact that piezo channel conformation is incompatible with planar membranes and electron microscopic images reveal local membrane curvature in Piezo occupied areas in lipid vesicles. But further studies about the natural state of Piezo channels in resting membranes in cells need to be elucidated. Cry-electron imaging of Piezo1 showed that it tends to adopt different degrees of curvature when reconstituted in lipid vesicles depending on the size and hence, curvature of lipid vesicles. Application of mechanical force causes flattening of Piezo1 with concomitant expansion of Piezo1 area consistent with open channel configuration [397]. Hence, changes in the lateral membrane tension can cause reversible changes in the Piezo1 conformation leading to its in-plane flattening and channel opening [395, 397] (Fig. 4-2-2).

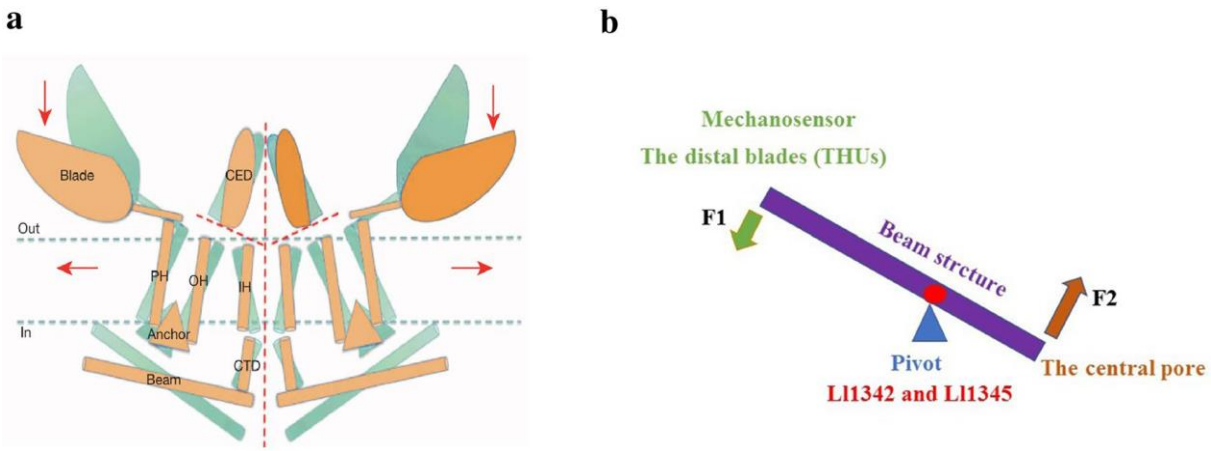

Figure 4-2-2. Gating of Piezo1 channels. Piezo1 channels senses changes in membrane tension. Lateral membrane stretch is sensed by force-sensing extracellular blades which causes change in Piezo1 structure, leading to its flattening and subsequent opening of the central pore. The blue model represents closed state of the channel while the orange model represents the open state (a). While the blades serve as force sensors, the beam region act as transducers of force through a lever-like mechanism. Upon exertion of external force on the distal blades, the beam (specifically amino acid residues, Ll1342 and Ll1345) acts as a fulcrum and transduces the force to the central pore which increases its diameter causing the channel to open (b). *(Figure adapted from Fang et.al. Cell Biosci. 2021[376].)*

4.2.2 Effect of cytoskeletal and ECM interactions on Piezo gating

Although the above reports conclusively show Piezo1 can be gated solely through changes in the lipid bilayer tension profile, there are many reports that show Piezo1 activity is regulated and modified through its interactions with cytoskeletal and ECM components [398]. During curvature-induced Piezo activation, different patch clamp configuration was applied to induce opposite curvatures [394]. It was observed that although Piezo1 was activated during both type curvature formation, its activity varied significantly in terms of current amplitude and threshold sensitivity. Concave and convex-curved membrane employ different degrees of cytoskeletal tethering on account of their differential geometry. Threshold forces required to activate Piezo1 differed between cell-attached versus inside-out configurations of patch clamp [398]. Since the cytoskeletal content associated with these configurations also varied, it is very likely that cytoskeletal contacts tune Piezo1 activity. Report by Cox et.al. [399] showed that Piezo1 proteins reconstituted in HEK293 membrane blebs devoid of any cytoskeleton were activated by membrane tension, confirming Piezo1 gating in response to lipid bilayer tension. But forces required for Piezo1 gating in cytoskeleton-free membrane bleb were

lower in magnitude as compared to that required for gating in whole cells. This increased sensitivity of Piezo1 to mechanical forces in the absence of cytoskeleton shows that cytoskeletal interactions tune Piezo1 responsiveness to tension. The cortical cytoskeleton confers a degree of 'mechanoprotection' to the cell by resisting changes in membrane deformation in response to mechanical stimuli thereby maintaining structural integrity [400]. Hence, presence of cytoskeletal interactions increases the threshold force required for Piezo1 gating. Piezo1 channels in whole cell is characterised by rapid inactivation post-stimulation. However, Piezo1 channels in artificial lipid membrane do not display such inactivation kinetics, suggesting that other proteins and cytoskeletal interactions regulate its activity [399,400]. Thus, although cytoskeletal interactions are not needed for force-induced Piezo1 gating, cytoskeletal tethering does influence gating kinetics and force sensitivity (Fig. 4.2.2).

Piezo activity is also regulated by interactions with the ECM (Fig. 4-2-3). Studies have shown their preferential localisation in regions of cell contact with the ECM [401]. Piezo channels localised to these contact regions show considerable increase in force sensitivity, as evident by lower magnitude forces needed to activate them in these sites [401-403]. AFM cantilever was used to apply pushing and pulling force to Piezo1 overexpressing cells and fluorescence - based Ca^{2+} detection was performed to measure Piezo1 response [404]. The AFM cantilever were coated with various ECM proteins to mimic Piezo1-ECM interaction. Piezo1 activation in response to pushing forces was unaffected by ECM coating suggesting that pushing force-mediated Piezo1 response was independent of ECM interactions [404]. When Piezo1 was subjected to pulling forces by means of ECM-coated cantilever, threshold force required for stimulation was well below threshold pushing forces required for the same [404]. Thus, this study suggests that ECM interaction along with directionality of applied forces may modulate Piezo1 response. Modulation of Piezo1 activity through ECM interactions was mainly

mediated through Collagen IV component of the ECM [404]. It has been shown that Piezo1 activity is regulated by ECM interactions in aggressive gliomas [405]. Piezo1 tends to localise in focal adhesion sites of ECM contact, where they enhance ECM stiffness through interactions with ECM components and positive feedback signalling.

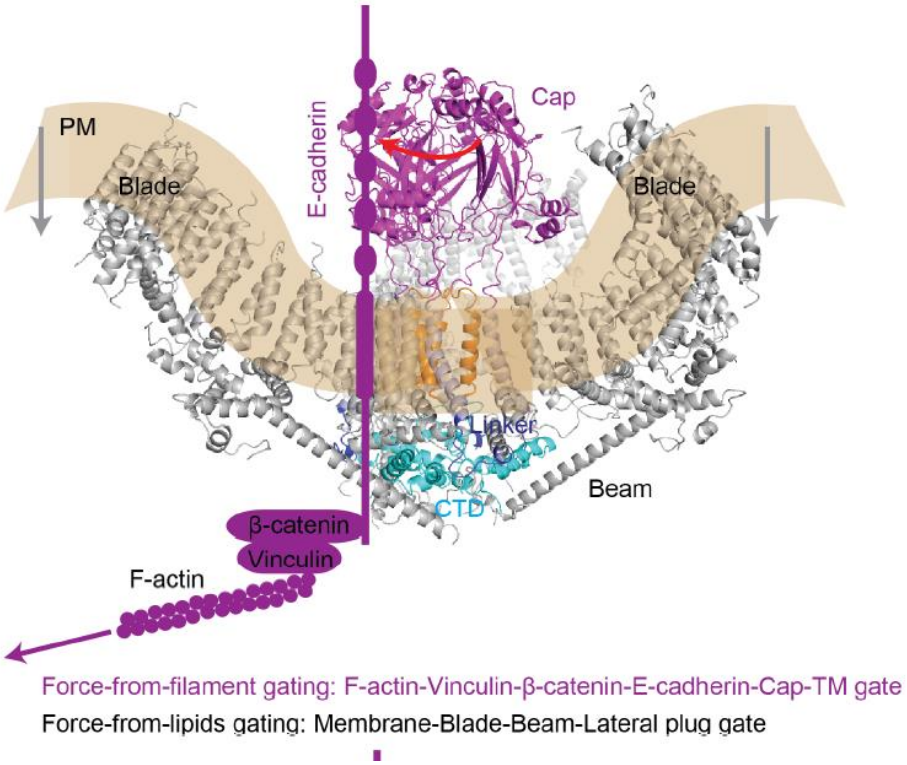

Figure 4-2-3. Influence of cytoskeletal tethering and ECM interaction on Piezo1 gating. ECM components like E-cadherin interact with the cap domain of Piezo1, thus tethering Piezo1 to the ECM. The cytosolic domain of the Piezo1 subunit interact with actin cytoskeleton through adaptors β-catenin and vinculin. This interaction with the ECM and cytoskeletal components regulates threshold sensitivity of Piezo1 to mechanical force, thus modulating its gating capacity. *(Adapted from Yang et.al. bioRxiv 2020.05.12.092148 [401])*

Piezo1 gating studies with intact cytoskeletal and ECM interactions is a closer simulation of physiological conditions and thus can provide a better understanding of channel mechanics.

It was also shown that STOML3 which is required of touch sensation, significantly modulates Piezo1 activity in rat sensory neurons [406]. By means of elastomeric pillar arrays, mechanical stimulus was applied to a defined area of the cell by deflecting a single pilus. Piezo channels showed acute sensitivity at substrate-cell interface. This significant sensitisation of Piezo channels by STOML3 ensures that stimuli applied on the skin surface maintains sufficient threshold values despite considerable attenuation by the time they reach nerve endings in the deeper skin layers [406]. In yet another studies, it was found that depletion of plasma membrane phosphoinositides, PI(4,5)P2 and PI(4)P that occurs downstream of TRPV1 activation results in Piezo channel inhibition [407]. Moreover, it has been shown that Piezo1 signalling leads to alterations in the composition of the lipid-protein bilayer of the cell membrane which in turn affects Piezo1 activity [408]. Piezo1 activity is also dependent on cholesterol-dependent formation of Piezo1 clusters [409]. Cholesterol depletion using methyl-β-cyclodextrin increases threshold forces required for activation. These findings suggest that a despite its inherent mechanosensitive property, a number of membrane and cellular components modulate Piezo channel activity.

4.3 Physiological roles of Piezo channels

Piezo-mediated mechanotransduction has been implicated in a wide range of physiological and cellular processes (Fig. 4-3). Abnormal Piezo signalling has been associated with pathogenesis in various disease conditions. Role of Piezo mechanotransduction in physiological processes and disease pathogenesis has been briefly described in the following section.

Regulation of stem cell differentiation

Stem cells are sensitive to numerous chemical, biological and biophysical cues from their microenvironment. The stem cell niche consists of various soluble or surface bound signalling molecules, an interactive network of a heterogenous of population of cells, the ECM and the mechanical microenvironment [410]. The biophysical cues in the stem cell niche play an indispensable role in determining stem cell fate [411]. Piezo1 mediated mechanostransduction has been found to play a crucial role in directing the fate of a number of stem cells. Human neural stem/progenitor cells (hNSPCs) highly express Piezo1 [412]. hNSPCs are highly sensitive to stiffness properties of the ECM [412]. These cells generate stiffness-dependent traction forces on the substrate which is sensed by Piezo1. Piezo1 activation on rigid substrates favour neurogenesis, while inhibition of Piezo1 directs the stem cell fate towards astrocytes formation. Nuclear translocation of transcriptional coactivators Yap/Taz downstream of Piezo1 activation was shown to affect lineage determination of these cells [412]. Similarly, Piezo1 activation also favours osteoblast differentiation over adipocyte differentiation of bone-marrow derived mesenchymal stem cells [413]. Studies have shown that bone mass is strongly correlated with physical activity, or in other words a mechanically stimulated microenvironment favours bone generation [414]. Piezo1 activation in response to hydrostatic

pressure results in upregulation of the bone morphogenetic protein 2 (BMP2) that drives osteogenesis [413]. It has recently been shown that enteroendocrine precursor cells in the Drosophila midgut highly express Piezo1 channels and mechanical activation of these channels mediates proliferation and differentiation of these precursors to enteroendocrine (EE) cells [415]. These EE cells are involved in a number of intestinal functions. Piezo1 mediates differentiation of these precursors to EE by Ca^{2+}-dependent inhibition of Notch signalling, while mediating proliferation of these cells through Ca^{2+}-dependent phosphorylation of ERK [415]. The gastrointestinal tract provides a mechanically stimulated environment that induces differentiation of cell types that regulate intestinal functions.

Regulation of vascular structure and function

Piezo1 channels mediate shear stress response in endothelial cells [416]. Piezo1-/- was embryonically lethal and embryos were characterised by severely under developed vascular structures with very few fully formed blood vessels. Endothelial cell migration in response to vascular endothelial growth factor (VEGF) was driven by Piezo1 activity. Piezo1 activity in response to shear stress was also found to trigger Ca^{2+}-dependent calpain 2 activation, that is involved in endothelial cells alignment by modulating actin cytoskeleton and focal adhesion turnover [416]. Maintenance of blood vessel tone in response to blood flow is essential for controlling arterial blood pressure. A number of factors that mediate blood vessel vasodilation in response blood flow shear stress are released by endothelial cells [417]. One of the major vasoactive factors released from endothelial cells in response to shear stress is nitric oxide (eNOS). It has recently been demonstrated that Piezo1 mediated sensing of shear stress leads to ATP release that activates purinergic receptors that results in downstream

activation of Akt pathway and phosphorylated eNOS production [418]. Thus, Piezo1 activity is required for maintaining blood pressure homeostasis.

Piezo1 is highly expressed in smooth muscle cells lining small-diameter resistance arteries particularly caudal and cerebral artery [419]. Resistance arteries undergo intense remodelling of the smooth muscle cells lining the blood vessel lumen in response to hypertension so as to maintain normal blood pressure [420]. Although loss of Piezo1 did not affect basal myogenic tone of these blood vessels, these channels mediated arterial remodelling under hypertensive conditions. Piezo1 activation under these conditions resulted in downstream activation of Ca^{2+}-dependent transglutaminases (TG) that is involved in structural remodelling of small arteries in response to high blood pressure [419]. Removal of the mechanoprotective influence of the cytoskeleton by specifically deleting the smooth muscle actin crosslinking filamin A, (smFlnA) increased the number of Piezo1 channels that were activated in small arteries in the absence of hypertension. The extent of arterial wall thickening significantly correlated with increased Piezo1 channel activity which was reversed when either of the Piezo1 alleles were deleted along with FlnA [419]. These findings indicate that mechanotransduction by Piezo1 channels play a crucial role in maintaining vascular structure and function in response to blood flow and pressure.

Chondrocyte mechanotransduction

Chondrocytes are subjected to considerable mechanical strain. It is known that post traumatic injury can lead to chondrocyte death that may culminate in debilitating osteoarthritis. Lee at.al. [421] showed that inhibiting Piezo channels with GsMTx4 leads to significant protection from mechanical injury triggered cell death. Inhibition of dynamin GTPase significantly strengthened GsMtx4 inhibition possibly by affecting membrane curvature and enhancing

insertion of GsMTx4. Both Piezo1 and Piezo2 mediate mechanically activated currents in chondrocytes and is believed to confer mechanosensitivity to these cells [421]. Further molecular details of the mechanotransduction pathway need to be elucidated. This finding could generate new therapeutic targets for treating degeneration of cartilage post injury and controlling posttraumatic arthritis.

Maintenance of epithelial cell homeostasis

Piezo1 activity has been shown to regulate epithelial cell density [422]. In cell-sparse areas cells tend to stretch, which activates these channels downstream of which, cell proliferation is triggered. In regions of cell crowding Piezo1 activation, however, induces extrusion of cells that will be destined for apoptosis [423]. This distinct response could be attributed to the ability of these channels to sense differential tension in these situations by localizing to different subcellular compartments. In regions of low cell density low levels of Piezo1 mainly resides in the nuclear envelope and accumulates over time. At higher densities they localise to the plasma membrane and endoplasmic reticulum where they mediate cell proliferation. At cell crowding stage they form large cytoplasmic aggregates [423]. More work has to be done to elucidate the differential response depending on kinds of the membrane tension these channels encounter.

Regulation of red blood cell (RBC) volume

Gain-of-function mutations of Piezo1 results in severely dehydrated RBCs, a condition termed as dehydrated hereditary stomatocytosis (DHS) associated with mild hemolysis [424]. RBCs are subjected to significant mechanical forces in circulation. Piezo1 mediated influx of Ca^{2+} in response to these forces, activate KCa3.1 or Gardos channels that allow efflux of K^+ and H2O resulting in RBC dehydration or volume reduction [425]. This Piezo1-mediated regulation of cell

volume aids a number of physiological process including facilitating movement of RBCs through narrow capillaries or concentration of haemoglobin in the cell periphery, that accelerate release of oxygen from haemoglobin. Loss of Piezo1 function in RBCs leads to overhydrated and osmotically fragile RBCs [425]. Interestingly, gain-of-function Piezo1 conferred resistance to malarial infection in mice [426]. RBC dehydration was primarily responsible for attenuated parasite growth and protection against cerebral malaria in these mice. Remarkably, about one-third of African population carry a gain-of-function Piezo1 mutation, E756del [426]. This mutant allele shows a high allelic frequency of 9%-23% in individuals of African origin. RBCs isolated from donors carrying this mutation displayed morphologies similar to those as hereditary xerocytosis as described earlier. These RBCs also showed significantly lower parasite load when infected with Plasmodium falciparum in comparison to RBCs isolated from non-carriers. These findings suggest that is gain-of-function Piezo1 mutant allele is under strong positive selection in African populations regions since malaria is highly prevalent in this region [426]. Although genome-wide association studies could not detect this mutant Piezo1 locus among the genetic loci responsible for conferring malarial resistance, this study provides strong experimental evidence and this Piezo1 locus can be further analysed in endemic malarial populations. Similar loss or gain-of-function Piezo1 mutations can be examined for their association with other disease phenotypes, that will provide critical understanding of the role of general mechanotransduction in physiological processes.

Light touch sensation and nociception

Piezo2 has been shown to mediate light touch sensation [427]. The merkel cell-neurite complex in the skin is a receptor for gentle touch [428]. Merkel cell and the afferent nerve fibres that

innervate them form synapses, that transmit gentle touch sensation in skin. Piezo2 is highly expressed in Merkel cells and synaptic nerve fibres [429]. Deletion of epidermal Piezo2 drastically reduced the ability of these cells to mediate slowly adapting currents in response to mechanical touch. Gentle touch is sensed by these cells that produces sustained depolarization which ultimately triggers firing of slowly adapting currents in the afferent nerve fibres. Piezo2 deletion reduced the frequency and rates of firing in the afferent nerves in response to light touch or low mechanical forces [429,430]. Mice with skin-specific Piezo2 deletion were less responsive to light touch triggered behavioural tests [428]. These findings suggest that Piezo2 enabled mechanotransduction in these Merkel cell-neurite complexes significantly contribute to the ability these skin complexes to respond to finer spatial and textural details like surface, edge and curvature of objects [429]. Since loss of Merkel cells-specific Piezo2 function did not completely abrogate touch responses this suggested whether similar process of mechanotransduction occurs in other touch receptors like LTMRs (low-threshold mechanoreceptors) and nociceptors. Neural crest cells derived from human embryonic stem cells are can be differentiated to sensory neurons in vitro. These neurons express genes characteristics of LTMRs and thus facilitates exploring the mechanosensory properties of these cells [431]. Differentiation of these progenitor cells into LTMRs is characterized by distinct upregulation of Piezo2 expression [432]. Piezo2-/- neurons failed to show any mechanically activated currents while Piezo2+/- showed intermediate levels of mechanically-induced currents [432]. These findings indicate that Piezo2 mechanotransduction is widespread in a number of touch receptors. The molecular mechanisms downstream of Piezo2 activation in light touch sensation in LTMRs will need to be elucidated. Mechanical allodynia is a condition characterised by overt painful sensitivity to innocuous touch [433]. Overexpression of Piezo2 in LTMRs induce painful behavioural response in mice in response

to light stimulus [433]. Capsaicin-mediated activation of nociceptive TRPV1 channels increases sensitivity of neurons to peripheral touch and induces mechanical allodynia. Capsaicin-treated wild-type mice exhibited painful behaviour in response to gentle stroke but Piezo2-deficient mice did not exhibit any such response [434]. Nerve injury-dependent similar painful responses to light stimulus was also abolished in Piezo2-deficient mice. Nociceptors are high-threshold receptors that sense harmful mechanical stimuli. Loss of Piezo2 resulted in partial attenuation of nociceptive responses in mice [435]. These findings imply that Piezo2 plays an important role in mechanical allodynia in LTMRs and nociception in nociceptors. Thus, Piezo2 can prove to be viable target in treating abnormal painful responses to mechanical stimulus.

Proprioception

Proprioception is the ability to sense the position of our body in the environment and is required for basic functions like walking, maintaining equilibrium or limb movements [436]. Proprioception is mediated by a specialized group of sensory neurons that innervate muscle spindle fibres where they sense muscle stretch and Golgi tendon organs where they sense muscle tone [436]. Piezo2 has been found to be highly expressed in the nerve endings of these proprioceptive neurons [437]. These neurons mostly exhibited rapidly activating (RA) mechanical currents similar to Piezo2. Although loss of Piezo2 function in adult mice did not drastically affect proprioception, it was possible that deletion of Piezo2 from birth would result in severe impairment of proprioceptive abilities. Indeed, postnatal mice with Piezo2 knockout (KO) in parvalbumin-expressing proprioceptive neurons showed severe defects in limb positioning and coordinated limb movements [438]. These KO mice did not show any considerable structural or numerical changes in the sensory neurons suggesting that these neurons were functionally unable to sense and transduce information. Piezo2-deficient

neurons elicited low levels of RA currents in response to mechanical stimulus and consequent action potential was generated in only a small subset of these neurons. Also, only a small percentage of muscle fibres afferent nerves showed firing in response to mechanical stretch in Piezo2 KO condition [437,438]. These findings suggest that mechanotransduction by Piezo2 is critical for proprioception mice. Although Piezo2 function in human proprioception has not been explored Piezo2 mutations were found to be associated with distal arthrogryposis type 5 [439] and Marden-Walker syndrome [440]. These syndromes are characterised by severe defects in muscle joints, myopathy, progressive scoliosis, severely impaired proprioception and sensory ataxia [440]. These findings indicate that Piezo2 may play a similar role in human proprioception the mechanistic details of which need to delineated.

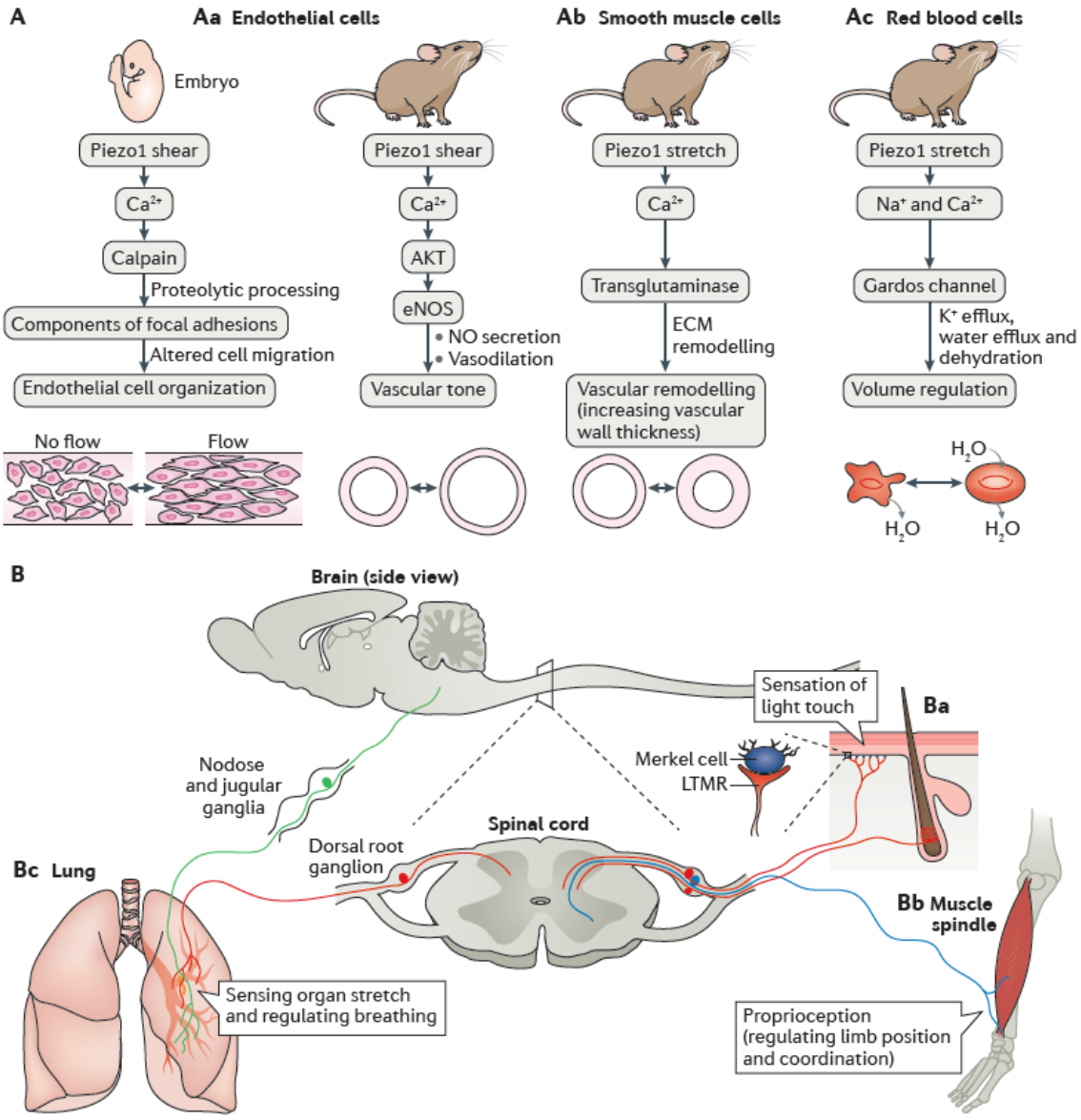

Figure 4-3. Role of Piezo channels in physiological processes. Piezo1 mechanotransduction is required for development of endothelial blood vessels. Piezo1 responds to shear stress and regulates alignment of the endothelial cells during blood vessel formation (Aa). Piezo1 also regulates blood vessel tone through nitric oxide (NO) signalling in response to shear stress. This is critical for regulation of blood pressure (Aa). Piezo1 also regulates remodelling of the smooth muscle cell lining of the blood vessels. In doing so, it helps regulate blood pressure, especially during conditions of hypertension when arterial wall thickening is observed (Ab). Red blood cells (RBCs) experience significant mechanical stress in circulation. Piezo1 has been shown to regulate RBC volume in response to external stress. In response to force, activated Piezo1 channels allow influx of extracellular cations while driving downstream efflux of

potassium ions and water, thus regulating its volume according to physical cues (Ac). Piezo1 channels have been mostly implicated in regulation of touch sensitivity, proprioception and respiration. They are highly expressed by Merkel cells in the dorsal root ganglion of the spinal cord which mediate low-threshold touch sensitivity (Ba). They are also expressed highly in nerve endings of skeletal muscle fibres where they help regulate position and equilibrium of limbs by sensing muscle stretch (Bb). Sensory neurons that innervate lung cells also express Piezo2 which senses muscle stretch and relay the signal to the central nervous system, thus, regulating respiration (Bc). *(Adapted from Murthy et.al. Nat Rev Mol Cel Biol. 2017 [441])*

Role of Piezo channels in disease pathogenesis

A recent study by Zhao et.al. [442] found that Piezo1 played a significant role in regulation of adipocyte function in development of insulin resistance in obesity. Adipocytes show immense plasticity by undergoing changes in volume and size especially during obesity. Piezo1 expression adipocytes was shown to regulate adipocyte activity by suppression of proinflammatory response in obesity. Loss of Piezo1 signalling led to accelerated development of insulin resistance, heightened proinflammation and lipolysis in high fat diet-induced obese mouse models. Suppression of adipocyte inflammation by Piezo1 during obesity is suspected to be mediated through Piezo1-dependent inhibition of proinflammatory TLR4 pathway [442]. Adipocyte Piezo1 upregulation during obesity can be considered to be an adaptive response to cope with increased inflammation.

Role of Piezo mechanotransduction in cancer progression has been a subject of intensive study considering the importance of changing mechanical environment during tumour formation and progression. Increased expression of Piezo1 and Piezo2 correlated with better prognosis and survival in non-small cell lung carcinoma (NSCL) [443]. Analysis of human NSCL tissues showed increased Piezo1 deletion rates while Piezo2 showed higher mutation

frequencies. Elucidation of mechanisms involving Piezo-mediated inhibition of NSCL is needed to develop diagnostic or therapeutic strategies. It has also been found that when cancer cells are subjected to cyclical stretch, they undergo apoptosis through Piezo1-activated signalling. Ca^{2+} downstream of Piezo1 activation triggers calpain protease activation and downstream mitochondrial apoptosis [444]. Other studies have also reported that dysregulated Piezo1 and Piezo2 activity is associated with aggravated forms of cancer [445].

Gain-of-function mutations in Piezo1 has been associated with protection from cerebral malaria in mice through inhibiting growth of *Plasmodium falciparum* in RBCs [426]. Gain-of-function Piezo1 E756del allele is highly enriched in African populations, suggesting their selection in malaria-infested populations. A recent study found a positive correlation between Piezo1 E756del allelic frequency and protection against cerebral malaria in a cohort of Gabonese children [446]. The RBCs of individuals expressing this Piezo1 allele displayed normal RBC morphology, although infected cells expressed reduced levels of *P. falciparum* virulence protein, PfEMP-1 [446]. Hence, Piezo1 expression levels and allelic type strongly influence susceptibility to malarial infections.

Thus, Piezo channels play a dominant role in mediating mechanotransduction in various physiological processes and have also been associated with altered or diseased states.

Chapter 5: Role of Piezo 1 mechanosensors in T cell activation

Piezo1 activity in RBCs was particularly intriguing, and led us to think whether these mechanosensors played a similar role in T cells which also belonged to the hematopoietic lineage. BIOGPS database showed that Piezo1 channels are highly expressed in the human immune cell compartment particularly in $CD4^+$ and $CD8^+$ T lymphocytes (Fig. 5-1 A) while Piezo2 channels show reduced expression (Fig. 5-1 B). For my thesis, I aimed to study the role of Piezo1 channels in T cell mechanotransduction. The following sections will describe the role of Piezo1 activity in two aspects of T cell function where mechanotransduction-mediated signalling is crucial – T cell activation and migration.

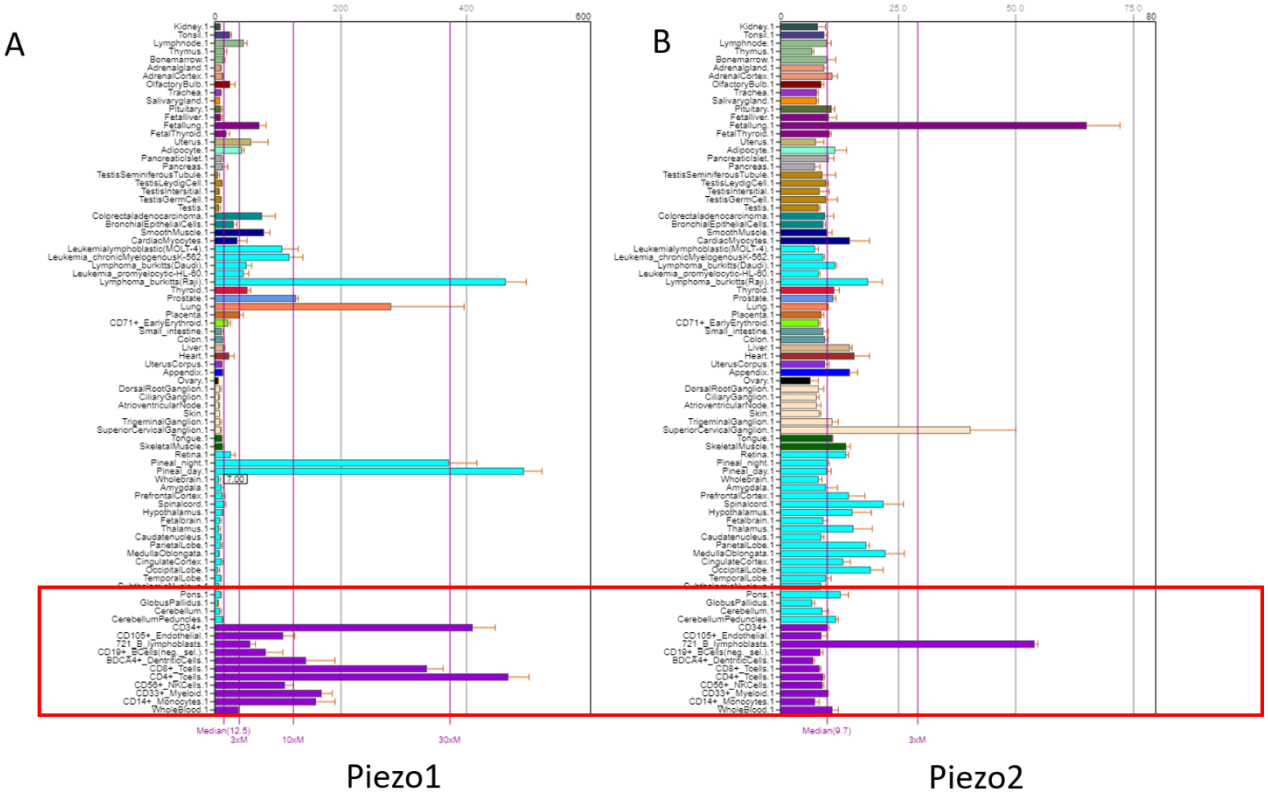

Figure 5-1. BIOGPS gene expression/activity chart of human Piezo1 and Piezo2. This graph represents human tissue-specific Piezo1 (A) and Piezo2 (B) mRNA distribution. The graph

shows high expression of Piezo1 channels in immune cell subsets, particularly, $CD4^+$ and $CD8^+$ T lymphocytes (A) as compared to Piezo2 channels (B). *(Adapted from biogps.org)*

5.1 Generation of mechanical forces during T cell activation

T cells bind APCs through TCR and cognate pMHC interactions. A productive TCR-pMHC interaction results in TCR triggering, leading to TCR activation and induction of downstream signalling pathways, that bring about T cell effector phenotype and function [311]. Efficient TCR triggering requires close T cell-APC interaction which is facilitated through formation of a stable immunological synapse [311]. The immunological synapse serves as the hub of information exchange between cellular partners, and also acts as the centre of TCR activation-induced signalling. The immunological synapse consists of distinct signalling zones arranged in a concentric manner. These zones are called supramolecular activation clusters (SMACS) and each comprises a distinct composition of signalling protein components [311,447] (Fig. 5-2-A). The central SMAC (cSMAC) primarily consists of TCR molecules and co-stimulatory proteins like CD28, signalling partners like Lck kinases. The cSMAC is surrounded by peripheral SMAC (pSMAC) that mainly contains adhesion proteins like integrins. The outward most zone, the distal SMAC (dSMAC) mainly contains bulky proteins with large ectodomains like CD45 tyrosine phosphatase and CD43. The dSMAC also consists of a ring of polymerised F-actin network. The immunological synapse is a dynamic structure that undergoes constant rearrangement. Active actin polymerisation at the dSMAC along with myosin-mediated contraction drives retrograde actin flow which triggers mobilisation of TCR microclusters and integrin receptors towards the centre of the synapse [447]. T cells also extend membrane-cytoskeletal protrusions towards APC surface or target cells in the process of antigen scanning or target cell killing [311,447]. Extension and retraction of membrane extensions are facilitated by actin-cytoskeletal rearrangement and membrane stretching. Target cell lysis during CTL activity requires directed release of lytic granules across the synapse. This is facilitated by

cortical actin remodelling at the synapse [334]. All these events leading to the formation, and maintenance of an active synapse results in generation of considerable mechanical forces that regulate signalling components activity which will be discussed in the following section [223,311]. Disrupting cytoskeletal activity through inhibition of actin nucleation factor Arp2/3 or myosin light chain kinase activity, or promoting actin depolymerisation shows a dramatic reduction of forces measured at the immunological synapse (Fig. 5-2-B). Abolishment of mechanical forces severely impairs TCR activation and downstream signalling [223,311]. The cortical cytoskeleton is maintained in a steady state level of tension because of mechanical activity. Since the T cell membrane is tightly tethered to the actomyosin network, any change in their state will produce consequent changes in the T cell membrane tension [448]. T cells can sense APC surface rigidity and responds changes in mechanical stiffness. Interacting T cells and APCs experience shear stress in circulation and these forces have been shown to regulate binding affinity of adhesion receptors [223,331]. T cells scan the APC surface for specific antigenic cues through extending tiny microvilli projections on the APC surface. A study reported that antigen scanning is facilitated by unconventional myosin 1g (Myo1g) motor-mediated generation of membrane tension that increases meandering ability of T cells [449]. Improved T cell meandering and interactions with APC accentuates T cells capacity to search of cognate antigens. On encounter with cognate pMHC complex, they bind through TCR-pMHC interaction. This process of antigen searching and binding involves close interaction of apposing membrane and it produces significant changes in the T cell membrane tension, a cue which can be sensed by the T cell and guide its response. Thus, T lymphocytes are subjected to diverse external or cell-intrinsic mechanical cues that are somehow guide T cells to optimal activation and signalling. Abolishment of mechanical forces impairs optimal T cell activation [223,311]. Since no dedicated mechanosensor has been identified for T cell activation

through mechanotransduction, the aim of my research was to study the plausible role of Piezo1 mechanosensors in T cell activation.

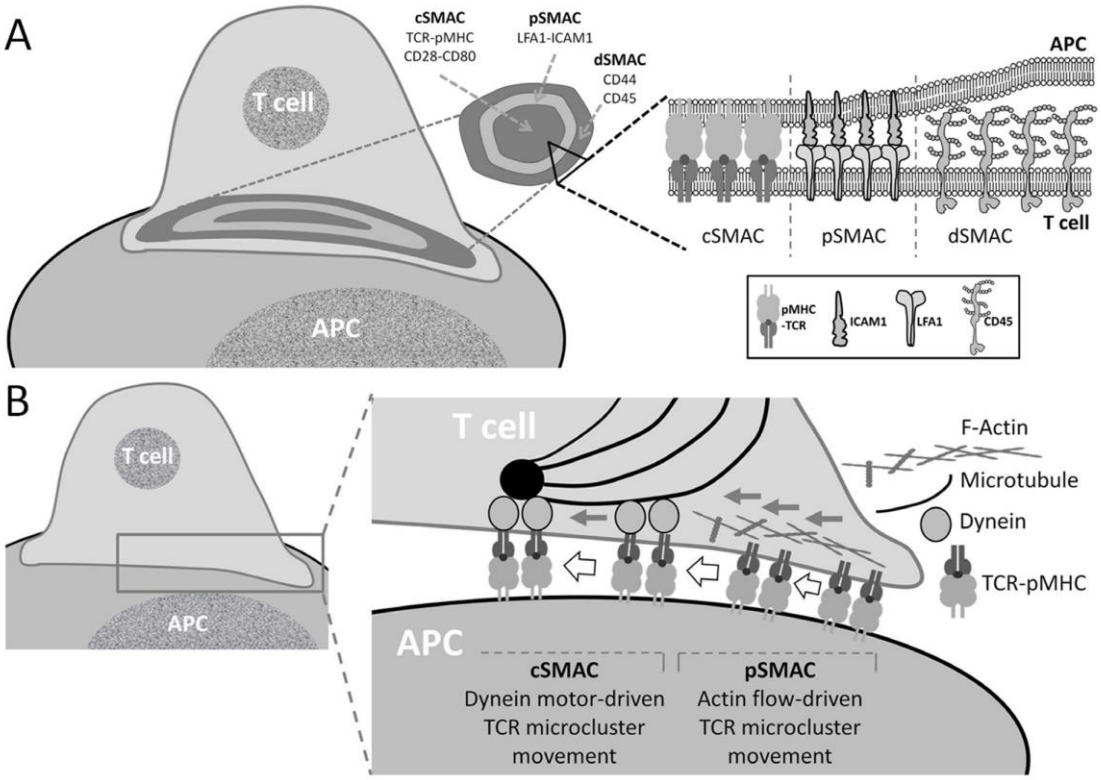

Figure 5-2. Formation of the T cell-APC immunological synapse. T cell-APC interaction is characterised by the formation of a signalling-proficient region known as the immunological synapse. The immunological synapse can be divided into 3 distinct regions arranged in a concentric manner. They are called supramolecular activation clusters (SMACs) (A). The central region (cSMAC) comprises antigen-bound TCR clusters, associated co-stimulatory molecules and signalling kinases. cSMAC is surrounded by peripheral region (pSMAC) formed by adhesion molecules like integrins. The outermost concentric ring or the distal SMAC (dSMAC) consists of bulky moieties like CD45 and CD44. These proteins provide steric hinderance during T cell-APC adhesion and thus excluded from the signalling hub (A). Spatial

distribution of T cell signalling components and formation of these distinct signalling domains is driven by actomyosin cytoskeletal activity. Pushing forces generated by actin polymerisation in response to TCR stimulation concentrates TCR clusters from the periphery to the cSMAC region. Activity of myosin and myosin-associated motor proteins like dynein triggers actin retrograde flow which produces significant mechanical forces at the immunological synapse (B). *(Figure adapted from Liu & Ganguly. Crit. Rev. Immunol. 2019 [311])*

Chapter 6. Piezo1 is highly expressed in human T lymphocytes

6.1 Introduction

Numerous reports confirm the significance of mechanotransduction in T cell activation, downstream signalling and effector functions. The identity of a dedicated mechanosensor in T cell mechanotransduction has remained tenuous at best. Since Piezo channels have been widely implicated in numerous mechanical force-regulated cellular processes, including red blood cells, we speculated the potential role of these mechanosensors in T cell activation.

6.2 Methods

Isolation of human T lymphocytes

PBMC isolation: 10ml blood was taken from healthy volunteers through informed consent according to ethical guidelines. Human peripheral blood mononuclear cells (PBMCs) were isolated from fresh blood using ficoll-gradient centrifugation. Briefly, blood was diluted at 1:1 ratio in 1X PBS and gently layered onto ficoll (HiSep LSM 1077, Himedia) layer followed by centrifugation at 2500rpm, 25˚C at minimum acceleration and break. After centrifugation, the PBMC layer appeared in between topmost plasma layer and lower ficoll layer. PBMCs were collected after the topmost layer consisting of plasma and platelets was discarded. PBMCs were washed with 1X PBS. Contaminating RBCs were removed by incubation in RBC lysis buffer for 10 minutes at room temperature. Lysis was stopped by adding excess 1X PBS followed by centrifugation at 1500rpm, 5mins, 4˚C.

Magnetic activated cell sorting (MACS): $CD4^+$ and $CD8^+$ T lymphocytes were isolated through magnetic immunoselection using $CD4^+$ and $CD8^+$-specific microbeads according to manufacturer's protocol. Briefly, PBMC pellet was resuspended in 500µL of MACS buffer and

appropriate volume of $CD4^+$ or $CD8^+$ microbeads (Miltenyi Biotec) was added to the cell suspension followed by incubation at 4˚C for 20 mins under rotating conditions. After incubation, excess unbound beads were washed by adding excess MACS buffer and centrifugation at 1500rpm, 5mins, 4˚C. Bead-bound cells were passed through LS (large-sized) magnetic columns followed by washing with excess cell-free MACS buffer. $CD4^+$ and $CD8^+$ T lymphocytes were isolated through plunging of the column-bound positive fraction. Isolated T lymphocytes were cultured in RPMI+10% FBS at 37˚C, 5% CO_2.

Real-time quantitative PCR studies

RNA isolation: For quantitation of Piezo1 and Piezo2 expression in $CD4^+$ and $CD8^+$ T cells, RNA was extracted from these subsets using TRIzol method. Briefly, cells were resuspended in 800µL of TRIzol reagent (RNAiso Plus, Takara). 200µL of chloroform was added and mixed thoroughly followed by room temperature, 15 minutes incubation and centrifugation at 13500rpm, 4˚C, 15 minutes to allow separation of RNA-containing aqueous layer. RNA was precipitated by adding equal volume of isopropanol to the aqueous layer and 15-minutes incubation at room temperature followed by centrifugation at 13500rpm, 15 minutes, 4˚C. Excess salts were removed by washing with 70% ethanol. After drying of ethanol, RNA pellet was resuspended using appropriate volume of nuclease-free water.

cDNA preparation: cDNA was prepared using reverse transcriptase-based cDNA synthesis kit (Thermo scientific fisher).

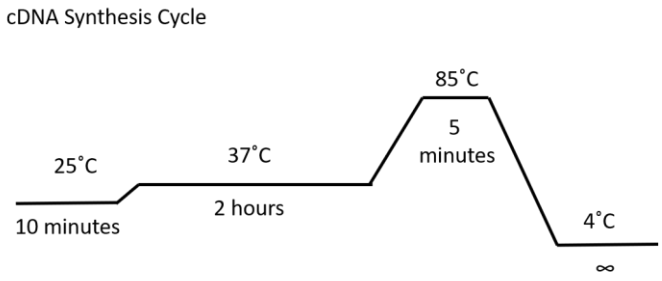

Quantitative PCR analysis: Primers against FAM38A (Piezo1) and FAM38B (Piezo2) were designed using NCBI PRIMER-BLAST tool. SyBr green-based quantitative PCR was subsequently performed on Quantstudio 3 and relative gene expression was measured using 18S as a housekeeping standard gene.

Confocal microscopy

In order to check distribution of Piezo1 proteins in $CD4^+$ T cells, human $CD4^+$ T cells were isolated from blood. Coverslips were coated with 2mg/ml poly-L-lysine at room temperature for 1 hour followed by washing with 1X PBS and drying. $CD4^+$ T cells were allowed to attached to poly-lysine coated coverslips for 2 hours at 37˚C. Unbound cells were removed by washing gently with 1X PBS twice. Duration of each 1X PBS wash was 1 minute. Cells were fixed with 4% paraformaldehyde at room temperature for 15 mins. PFA was removed by washing with 1X PBS three times followed by permeabilization with acetone for 2 minutes at room temperature. Cells were subsequently washed thrice with 1X PBS. Blocking was performed with 3% Bovine-serum albumin in 1X PBS for 1 hour at room temperature followed by washing thrice with 1X PBS. Goat anti-human Piezo1 antibody was added at a concentration of 1:25 (stock dilution) in 1X PBS and allowed to bind for 1 hour at room temperature in a moist chamber. Unbound antibody was removed by gently washing three times with 1X PBS. This was followed by addition of alexa-647 conjugated anti-goat IgG secondary antibody and PE-conjugated anti-CD4 antibody (1:25 dilution). This was allowed to incubate for 1 hour at room

temperature in a moist chamber followed by washing three times with 1X PBS. After antibody incubation, DAPI was added at a concentration of 1ug/ml in 1X PBS and was allowed to stain for no more than 1 minute. Excess DAPI was removed by washing extensively with 1X PBS. Stained coverslips were mounted on microscopy slides containing Vectashield mounting medium. Images were acquired on Leica TCS SP8 confocal microscope.

6.3 Results

Piezo1 is highly expressed in human T lymphocytes: qPCR analysis of human $CD4^+$ and $CD8^+$ T lymphocytes showed that Piezo1 is highly expressed while Piezo2 expression is negligible (Fig. 6-A). This confirms reports by public databases like BIOGPS portals. Piezo1 distribution in $CD4^+$ T lymphocytes was assessed through confocal microscopy and it was found that resting $CD4^+$ T cells showed Piezo1 residing in both cytoplasmic vesicles as well the plasma membrane (Fig. 6-B). Thus, Piezo1 is uniformly distributed between cytoplasmic, nuclear and membrane compartments in resting $CD4^+$ T cells.

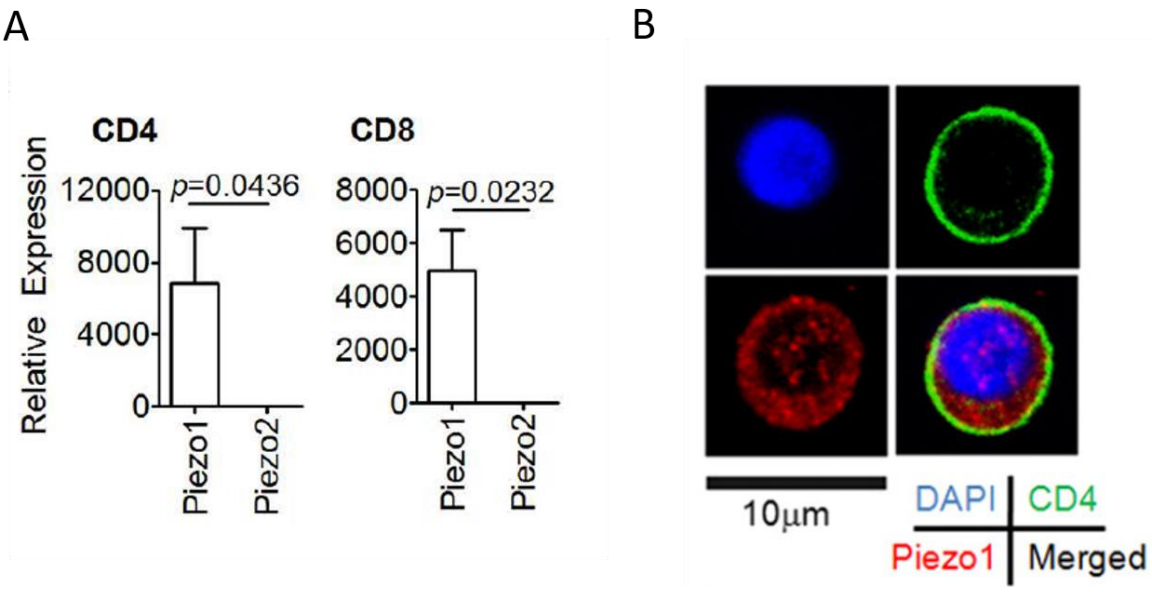

Figure 6. Piezo1 is highly expressed in human T lymphocytes. (A) Quantitative PCR analysis showed that human $CD4^+$ and $CD8^+$ T lymphocytes show high expression levels of Piezo1 but not that of Piezo2. n= 3. (B) Confocal imaging of human $CD4^+$ T cells shows that Piezo1 is uniformly distributed in cytoplasmic and membrane compartments of resting T cells. Paired t-test was performed to calculate statistical significance. *(Adapted from Liu et.al. J Immunol. 2018. [311])*

6.4 Discussion

Quantitative PCR studies confirmed high expression of Piezo1 mechanosensors in human $CD4^+$ and $CD8^+$ T lymphocytes. T lymphocytes, however lacked Piezo2 expression. Confocal imaging showed distinct cellular distribution of Piezo1 mechanosensors in $CD4^+$ T lymphocytes, thus, making it a highly probable candidate that drives T cell activation by sensing mechanical cues during T cell interaction with cognate APCs.

Chapter 7. Optimal T cell receptor (TCR) activation requires Piezo1

7.1 Introduction

The T cell receptor (TCR) complex consists of the heterodimeric TCR molecule (αβ or γϑ) and associated CD3 subunits (Ɛγ, Ɛϑ, ζ ζ) [450]. The TCR molecule recognises cognate antigen-MHC complexes on APCs. Owing to their short cytoplasmic tail, they are unable to transduce downstream signalling. CD3 complex has a short N-terminus extracellular region followed by transmembrane domain and long cytoplasmic tails that contain ITAM (immunoreceptor tyrosine activation) motifs [53,451]. Antigen recognition by the TCR molecule induces changes to the signalling-competent CD3 subunits that initiates downstream signalling pathways specific to TCR activation. TCR ligation with cognate pMHC induces auto and trans-phosphorylation of ITAM motifs in the CD3 cytoplasmic tails mediated by protein tyrosine kinases like Lck and Fyn. Phosphorylated tyrosine in ITAMs serve as docking sites for signalling proteins like kinases and adaptor proteins that has the SH2 domain (Src homology 2 domain). ZAP-70 protein, a member of the Syk kinase family is one the earliest protein to be recruited to phosphorylated ITAMs. Bound ZAP-70 undergoes phosphorylation to form phosphorylated ZAP-70 (pZAP70), one of the earliest markers of TCR activation. pZAP70 phosphorylates adaptor proteins like transmembrane LAT (linker of activated T cell) and cytosolic SLP-76 (SH2 domain containing leukocyte phosphoprotein) enabling formation of a T cell signalosome [53,451]. The T cell signalosome recruits effector molecules like phospholipase Cγ-1, phosphoinositide 3-kinase (PI3K), and the adapters growth factor receptor-bound protein 2 (GRB2), etc. These molecules trigger downstream signalling pathways like Ca^{2+} influx and subsequent activation of effectors like mitogen-activated protein (MAP) kinases, protein kinase C (PKC) and calcineurin. These signalling pathways lead to activation and nuclear

translocation of key transcription factors like NFAT, NF-κB and AP-1-dependent pathways that regulate T cell effector response like proliferation, cytokine production, migration etc [53,451]. T cell activation can be quantified by measuring levels of T cell activation markers. As mentioned before, pZAP70 serves as one of the earliest markers of TCR crosslinking and activation [452]. Other activation markers include surface expressed CD69, a type II C-lectin receptor [453]. CD69 is expressed within 24 hours of TCR stimulation although its mRNA is observed as early as within 1-2 hours of stimulation. CD69 expression regulates many aspects of T cell activation including T cell differentiation, cytokine production, T cell retention in inflamed tissues or lymph nodes [453], etc. The IL-2 receptor α chain, CD25 is another marker of T cell activation [454]. Its expression is upregulated between 24-48 hours of TCR stimulation. Its upregulation allows T cells to express high affinity form of the IL2 receptor consisting of α, β and γ chains which facilitates high-affinity binding to IL-2 cytokine that induces T cell proliferation and its clonal expansion [454]. Finally, extent of T cell proliferation also determines levels of T cell activation. The following section will delve into the plausible role of Piezo1 mechanosensors in optimal T cell activation. Using siRNA-mediated downregulation of Piezo1, I checked whether human T cell activation by means of TCR crosslinking was affected on Piezo1 knockdown. I performed real-time and flow cytometric based quantification of T cell activation markers on TCR crosslinking after Piezo1 downregulation.

7.2 Methods

siRNA-mediated Piezo1 knockdown

Human Piezo1-specific esiRNAs (pool of siRNAs) was used to downregulate Piezo1 activity in human $CD4^+$ and $CD8^+$ T lymphocytes. 150nM of Piezo1 esiRNA was electroporated into 3-4 million $CD4^+$ and $CD8^+$ T cells in a final volume of 100ul of RPMI without FBS, using Bio-rad

Gene Pulser XL. The cells were electroporated using an exponential decay pulse of 250V and 950µF resistance in a 2mm cuvette. As control, 150nM of EGFP siRNA (siRNA targeting GFP) was similarly electroporated in control cells. The cells were incubated in complete RPMI for 3 days to allow sufficient Piezo1 knockdown before activation studies.

Culture and activation of human T lymphocytes

Approximately 200,000 cells/well were cultured in a 96-well flat-bottomed plate. Human $CD4^+$ and $CD8^+$ T lymphocytes were activated in two ways – a) T cells were activated using TCR-crosslinking anti-CD3 and anti-CD28 soluble antibodies to mimic T cell activation in the absence of mechanical force b) They were activated using anti-CD3/CD28 coated dynabeads. These dynabeads consists of inert, superparamagnetic beads, approximately 4.5µm in diameter. These beads are covalently coupled to anti-CD3 and CD28 antibodies. These beads resemble APCs due to their similar sizes and expression of TCR-crosslinking ligands. Activation of T cells using bead-immobilised antibodies will exert mechanical forces on the T cells in addition to facilitating TCR crosslinking due to bead size and rigidity. T cells were stimulated with 2µg/ml each of anti-CD3 and CD28 soluble antibodies or with bead-immobilised CD3/CD28 antibodies in a cell: bead ratio of 1:1. T lymphocytes were stimulated under these conditions for different time durations depending on expression kinetics of activation markers.

Real-time quantitative PCR studies

To measure levels of Piezo1 downregulation, control-transfected T cells (designated as wild-type, WT T cells, henceforth) and Piezo1 siRNA-transfected T cells were collected on day 3 post-transfection. RNA was isolated followed by cDNA preparation and qPCR was performed using human Piezo1-specific primers. Data was analysed to measure relative expression of

Piezo1 using 18S as housekeeping standard. Piezo1 knockdown efficiency was expressed as fold knockdown of Piezo1 -

$$\frac{\text{Piezo1 relative expression in control siRNA-transfected cells} - \text{Piezo1 relative expression in Piezo1 siRNA-transfected cells}}{\text{Piezo1 relative expression in control cells}}$$

For measurement of CD69 upregulation in response to TCR stimulation, ≈200,000 $CD4^+$ and $CD8^+$ T cells (both WT and Piezo1-deificient) were stimulated with soluble or bead-immobilised anti-CD3/CD28 for 1.5 hours. Cells were collected in TRIzol and qPCR using human CD69-specific primer was performed.

Flow cytometric-based quantification of T cell activation markers

For measuring T cell activation markers, ≈200,000 human $CD4^+$ and $CD8^+$ T cells (control and knockdown cells) were stimulated with soluble αCD3/CD28 antibodies or bead-immobilised αCD3/CD28 antibodies and collected at different time-points depending on the expression kinetics of concerned activation marker. CD69 surface upregulation was measured at 18 hours post TCR stimulation while CD25 surface expression was measured 36 hours post TCR stimulation.

Intracellular staining of pZAP70: For measurement of phosphorylated ZAP70 (pZAP70) levels, cells were collected 1hour post TCR stimulation in 0.5% paraformaldehyde (PFA). Cells were washed at 1500rpm, 5mins, 4˚C. Cell permeabilization was performed by incubating cells in 0.1% saponin + FACS buffer (permeabilization) for 10 minutes on ice. Cells were subsequently washed with excess permeabilization buffer at 2400rpm, 5mins, 4˚C. Cells were incubated with PE-conjugated anti-phospho ZAP70 antibody (BD Bioscience) in 50µL permeabilization buffer for 20 minutes on ice. Excess antibody was removed by washing with excess

permeabilization buffer followed by excess FACS buffer. Cells were fixed in 1% PFA and acquired on BD LSR Fortessa II.

Staining of surface activation markers: For CD69 and CD25 surface staining, TCR-stimulated control and Piezo1-deficient cells were collected 18 hours and 36 hours respectively post TCR stimulation. Collected cells were washed in FACS buffer at 1500rpm, 4˚C for 5mins. They were incubated with anti-CD69-PE or anti-CD25-APC antibodies ((BD Bioscience) for 20 minutes on ice. This was followed by washing with excess FACS buffer and fixation in 1% PFA. Stained samples were acquired on BD LSR Fortessa II.

T cell proliferation assay

In order to quantify T cell expansion, control and Piezo1 siRNA-transfected $CD4^+$ and $CD8^+$ T cells were stained with cell trace dyes - Carboxyfluorescein succinimidyl ester (CFSE) or cell trace violet (CTV, Thermo Scientific Fischer). Cell trace dyes are cell permeant fluorescent dyes that bind to amine groups in intracellular cytosolic proteins. On cell proliferation, due to division of cell matter, these dyes tend to get diluted with subsequent cell divisions. Hence, reduction of fluorescent intensity can be used to measure extent of cell proliferation.

Briefly, 3.5nM of dye was added to 1.5-2 million control and Piezo1 siRNA-transfected cells resuspended in 1.5-2.0 ml of 1X PBS. Cells were thoroughly resuspended and incubated in dark at room temperature for 20 minutes with intermittent shaking to allow uniform staining. After 20 minutes, excess complete RPMI was added and cells were washed at 1500rpm, 4˚C for 5 minutes. Stained transfected cells cultured in complete RPMI and were stimulated with soluble αCD3/CD28 or bead-immobilised αCD3/CD28. Cells were collected on day 4 post-stimulation. The extent of dye dilution (reduced fluorescent intensity) as a result of cell proliferation was measured on BD LSR flow cytometer.

7.3 Results

Piezo1 is essential for optimal TCR triggering: As described in the previous chapters, T cell activation requires efficient generation and sensing of mechanical forces. In order to find out whether Piezo1 mechanosensors which are highly expressed in human T lymphocytes, play any role in T cell activation, we downregulated Piezo1 protein through Piezo1-specific siRNA-mediated knockdown. Isolated $CD4^+$ and $CD8^+$ T cells were transfected with either control siRNA or Piezo1-specific siRNA. Control and Piezo1-downregulated cells were then stimulated with either soluble forms of TCR-crosslinking antibodies or bead-immobilised forms of TCR-crosslinking antibodies, αCD3/CD28. Using bead-immobilised antibodies to crosslink and activate TCR mimics TCR activation by ligands presented on APCs since beads bound to T cell surface exert considerable mechanical force on the T cell surface (Refer to section 7.2). T cell activation in response to different forms of TCR crosslinking was measured by quantifying expression of activation markers at different time-points post-stimulation. T cell activation in control and Piezo1-deficient T cells was measured by quantifying early activation markers like phosphor-ZAP70 and CD69 expression levels and late activation markers like CD25 and cellular proliferation. As expected, bead-immobilised TCR crosslinking antibodies were much more efficient at TCR activation as compared to TCR crosslinking by soluble αCD3/CD28 antibodies (Fig. 7-A-G). This provides further validation to previous studies that bead-bound or surface immobilised TCR crosslinking antibodies are much more efficient than soluble antibodies at TCR triggering and downstream activation due to generation of mechanical forces during TCR interaction with the former. Downregulation of Piezo1 led to significant reduction of TCR activation in response to bead-immobilised TCR crosslinking antibodies. Piezo1-deficient T cells showed reduced levels of phosphorylation of ZAP70 (pZAP70)

downstream of TCR-crosslinking (Fig. 7-A). Interestingly, when we compared reduction of pZAP70 induction in Piezo1-deficient T cells relative to control cells, there was strong positive linear correlation between reduction of pZAP70 levels and Piezo1 knockdown efficiency (Fig. 7-B). Cells with higher Piezo1 downregulation levels showed greater abrogation optimal TCR activation in terms of pZAP70 induction. In order to assess effects of Piezo1-downregulation on TCR activation, we only used those experiments for analysis where Piezo1-knockdown efficiency was more than 40% (Fig. 7-G). Piezo1 downregulation also strongly impaired upregulation of CD69 mRNA and surface expression (Fig. 7-C and 7-D) in response to TCR crosslinking by bead-immobilised αCD3/CD28. Piezo1-deficient $CD4^+$ and $CD8^+$ T cells also showed markedly reduced proliferation capacity in response to TCR triggering as measured by reduction in high-affinity IL-2 receptor, CD25 upregulation (Fig. 7-E) and cell proliferation (Fig. 7-F). These results show that Piezo1 activity is crucial for human TCR activation. Loss of Piezo1 impairs T cells' capacity to optimally respond to TCR stimulation.

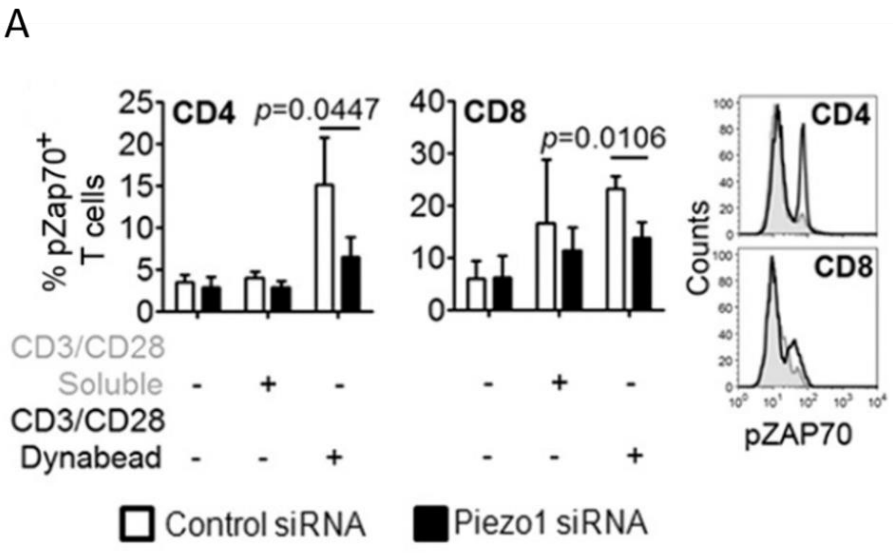

Figure 7-A. Loss of Piezo1 impairs upregulation of phospho-ZAP70 in response to TCR triggering. Human $CD4^+$ and $CD8^+$ T cells were transfected with control and Piezo1-specific siRNA and stimulated with soluble TCR crosslinking αCD3/CD28 antibodies or bead-immobilised αCD3/CD28 antibodies. Phosho-ZAP70 levels were measured 1hour post TCR stimulation. Bead-immobilised αCD3/CD28 triggered greater levels of phosphorylation of ZAP70 (pZAP70) on TCR activation as compared to soluble αCD3/CD28. There is significant reduction in pZAP70 induction in response to immobilised TCR antibody crosslinking in Piezo1-deficient $CD4^+$ (left panel) and $CD8^+$ (middle panel) T lymphocytes as compared to control cells. Right panel: Representative histograms of pZAP70 expression levels in $CD4^+$ and $CD8^+$ T lymphocytes in response to αCD3/CD28 dynabeads (Black outline: control cells; grey-shaded area: Piezo1 knockdown cells). Paired t-test was performed to calculate statistical significance. *(Adapted from Liu et.al. J Immunol. 2018. [311])*

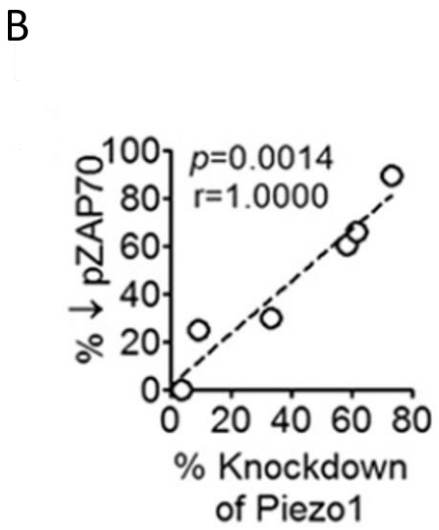

Figure 7-B. Correlation between extent of Piezo1 downregulation by siRNA-mediated knockdown and reduction in phosphor-ZAP70 levels. Piezo1 knockdown efficiency was calculated by measuring percentage reduction in Piezo1 mRNA relative expression in Piezo1

siRNA-transfected cells as compared to control siRNA-transfected cells. Similarly, reduction in pZAP70 induction was calculated as percent decrease in pZAP70 levels in Piezo1-deficient T cells as compared to control T cells, in response to TCR triggering by bead-immobilised TCR crosslinking antibodies. Reduction in pZAP70 induction in response to TCR activation showed strong positive linear correlation with Piezo1 knockdown efficiency. Spearman's Rank Correlation was performed to calculate correlation coefficient and *p*-value. *(Adapted from Liu et.al. J Immunol. 2018.* [311]*)*

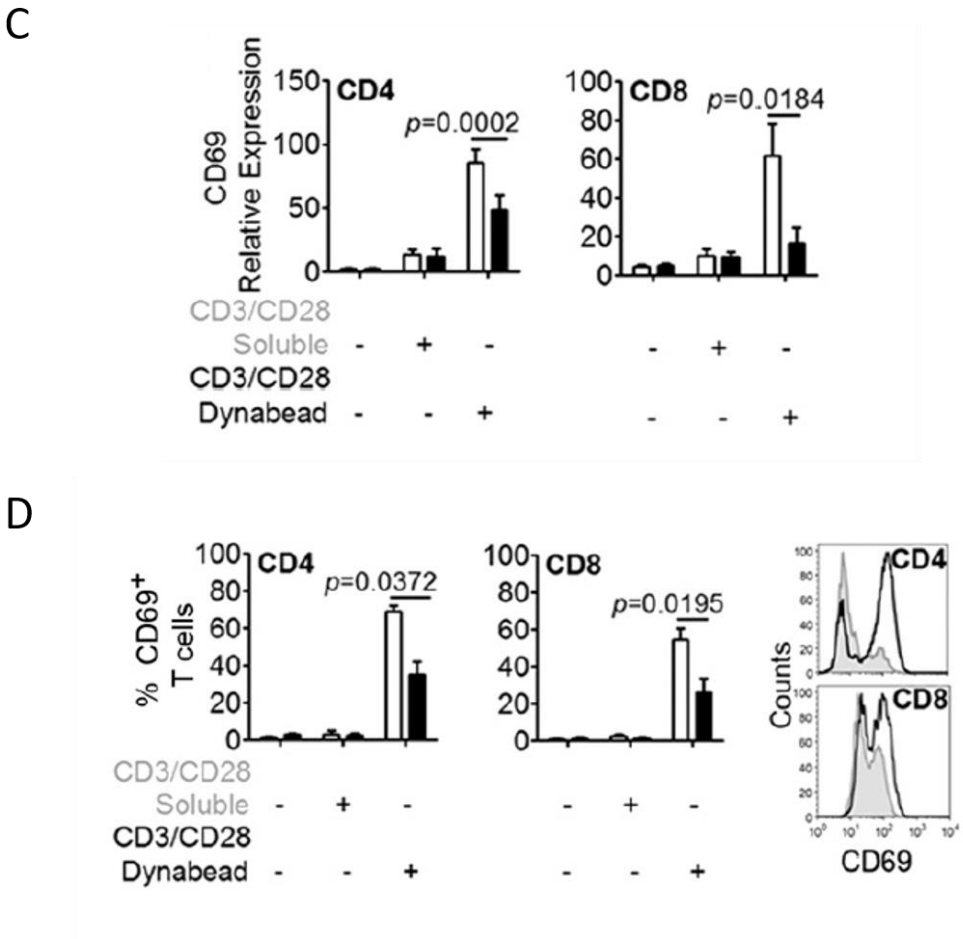

Figure 7- C & D. Piezo1-deficient human CD4⁺ and CD8⁺ T lymphocytes showed reduced CD69 upregulation response to TCR triggering. Bead-immobilised αCD3/CD28 induced more proficient CD69 upregulation as compared to soluble counterparts. siRNA-mediated Piezo1

knockdown however, significantly reduced CD69 mRNA (C) and CD69 surface (D) activation marker expression as measured 1 hour and 18 hours post stimulation with αCD3/CD28 dynabeads, respectively. Lower right panel: Representative histograms of CD69 surface expression levels in $CD4^+$ and $CD8^+$ T lymphocytes in response to αCD3/CD28 dynabeads (Black outline: control cells; grey-shaded area: Piezo1 knockdown cells). Paired t-test was performed to calculate statistical significance. *(Adapted from Liu et.al. J Immunol. 2018. [311])*

E

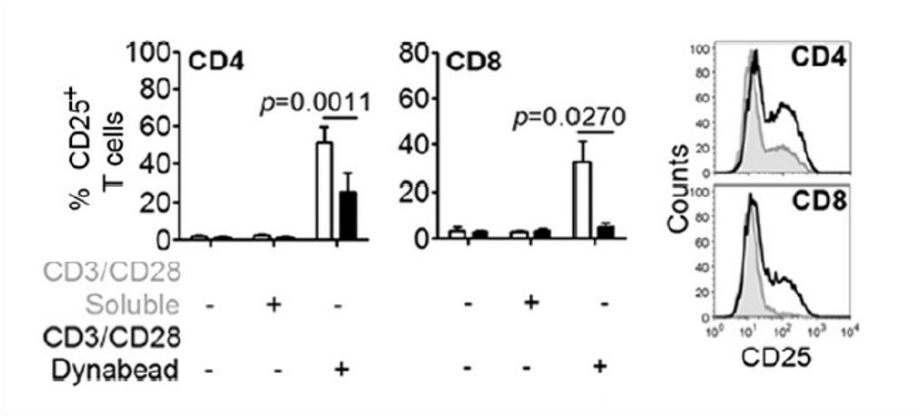

F

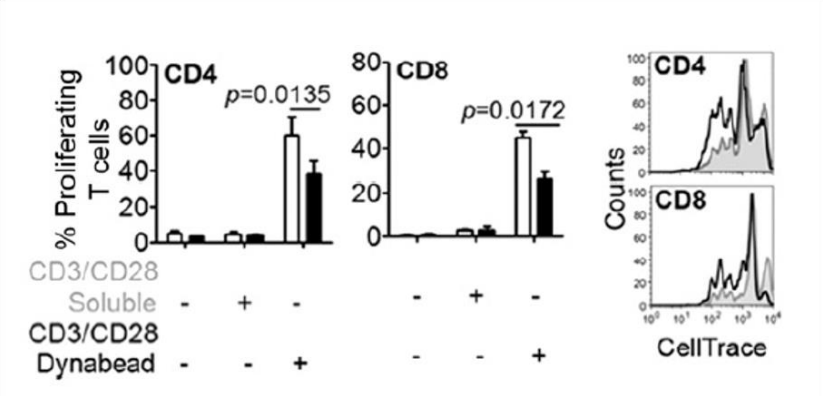

Figure 7-E & F. Loss of Piezo1 impairs proliferative capacity of human $CD4^+$ and $CD8^+$ T lymphocytes. Piezo1-deficient $CD4^+$ (E, left panel) and $CD8^+$ (E, middle panel) T cells showed distinct reduction in the upregulation of the proliferative cytokine IL-2 high-affinity receptor, CD25 surface marker in response to TCR crosslinking by αCD3/CD28 dynabeads. CD25 surface expression was measured 36 hours after T cell stimulation. Moreover, we also see a significant

reduction of $CD4^+$ (F, left panel) and $CD8^+$ (F, middle panel) T lymphocyte proliferation on day 4 of stimulation of αCD3/CD28 dynabeads under conditions of reduced Piezo1 activity. Right panel: Representative flow cytometry histogram plots of CD25 surface expression (E, right panel) and T cell proliferation (F, right panel) in response to TCR triggering by αCD3/CD28 dynabeads (Black outline: control cells; grey-shaded area: Piezo1 knockdown cells). Paired t-test was performed to calculate statistical significance. *(Adapted from Liu et.al. J Immunol. 2018. [311])*

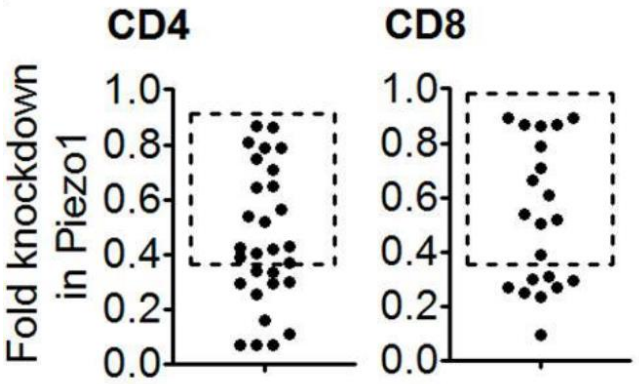

Figure 7-G. Piezo1 knockdown efficiency in human $CD4^+$ and $CD8^+$ T lymphocytes. Piezo1 was downregulated through siRNA-mediated knockdown in both $CD4^+$ and $CD8^+$ T lymphocytes. Knockdown efficiency was calculated through fold knockdown of Piezo1 (section 7.2). Experiments which showed at least 40% Piezo1 knockdown were considered for further activation or functional studies. *(Adapted from Liu et.al. J Immunol. 2018. [311])*

7.4 Discussion

Hence, these results confirm that Piezo1 activity is absolutely crucial for TCR activation in response to TCR-crosslinking antibodies. As expected TCR activation by αCD3/CD28 dynabeads achieved significantly stronger T cell activation as compared to TCR activation with

soluble αCD3/CD28. This finding is consistent with earlier reports where immobilised TCR ligands were more potent activators of T cells as compared to soluble TCR ligands. When T cells are presented with TCR-binding ligands bound to rigid surfaces like magnetic beads or plastic surfaces or synthetic matrices, there is considerable mechanical interactions between the T cell surface and ligand-bound surface. As reviewed and proved extensively in previous studies, these mechanical interactions are crucial for T cell activation. When generation of mechanical forces and tension are abrogated, T cells fail to achieve optimal activation. The above experiments show that Piezo1 activity is essential for optimal activation of T cells in response to TCR triggering.

Chapter 8. Piezo1 is essential for efficient antigen priming of human T lymphocytes by APCs.

8.1 Introduction

T cell activation requires efficient presentation of TCR-cognate antigens coupled with MHC molecules on APCs. As described earlier, T cell interaction with cognate APC is characterised by dynamic changes in membrane tension and generation of mechanical forces that are essential for T cell response [331]. We tried to study the role of Piezo1 mechanosensors in T cell priming by APCs by culturing T cells with allogeneic and autologous monocyte-derived dendritic cells (moDCs) that act as APCs.

Allogeneic stimulation of T lymphocytes involves co-culturing T cells with target cells or monocyte-derived dendritic cells from a different donor [455]. The process of thymic T cell positive selection creates a repertoire of self-MHC restricted T cells that recognise antigens complexed with self-MHC molecules. This process of antigen recognition by T cells underlies conventional T cell-mediated immune response. T cell alloreactivity is however, a remarkable exception to this process [456]. Alloreactive T cells are capable of recognising foreign peptide – foreign MHC complexes. They respond to peptides complexed with allogenic MHC molecules that were not present at the time of development. Thus, alloreactive T cells break the barrier of self-MHC restriction during antigen presentation by target cells. It has been suggested that since there is no active process that selects or eliminates T cells on the basis of their ability to interact with non-self MHC molecules; T cell alloreactivity could stem from TCR's inherent affinity for the MHC surface. T cell stimulation in response to allogeneic APCs can be explained on the basis of recognition of alloantigens like MHC molecules or other minor antigens on

donor cells. Naïve T cells can directly recognise foreign MHC antigens on allogeneic DCs through a process known as direct allorecognition. Unlike conventional T cell stimulation, direct allostimulation leads to polyclonal activation of T cells. Direct recognition of allogeneic MHC antigens can be facilitated due to abundant expression and polymorphism of MHC antigens on donor DCs that may enable their direct, peptide-independent and low affinity binding to many T cells of ranging specificities [457]. Another theory that explains allostimulation of T cells states that T cells can recognise defined peptides bound to allo-MHC molecules on donor cells. Allostimulation of T cells can also be facilitated through indirect allorecognition in which alloantigens on donor cells can be taken up and processed by self-APCs such that they are presented as complexes with self-MHC molecules [457]. This form of antigen recognition is evident in transplant rejection and graft-versus-host disease [457]. There is also increasing evidence of semi-direct form of allorecognition in which exchange of MHC class I and class II molecules between donor and recipient DCs (MHC cross-dressing) may enable T cell activation by allogeneic DCs leading to transplant rejection [456,457]. Allogeneic T cell stimulation requires T cell culture with APCs derived from a different donor. T cell activation is thus, mediated through direct recognition of alloantigens.

Autologous stimulation of T cells involves culturing of T cells with APCs derived from the same donor [458]. Isolated APCs are primed with specific antigens during which they take up antigens and present antigenic epitopes on their surface after antigen processing. Primed APCs are co-cultured with autologous T cells. T cells specific for the antigen will get activated in response to peptide-MHC complexes on APCs and undergo subsequent proliferation. This technique is used to study the conventional self-MHC restricted T cell response.

We used these two forms of T cell activation through interaction with APCs to study the role of Piezo1 mechanosensors in T cell priming by APCs.

8.2 Methods

Generation of monocyte-derived dendritic cells (moDCs)

Human monocytes are able to rapidly differentiate into DCs in the presence of GM-CSF and IL-4. These moDCs can trigger significant T cells expansion when primed with exogenous antigens. Hence, in-vitro generated moDCs can act as efficient APCs. Human monocytes were isolated from blood of healthy volunteers using monocyte-specific CD14 microbeads through magnetic immunoselection. ≈ 500,000 $CD14^+$ monocytes were cultured in each well of a 24-well plate in RPMI + 10% FBS. 50ng/ml each of recombinant human GM-CSF (ebioscience) and IL-4 (Tonbo Bioscience) were added to each well and cells were cultured for 4 days. moDCs were collected after 4 days of culture and washed with 1X PBS. Pellet was resuspended in appropriate volume of RPMI + 10% FBS.

Allogenic T cell stimulation

Human $CD4^+$ and $CD8^+$ T cells were isolated from a different donor and electroporated with EGFP control siRNA or Piezo1-specific siRNA. On day 3 post-transfection, transfected $CD4^+$ and $CD8^+$ T cells were collected and stained with cell trace dyes (CFSE or CTV) using the same protocol as described in section 3.2.2. moDCs (collected after 4 days of monocyte stimulation) were co-cultured with control or Piezo1 siRNA-transfected allogeneic T cells (loaded with cell trace dyes) in a ratio of 1:5 (moDC/T cell). Proliferation of transfected T cells in response to allogeneic moDC stimulation was measured after 4 days of co-culture through flow cytometry-based detection of cell trace dye dilution.

Autologous T cell stimulation

moDCs were generated from CD14-expressing monocytes isolated from tetanus-immunized donors 7-10 days post-vaccination. Generated moDCs were primed with 2IU/ml of tetanus toxoid (Serum Institute of India) for 24 hours before their co-culture with autologous effector T cells. Human effector $CD4^+$ T lymphocytes were isolated from the same tetanus-vaccinated donor which ensured presence of tetanus-specific effector T cells. Briefly, isolated $CD4^+$ T cells were further incubated with $CD45RA^+$ microbeads. Excess unbound $CD45RA^+$ microbeads were washed and cells were subsequently passaged through MS (medium-sized) magnetic columns. $CD4^+$ effector T cells were collected as the CD45RA-negative cell fraction (flow-through). CD45RA-negative effector $CD4^+$ T lymphocytes were electroporated with EGFP control siRNA or Piezo1-specific siRNA. On day 3 post-transfection, transfected effector $CD4^+$ T cells were collected and stained with cell trace dyes (CFSE or CTV). Tetanus toxoid-primed moDCs were co-cultured with control or Piezo1 siRNA-transfected autologous effector $CD4^+$ T cells (loaded with cell trace dyes) in a ratio of 1:5 and 1:10 (moDC:T cell). Co-culture of autologous effector T cells with unprimed moDC was used as a negative control during measurement of T cell proliferation. Proliferation of transfected effector $CD4^+$ T cells specific for tetanus toxoid in response to primed moDC stimulation was measured after 4 days of co-culture through flow cytometric detection of cell trace dye dilution.

8.3 Results

Piezo1 downregulation causes significant attenuation of T cell priming by APCs: moDCs triggered efficient proliferation of allogenic $CD4^+$ T lymphocytes on co-culture. Piezo1 knockdown however, severely impaired T cell proliferation in response to stimulation by allogeneic APCs (Fig. 8.3-A). Similar results were observed when effector $CD4^+$ T cells were

primed by autologous APCs bearing tetanus toxoid antigen. moDCs isolated from tetanus-vaccinated donors were primed by tetanus toxoid. Primed moDCs were subsequently co-cultured with CD45 RA-negative effector $CD4^+$ T cells isolated from the same immunised donor which allowed specific antigen presentation and proliferation of tetanus toxoid-specific effector $CD4^+$ T cells. $CD4^+$ effector T cells showed efficient proliferation in response to tetanus toxoid-primed moDCs as compared to unprimed moDCs (Fig. 8.3-B). $CD4^+$ effector T cell proliferation also showed graded response with higher moDC : T cell ratios showing greater T cell proliferation outcomes. Loss of Piezo1 activity through Piezo1 downregulation resulted in drastic decrease in T cell priming and subsequent proliferation in response to autologous antigen presentation (Fig. 8.3-B). Thus, T cell priming by APCs require efficient Piezo1 activity.

A

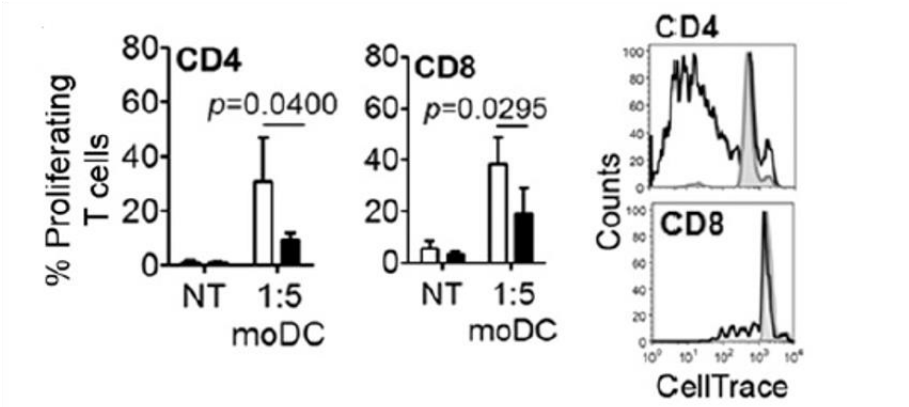

B

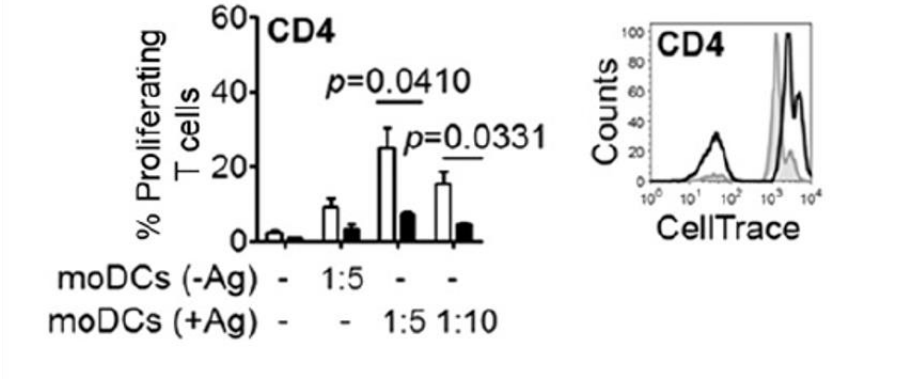

Figure 8-A, B. Loss of Piezo1 abolishes T cell priming by APCs. Piezo1-deficient $CD4^+$ (A, left panel) and $CD8^+$ (A, middle panel) T lymphocytes showed drastic reduction in proliferation in response to stimulation by allogeneic moDCs as measured by flow cytometry after 4 days of co-culture. Right panel: Representative histograms of T cell proliferation in response to allogeneic moDCs as measured by reduction in Cell trace MFI (Black outline: control cells; grey-shaded area: Piezo1 knockdown cells). Downregulation of Piezo1 also interfered with priming of effector $CD4^+$ T cells in response to autologous moDCs loaded with tetanus toxoid. Piezo1-downregulated $CD4^+$ effector T cells showed significant impairment of cell proliferation in response to autologous stimulation as measured by flow cytometry (B, right panel). Control and Piezo1 siRNA transfected $CD4^+$ effector T cells were cultured with

autologous moDCs at ratios of 1:5 and 1:10 (moDC/T cell) and cell proliferation was assessed after 4 days of co-culture. Right panel: Representative histograms of T cell proliferation in response to autologous moDCs (1:5 co-culture) as measured by reduction in Cell trace MFI (Black outline: control cells; grey-shaded area: Piezo1 knockdown cells). Paired t-test was performed to calculate statistical significance. *(Adapted from Liu et.al. J Immunol. 2018. [311])*

8.4 Discussion

T cell activation response to APC priming by means of in-vitro T cell-APC co-culture is a closer representation of physiological activation of T cells in response to binding cognate pMHC complexes on APCs. We attempted to study T cell responses under more physiological conditions by co-culturing human T lymphocytes with allogeneic or autologous in-vitro generated moDCs that act as efficient APCs. Under these conditions, we found that Piezo1 is essential for T cell activation through efficient antigen priming by APCs. Loss of Piezo1 activity through Piezo1 downregulation significantly attenuated T cell proliferation in response to antigen presentation by APCs.

Chapter 9. Piezo1 agonist strengthens TCR activation by TCR crosslinking.

9.1 Introduction

As discussed previously, it is well known that TCR activation by antibody-mediated TCR crosslinking is much more potent when TCR crosslinking antibodies are presented to the T cells in immobilised forms compared to their presentation in soluble forms [311]. TCR-crosslinking antibodies can be immobilised either on culture dish surfaces (surface coated αCD3/CD28) or on inert beads (αCD3/CD28-coated dynabeads). The difference in T cell activation potency by these two forms of antibody presentation can be attributed to the involvement of mechanical forces when immobilised TCR-crosslinking antibodies are used. Upon binding, surface or bead-coated antibodies exert a certain degree of drag forces on the T cell surface similar to those exerted by the APCs when they interact with T cells. Soluble TCR-crosslinking antibodies, on the other hand, fail to evoke such mechanical force-mediated response [311]. In order to analyse the role of Piezo1 mechanosensors in a gain-of-function context, we measured T cell activation response in the presence of the Piezo1 agonist, Yoda1. Since T cells do not achieve optimal activation in response to soluble αCD3/CD28, we checked if Piezo1 activation through addition of Yoda1 can potentiate TCR activation under these conditions of suboptimal TCR triggering.

Yoda1

Yoda1 is a chemical agonist of Piezo1 [459]. It can activate Piezo1 in the absence of any external mechanical force and can hence, be used for Piezo1 gain-of-function studies. Yoda1 was discovered by Syeda et.al. [459] when a large number of low-molecular weight compounds

were screened for their ability to trigger influx of extracellular Ca^{2+} in Piezo1-overexpressed HEK293 cells. HEK293 cells show very little Piezo1 activity unless Piezo1 is overexpressed. Yoda1 was able to induce influx of extracellular Ca^{2+} in Piezo1-overexpressed HEK293 cells but not in vector-transfected cells. Chelation of extracellular Ca^{2+} but not intracellular Ca^{2+} abolished Yoda1 activity, further confirming that it activates Piezo1 and causes passage of extracellular Ca^{2+} (Fig. 9-1-A). Yoda1 also showed selectivity for Piezo1 channels and did not activate overexpressed Piezo2 channels [459].

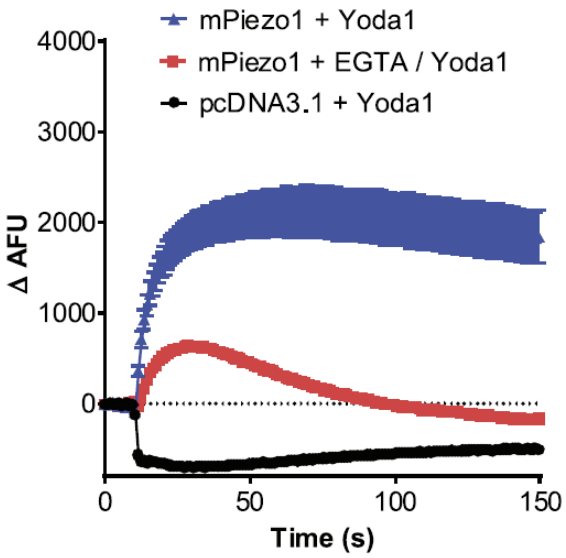

Figure 9-1-A. Yoda1 is a chemical agonist of Piezo1. HEK293 cells were either transfected with mPiezo1 expressing construct or control vector, pcDNA3.1. Addition of 25µM Yoda1 to mPiezo1-transfected cell produced influx of extracellular Ca^{2+} as measured by increase in fluorescence of Ca^{2+}-binding dye (blue line). When extracellular Ca^{2+} was chelated by EGTA, Yoda1 failed to induce Ca^{2+} influx (red line). Control vector-transfected HEK293 did not respond to Yoda1. *(Adapted from Syeda et.al. Elife. 2015. [459])*

Yoda1 structure can be divided into 3 moieties (Fig. 9-1-B). It has a 2,6 dichlorophenyl ring which has been shown to be necessary for its activity [460]. Any change in this moiety results

in loss of Yoda1 activity. The other two moieties consist of a pyrazine ring and a thiadiazole group [460]. In order to decipher Yoda1-mediated gating of Piezo1 channels, chimeric mouse Piezo1 proteins were synthesised [461]. Piezo1 chimeras consisted of wild-type subunits that could bind Yoda1 and mutant subunits that were insensitive to Yoda1. It was observed that presence of even a single Yoda1 responsive wild-type subunits led to Piezo1-derived signals similar to wild-type Piezo1 channels [461]. This means that productive Yoda1 binding to a single subunit could relay the signal to other Piezo1 subunits causing it to open. A recent study based on electrophysiology, Ca^{2+} fluorescent imaging and all-atom molecular dynamic simulation showed that Yoda1 binds to a small hydrophobic pocket domain which is situated at an approximate distance of 40Å from the central ion-conducting pore [462]. Yoda1 binding led to tension-induced allosteric conformational changes in Piezo1 subunits. This produces drastic reduction in the magnitude of threshold force required for Piezo1 activation. Yoda1 binding produces a wedge-like effect that causes gating of Piezo1 channels [462] (Fig. 9-1-C).

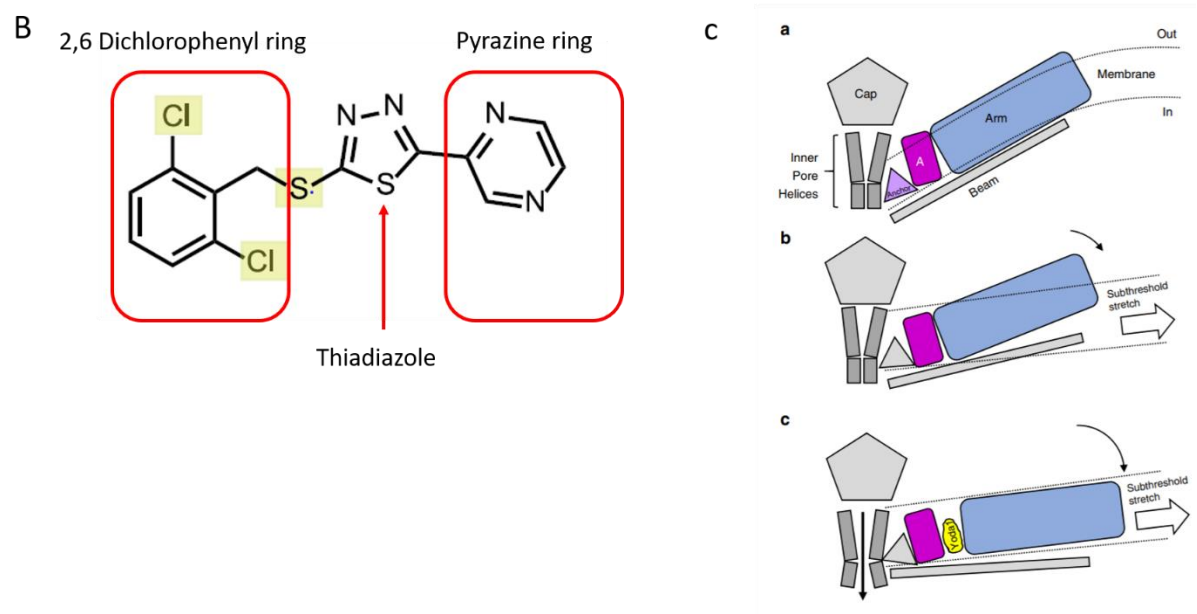

Figure 9-1-B, C. Structure and gating mechanism of Piezo1 agonist Yoda1. (B) Yoda1 consists of 3 main groups – 2,6 dichlorophenyl ring, a pyrazine ring and thiadiazole group. (C) Under resting conditions, each Piezo1 arm is flexed according to membrane curvature (a). Application of suboptimal mechanical force and subsequent slight membrane stretching cause the Piezo1 arms to extend to a certain degree but does not open the channel (b). Binding of Yoda1 causes tension-induced allosteric modification of subunit arrangement and which causes complete flattening of subunit arms and channel opening (c). *(Fig. B-Adapted from Evans et.al. Br J Pharmacol. 2018 (B).* [460] *& Fig. C-Lacroix et.al. Nat Commun. 2018 (C).* [461]*)*

9.2 Methods

Synthesis of Yoda1: Yoda1 was synthesised by Dr. Barnali Paul under the guidance of Dr. Arindam Talukdar from the department of Organic and Medicinal Chemistry, CSIR-IICB, Kolkata. A brief schematic of Yoda1 synthesis has been given below (Fig. 9-2-A-D).

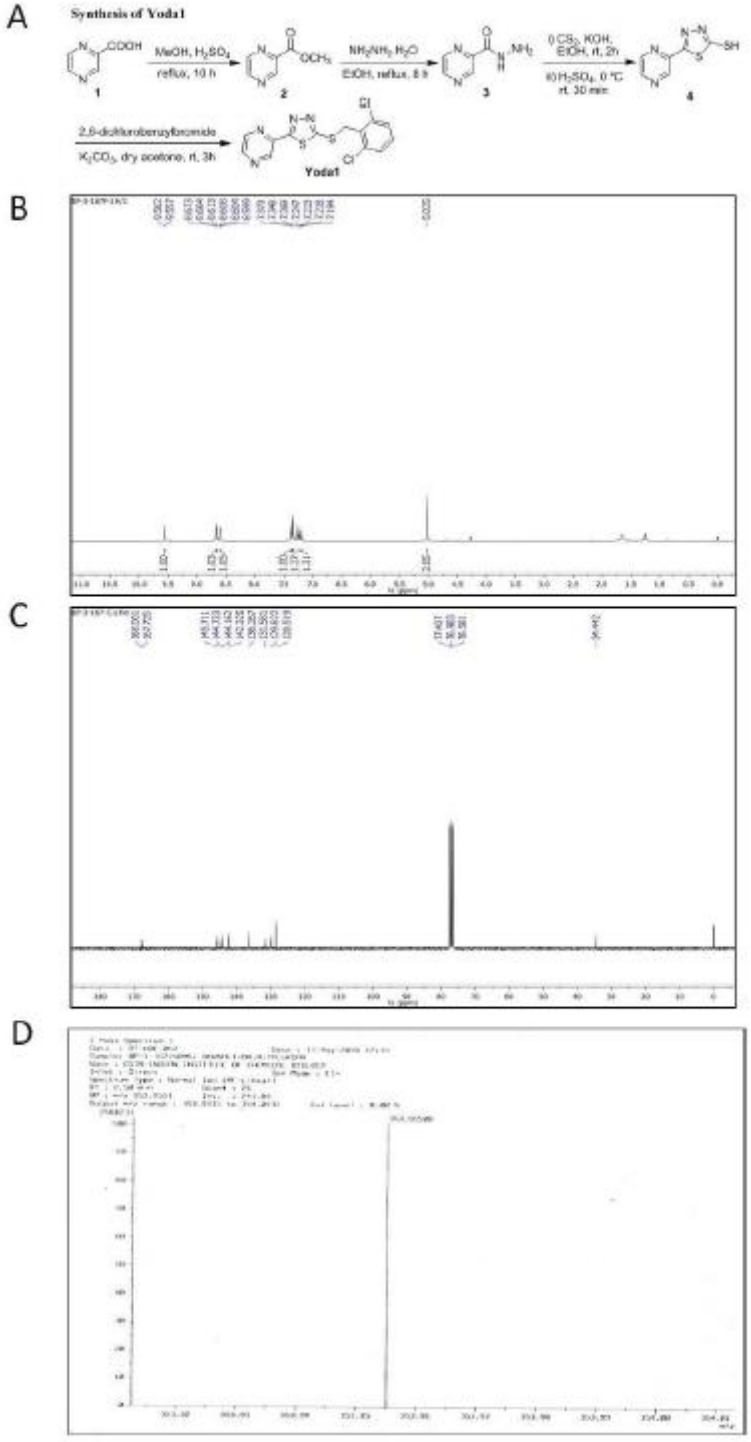

Figure 9-2. Schematic for Yoda1 synthesis. (A) Yoda1 synthesis reaction steps. (B) Purity check of synthesised Yoda1 by ^{1}H NMR (Nuclear magnetic resonance) in $CDCl_3$. (C) ^{13}H NMR in $CDCl_3$. (D) EI-HRMS (Electron ionization- high resolution mass spectrometry). (Done by Dr. Barnali Paul.) *(Adapted from Liu et.al. J Immunol. 2018. [311])*

Yoda1 reconstitution

Yoda1 was reconstituted in 0.22µm-filtered DMSO at a stock concentration of 25µM. Reconstituted Yoda1 solution was stored in 4˚C. Working dilutions were made in 1X PBS. Molecular weight of Yoda1: 355.27

Activation of T lymphocytes with Yoda1

Isolated $CD4^+$ and $CD8^+$ T lymphocytes were seeded at a density of 200,000 cells per well in a final volume of 100µL of complete RPM1. 2µg/ml each of soluble anti-CD3 (eBioscience) and anti-CD28 (eBioscience) were added to the cells in the presence or absence of 15µM of Yoda1. Cells were treated for 1 hour after which they were harvested and checked for expression of phospho-ZAP70 and CD69 mRNA. Staining of phosphor-ZAP70 and PCR quantification of CD69 mRNA were carried as described in the previous sections. Untreated cells were used as control. Briefly, $CD4^+$ and $CD8^+$ T lymphocytes were permeabilised in FACS buffer + 0.1% saponin and stained with anti-phosphoZAP70 antibody for 20 minutes on ice, followed by washing and fixation in 0.1% paraformaldehyde. For CD69 mRNA quantification, RNA was isolated by TriZOL-based method. After cDNA synthesis, SyBr green-based quantitative PCR was performed with human CD69 primers using 18S as relative control.

Specificity of Yoda1-mediated T cell activation

$CD4^+$ T lymphocytes were electroporated with control and Piezo1-specific siRNA. Transfected cells were collected on day 3 post-transfection and stimulated with 2µg/ml of anti—CD3 and anti-CD28 antibodies with and without 15µM Yoda1. Cells for stimulated for 1 hour after

which they were collected in TRIzol and CD69 mRNA induction was measured by quantitative PCR.

9.3 Results

Piezo1 activation by Yoda1 significantly potentiates TCR activation: Downregulation of Piezo1 expression strongly impaired TCR activation in response to immobilised TCR crosslinking antibodies. We wanted to check if activation of Piezo1 in the absence of external mechanical forces would increase TCR activation in response to suboptimal triggering. We used Yoda1, a chemical agonist of Piezo1 to activate Piezo1 in the absence of any mechanical cues. TCR-crosslinking by soluble αCD3 and αCD28 antibodies produces weak TCR activation. Addition of Piezo1 agonist, Yoda1, to $CD4^+$ and $CD8^+$ T lymphocytes significantly increased T cell activation in response to suboptimal triggering by soluble αCD3 and αCD28. $CD4^+$ and $CD8^+$ T lymphocytes showed significant upregulation of phosphorylated ZAP70 (Fig. 9-3-A) and CD69 mRNA (Fig. 9-3-B) when T cells were activated in response to soluble αCD3 and αCD28 supplement with Yoda1.

In order to check specificity of Yoda1-mediated T cell activation, control and Piezo1 siRNA-transfected $CD4^+$ T cells were stimulated with soluble anti-CD3 and anti-CD28 antibodies in the presence or absence of Yoda1. CD69 upregulation in response to Yoda1 potentiation of TCR triggering was only observed in control cells. Piezo1 downregulation led to significant reduction of Yoda1-mediated CD69 activation thus confirming that Yoda1 enhances TCR triggering through activation of Piezo1 (Fig. 9-3-C). Yoda1 alone failed to induce $CD4^+$ T cell activation showing that Piezo1 activation in the absence of specific TCR triggering will not activate T cells.

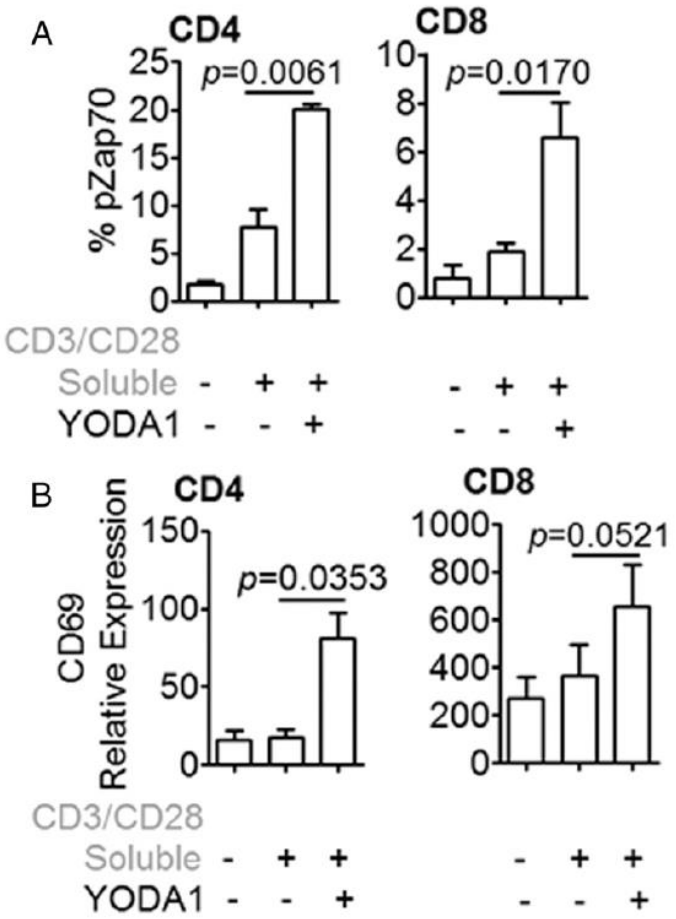

Figure 9-3-A, B. Piezo1 agonist enhances TCR activation. Isolated human $CD4^+$ and $CD8^+$ T lymphocytes were stimulated with soluble αCD3 and αCD28 antibodies in the presence or absence of 15µM Yoda1. (A) Addition of Yoda1 significantly increased levels of phosphorylated ZAP70 in response to TCR activation by soluble αCD3 and αCD28 antibodies. (B) Addition of Yoda1 significantly upregulated induction of CD69 mRNA expression in response to TCR activation by soluble αCD3 and αCD28 antibodies. Paired t-test was performed to calculate statistical significance. *(Adapted from Liu et.al. J Immunol. 2018. [311])*

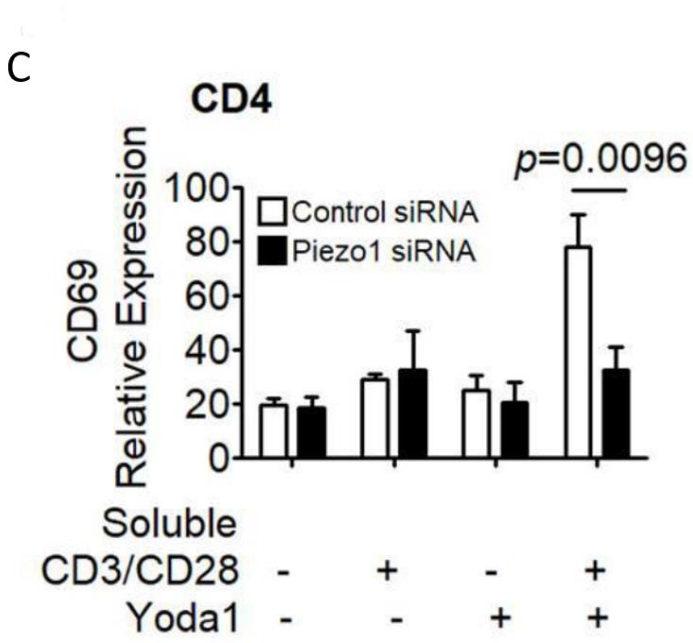

Figure 9-3-C. Specificity of Yoda1-mediated TCR activation. Control and Piezo1 siRNA-transfected $CD4^+$ T cells were stimulated with soluble anti-CD3 and anti-CD28 antibodies in the presence and absence of Yoda1. Soluble TCR crosslinking antibodies alone failed to upregulate CD69 expression. Addition of Yoda1 upregulated TCR activation by soluble antibodies which was significantly impaired on Piezo1 downregulation. Yoda1 alone failed to induce T cell activation in the absence of TCR triggering. *(Adapted from Liu et.al. J Immunol. 2018.* [311]*)*

9.4. Discussion

It's a widely known that in-vitro activation of $CD4^+$ and $CD8^+$ T lymphocytes by TCR crosslinking antibodies is much more efficient when these antibodies are coated on the surface of the culture plate or covalently immobilised on rigid microbeads. TCR crosslinking antibodies added to T lymphocytes in soluble form are inefficient at activating T cells. T cell interaction with surface-coated or microbead-bound TCR antibodies will lead to generation of mechanical tension or drag on the T cell membrane. This mechanical interaction is similar to what is

observed when T cells interact with APCs. Mounting research on the importance of mechanical force on T cell function suggests that this mechanical signal is essential for T cell activation. Since binding of soluble TCR-crosslinking antibodies fail to generate any such mechanical force, they are rather inept at activating T cells. Our first set of experiments provide strong evidence that Piezo1 mechanosensor is important for optimal T cell activation through microbead-bound TCR crosslinking antibody. We sought to increase soluble αCD3/αCD28-mediated T cell activation by chemically activating Piezo1 in the absence of any mechanical force. Our results show that chemical activation of Piezo1 by Yoda1 strongly accentuates TCR activation in the absence of mechanical force. Thus, Piezo1 agonist, Yoda1, can act as a strong surrogate for mechanical forces and can be used for optimal activation of T cells in response to TCR crosslinking where mechanical forces are not actively generated. Yoda1-mediated enhanced T cell activation was significantly reduced in Piezo1-deficient T cells, thus confirming that it acts through by specifically activating Piezo1 mechanonsensors. Moreover, Yoda1 in the absence of specific TCR crosslinking failed to activate T cells. Thus, non-specific activation of Piezo1 does not activate T cells. Piezo1 activation in the presence of specific TCR crosslinking is required for optimal T cell activation which is crucial for preventing non-specific activation of T cells in response to ubiquitous mechanical forces.

We however, could not observe enhanced Yoda1-mediated TCR activation at later time-points. This could be attributed to the nature of Yoda1-mediated Piezo1 activation. Piezo1 gating shows rapid inactivation kinetics. They are inactivated within mill-seconds of gating in response to mechanical force so as to prevent constant influx of extracellular cations. Yoda1 binding, however makes Piezo1 insensitive to inactivation by stabilising the open state of Piezo1. Thus, Yoda1 binding could render the cell toxic at latter time-points.

Chapter 10. TCR crosslinking by immobilised antibodies causes Piezo1 spatial redistribution

10.1 Introduction

Resting T lymphocytes show uniform distribution of Piezo1 through the entire cell. In an attempt to discover how Piezo1 senses mechanical forces during T cell activation, we checked if T cell interaction with bead-immobilised TCR crosslinking antibodies produced any effect on Piezo1 spatial distribution. Piezo1 in epithelial cells has been shown to undergo spatial redistribution depending on spatial map of mechanical cues [423]. The balance between epithelial cell division and apoptosis has to be critically governed so as to maintain barrier integrity while simultaneously preventing any dysregulated cell growth [105]. A report showed that Piezo1-mediated mechanotransduction regulated epithelial cell homeostasis [422,423]. When epithelial cells become too crowded as a result of increased cell division, Piezo1 senses mechanical cues generated by overcrowding and triggers cell apoptosis. On the other, when cells are subconfluent, Piezo1 channels are activated by membrane stretch and triggers cell division. It has been observed that at low cell densities, Piezo1 channels mainly localise to the cell nucleus where it does not sense cell stretch. This could be owing to the reason that low cell density already necessitates high cell division so Piezo1 regulation is not needed. Under conditions of confluency, Piezo1 localises to the cell membrane in regions where cells are spaced out and widely spread [423]. Piezo1 senses membrane stretch in these areas and triggers cell division. In areas where cells are very crowded Piezo1 forms large cytoplasmic aggregates where it triggers cell death. Hence, Piezo1 actively migrates to sites where it can

sense mechanical cues and trigger an appropriate response [423]. We wanted to check if Piezo1 exhibits a similar behaviour when T cells undergo activation.

10.2 Methods

$CD4^+$ T lymphocyte isolation: Human $CD4^+$ T lymphocytes were isolated from PBMCs by magnetic immunoselection as described before.

Confocal microscopy

Coating of coverslips: 13mm round glass coverslips were wiped with absolute ethanol. The coverslips were then coated with 150µL of 2mg/ml poly-L-lysine for 1 hour at room temperature. Coated coverslips were then washed thrice with 1X PBS and allowed to dry at 37˚C.

Cell seeding and stimulation: Approximately 200,000 CD^+ T cells in 150µL of complete RPMI were seeded on coated coverslips. Cells were allowed to bind to coverslips at 37˚C for 2 hours. Microbead-coated anti-CD3/anti-CD28 antibody was added to the cells in a 1:1 cell:bead ratio. Antibody was allowed to bind for 30 minutes.

Staining: After 30 minutes of stimulation with bead-immobilised anti-CD3/-anti-CD28, cells were washed twice with 1X PBS. 150µL of 4% paraformaldehyde was added and incubated at room temperature for 15 minutes. Cells were then washed thrice with 1X PBS followed by permeabilization with acetone for 2 minutes at room temperature. 3% Bovine-serum albumin in 1X PBS was subsequently added for blocking for 1 hour at room temperature. After washing thrice with 1X PBS, anti-human Piezo1 antibody was added at a concentration of 1:25 stock dilution (Santa Cruz Biotechnology). Primary antibody incubation was done for 1 hour at room temperature in a humidified chamber. Excess antibody was washed thrice with 1X PBS

followed by secondary Alexa 647-conjugated anti-goat antibody. PE-conjugated anti-CD4 was also added as the T cell marker at a dilution of 1:25 from stock. Secondary antibody incubation was done for 1 hours, followed by washing thrice with 1X PBS. 1µg/ml of DAPI in 1X PBS was added to the cells and stained for 1 minute after which cells were thoroughly washed 4 times with 1X PBS. Stained coverslips were mounted on a microscopic glass slide using 7µL of VECTASHIELD antifade mounting medium.

Image acquisition: Cells were imaged on a Leica TCS SP8 microscope at a magnification of 60X oil immersion. Alexa-647 signal was detected using the 638nm laser. PE signal was detected using the 488nm laser and DAPI signal was detected using the 405nm laser.

Analysis of Piezo1 spatial distribution: Image analysis was performed using ImageJ software. In order to measure Piezo1 spatial distribution, we took two circular ROIs (region-of-interests) of two different fixed diameters. The ROI with the larger area was used to measure mean Piezo1 fluorescence over the entire cell area. The ROI with the smaller area was used to measure mean Piezo1 fluorescence over the central area of the cell. The ratio of mean Piezo1 fluorescence between the larger ROI and the smaller ROI was calculated which gave us a measure of Piezo1 distribution. A higher ratio meant that Piezo1 localised to cell peripheral areas while a smaller ratio meant no such preferential localisation.

10.3 Results

Image analysis showed that while untreated $CD4^+$ T cells showed uniform distribution of Piezo1, $CD4^+$ T cells that were bound to bead-immobilised anti-CD3/anti-CD28 antibody showed preferential peripheral distribution (Fig. 10-A). The peripheral distribution was evident due to higher intensity ratios of mean Piezo fluorescence over entire cell versus the central part of the cell (Fig. 10-B). In coverslips which were treated with bead-immobilised

anti-CD3/anti-CD28 antibody, cells which did not bind the TCR crosslinking antibodies, did not show any selective distribution of Piezo1 proteins (Fig. 10-B). Hence, $CD4^+$ T lymphocytes actively redistribute Piezo1 proteins when they bind to immobilised TCR-crosslinking antibodies. Piezo1 preferentially migrates to peripheral areas of the cell.

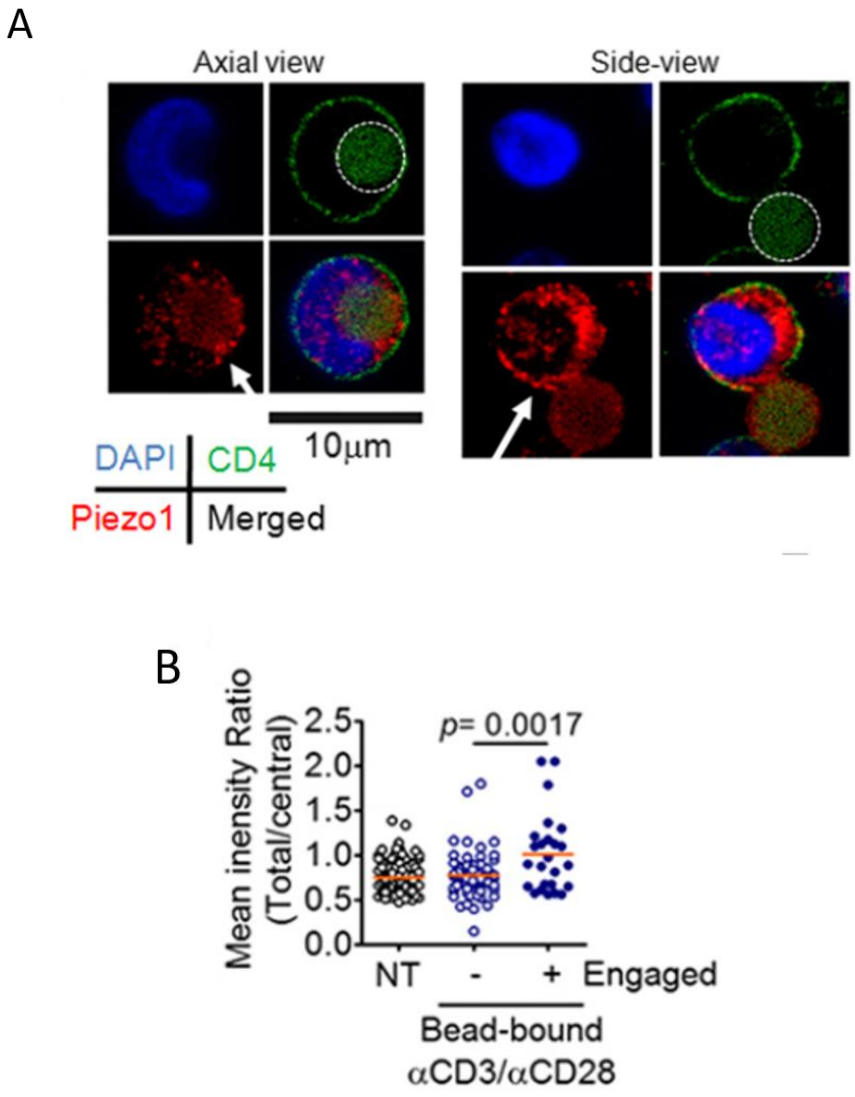

Figure 10. Piezo1 undergoes spatial redistribution on TCR crosslinking. TCR binding to bead-bound αCD3/αCD28 antibodies induces Piezo1 redistribution towards peripheral regions of the cell. (A) Representative confocal image of human $CD4^+$ T lymphocytes bound to bead-bound αCD3/αCD28 antibody. Piezo1 (red) is localised to cell peripheral regions near the T

cell-bead synapse as indicated by white arrows. Left panel: axial view of antibody bound-T cell; Right panel: Side view of antibody-bound T cell. White dashed line indicated bead-bound αCD3/αCD28 antibodies. Green: CD4 fluorescence; Blue: DAPI fluorescence. (B) Mean fluorescence of Piezo1 (red) was measured over total cell area and central cell area. The mean fluorescence intensity ratio between total versus central cell area was calculated for untreated $CD4^+$ T cells and antibody-treated $CD4^+$ T cells that were bound and unbound to bead-immobilised αCD3/αCD28 respectively. $CD4^+$ T cells bound to TCR-crosslinking antibody showed higher mean fluorescence intensity ratio indicating a peripheral distribution of Piezo1 in these cells. *(Adapted from Liu et.al. J Immunol. 2018. [311])*

10.4 Discussion

Piezo1 is uniformly distributed between cytoplasmic vesicles and membrane regions in resting $CD4^+$ T cells. When T cells bind to bead-immobilised anti-CD3/anti-CD28 antibodies, there is active Piezo1 mobilisation to peripheral regions of the bound cell. This Piezo1 redistribution is necessary since it positions these mechanosensors in regions where they can actively sense mechanical force and transduce it to intracellular signals. Resting $CD4^+$ T cells do not experience localised mechanical cues. When T cells bind to APCs expressing cognate antigens, there is localised force generation at the synapse. The T cell surface consequently experience significant membrane tension and force. Upon APC interaction, Piezo1 selective distribution to the peripheral regions surrounding the synapse enables it to sense mechanical forces generated at the cell surface and trigger a downstream signalling response. Piezo1 mobilisation in response to mechanical cues can be a crucial aspect of its regulation of T cell activity.

Chapter 11. Piezo1 is essential for influx of Ca^{2+} in downstream of TCR crosslinking

11.1 Introduction

Ca^{2+} signalling is one of the crucial aspects of T lymphocyte activation. Ca^{2+} mobilisation downstream of TCR activation triggers signalling pathways that regulate T lymphocyte proliferation, metabolic activities, cytokine production and T lymphocyte differentiation [463]. There are several channels and transporters expressed on the T cell membrane as well in intracellular organelles like endoplasmic reticulum, mitochondria and lysosomes that facilitate Ca^{2+} uptake and efflux [463]. The activity of these channels is crucial for maintaining appropriate cytosolic and organellar Ca^{2+}- levels. TCR binding to cognate peptide-MHC on APCs triggers phosphorylation and activation of phospholipase Cγ1 (PLCγ1) [463]. Activated PLCγ1 hydrolyses phosphatidylinositol-4,5-bisphosphate (PtdIns(4,5)P2) into inositol-1,4,5-trisphosphate (Ins(1,4,5)P3) and diacylglycerol (DAG). Soluble (Ins(1,4,5)P3) activates its cognate receptor on the endoplasmic reticulum (ER) membrane which mobilises ER Ca^{2+} into the cell cytosol. Depletion of ER Ca^{2+} level stimulates the plasma membrane-resident Ca^{2+} channels and transporters through a mechanism known as store-operated Ca^{2+} entry (SOCE) [463]. This form of influx of extracellular Ca^{2+} during SOCE has been shown to occur through activation of CRAC (Ca^{2+} release-activated Ca^{2+}) channels on the plasma membrane. Induction of SOCE is facilitated by ER-resident stromal interaction molecule 1 and 2 (STIM1 and STIM2). STIM1 and STIM2 senses Ca^{2+} levels in the ER. Mobilisation of ER Ca^{2+} into the cytosol as results of TCR activation reduces ER Ca^{2+} levels and release of bound Ca^{2+} from STIM proteins. This leads to aggregation of STIM proteins and their mobilisation to the T cell synapse where

they activate ORAI CRAC channel and induces SOCE [463]. Other channels that mediate Ca^{2+} entry across the plasma membrane include transient receptor potential (TRP) channels, voltage-activated Ca^{2+} channels and purinergic ionotropic receptors (P2RXs). Cytosolic Ca^{2+} is rapidly distributed between various organelles like the mitochondria or endolysosomes where it enhances ATP production and metabolism; and vesicular trafficking of signalling molecules respectively [463]. These events are essential in the activation and regulation of signalling pathways necessary to maintain T cell function.

Piezo1 channels are mechanically gated ion channels that allow passage of extracellular non-selective cations across the plasma membrane into the cell [374]. Influx of extracellular Ca^{2+} through activated Piezo1 has been implicated in a number of physiological processes. Since Piezo1 activation is essential for TCR activation, we sought to check if Ca^{2+} influx downstream of TCR crosslinking is affected by Piezo1 activity.

11.2 Methods

Flow cytometric-based quantification of Ca^{2+} influx.

Ca^{2+} indicators dyes: Ca^{2+} indicators are fluorescent dyes that show either a change in their fluorescence spectra or in their fluorescent intensity upon binding Ca^{2+}. Dyes like Fluo-3 and Fluo-4 show approximately >100-fold increase in their fluorescent intensity upon binding Ca^{2+}. Increase in cytosolic Ca^{2+} levels in response to appropriate trigger will cause increase in fluorescence intensity of cells loaded with these dyes which can detected and quantified by flow cytometry, immunofluorescence microscopy or through microplate reader-based assays. Other indicators show a shift in their excitation or emission spectra upon binding Ca^{2+}. For example, the Ca^{2+}-free form of Fura-2 shows peak excitation at ≈380nm while the Ca^{2+}-bound form shows peak excitation at ≈340nm. Excitation at both these wavelengths will result in

decrease in emission intensity of the Ca^{2+}-free form of the dye (at 380nm excitation) and simultaneous increase in emission intensity of the Ca^{2+}-bound dye (at 340nm excitation) on Ca^{2+} influx. Ratio of fluorescence intensity over these two excitation wavelengths can be used to measure Ca^{2+} response. Similarly, Indo-1 shows dual emission range corresponding to Ca^{2+}-bound (405nm emission) and Ca^{2+}-free (475nm emission) forms. The proportion of these two forms of dye will change upon Ca^{2+} influx and hence, ratio of fluorescence intensity at these two wavelengths will give us a measure of Ca^{2+} response. Combination of indicator dyes can also be used in order to perform a ratiometric Ca^{2+} response analysis. Fluo-3AM and Fluo-4AM is sometimes used in combination with Fura-red. The Ca^{2+}-bound form of Fluo-3/4AM and the Ca^{2+}-free form of Fura-red are activated at a single excitation wavelength of 488nm. Upon increase in cytosolic Ca^{2+} levels intensity of Ca^{2+}-bound Fluo-3/4AM will increase while Ca^{2+}-free Fura-red will decrease. Ratio of emission intensities of these two dyes will give us an accurate measure of degree of Ca^{2+} response.

Staining of $CD4^+$ and $CD8^+$ T lymphocytes with Ca^{2+}-sensor dye, Fluo-3AM: In order to measure Ca^{2+} response on TCR activation, we loaded $CD4^+$ and $CD8^+$ T lymphocytes with the Ca-sensor fluorescent dye-Fluo-3AM. Fluo-3AM (1-[2-Amino-5-(2,7-dichloro-6-hydroxy-3-oxo-9-xanthenyl)phenoxy]-2-(2-amino-5-methylphenoxy)ethane-N,N,N',N'-tetraacetic acid, pentaacetoxymethyl ester) is a fluorescent dye that has an excitation wavelength of 488nm. Upon binding of Ca^{2+}, it shows >100-fold increase in its fluorescence intensity (Figure 11-1).

Isolated $CD4^+$ and $CD8^+$ T lymphocytes were resuspended in 1X PBS + 1.2mM calcium chloride ($CaCl_2$) at a concentration of 1-2 million cells/ml. 2µM of Fluo-3AM was added to the cells and resuspended gently. The AM (acetoxymethyl) ester of the dye renders the dye non-polar and hence, cell-permeable. The cells were incubated at 37˚C for 30-35 minutes during which cells

were taking up the dye. After incubation, cells were washed with excess 1X PBS + 1.2mM $CaCl_2$ at 1500rpm, room temperature for 5 minutes. After washing, the cells were resuspended in appropriate volume of 1X PBS + 1.2mM $CaCl_2$ and incubated at room temperature for additional 15 minutes in dark. The AM ester of Fluo-3AM facilitates passive uptake of the dye by the cell. But once inside the cell, the dye should be able to bind free Ca^{2+} for which the AM ester has to be cleaved off. Incubation at room temperature allows cell-intrinsic esterases to cleave off the AM ester group thus rendering the dye capable of binding Ca^{2+}.

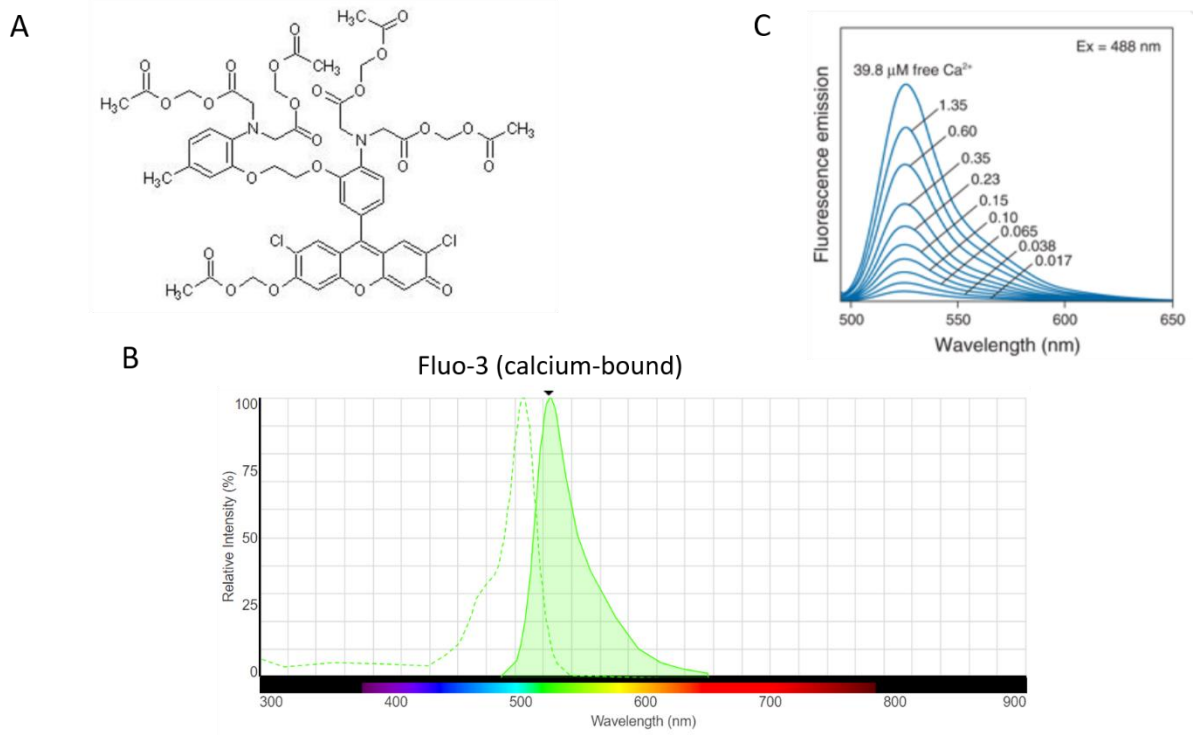

Figure 11-1. Fluo-3AM. (A) Structure of Fluo-3AM. (B) Excitation and emission curve of Ca-bound form of Fluo-3AM. (C) Ca^{2+}-dependent increase in emission fluorescence intensity of Fluo-3AM.

(Adapted from https://www.thermofisher.com/order/catalog/product/F1241#/F1241)

Flow cytometric measurement of Ca^{2+} influx in response to Piezo1 knockodwn

In order to study the role of Piezo1 in TCR-mediated Ca^{2+} response, Piezo1 expression in $CD4^+$ and $CD8^+$ T lymphocytes was downregulated through siRNA-mediated knockdown as described before. Control and Piezo1-siRNA transfected T lymphocytes were stained with Fluo-3AM and described above. Time-kinetics of Ca^{2+} influx was then measured in BD LSR fortessa. Stained transfected cells were resuspended to a density of around 200,000-300,000 cells in 500µL of 1X PBS + 1.2mM $CaCl_2$ buffer. Baseline fluorescence of cells was acquired for 2 minutes followed by addition of anti-CD3/CD28 dynabeads in a ratio of 1:1. Ca^{2+} influx in response to TCR crosslinking was measured for the remaining duration. Ca^{2+} response was measured as increase in fluo-3AM fluorescence intensity versus time.

Flow cytometric measurement of Ca^{2+} influx in response to Piezo1 agonist, Yoda1

Similarly, untransfected wild-type $CD4^+$ and $CD8^+$ T lymphocytes were stained with Fluo-3AM as described above. Baseline fluorescence of cells were acquired for 2 minutes followed by addition of soluble 2µg/ml anti-CD3 and 2µg/ml anti-CD28 antibodies with and without 15µM Yoda1. Ca^{2+} influx was measured as increase in Fluo-3AM fluorescence intensity for the remaining 8 minutes.

In order to check sourcing of Ca^{2+} during influx response, $CD4^+$ T lymphocytes were incubated with 1mM EGTA prior to acquisition. EGTA is a Ca^{2+} chelator and is cell-impermeant. Hence, it chelates extracellular Ca^{2+} in the medium. It can thus, be used to check of Ca^{2+} response is due to extracellular Ca^{2+} sources.

11.3 Results

Loss of Piezo1 impairs Ca^{2+} response downstream of TCR triggering. We studied the effect of Piezo1 on Ca^{2+} response downstream of TCR crosslinking by measuring Ca^{2+} influx in response to bead-immobilised anti-CD3/anti-CD28 on Piezo1 downregulation. We found that both human $CD4^{+}$and $CD8^{+}$ T lymphocytes (Fig. 11-2-A) responded to bead-immobilised anti-CD3/anti-CD28 by showing significant Ca^{2+} influx. siRNA-mediated Piezo1 downregulation completely abolished Ca^{2+} influx on TCR crosslinking.

Piezo1 agonist, Yoda1 significantly increased Ca^{2+} influx in response TCR crosslinking by soluble anti-CD3 and anti-CD28 antibodies. As expected TCR binding to soluble forms of TCR crosslinking antibodies failed to induce any Ca^{2+} influx in both $CD4^{+}$ and $CD8^{+}$ T lymphocytes. When soluble anti-CD3 and anti-CD28 were supplemented with Piezo1 agonist, Yoda1, there was a distinct increase in Ca^{2+} influx response, thus confirming that Piezo1 activity is essential for Ca^{2+} influx downstream of TCR crosslinking (Fig. 11-2-B). In order to check the specificity of Yoda1-mediated enhanced Ca^{2+} response, we measured Ca^{2+} influx in Piezo1-downregulated $CD4^{+}$ T cells. Yoda1-mediated accentuated Ca^{2+} influx in response to soluble anti-CD3 and anti-CD28 antibodies was abolished when Piezo1 was silenced (Fig. 11-2-C). Moreover, when extracellular Ca^{2+} chelator, EGTA was added to the cells prior to TCR activation, Ca^{2+} influx in response to Yoda1 was completely abolished thereby indicating that Piezo1 activation during TCR triggering causes influx of extracellular Ca^{2+} (Fig. 11-2-D).

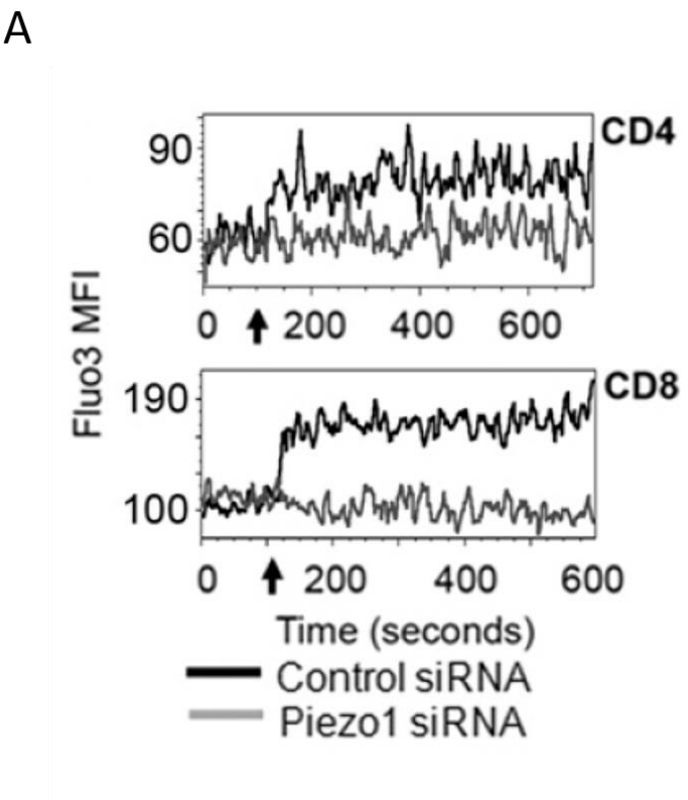

Figure 11-2-A. Loss of Piezo1 abolishes Ca^{2+} influx in response to TCR activation by bead-immobilised αCD3/αCD28 antibodies. Control and Piezo1 siRNA-transfected $CD4^+$ and $CD8^+$ T lymphocytes were stimulated with anti-CD3/CD28 dynabeads in a ratio of 1:1 at indicated time points (black arrow). Ca^{2+} influx was measured after stimulation as increase in mean fluorescence intensity (MFI) of Ca^{2+} indicator, Fluo-3AM relative to baseline fluorescence. Representative flow cytometry plots show complete abrogation of Ca^{2+} influx when Piezo1 is downregulated in $CD4^+$ (upper panel) and $CD8^+$ (lower panel) T lymphocytes. *(Adapted from Liu et.al. J Immunol. 2018. [311])*

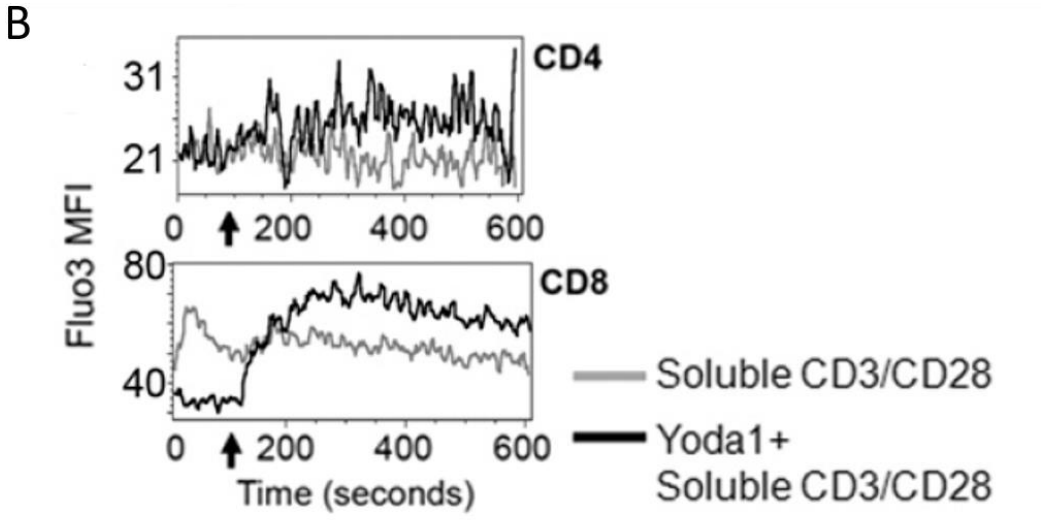

Figure 11-2-B. Yoda1 enhances Ca^{2+} influx response on TCR crosslinking by soluble anti-CD3 and anti-CD28 antibodies. TCR crosslinking by soluble anti-CD3 and anti-CD28 antibodies failed to induce any Ca^{2+} influx. Addition of Piezo1 agonist, Yoda1 in addition to soluble anti-CD3 and anti-CD28 antibodies, induced Ca^{2+} influx as measured by increase in Fluo-3AM mean fluorescence intensity (MFI) in both $CD4^+$ (A) and $CD8^+$ (B) T lymphocytes. Soluble anti-CD3 and anti-CD28 antibodies with or without Yoda1 were added at indicated time-points (black arrow) after measurement of baseline fluorescence. *(Adapted from Liu et.al. J Immunol. 2018.* [311]*)*

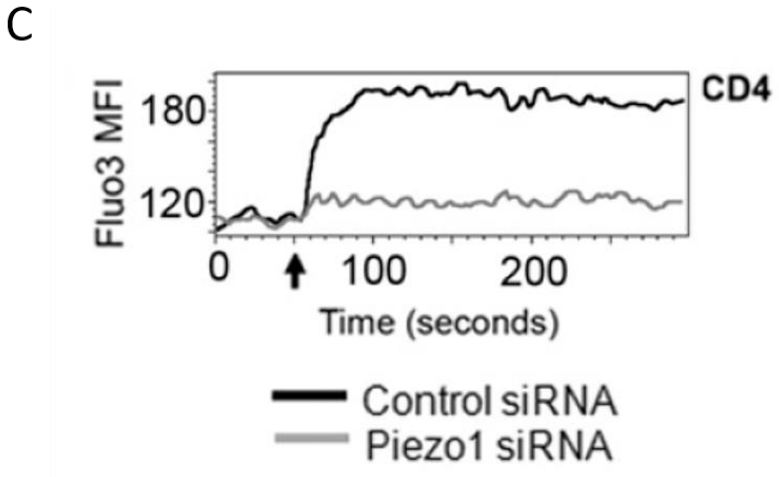

Figure 11-2-C. Specificity of Yoda1-induced Ca^{2+} influx in response to soluble anti-CD3 and anti-CD28 antibodies. Control and Piezo1 siRNA-transfected human $CD4^+$ T cells were loaded with Ca^{2+}-indicator, Fluo-3AM. After measurement of baseline fluorescence, transfected cells were stimulated with soluble anti-CD3 and anti-CD28 antibodies supplemented with Yoda1. Piezo1 downregulation significantly abolished Ca^{2+} influx in response to Yoda1 thus confirming its Piezo1 specificity. Ca^{2+} influx in response to stimulation was measured as increase in Fluo-3AM mean fluorescence intensity relative to baseline fluorescence. *(Adapted from Liu et.al. J Immunol. 2018. [311])*

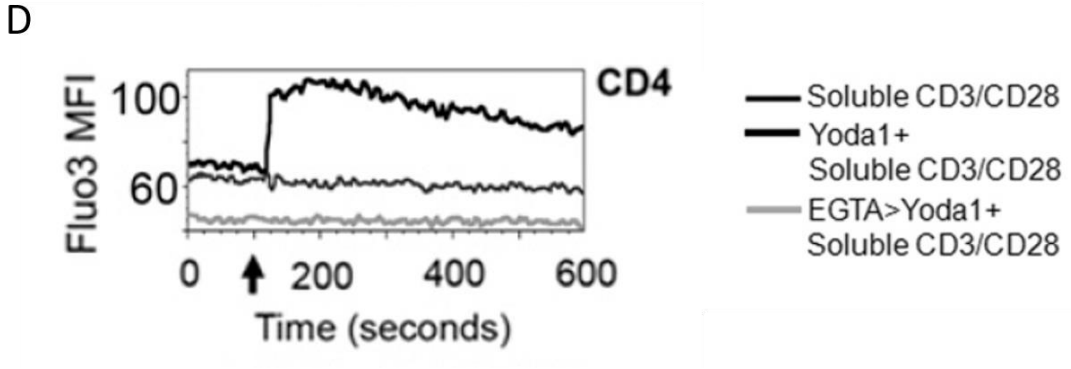

Figure 11-2-D. Yoda1 mediates influx of extracellular Ca^{2+}. Piezo1 activation allows passage of extracellular Ca^{2+}. Fluo-3AM-loaded $CD4^+$ T lymphocytes were stimulated with soluble anti-CD3 and anti-CD28 antibodies in the presence or absence of Yoda1. Yoda1 significantly increased Ca^{2+} response on TCR crosslinking. When cells were incubated with EGTA which chelates extracellular Ca^{2+}, Yoda1-induced enhanced Ca^{2+} response was significantly abolished indicating that Yoda1-mediated Piezo1 activation allows influx of extracellular Ca^{2+}. *(Adapted from Liu et.al. J Immunol. 2018. [311])*

11.4 Discussion

Mobilisation of intracellular Ca^{2+} and influx of extracellular Ca^{2+} is a crucial aspect of TCR signalling. When T cells bind to cognate antigens expressed on APCs, a cascade of signalling events are triggered that increases cytosolic Ca^{2+} levels through these mechanisms. Increased cytosolic Ca^{2+} is subsequently mobilised into different intracellular organelles where a number of metabolic and transcription pathways are triggered that govern T lymphocyte function. Piezo1 activation also allows passage of extracellular Ca^{2+} into the cell cytosol. This led us to wonder if Piezo1-mediated Ca^{2+} response contributes to TCR-mediated Ca^{2+} response. We found that Piezo1 deficiency in human $CD4^+$ and $CD8^+$ T lymphocytes led to significant abolishment of Ca^{2+} response on TCR stimulation by bead-bound anti-CD23/CD28. Similarly, addition of Piezo1 agonist, Yoda1 caused significant potentiation of Ca^{2+} influx in response to suboptimal TCR triggering by soluble anti-CD3 and anti-CD28 antibodies. Yoda1-induced enhanced Ca^{2+} response is Piezo1-specific since downregulation of Piezo1 completely abolished Ca^{2+} influx. Addition of the extracellular Ca^{2+}, chelator EGTA, also abrogated Ca^{2+} response in response to soluble TCR crosslinking antibodies supplemented with Yoda1, thus confirming that Ca^{2+} response on Piezo1 activation during TCR crosslinking is mediated through extracellular Ca^{2+} sources. Hence, Piezo1 activation during TCR triggering mediates influx of extracellular Ca^{2+} which is crucial for T cell activation.

Chapter 12. Piezo1 activation during TCR triggering induces downstream Ca^{2+}-dependent Calpain pathway

12.1 Introduction

Intracellular calcium acts as a potent second messenger triggering a number of intracellular signalling pathways leading to activation of a range of transcription factors that regulate T cell effector functions. TCR crosslinking triggers a number of downstream signalling pathways including PKCϴ-IKK-NFκB pathway, mTOR pathway, Ras-Erk1/2-AP-1 pathway [451]. Since Ca^{2+} signalling appears to play a crucial role in Piezo1-mediated TCR signalling, we decided to assess pathways that are directly regulated by cytosolic Ca^{2+}. Ca^{2+}-dependent NFAT pathway was one such promising candidate. The NFAT (Nuclear factor of activated T cells) family of proteins are transcription factors that are activated in response to intracellular Ca^{2+} [463]. NFAT proteins have a highly conserved DNA-binding domain known as the REL-homology region (RHR). Binding of calcium to calmodulin induces calmodulin-dependent activation of calcineurin phosphatase. Dephosphorylation of NFAT by calcineurin triggers its activation and subsequent localisation to the nucleus where it binds to NFAT promoters via its RHR domain and induces expression of T cell activation genes like IL-2 [463].

Ca^{2+} signalling is crucial during formation of a stable synapse between T cell and APC. T cells continuously move on the APC surface while scanning for specific antigens [463,464]. Once they encounter cognate antigen-MHC on the APC surface, they must stop movement and form stable contacts so as to facilitate efficient T cell activation. Blocking increase in intracellular Ca^{2+} levels failed to achieve actin cytoskeletal reorientation in the T cell-APC contact region and subsequent formation of a stable immunological synapse [465]. Ca^{2+}-dependent calpain

pathway is essential for actin cytoskeletal reorientation [466]. Calpains are Ca^{2+}-dependent cysteine proteases that act on actin cytoskeletal-associated proteins [466,467]. Calpains consist of a catalytic domain and a regulatory domain. Binding of Ca^{2+} induces a conformational change and subsequent dissociation of the regulatory subunit from the catalytic domain leading to its activation [467]. Calpain substrates include membrane-cytoskeletal tether protein, talin, actin-crosslinking protein, α-actinin, actin binding protein, cortical proteins like spectrin and ankyrin [467]. Calpain has also been shown to regulate integrin, focal adhesion kinase and protein kinase C activities all of which affect TCR signalling [467,468]. Hence, Ca^{2+}-dependent activation of the calpain pathway also seemed a potential effector of Piezo1 response in T lymphocytes.

12.2 Methods

Studying the role of Ca^{2+}-dependent NFAT pathway in Piezo1-mediated T cell activation: Cyclosporin A is an inhibitor of calcineurin phosphatase. Addition of cyclosporin A prevents calcineurin-dependent dephosphorylation and activation of NFAT and its subsequent nuclear translocation. Thus, it can be used as an inhibitor of Ca^{2+}-dependent NFAT pathway.

$CD4^+$ T lymphocyte activation

Human $CD4^+$ T lymphocytes were isolated from PBMCs as described earlier. Approximately 200,000 cells were seeded in 100µl of RPMI + 10% FBS. 2µg/ml each of soluble anti-CD3 and anti-CD28 antibodies were added in the presence of absence of Piezo1 agonist, Yoda1. 2.5µM of cyclosporine A was added to the cells 1 hour prior to treatment in order to achieve efficient blocking of the NFAT pathway. Untreated cells were used as control. $CD4^+$ T lymphocytes were collected in TRIzol after 1 hour of stimulation and relative expression of CD69 mRNA was measured by quantitative PCR as described before.

Studying the role of Ca^{2+}-dependent calpain pathway in Piezo1-mediated T cell activation

PD150606

PD150606 is a non-peptide and uncompetitive inhibitor of calpain. It is cell permeable and binds to the calmodulin-like domain of calpain causing its inhibition. It is highly selective for calpain.

$CD4^+$ T lymphocyte activation

Human $CD4^+$ T lymphocytes were isolated from PBMCs as described earlier. Approximately 200,000 cells were seeded in 100µl of RPMI + 10% FBS. 2µg/ml each of soluble anti-CD3 and anti-CD28 antibodies were added in the presence of absence of Piezo1 agonist, Yoda1 (15µM). 100µM of PD150606 was added to the cells 1 hour prior to treatment in order to achieve efficient blocking of the NFAT pathway. Untreated cells were used as control. $CD4^+$ T lymphocytes were collected and lysed in TRIzol after 1 hour of stimulation. Relative expression of CD69 mRNA was measured by quantitative PCR as described before.

12.3 Results

Ca^{2+}-dependent calpain activation mediate Piezo1 function in T cell activation. We attempted to identify the signalling component activated downstream of Piezo1-mediated influx of Ca^{2+} during T cell activation. Isolated human $CD4^+$ T lymphocytes were activated with soluble TCR crosslinking antibodies in the presence or absence or Piezo1 agonist, Yoda1. As expected, T cell achieved optimal activation on TCR crosslinking in the presence of Yoda1, measured by increased CD69 mRNA expression. Calcineurin inhibitor, Cyclosporin A (CsA) or calpain inhibitor, PD150606 was added to the cells prior to stimulation to block the Ca^{2+}-dependent NFAT and calpain signalling pathway respectively. Cyclosporin A-dependent inhibition of the

NFAT signalling pathway did not affect Yoda1-mediated optimal T cell activation (Fig. 12-B). On the other hand, inhibition of the calpain pathway almost completely abolished Yoda1-mediated heightened T cell activation (Fig. 12-A).

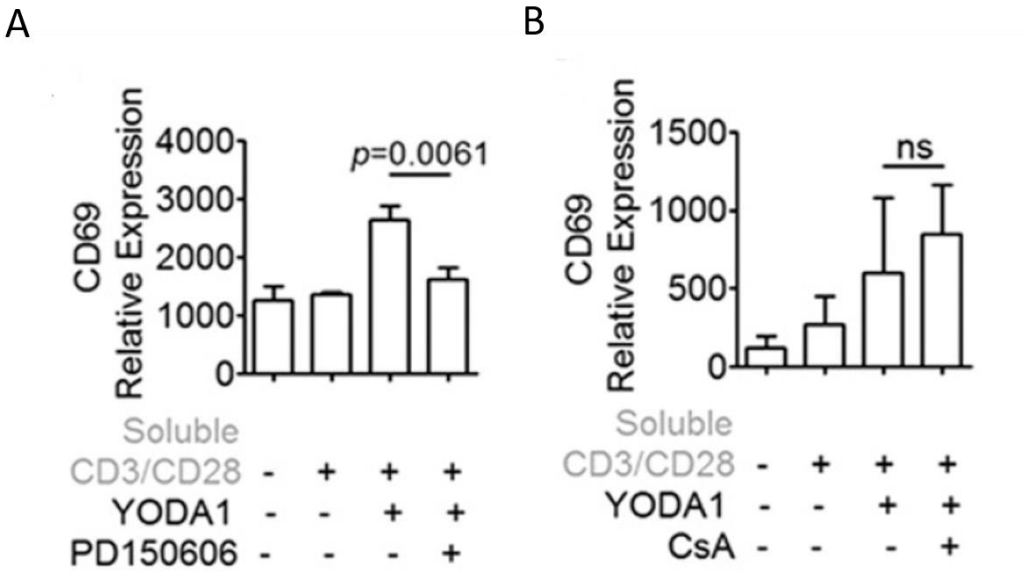

Figure 12. Piezo1-mediated Ca^{2+} influx drives T cell activation through downstream calpain activation. Inhibition of Ca^{2+}-dependent calpain pathway by PD150606 in $CD4^+$ T lymphocytes abolished Yoda1-mediated optimal T cell activation in response to soluble anti-CD3 and anti-CD28 antibodies (A). Inhibition of the calcineurin-NFAT signalling pathway by cyclosporin A (CsA) did not affect Yoda1-mediated optimal CD69 activation by soluble anti-CD3 and anti-CD28 antibodies (B). *(Adapted from Liu et.al. J Immunol. 2018. [311])*

12.4 Discussion

We sought to identify signalling pathways that mediate Piezo1 function during T cell activation. Piezo1-dependent T cell activation depends on influx of Ca^{2+} as observed in the previous section. Moreover, since downregulation of Piezo1 severely impaired T cell

activation even in early stages of TCR triggering (phospho-ZAP70 and CD69 induction), we decided to assess specific pathways that are activated early on during TCR triggering and regulated directly by intracellular Ca^{2+} levels. The Ca^{2+}-dependent NFAT pathway and Ca^{2+}-regulated calpain signalling pathway are viable candidates since they are activated proximal to TCR triggering and are directly activated by cytosolic Ca^{2+}. We inhibited each of these pathways and measured if optimal T cell activation as induced by Piezo1 agonist, Yoda1 under suboptimal TCR triggering conditions (soluble TCR crosslinking antibodies) was affected at all. Yoda1-mediated optimal CD69 activation was not affected if the calcineurin-NFAT pathway was blocked which suggested that Piezo1-mediated influx of Ca^{2+} probably did not trigger this pathway. On the other hand, inhibition of the calpain pathway resulted in a sharp reduction CD69 activation response to Yoda1 and TCR crosslinking. This prompted us to conclude that Ca^{2+} influx on Piezo1 activation during TCR triggering activated cytosolic calpain which led to optimal T cell activation.

Chapter 13. Piezo1-mediated activation of the calpain pathway triggers polymerisation and re-organisation of the actin cytoskeletal scaffold during T cell activation

13.1 Introduction

When T lymphocytes bind to APCs bearing cognate peptide-MHCs, they extend lamellipodia and pseudopodia-based membrane extensions towards the APC surface [469]. This process of efficient contact formation involves extensive actin cytoskeletal rearrangement in the interface [469]. Cytoskeletal reorganisation is characterised by heightened actin polymerisation along with active changes in actin-myosin contractile network. These cytoskeletal changes act together to recruit signalling components like TCR clusters, adaptor proteins and downstream signalling molecules at region of T cell-APC interface so as to form a compartmentalised region of active T cell activation and signalling called the immunological synapse (IS) [469]. Formation of a stable IS is crucial for optimal and sustained T cell activation. Actin dynamics at the IS divides it into 3 distinct regions called the supramolecular activation clusters (SMACs), each with its own specific role in the T cell activation process [311,447,469]. The central region of SMAC (cSMAC) contains TCR clusters and associated signalling molecules. cSMAC is surrounded by a region (peripheral or pSMAC) enriched in integrin LFA-1 and adhesion proteins. Proteins with large ectodomains like CD45 tyrosine phosphatses are mostly excluded and confined to the outermost region called the distal SMAC (dSMAC). The structure of the IS is tightly regulated by strength and nature of TCR-APC interaction. The IS is a dynamic structure where signalling components are constantly recruited or reorganised between the domains through actin-regulated processes. Active T cell signalling is confined to the

peripheral zones of the IS while the central region serves to downregulate activation by degrading TCR clusters and associated signalling molecules. Thus, reorganisation of the actin scaffold serves to form specialised membrane nanodomains that are rich in signalling components essential for optimal T cell activation [311,447,469]. As described in the previous chapter, calpains are cytosolic cysteine proteases that play a crucial role in actin cytoskeletal remodelling downstream of TCR activation. Inhibition of calpain impairs Yoda1-mediated TCR activation, thus implicating the activity of these proteases downstream of Piezo1-mediated Ca^{2+} signalling. We, therefore, attempted to confirm if Piezo1-mediated activation of the calpain pathway plays a similar role in actin cytoskeletal remodelling during T cell activation.

13.2 Methods

Measurement of actin polymerisation of Filamentous actin (F-actin) content in response to T cell activation

$CD4^+$ T lymphocytes were isolated from PBMCs of healthy volunteers. Approximately 200,000 cells were activated with soluble anti-CD3 and anti-CD28 antibodies (2µg/ml each) in the presence and absence of 15µM of Piezo1 agonist, Yoda1. Cells were stimulated for 30 minutes at 37˚C in the presence or absence of 100µM of Calpain I inhibitor, PD15606 (Cells were preincubated with PD15606 for 1 hour before stimulation). Effect of calpain inhibition on Yoda1-mediated TCR activation and actin polymerisation was analysed by measuring F-actin content by flow cytometry on BD LSR Fortessa II.

Flow cytometric assessment of F-actin content

After stimulation of $CD4^+$ T lymphocytes as described above, cells were collected and washed in FACS buffer and fixed in 4% paraformaldehyde for 45 minutes at room temperature. Cells

were then permeabilised in FACS buffer + 0.1% saponin for 30 minutes at room temperature followed by addition of Alexa 532 conjugated-phalloidin (1:500, vol:vol) for 30 minutes at room temperature. Phalloidin binds to F-actin and fluorescence intensity can be used to quantify increase in F-actin content or polymerised actin after stimulation. Cells were then washed and analysed in BD LSR II Fortessa.

Confocal imaging of actin polymerisation or F-actin content on T cell activation: Coverslips were coated with 2mg/ml poly-L-lysine for 1 hour at room temperature followed by washing with 1X PBS and drying. Approximately 100,000 $CD4^+$ T lymphocytes were allowed to attach to coated coverslips for 2 hours at 37˚C and 5% CO_2. Cells were stimulated with 2µg/ml each of TCR crosslinking, soluble anti-CD3 and anti-CD28 antibodies in the presence or absence of 15µM of Yoda1 and 100µM Calpain I inhibitor, PD15606. Stimulation was carried out for 30 minutes at 37˚C, 5% CO_2. After stimulation, cells were washed with 1X PBS and fixed with 4% paraformaldehyde for 1 hour at room temperature. Blocking and permeabilization were performed with 3% Bovine-serum albumin in 0.1% Triton X-100 for 30 minutes at room temperature followed by washing thrice with 1X PBS. Alexa 532-conjugated phalloidin was added to the cells at a concentration of 1:100 in 1X PBS and incubated at room temperature for 30 minutes. Cells were washed thrice with 1X PBS followed by addition of 1µg/ml DAPI for 1 minute. After washing, cells were mounted on 7µl VECTASHIELD antifade mounting media.

Image acquisition

Images were acquired using Olympus IX81 microscope with a Yokogawa CSU-X1 spinning disc system. 3D images were acquired through Z-stack imaging where each Z-step corresponded to 0.25µm.

Image analysis: Gaussian filtering was applied for 3D volume rendering and image construction using Imaris 7. Images were captured from multiple fields containing approximately 25 to 50 cells. The average surface area of F-actin was calculated in order to quantify F-actin content in differently stimulated cells.

Co-localisation of polymerised F-actin scaffold and Piezo1

13mm glass coverslips were coated with 2mg/ml poly-L-lysine for 1 hour at room temperature and washing thrice with 1X PBS. After drying, approximately 100,000 $CD4^+$ T lymphocytes were allowed to attach to coated coverslips for 2 hours at 37˚C and 5% CO_2. Anti-CD3/CD28-coated dynabeads were then added in a ratio of 1:1 (as described by manufacturer's protocol) and incubated for 30 minutes at 37˚C. Cells were washed with 1X PBS and fixed with 4% paraformaldehyde for 45 minutes at room temperature. Cells were washed thrice with 1X PBS and blocked with 3% bovine-serum albumin in 1X PBS containing 0.1% Triton X-100 for 1 hour at room temperature. Goat anti-human Piezo1 antibody was added at a concentration of 1:25 (vol:vol) and incubated at room temperature for 1 hour. Cells were washed thrice with 1X PBS. Anti-goat alexa 594 was added at a concentration of 1µg/ml and incubated for 1 hour at room temperature. Alexa 532-conjugated phalloidin was added at a concentration of 1:100 and incubated for 30 minutes at room temperature. Cells were washed thrice with 1X PBS. 1µg/ml of DAPI was added for a minute and washed thrice thoroughly with 1X PBS. Coverslips were mounted on 7µl VECTASHIELD antifade mounting media.

Image acquisition

Images were acquired using Olympus IX81 microscope with a Yokogawa CSU-X1 spinning disc system.

Measurement of actin polymerisation of Filamentous actin (F-actin) content in response to T cell activation after Piezo1 downregulation

$CD4^+$ T lymphocytes were isolated from PBMCs of healthy volunteers. Approximately 2-3 million cells were electroporated with control EGFP siRNA and Piezo1 siRNA. On day 3 post-electroporation, cells were collected and approximately 200,000 cells/ well cultured and stimulated with bead-immobilised anti-CD3/CD28 antibodies (1:1, bead : cells) for 30 minutes. After stimulation, cells were washed and fixed in 4% paraformaldehyde for 45 minutes at room temperature. Cells were permeabilised in 0.1% saponin buffer for 30 minutes and stained with alexa 532-conjugated phalloidin at a concentration of 1:100 (volume : volume) for 30 minutes. Cells were washed and acquired in BD Fortessa LSR II.

13.3 Results

Piezo1 agonist stimulates calpain-mediated polymerisation of actin downstream of TCR crosslinking. TCR activation triggers a cascade of signalling events which lead to reorganisation of the cytoskeletal actin scaffold and formation of the immune synapse. As observed before (Chapter 9), addition of Piezo1 agonist, Yoda1, significantly potentiates T cell activation in response to soluble forms of TCR crosslinking antibodies (Fig. 13-A, B). We measured increase in actin polymerisation through flow cytometric quantification of F-actin content in response to 30 minutes of TCR stimulation. TCR crosslinking by soluble anti-CD3 and anti-CD28 antibodies triggered a marginal increase in F-actin content in comparison to untreated cells. Addition of Piezo1 agonist, Yoda1, on the other hand, significantly increased actin polymerisation in response to TCR crosslinking by soluble antibodies. Yoda1-mediated cytoskeletal actin polymerisation was however, abrogated in the presence of calpain I inhibitor, PD15606, thus confirming that the role of Piezo1 in optimal T cell activation is

mediated through Ca^{2+}-dependent calpain pathway (Fig. 13-A, B). Similarly, 3D confocal imaging confirmed that Piezo1 activation through Yoda1 potentiates polymerisation and remodelling of the actin scaffold in response to TCR crosslinking as measured by increase in average surface area of F-actin in stimulated cells. 3-D images of the cells were constructed and same-intensity thresholding was applied to all the cells. The average surface area of these phalloidin-stained cells was then calculated. Inhibition of calpain significantly reduced actin polymerisation in response to Yoda1 as measured by reduction in phalloidin-bound F-actin surface area, thus affirming its role downstream of Piezo1 activation (Fig. 13-C, D). Isolated $CD4^+$ T lymphocytes stimulated with bead-immobilised anti-CD3/CD28 antibodies showed a strong increase in F-actin content which was significantly reduced on Piezo1 downregulation (Fig. 13-E, F). Confocal imaging of $CD4^+$ T lymphocytes stimulated with bead-bound anti-CD3/CD28 antibodies showed strong co-localisation of Piezo1 and actin cytoskeleton after 30 minutes of stimulation (Fig. 13-G).

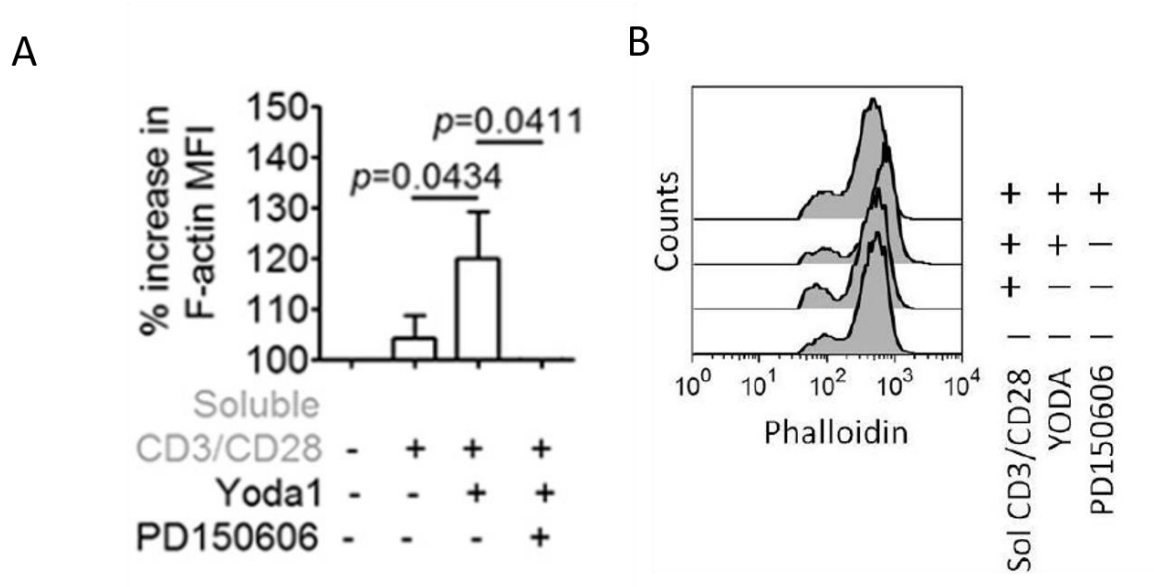

Figure 13-A-B. Piezo1 agonist Yoda1 reorganises the actin cytoskeletal scaffold during TCR activation. F-actin content was quantified through flow cytometric measurements after 30

minutes of CD4⁺ T cell stimulation with soluble forms of TCR crosslinking anti-CD3 and anti-CD28 antibodies in the presence or absence of Yoda1 and preincubated Calpain I inhibitor, PD15606. Data is representative of at least 3 independent experiments (A). Representative flow cytometry plots overlay of F-actin content in response to T cell stimulation (B). *(Adapted from Liu et.al. J Immunol. 2018. [311])*

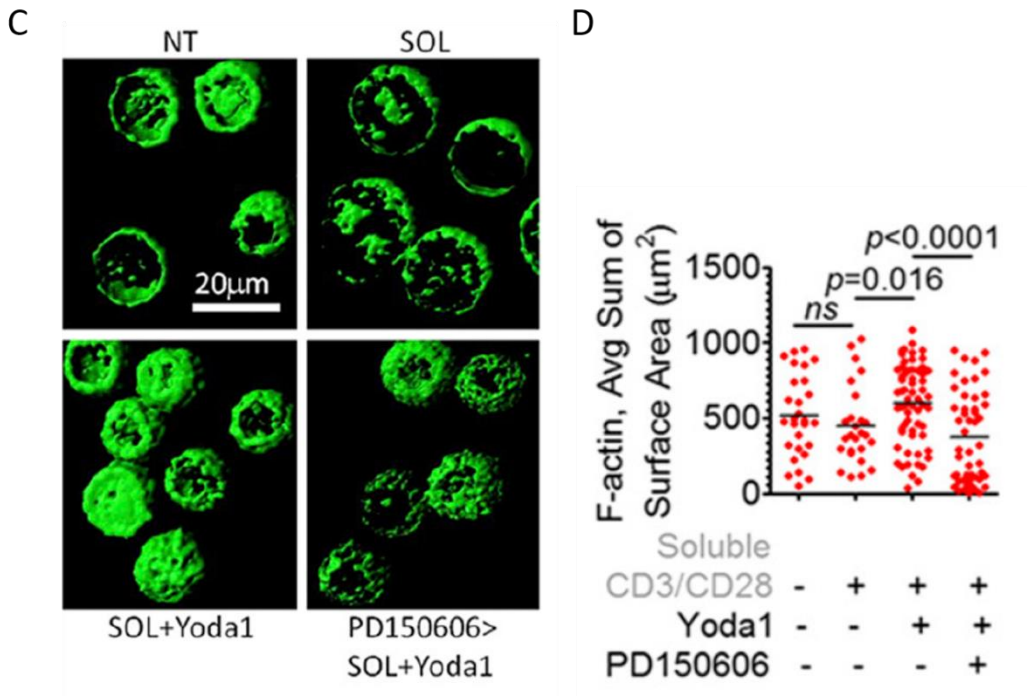

Figure 13-C-D. 3-D confocal imaging of F-actin content in CD4⁺ T lymphocytes. CD4⁺ T lymphocytes were stimulated with soluble TCR crosslinking antibodies for 30 minutes. Piezo1 agonist, Yoda1 was added to determine its effect on actin polymerisation during T cell activation in the presence or absence of calpain I inhibitor. Cells were stained with Alexa 532-conjugated phalloidin for F-actin quantification. Representative 3-D confocal images of F-actin content in stimulated CD4⁺ T lymphocytes stained with fluorochrome-conjugated phalloidin (C). Statistical analysis of F-actin content measured as average sum of F-actin surface area of thresholded stimulated CD4⁺ T lymphocytes (D). *(Adapted from Liu et.al. J Immunol. 2018. [311])*

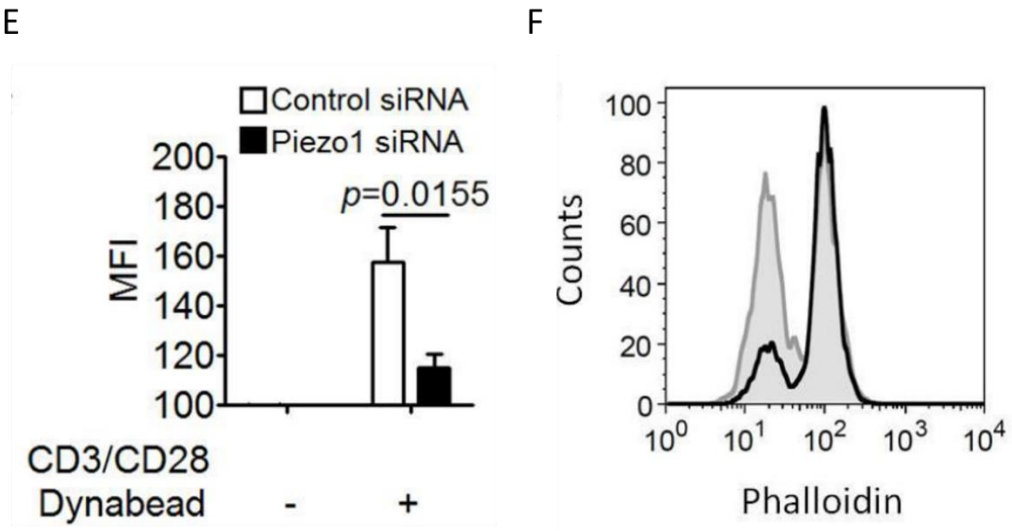

Figure 13-E-F. Piezo1 downregulation abolished increase in F-actin polymerisation in response to TCR stimulation. $CD4^+$ T lymphocytes were transfected with control and Piezo1-specific siRNAs. After knockdown, transfected cells were stimulated with bead-immobilised anti-CD3/CD28 antibodies for 30 minutes. Bead-immobilised TCR crosslinking antibodies produced a strong increase in T cell F-actin signal which was significantly reduced on Piezo1 downregulation. Data representative of at least 3 independent experiments (E). Representative flow cytometry plots of F-actin content in phalloidin stained $CD4^+$ T cells stimulated with bead-bound anti-CD3/CD28 antibodies. Black outline: Control siRNA-transfected cells. Grey-shaded area: Piezo1 knockdown cells. *(Adapted from Liu et.al. J Immunol. 2018.* [311]*)*

G

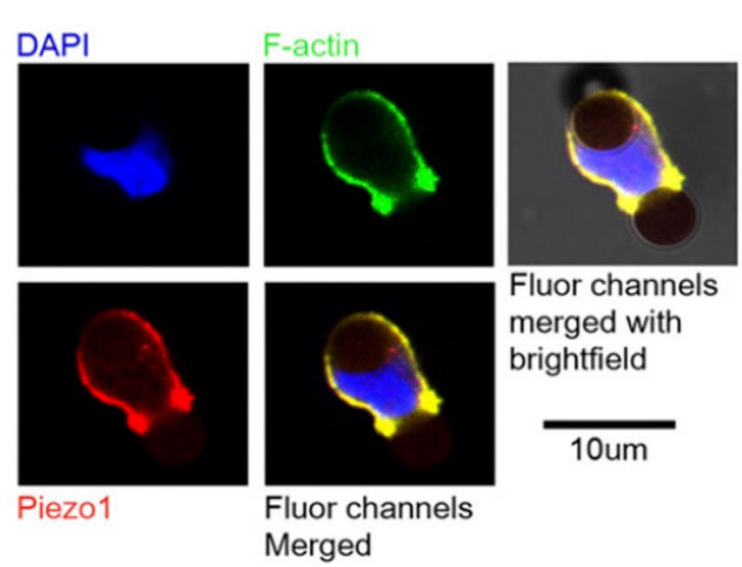

Figure 13-G. Piezo1 co-localises with actin cytoskeleton in stimulated CD4⁺ T cells. CD4⁺ T lymphocytes were stimulated with bead-immobilised anti-CD3/CD28 antibodies for 30 minutes. Cells bound to bead-immobilised TCR-crosslinking antibodies showed a strong co-localisation of Piezo1 with the actin cytoskeletal scaffold thus confirming their closely-regulated dynamics. *(Adapted from Liu et.al. J Immunol. 2018. [311])*

13.4 Discussion

Results from the previous section (3.8.3) confirmed that Piezo1 mediates its function through Ca^{2+}-dependent calpain activation downstream of T cell stimulation. Inhibition of calpain abolishes the ability of Piezo1 to facilitate T cells activation under optimal stimulating conditions (bead-immobilised anti-CD3/CD28 antibodies as compared to weakly stimulating soluble anti-CD3 and anti-CD28 antibodies) as well as in the presence of Piezo1 agonist, Yoda1. Calpain activation has been associated with cytoskeletal actin polymerisation. Polymerisation and reorganisation of cortical actin is a crucial aspect of optimal T cell activation since it results in the formation of the active signalling-competent immunological

synapse between the T cell and cognate APC membrane interface. Numerous studies have shown that interfering with actin polymerisation through addition of inhibitors like latrunculin A, strongly impairs formation of the immunological synapse and abrogates optimal T cell activation. We attempted to identify if Piezo1-mediated calpain activation plays a similar role in cortical actin polymerisation during T cell activation. We measured F-actin (polymerised actin) content in response to various forms of TCR stimulation through flow cytometry and 3-D confocal imaging. As expected, TCR stimulation with weakly activating soluble anti-CD3 and anti-CD28 antibodies produced a marginal increase in F-actin content which was drastically enhanced when Piezo1 was exogenously activated with its agonist, Yoda1. Yoda1-mediated increase in F-actin content was however, significantly reduced in the presence of calpain inhibition. Moreover, activation of $CD4^+$ T lymphocytes with strongly activating bead-immobilised anti-CD3/CD28 antibodies resulted in a strong F-actin signal which was significantly impaired on Piezo1 downregulation. Thus, Piezo1 activation during T cell stimulation under optimal conditions, triggers activation of Ca^{2+}-dependent calpain that subsequently triggers actin polymerisation and remodelling of the cortical actin scaffold resulting in formation and stabilisation of the immune synapse. Piezo1-deficient T cells fail to undergo actin cytoskeletal remodelling and immune synapse stabilisation, thus, failing to achieve optimal T cell activation.

Chapter 14. Conclusion

Interaction between T lymphocytes and APCs bearing cognate peptide-MHCs is characterised by the generation of mechanical forces that govern their function and fate [311]. Optimal activation of T cells is crucially dependent on their ability to sense and respond to mechanical cues like alterations in membrane tension or shear stress experienced on their surface during interaction with APCs [311]. Changes in the mechanical properties of the environment strongly affect T cell activation and function. Any form of external interference that abolishes mechanical forces during interaction with APCs, results in defective T cell activation and function. Although various studies have elucidated the imperativeness of mechanical cues in T cells activation, no dedicated mechanosensor was identified until recently [470]. In the above study, we have identified Piezo1 channel as a T cell mechanosensor that is essential for optimal T cell activation. Piezo1 channels belong to a family of evolutionarily conserved ion channels that senses mechanical cues [311]. Studies have shown that Piezo1 senses changes in membrane tension and gets activated in response to membrane stretch. Upon activation, Piezo1 opens and allows influx of extracellular cations like Ca^{2+} and Na^{+} [311]. As described earlier, T cell interaction with cognate APCs results in generation of mechanical forces which leads to changes in T cell membrane tension that regulates T cell activation. In-vitro studies have shown that TCR crosslinking antibodies immobilised on a solid surface like inert beads or coated matrices are more efficient at stimulating T cells as compared to soluble forms of crosslinking antibodies, suggesting the importance of mechanical interactions [311]. In our study, we used two different forms of TCR crosslinking antibodies in order to simulate altered mechanical dynamics on the T cell surface – a. TCR crosslinking antibodies (anti-CD3 and anti-CD28) immobilised on beads sized approximately 4.5µm which will exert mechanical stress

on the T cell surface (similar to T cell interaction with APCs) and b. soluble forms of anti-CD3 and anti-CD28 antibodies which do not exert any mechanical force on the T cell surface upon binding [311,470]. As anticipated, bead-immobilised TCR crosslinking antibodies triggered efficient T cell stimulation while soluble forms of antibodies failed to optimally activate T cells [470]. siRNA-mediated Piezo1 knockdown, however abolished the capacity of bead-immobilised TCR crosslinking antibodies to optimally activate T cells, thus confirming that Piezo1-mediated mechanotransduction is crucial. T cell activation in response to allogenic or autologous APCs was also strongly dependent on the presence of Piezo1 channels. Gain-of-function studies involving Piezo1 agonist, Yoda1 showed that its addition significantly enhanced the ability of otherwise weakly-activating soluble anti-CD3 and anti-CD28 antibodies to trigger optimal T cell activation. Flow cytometric measurements revealed that Piezo1 activation during T cell stimulation results in influx of extracellular Ca^{2+} which triggers activation of downstream calpain pathway. Piezo1-mediated activation of the Ca^{2+}-dependent calpain pathway results in enhanced polymerisation actin and remodelling of the cytoskeletal actin scaffold which is characteristic of T cell activation and formation of a stable immunological synapse between T cells and APCs (Fig. 14) [470]. Thus, this study provides first evidence of a T cell-committed mechanosensor, Piezo1, that plays an indispensable role in T cell activation. We have tried to develop a model of Piezo1-mediated T cell activation involving Ca^{2+} signalling and calpain-dependent cytoskeletal actin reorganisation [470]. Further mechanistic studies are required to provide a detailed evaluation of Piezo1-mediated signalling in T cell activation.

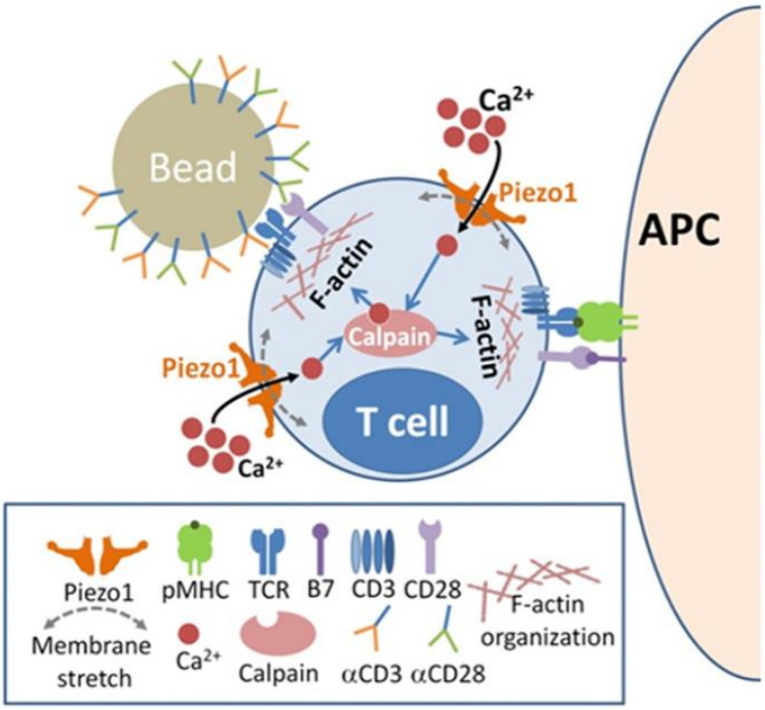

Figure 14. Proposed model for role of Piezo1 mechanotransduction in optimal human T cell activation. Interaction between T cell and APC results in generation of mechanical forces and altered T cell membrane tension. Piezo1 channels on the T cell surface are gated in response to altered membrane tension which allows influx of extracellular Ca^{2+}. Increase in cytosolic Ca^{2+} level triggers calpain activation. This subsequently triggers actin polymerisation and remodelling of the actin cytoskeleton, characteristic of immune synapse formation and stabilisation thereby resulting in optimal T cell activation. *(Adapted from Liu et.al. J. Immunol. 2018.* [470]*)*

Chapter 15. Mechanical aspects of T lymphocyte migration

15.1 Role of mechanical cues in immune cell migration

Immune cells migrate through complex tissue microenvironment during an immune response. An effective immune response requires directed migration towards the inflamed peripheral site and to secondary lymphoid organs to generate long-term adaptive immune response [471]. Different tissue sites, diseased conditions and degree of inflammation present different mechanical microenvironments to migrating immune cells [90,91]. Immune cells sense and adapt to varying mechanical cues provided by its surroundings during migration. Studies have shown that generation of mechanical force and subsequent transfer of momentum to the surroundings are essential for efficient migration [231]. The dynamically changing cellular actomyosin contractile network during cell migration is responsible for generation of mechanical forces [231]. Actin polymerisation at the leading edge of a moving cell forms membrane-based extensions like lamellipodia and pseudopodia that exerts force against the environment and pushes the cell forward. Myosin II-based contractions of the actin fibres generates contractile or traction forces at the trailing edge that pulls the cell forward thereby facilitating cell movement [231]. Integrin-based focal adhesion complexes allow transfer of momentum to the surroundings [231]. It has also been shown that 3D geometric confinement affects mode of immune cell migration [231,472]. Migration on 2D surfaces requires focal adhesion-based anchoring [231]. Migration of leukocytes on vascular endothelial cells requires contact-based adhesion to allow leukocyte crawling in the blood vessels while resisting shear stress generated by blood flow [219,231]. Confined 3D migration, on the other hand is usually adhesion-independent, otherwise known as ameboid mode of migration [473]. Nonadhesive mode of confined migration is facilitated by retrograde flow of actin steered by myosin II-

based contractions. It was recently shown that adhesion-independent migration is driven through retrograde flow of the plasma membrane [474]. This is facilitated by balanced rates of membrane endocytosis at the cell trailing edge followed by directed flow of membrane to the cell leading edge. Directional membrane flow generates tangential viscous forces in the 3D environment that results in cell propulsion through the environment [474]. These forces have been shown to act through triggering RhoA activity and allowing directed migration and migration speeds were significantly higher than adhesion-based mode of movement [474]. Moreover, it has been shown that leukocyte transmigration across the blood vessels is enabled by its capacity to scan the microenvironment and preferentially migrate through the path of least resistance by choosing larger pore sizes [344]. Leukocytes regulate the position of their nucleus and associated microtubules, allowing them to assess mechanical resistance. Leukocyte polarity is essential to maintain directional migration. Leukocytes including T lymphocytes redistribute their membrane and cytoplasmic components in response to a chemotactic gradient, which generates cell polarity. This is crucial in directional cell movement [475]. Mechanical parameters are a crucial consideration during generation and maintenance of cellular polarity [476]. Cell polarity is generated by formation of a cell leading edge where signalling components are confined. It has been widely believed that in order to prevent formation of additional leading edges, the leading edge produces inhibitors that sequesters signalling components to the leading edge [477]. These inhibitors prevent polarised signalling molecules from diffusing to the rest of the cell, thereby maintaining cell polarity. A recent study however, showed that this mechanism is not sufficient to maintain cell polarity during movement. It was shown that formation of a leading-edge pseudopodia results in doubling of membrane tension in the area, which inhibits diffusion of polarised signalling components like polymerised actin and Rac1 to the rest of the cell [477]. When neutrophils

make contact with a surface, the resultant localised increase in membrane curvature at the region of contact triggers generation of cell polarity by breaking cell symmetry and initiation of actin cytoskeleton polarisation [477]. Thus, mechanical parameters play a significant role in regulating immune cell migration (Fig. 15).

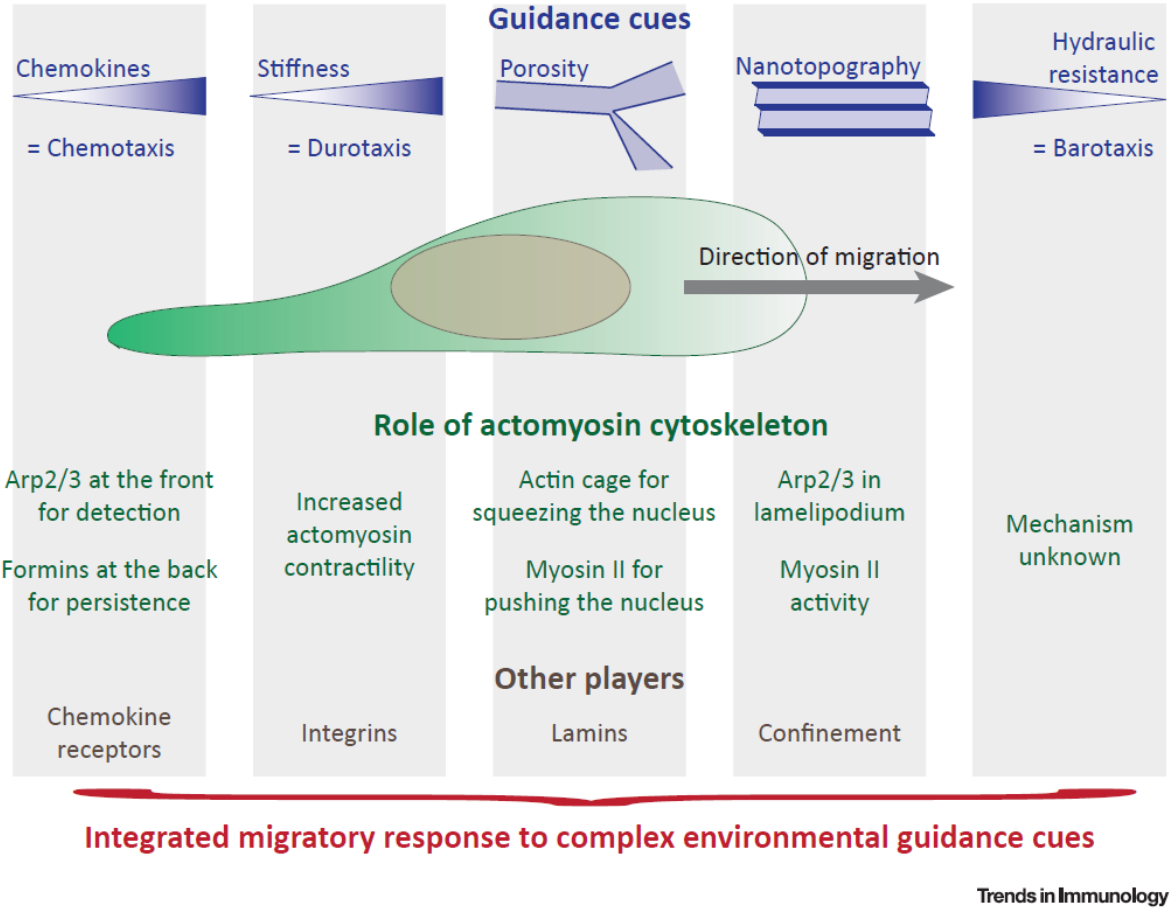

Figure 15. Interplay between environmental cues and cytoskeleton scaffold during immune cell migration. Migrating immune cells encounter diverse mechanical cues from their tissue microenvironment. Migrating immune cells modulate their migratory patterns according to environmental mechanical properties that include tissue porosity, tissue stiffness as determined by ECM components, topographical cues and hydraulic pressure (a parameter widely important in inflamed tissues characterised by localised swelling). Migrating immune cells also show chemotactic behaviour by migrating along chemokine gradients. All these

parameters provide diverse mechanical stimulus that is mostly transduced through changes in the cells' actomyosin network, resulting in cells' migratory behaviour. Immune cell migration is regulated by a feedforward loop involving environmental, cell-extrinsic mechanical stimulus and subsequent triggering of cytoskeletal changes and generation of cell-intrinsic forces. Moving cells generate a form of polarity triggered by Arp 2/3-mediated actin polymerisation at leading lamellipodia, and actin retrograde flow to the rear uropod through myosin contractions. This mechanism propels the cell in the forward direction. Nuclear positioning and mechanotransduction plays an important role in 3D migration which is also regulated by the actomyosin contractile network. Integrin-based contacts also facilitate leukocyte rolling and diapedesis across blood vessels to tissue sites. Other factors like chemokine gradient and degree of confinement also affect immune cell migratory modes. *(Adapted from Moreau et.al. Trends Immunol. 2018 [231].)*

15.2 Role of mechanical cues in T lymphocyte migration

It has been shown that shear stress generated by circulating blood regulate T cell migration along the endothelial blood vessel [338]. T cell extravasation across the blood vessels through high endothelial venules (HEVs) primarily requires T cell firm attachment to the endothelial wall by resisting detachment because of high shear stress in the surroundings. This firm attachment is mediated through interaction between T cell integrins and endothelial selectins. Integrin-mediated arrest on the blood vessel is tightly regulated by forces generated from shear stress [338]. Atomic force microscopy-based measurements characterise this interaction as a catch bond whose strength and stability increases with force at lower shear stress magnitudes [219,220]. Force-triggered conformational changes in the interacting

integrin/selectin domains allows stable interaction. Thus, mechanical forces facilitate firm attachment between T cells and endothelial cells so as to enable their transmigration to lymph nodes or inflamed peripheral tissues [228,337].

T cells also display a characteristic phenotype known as durotaxis which is their preference to migrate towards stiffer substrates [340]. Altered physiological conditions like inflammation and tumor formation are associated with changes in the stiffness properties of the microenvironment. Tumor progression is characterised by changes in the mechanical properties of the extracellular matrix (ECM) which affect infiltration of T lymphocytes [478]. Usually, tumor microenvironment is characterised by increase in stiffness due to ECM remodelling by collagen formation and crosslinking. T cell migration can be modulated by altering substrate stiffness with stiffer substrates allowing more efficient migration. T cells also exert greater traction forces on stiffer substrates [479]. A recent study developed nanostructured devices that allowed them to study the intricate relationship between mechanical signals provided by the tumor microenvironment and T cell migration [480]. They found that microtubule organisation and activity is essential for proper migration in response to diverse physical parameters of the tumor site. Pharmacological or genetic manipulation can help design cells that can optimally sense and adapt to varying mechanical properties in the tumor site, allowing their uniform infiltration during immunotherapy [480]. Thus, mechanical forces play a crucial role in efficient T lymphocyte migration which led us to delve into the plausible role of Piezo1-mediated mechanotransduction in this process.

Chapter 16. Role of Piezo1 channels in 2D migration of $CD4^+$ T lymphocytes

16.1 Introduction

An effective adaptive immune response to infection requires $CD4^+$ T lymphocytes binding to target antigens present on cognate APCs. Interaction between $CD4^+$ T lymphocytes with target cells is critically dependent on efficient migration to peripheral tissues as well as secondary lymphoid organs where long-term immune response is generated. APCs encounter target antigens on peripheral sites and carry them to secondary lymphoid organs where they activate naïve T lymphocytes [481]. Activated $CD4^+$ T lymphocytes undergo reprogramming so as to upregulate various receptors including those involved in migration. These cells regulate their migratory capacity which enable them to find APCs bearing target antigens in the peripheral tissues thereby eradicating peripheral infections. A functional immune response, therefore requires rapid scanning of the tissue microenvironment by $CD4^+$ T lymphocytes for cognate antigens [481]. As described earlier, T lymphocytes have to traverse through a complex range of varying tissue microenvironments ranging from peripheral blood circulation, to peripheral tissue sites and secondary lymph nodes. These locations provide vastly different architectural cues as well cellular interactions [231]. T cells adapt to these varying environmental conditions by switching between different modes of migration. Migration of T cells to lymph nodes and peripheral tissues requires T cell crawling on endothelial blood vessels. This 2-dimensional mode of migration involves T lymphocyte rolling on the surface of blood vessels, followed by adhesion to the surface endothelial layer mediated by integrins like LFA-1 (lymphocyte function-associated antigen-1; also known as $\alpha_L\beta_2$) binding to ICAM-1

(intracellular adhesion receptor 1) on the endothelial layer [481]. ICAM-1 is usually expressed at basal levels on the endothelial layer and its expression is upregulated significantly in response to inflammation [481]. Thus, LFA-1 and ICAM-1-mediated adhesion-based 2D migration is invaluable during an immune response. As described above, structural variations and inflammatory state of tissues provide distinct mechanical cues to migrating T lymphocytes [482]. In the following section, I tried to assess the role of Piezo1 mechanoregulation in ICAM-1-mediated 2D migration of T lymphocytes. Isolated $CD4^+$ T lymphocytes were allowed to migrate in the presence of chemokine CCL19 on ICAM-1 coated wells. T lymphocytes express lymphocyte-specific G-protein-coupled receptor (GPCR), CCR7, that binds to CCL19 and regulates T cell migration.

16.2 Methods

Isolation of $CD4^+$ $CD45RA^+$ naïve T lymphocytes

PBMCs were isolated from peripheral blood of healthy volunteers using the ficoll-gradient method. Briefly 10ml blood was diluted 1:1 with 1X PBS and was layered onto Hisep LSM 1077. Centrifugation was performed at 2500 rpm at an acceleration/brake of 1 and temperature, 25˚C. The middle buffy layer consisting of PBMCs were collected. RBCs were lysed and $CD4^+$ T lymphocytes were isolated after through positive magnetic immunoselection. 15µL of CD4 microbead was added and incubated under rotating conditions for 20 minutes. Excess, unbound beads were washed with excess MACS buffer at 1500rpm, 4˚C. Cells were passed through magnetic LS (large-sized) columns and column was washed with excess MACS buffer to remove unbound cells. $CD4^+$ T lymphocytes were collected through plunging of the positive fraction with MACS buffer. Isolated $CD4^+$ T lymphocytes were incubated in RPMI + 10% FBS at 37˚C, 5% CO_2 for 2 hours. $CD4^+$ T cells were

washed with 1X PBS at 1500rpm, 4˚C for 5 minutes followed by addition of 10µL of CD45RA microbead and incubation for 20 minutes at 4˚C. Excess unbound beads were washed with excess MACS buffer and cells were run through a fresh LS (large-sized) magnetic column followed by washing with excess MACS buffer. $CD4^+$ $CD45RA^+$ naïve T lymphocytes were collected by plunging of the positive fraction with MACS buffer.

Transfection of $CD4^+$ $CD45RA^+$ naïve T lymphocytes

Isolated cells were incubated for 1 hour at 37˚C prior to nucleofection. Nucleofection buffer (Lonza) was made by mixing 82µL of P3 primary buffer and 18µL of supplement 1 buffer. The mixture was diluted 1:1 with OPTI-MEM media and was used to transfect $CD4^+$ $CD45RA^+$ naïve T lymphocytes. 100µL of nucleofection buffer was used per cuvette. 150nM EGFP control siRNA and 150nM Piezo1 siRNA were used for transfection. Approximately 1-2 million $CD4^+$ $CD45RA^+$ naïve T lymphocytes were nucleofected per reaction using pulse specific for unstimulated human T lymphocytes- EO115, high functionality. Cells were cultured in RPMI + 10% FBS for 3 days to allow knockdown.

Live Cell imaging

Control and Piezo1-siRNA transfected $CD4^+$ $CD45RA^+$ naïve T lymphocytes were collected on day 3 post nucleofection. Cells were washed in 1X PBS at 1500rpm, 4˚C for 5 minutes.

Cell trace violet staining: Approximately 2 million cells were suspended in 2ml 1X PBS. 2.5µM Cell Trace Violet (CTV) dye was added to the cells and mixed thoroughly. Cells were stained at room temperature and in dark for 20 minutes with intermittent shaking. Cells were washed with excess RPMI + 10% FBS at 1500rpm, 5 minutes, 4˚C. Cells were washed once with RPMI + 10% FBS (without phenol red) + 20mM HEPES.

ICAM-1 coating: Each well of a 96-well plate were coated with 50µL 4µg/ml of recombinant human ICAM-1 overnight at 4˚C. The following day ICAM-1 was removed and wells were washed twice with 1X PBS and allowed to dry at room temperature.

Live cell microscopy: CTV-stained cells were seeded on ICAM-1-coated wells at a density of approximately 60000 cells per well. 0.5µg/ml of recombinant human CCL19 was added and incubated at 37˚C for 15 minutes. Cells were then imaged in the X-Y axis, in the DAPI emission filter using an EVOS immunofluorescence microscope for a total duration of 40 frames with 30 seconds per frame. Cells were acquired at a magnification of 20X. Acquisition was performed at room temperature. Cells were allowed equilibrate at room temperature for 5 minutes before acquisition.

Image analysis

Live cell tracking analysis was performed using Fiji version of ImageJ with help of ParticleTracker 2D/3D plugin. Intensity thresholding was performed before executing particle tracking analysis. The following migration parameters were calculated as described below.

Mean-squared displacement: Mean-squared displacement (MSD) was used to calculate the extent of T cell movement with respect to the cells' starting point or origin. It was calculated as follows:

$\sum_{i=0}^{i=n}(x_n - x_0)^2 + (y_n - y_0)^2$ where,

i = 0 is the starting frame, so x_0 and y_0 are the x and y-positions at the starting frame. i = n is the n^{th} frame, so x_n and y_n are the x and y-positions at the n^{th} frame.

Distance travelled: The total amount of distance migrated by the cell is calculated in terms of the sum of the Euclidean distance (ED) between two points on successive frames. It was calculated as follows:

Distance travelled between two successive frames = $\sqrt{(x_{n+1} - x_n)^2 + (y_{n+1} - y_n)^2}$

where, n = frame number; n + 1 = successive frame

Total distance travelled = $\sum_{i=0}^{i=n} \sqrt{(x_{n+1} - x_n)^2 + (y_{n+1} - y_n)^2}$

where, i = 0 is the starting frame while i = n is the n^{th} frame.

Speed of migrating cells = Total distance travelled / Total duration of time

Statistical significance was calculated using GraphPad Prism 5.0.

16.3 Results

Downregulation of Piezo1 in $CD4^+$ $CD45RA^+$ naïve T lymphocytes resulted in significant inhibition of the T cell migratory capacity. T lymphocytes showed impaired and reduced movement in the presence of 0.5µg/ml of recombinant human chemokine CCL19 on ICAM-1 coated dishes. $CD4^+$ naïve T cells deficient in Piezo1 showed significant reduction in adhesion-based T cell motility as measured by mean-squared displacement (Fig. 16-A) and total distance migrated (Fig 16-C). Representative cell tracks (Fig. 16-B) showed that control $CD4^+$ T lymphocyte showed extended movement with respect to its started point while Piezo1-deficient $CD4^+$ T lymphocytes showed restricted movement.

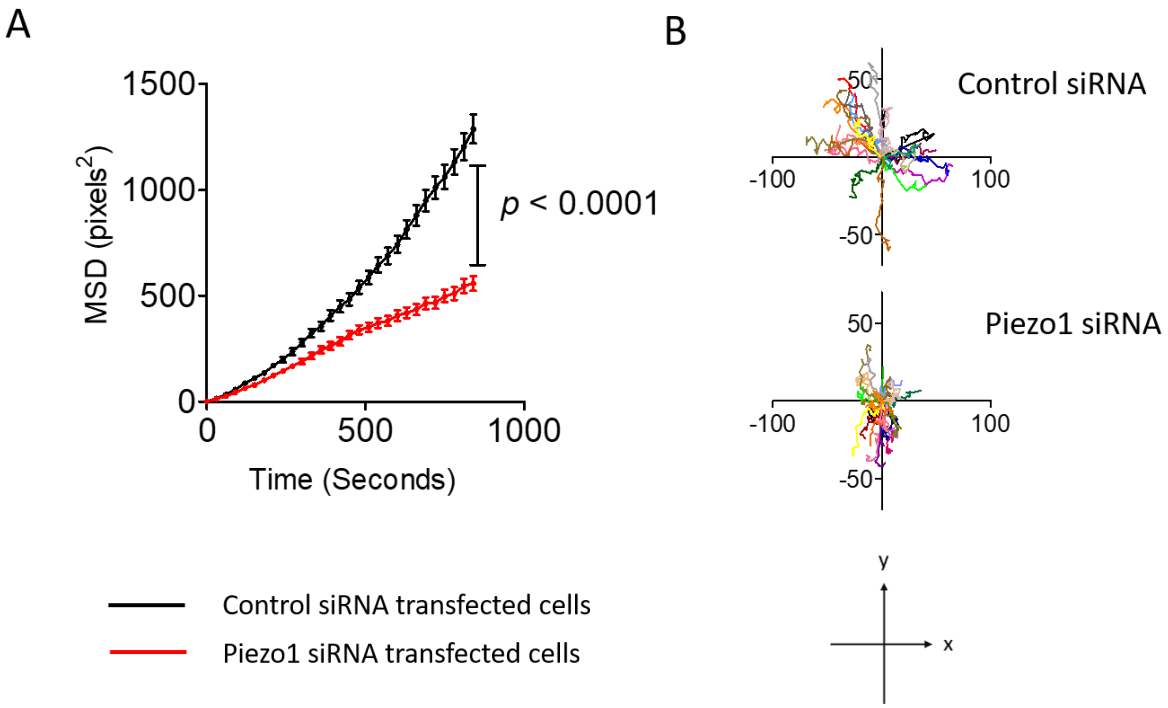

Figure 16-A, B. Piezo1 downregulation reduces migratory capacity of CD4⁺ naïve T lymphocytes in the presence of CCL19 chemokine. CD4⁺ naïve T lymphocytes showed significant reduction in calculated mean-squared displacement (MSD) in the presence of CCL19. n = 245 (Control siRNA and Piezo1 siRNA-transfected cells each). Black line: Control siRNA transfected CD4⁺ naïve T lymphocytes. Red line: Piezo1 siRNA transfected CD4⁺ naïve T lymphocytes (A). Representative migrating cell tracks calculated with respect to the cell's starting point. Total duration of tracks is 15 minutes. Each frame corresponds to 30 seconds. Top panel: Control siRNA cell tracks in the presence of CCL19. Bottom panel: Piezo1 siRNA transfected cell tracks in the presence of CCL19 (B). Unpaired t-test was performed to determine statistical significance.

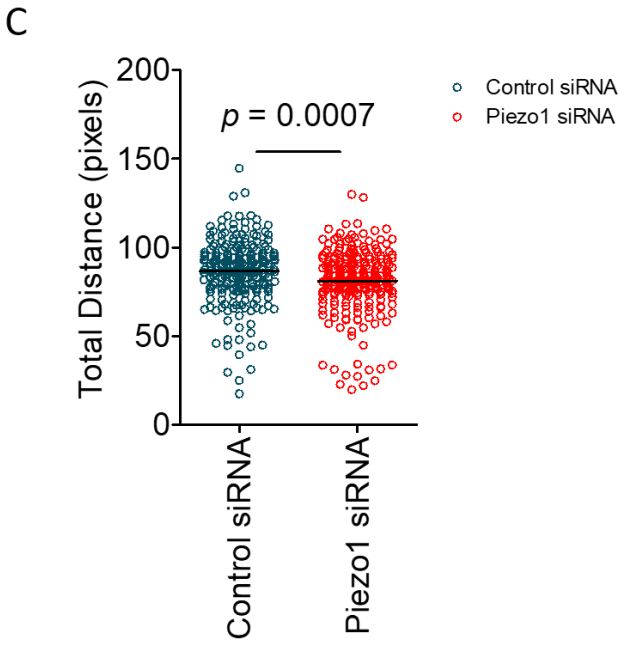

Figure 16-C. Piezo1 downregulation reduces mobility of CD4⁺ naïve T lymphocyte in response to CCL19. Total distance travelled in the presence of chemokine CCL19 was significantly reduced in Piezo1-deficient CD4⁺ T lymphocytes. Unpaired t-test was performed to determine statistical significance. Control siRNA-transfected cells, n = 245. Piezo1 siRNA-transfected cells, n = 246.

15.4 Discussion

T cell motility is closely regulated by mechanical signals provided by its surroundings. As discussed, T lymphocytes respond to mechanical cues by modulating their migration patterns. T lymphocyte trafficking is a complex process of traversing through diverse tissue microenvironment ranging from transmigration across tissue barriers to crawling and rolling on endothelial blood vessels. Since mechanical cues are an integral part of the migratory process, we sought to explore the plausible role of Piezo1 mechanosensors in the process of CD4⁺ T cell migration. We found that Piezo1 knockdown resulted in dramatically reduced capacity of CD4⁺ naïve T lymphocytes to migrate in response to chemokine stimulation. Cells

with downregulated Piezo1 expression travelled significantly lesser distance from its starting point thus, suggesting the importance of Piezo1-mediated mechanotransduction in T lymphocyte motility.

Chapter 17. Piezo1 downregulation impairs chemotactic migration of naïve CD4$^+$ T lymphocytes

17.1 Introduction

T lymphocytes migrate in response to chemokine gradients that enable them to move towards site of infection in peripheral tissues or home towards secondary lymphoid organs [481]. Chemokine-driven directed movement of T lymphocytes is crucial for an efficient immunosurveillance and adaptive immune response. Directional migration is mediated through a group of G protein-coupled receptors (GPCRs) expressed by T lymphocytes that respond to a range of chemokines [483]. Some of them include Chemokine (C–C motif) ligand 19 or CCL19 and CCL21 that bind to chemokine receptor CCR7, and CXCL12 or SDF1α that bind to receptor CXCR4 [483]. These chemokines are produced within lymphoid tissues or inflamed peripheral sites by resident tissue cells or innate immune cells and they act as directional cues for guided migration of T lymphocytes. Mature dendritic cells produce CCL19 upon antigen binding while CCL21 has been shown to be produced by vascular endothelial cells in mice [483,484]. Chemokine profiles and their corresponding receptor expression levels change in response to infections [484]. We wanted to assess the plausible role of Piezo1-mediated mechanotransduction in CD4$^+$ T lymphocytes chemotaxis. We used two different experimental setups to this end. The first allowed us to study the role of Piezo1 in transwell migration of naive CD4$^+$ T lymphocytes towards a chemokine gradient. The second system allowed us to study regulation of 2D chemotactic migration of naïve CD4$^+$ T lymphocytes in a millicell chamber where one can establish a chemokine gradient.

17.2 Methods

Isolation and transfection of $CD4^+$ $CD45RA^+$ naïve T lymphocytes

$CD4^+$ $CD45RA^+$ T lymphocytes were isolated from PBMCs of healthy volunteers by magnetic immunoselection (Described in detail in section 16.2). Isolated cells were transfected with 150ng/ml of control EGFP siRNA or Piezo1-specific siRNA by nucleofection using Amaxa 4D-Nucleofector (Detailed protocol in section 16.2), program EO-115. Transfected cells were incubated at 37˚C for 3 days to allow Piezo1 knockdown.

Transfection of Jurkat T cells

Jurkat T cells (Clone E6.1) were split and seeded at 100,000 cells per ml of RPMI + 10% FBS two days before transfection. Approximately 1-1.5 million cells were transfected per reaction. 82µl of SE Cell Line nucleofector solution (Lonza) was mixed with 18µl of P1 supplement buffer (Lonza). The buffer was diluted 1:1 with OPTI-MEM media. 180ng/ml of control EGFP siRNA or Piezo1 siRNA was added to 1-1.5 million cells in 100µl of nucleofection buffer. Nucleofection was performed using program specific for Jurkat E6.1 – CL120 in Amaxa 4D Nucleofecter. Transfected cells were cultured in RPMI + 10% FBS for 48 hours to allow Piezo1 downregulation. Media change was performed 24 hours after transfection to remove dead cells.

Transwell Chemotaxis assay

24-well plate with 0.5µm inserts (Merck Millipore) were used for this assay. 0.5µm inserts were coated with overnight with 4µg/ml of recombinant human ICAM-1 at 4˚C. Inserts were washed with 1X PBS the following day and allowed to dry at room temperature. Control and Piezo1-specific siRNA transfected $CD4^+$ naïve T lymphocytes were collected on day 3 post-nucleofection. Equal number of control and Piezo1 siRNA transfected cells (approximately 0.3

million to 0.5 million, depending on cell number) were seeded on ICAM-1 coated inserts in 100µl of RMPI + 10% FBS. Inserts were placed on each well of a 24-well plate. Each well contained 500µl of RPMI + 10% FBS with or without 0.5µg/ml of recombinant human CCL19. Cells were allowed to migrate for 5 hours at 37˚C, 5% CO_2. After 5 hours, inserts were placed on each well of a 24-well plate containing 500µl of chilled 1X PBS + 1mM EDTA to dislodge transmigrated cells from the lower wall of the inserts. Cells migrated in the bottom chamber were collected and centrifuged at 1500rpm for 5 minutes at 4˚C. The cell pellet was resuspended in a definite volume of RPMI + 10% FBS and cells were counted using a Neubauer Haemocytometer. Proportion of cells migrated to the lower chamber were calculated as the percentage of initially seeded cell number.

Transfected Jurkat cells were also similarly seeded in 0.5µm transwell inserts in a 24-well plate. Equal number of control siRNA or Piezo1 siRNA-transfected cells (approximately 300,000 -500,000 cells) were seeded on ICAM-1 coated inserts. 500µl of RPMI + 10% FBS containing 0.2µg/ml of CXCL12 or SDF1α was added to the lower chamber to create a chemokine gradient. Media without any chemokine was used a negative control. Cells were allowed to migrate for 1 hour at 37˚C after which further migration was stopped by placing the plate on ice. Inserts were placed on chilled 1X PBS + 1mM EDTA to dislodge cells that have transmigrated and attached on the lower wall of the insert. Migrated cells were collected and centrifuged at 1500rpm for 5 minutes at 4˚C and resuspended in a definite volume of media and counted using Neubauer's Haemocytometer.

Millicell µ-Migration chemotaxis assay

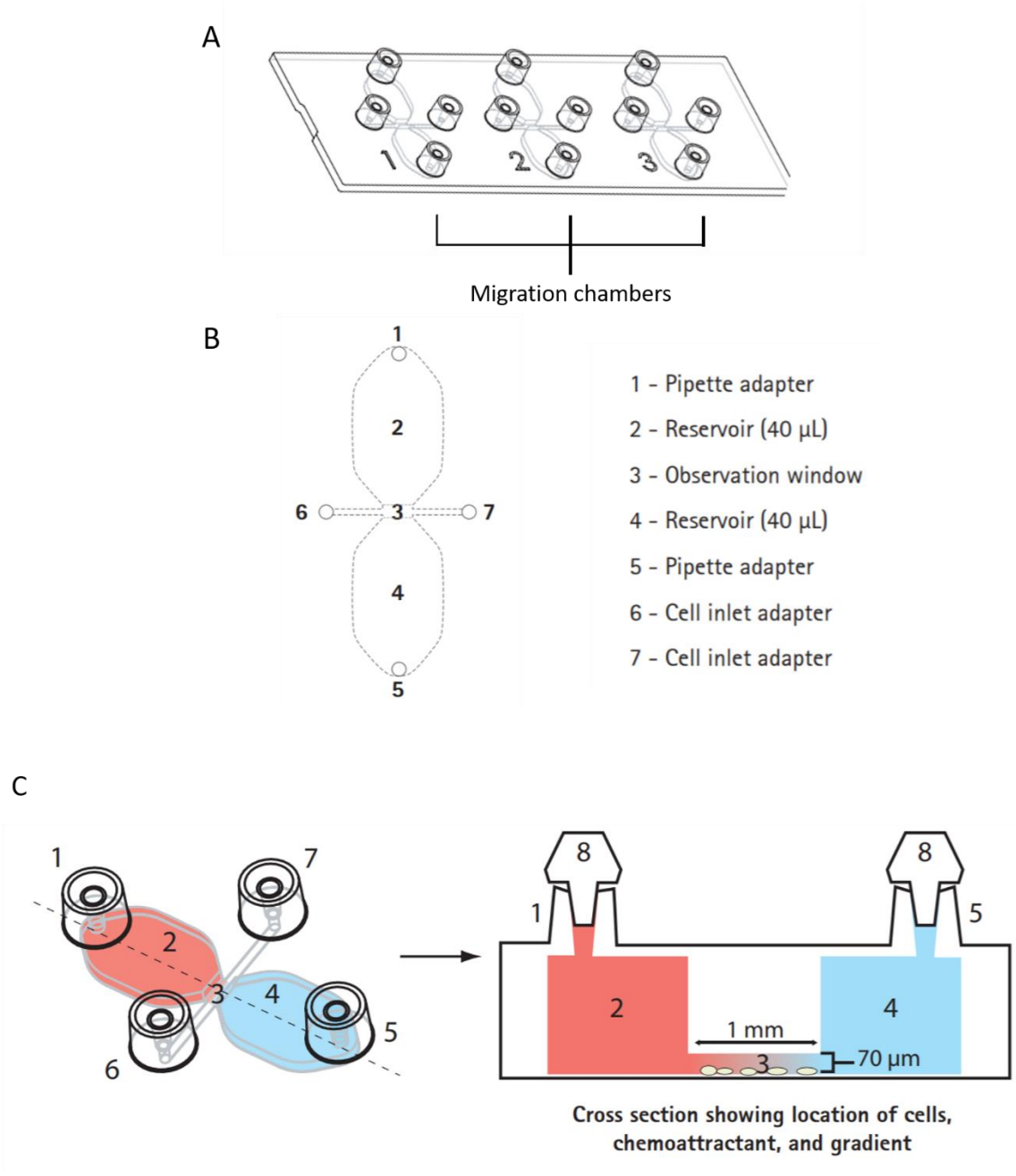

Figure 17-1. Millicell µ-Migration assay kit. Configuration of a µ-Migration slide (A). Configuration of each chamber of a µ-Migration slide (B). Establishment of a chemokine gradient in the chamber (C). *Adapted from Merck Millipore Millicell® µ-Migration Assay Kit brochure.*

Each µ-Migration slide contains 3 chambers (Fig. 17-1 A). Each chamber contains two reservoirs (Fig. 17-1 B) that can be filled with different concentrations of chemokine to

generate a chemokine gradient (Fig. 17-1 C). Movement of cells seeded in the observation window (Fig. 17-1 B & C) can be tracked by live cell time-lapse imaging.

Each chamber of a µ-Migration slide was coated with 4µg/ml of recombinant human ICAM-1. The slide was held at an angle of 30˚ along the long axis of the slide. 82µl of recombinant human ICAM-1 was pipetted onto adaptor 5 (Fig. 17-1 B) till the entire chamber was covered with the ICAM-1 solution. This setup was kept at 4˚C overnight. The chambers were washed the following day with 1X PBS after removing the ICAM-1 solution and dried at room temperature. After coating the migration chamber was filled with RPMI + 10% FBS containing 20mM HEPES through adaptor 5 (Fig. 17-1 B). Cell trace violet-labelled control and Piezo1 siRNA transfected cells were then seeded in the observation section (Fig. 17-1 B) through adaptors 6 and 7. Briefly a droplet of 8µl of 2-3 million cells was placed on adaptor 6 and equal volume was aspirated through adaptor 7 to allow the cells to enter the observation window. The slides were incubated at 37˚C for 30 minutes after which 18µl of chemokine CCL19 was added through adaptor 1 (Fig. 17-1 B) at a final concentration of 0.5µg/ml. The chemokine droplet was placed on adaptor 1 and an equal volume was aspirated through adaptor 5 to generate a chemokine gradient. This set up was placed at 37˚C for 30 minutes before time-lapse imaging using EVOS fluorescent microscope for a total duration of 35 frames with each frame corresponding to 30 seconds. Live cell imaging was performed at room temperature.

Image analysis

All cells were analysed using Fiji ImageJ plugin Particle 2D/3D Tracker. The following parameters were calculated.

Mean-squared displacement (MSD):

$\sum_{i=0}^{i=n}(x_n - x_0)^2 + (y_n - y_0)^2$ where,

i = 0 is the starting frame, so x_0 and y_0 are the x and y-positions at the starting frame. i = n is the n^{th} frame, so x_n and y_n are the x and y-positions at the n^{th} frame.

Total distance travelled = $\sum_{i=0}^{i=n}\sqrt{(x_{n+1} - x_n)^2 + (y_{n+1} - y_n)^2}$

where, i = 0 is the starting frame while i = n is the n^{th} frame.

Speed of migrating cells = Total distance travelled / Total duration of time

Chemotactic Index (CI) was used to assess the degree of directional migration of transfected $CD4^+$ naïve T lymphocytes. It was calculated as the ratio between the distance travelled at the last frame with respect to its starting point ($\sqrt{MSD}_{nth\ frame}$) and total distance travelled between each successive frame till the last time-point (total euclidean distance). A perfectly directional migration will cause these two parameters to be equal and hence, the ratio between them to be equal to 1.

Chemotactic Index (CI) = $\sqrt{MSD_{nth\ frame}}$/(Total distance travelled)

All statistical significance was calculated using GraphPad prism 5.0 using unpaired t-test.

17.3 Results

Downregulation of Piezo1 impaired 3D chemotactic transmigration of $CD4^+$ T lymphocytes.

$CD4^+$ naïve T lymphocytes were allowed to migrate across ICAM-1 coated 0.5µm pore-size inserts in response to 0.5µg/ml recombinant human CCL19 (Fig. 17-2 A). Transmigration was calculated as a percentage of originally seeded cells. $CD4^+$ T lymphocytes with downregulated Piezo1 expression showed significant reduction in the percentage of transmigrated cells as compared to control T lymphocytes (Fig. 17-2 B). Thus, Piezo1 on $CD4^+$ T lymphocytes is

essential for 3D transmigration of these cells in response to chemokine gradient. We also made similar observations in the acute T cell leukaemia cell line, Jurkat cells. Jurkat cells were transfected with control or Piezo1-specific siRNA. Jurkat cells deficient in Piezo1 showed significant reduction in percent migrated cells in the lower chamber (Fig. 17-2 C). Both primary $CD4^+$ T lymphocytes and Jurkat transfected cells showed minimal passive migration across transwells in the absence of any chemokine gradient (Fig. 17-2 B, C).

Loss of Piezo1 expression also resulted in inhibited $CD4^+$ naïve T lymphocytes motility in confined 2D migration in response to chemokine gradient. Millicell µ-migration chambers were used to set up a chemokine gradient (Described in section 17.2). 2D confined migration of $CD4^+$ naïve T lymphocytes was studied in response to CCL19 gradient on ICAM-1 coated µ-migration chambers. Loss of Piezo1 reduced motility of $CD4^+$ T lymphocytes as measured by mean-squared displacement (MSD) (Fig. 17-2 D). Piezo1 downregulated $CD4^+$ naïve T lymphocytes travelled lesser distance and thus showed lower migration speeds as compared to control transfected $CD4^+$ naïve T lymphocytes (Fig. 17-2 F, G). Representative tracks of these cells showed that control $CD4^+$ T lymphocytes showed directional persistence while $CD4^+$ T lymphocytes with downregulated Piezo1 failed to show any directionality during 2D movement in response to chemokine gradient (Fig. 17-2 E, I). We measured the chemotactic index (CI) of these moving cells that helped us evaluate their chemotactic capacity (Fig. 17-2 H, I). Piezo1-deficient $CD4^+$ T lymphocytes showed significantly reduced measurements of the chemotactic index. Piezo1 thus, regulates chemotactic response and directional persistence of naïve $CD4^+$ T lymphocytes.

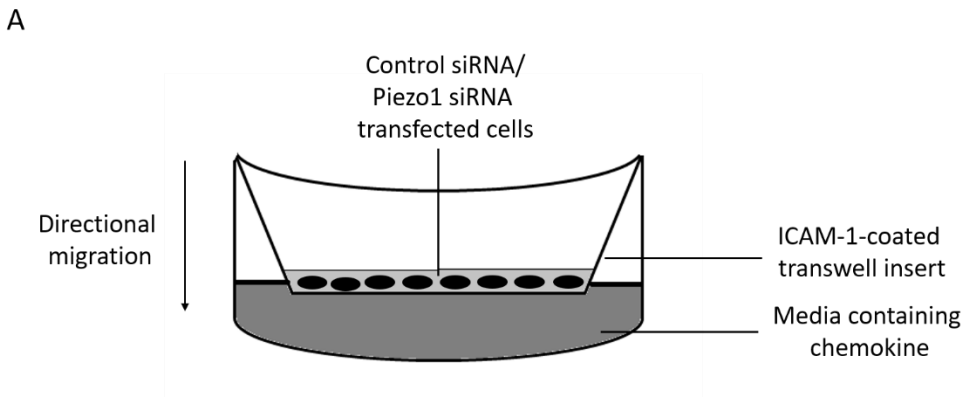

Figure 17-2 A. 3D transwell migration assay setup. The upper chamber consists of ICAM-1 coated insert where control or Piezo1-siRNA transfected $CD4^+$ T lymphocytes are seeded in equal numbers. The lower chamber consists of well filled with appropriate volume of media with and without recombinant human chemokine.

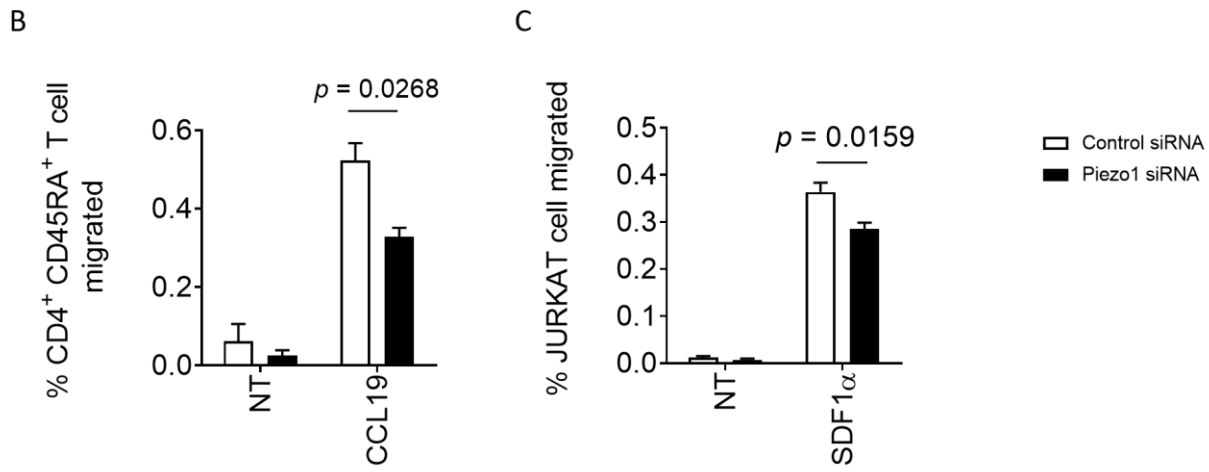

Figure 17-2 B, C. Piezo1 downregulation reduces 3D transwell migration of $CD4^+$ $CD45^+$ T lymphocytes. Control and Piezo1 siRNA-transfected $CD4^+$ naïve T lymphocytes were seeded on ICAM-1 coated 0.5µm transwell inserts. Cells were allowed to migrate for 5 hours towards the lower chamber well containing 0.5µg/ml CCL19 (primary $CD4^+$ naïve T lymphocytes) (B) or 0.2µg/ml CXCL12 (Jurkat cells) (C). Chemotaxis is measured as percentage of cells that have migrated to the lower chamber. Data is representative of at least 3 independent experiments.

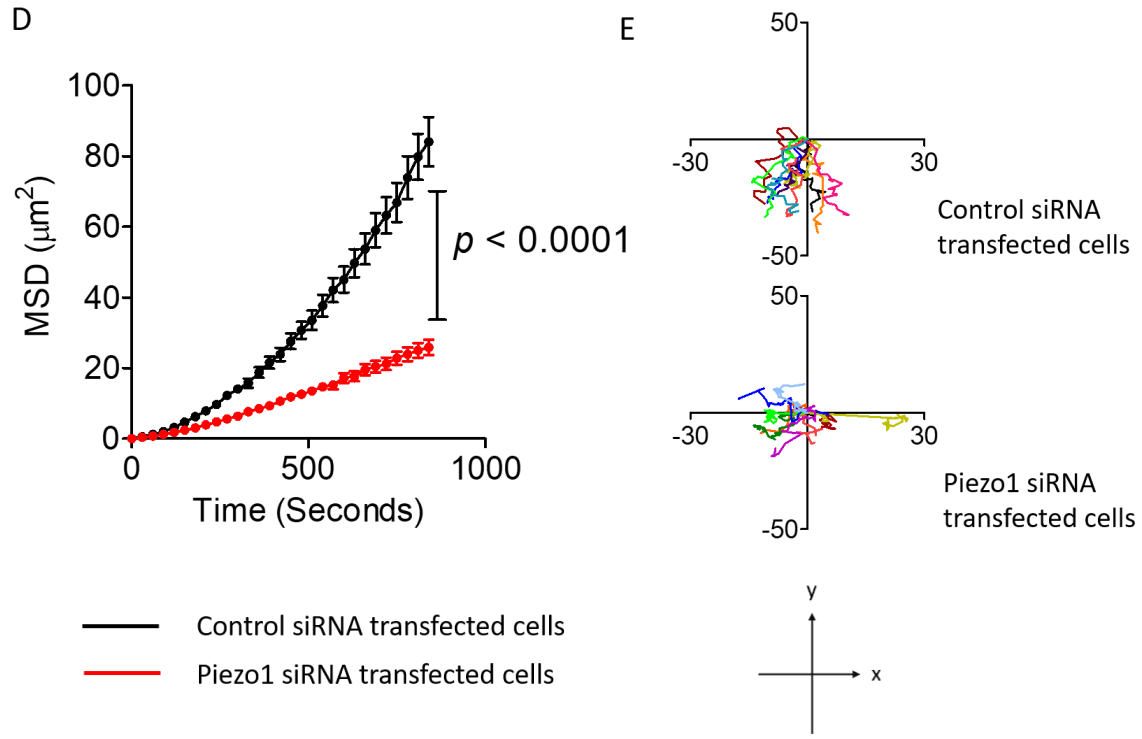

Figure 17-2 D, E. Piezo1 downregulation impairs motility of CD4⁺ naïve T lymphocytes in 2D confined chemotactic migration assay. Control and Piezo1 siRNA-transfected CD4⁺ T lymphocytes were seeded on ICAM-1 coated millicell μ-migration chambers. Recombinant human CCL19 was added at a final concentration of 0.5μg/ml in the top reservoir chamber (described in Fig. 4.2.2 C) and cell movement was evaluated through time lapse-imaging. Cells were acquired at rate of 30 seconds per frame for a total duration of 40 frames. Piezo1 downregulation significantly reduces chemokine-dependent cell motility as measured by mean-squared displacement (MSD) (D). Data is representative of at least 3 independent experiments. Control siRNA/Piezo1 siRNA transfected cells, n = 218 each. Representative cell tracks also shows that control CD4⁺ T lymphocytes extended movement while cells deficient in Piezo1 expression exhibited restricted motility (E). Representative cell tracks also shows that control CD4⁺ T lymphocytes showed directional persistence while tracks of Piezo1 downregulated cells failed to show any directionality (E).

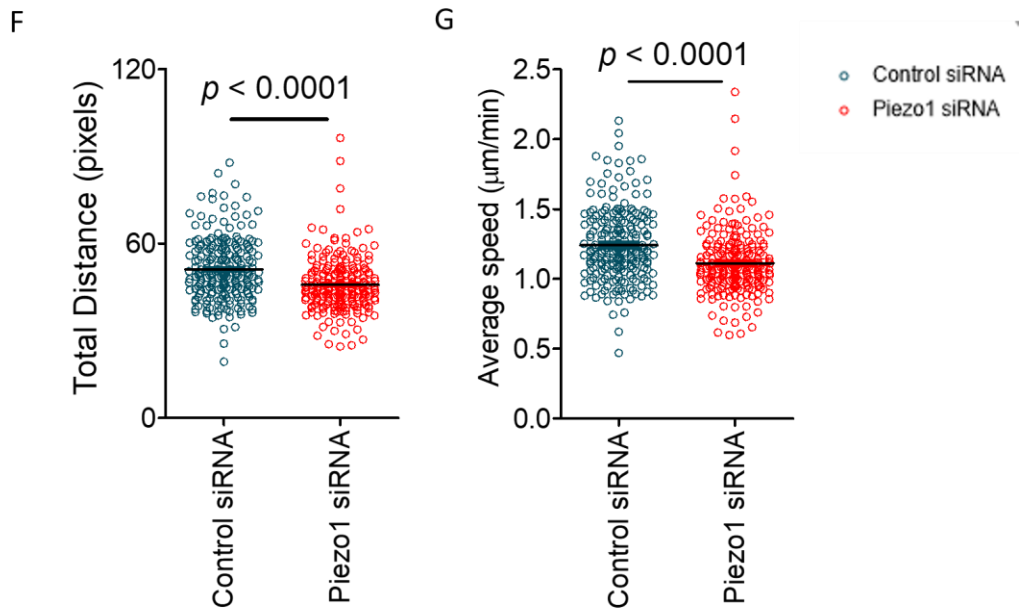

Figure 17-2 F, G. Piezo1 downregulation impairs 2D confined chemotactic motility of CD4⁺ naïve T lymphocytes. Control and Piezo1 siRNA-transfected CD4⁺ naïve T lymphocytes were seeded on ICAM-1 coated millicell μ-migration chambers. Recombinant human CCL19 was added at a final concentration of 0.5μg/ml in the top reservoir chamber (described in Fig. 17-1) and cell movement was evaluated through time lapse-imaging. Cells were acquired at rate of 30 seconds per frame for a total duration of 40 frames. Loss of Piezo1 reduced total distance migrated by CD4⁺ T lymphocytes in response to CCL19 (F). Cells also migrated with lower migration speeds in Piezo1 downregulated CD4⁺ T lymphocytes (G). Data is representative of at least 3 independent experiments. Control siRNA/Piezo1 siRNA transfected cells, n = 185 each.

H

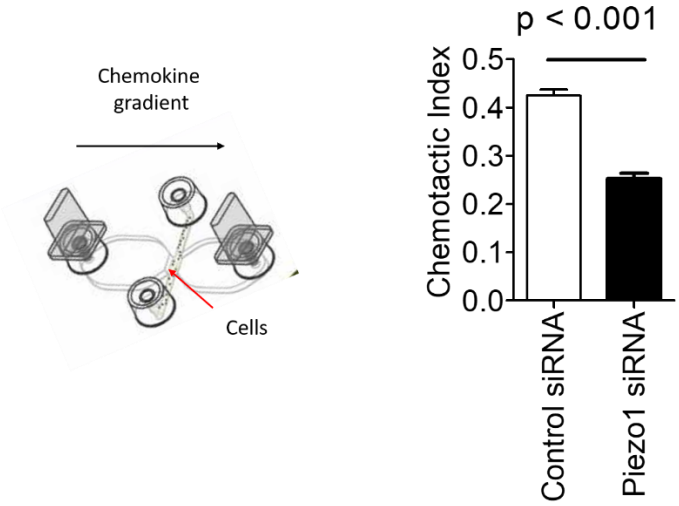

I

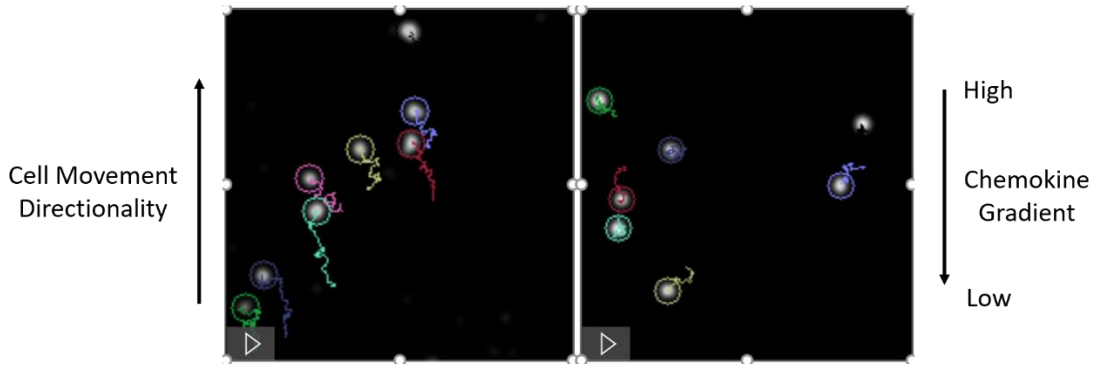

Figure 17-2 H, I. Piezo1 downregulation impairs 2D chemotactic migration of $CD4^+$ $CD45RA^+$ T lymphocytes. Chemotactic index (CI) was calculated as a measure of directed migration in response to CCL19 gradient in millicell µ-migration chamber. Piezo1 knockdown significantly reduced directional migration in response to chemokine gradient as compared to control cells as evident by lower chemotactic index (CI) values (H, right panel). Control siRNA/Piezo1 siRNA transfected cells, n = 159 each. Experimental setup of a millicell µ-migration chamber (H, left panel; details in section 17-2). Representative cell tracks of control and Piezo1 transfected $CD4^+$ naïve T lymphocytes along a CCL19 gradient (I).

17.4 Discussion

The process of T lymphocyte trafficking involves directed movement of these cells towards a chemokine source. This phenomenon is known as T cell chemotaxis and is essential for guided migration to peripheral sites of infection or homing to lymph nodes. Chemotactic migration requires T lymphocytes to respond to chemokine gradients and move across vascular endothelial layers through sites of high endothelial venules (HEVs). T lymphocyte migration also involves movement through confined capillary networks and the complex tissue microenvironment, all of which provide highly variable mechanical cues to migrating T cells. Existing studies have shown that T lymphocytes alter their migratory mode and pattern depending on the tissue microenvironment. We wanted to explore the potential role of Piezo1 regulation in chemotactic migration of $CD4^+$ T lymphocytes. We found that Piezo1 regulation is essential for 3D diapedesis across the endothelial barrier as well 2D confined migration in response to a chemokine gradient. Abrogation of Piezo1 resulted in significantly reduced 3D transmigration and 2D migration towards a chemokine gradient, thus alluding towards the potential role of Piezo1 in directional migration of $CD4^+$ naïve T lymphocytes.

Chapter 18. Downregulation of Piezo1 abolishes cytoskeletal actin polarity in response to chemokine

18.1 Introduction

Generation of cell polarity is characteristic of T lymphocyte migration [343,475]. During T lymphocyte migration, cytosolic and membrane components redistribute themselves so as to create a polarized cell state that facilitates cell movement. Migrating T lymphocytes extend multiple cytoskeleton-based membrane protrusions at the leading edge known as lamellipodia. The trailing end of migrating T lymphocytes have a single extension known as the uropod whose retraction drives the cell forward [481]. Moving T lymphocytes make contacts with the substrate mediated through integrin binding which act as focal points for generation of traction forces through localised formation and contraction actin fibres [475, 481]. Reorganisation of actin cytoskeletal scaffold is necessary to generate cell polarity. Formation of a cell leading and rear end is necessary for directional movement of T lymphocytes such as chemotaxis. Actin polymerisation at the cell's leading edge and its retrograde movement through myosin-based contractility is also necessary for the generation of traction forces that is crucial for cell migration [475,481]. Remodelling of the actin cytoskeleton is mediated by a number of factors including Rho family of GTPases, namely, Rho, Rac and Cdc42 [486]. They are activated upon chemokine binding to its receptor and trigger actin polymerisation at the cell's leading lamellipodia while driving myosin II-based contractions of from the rear end. Inhibition of actin polymerisation prevents generation of cell polarity and formation of leading edge lamellipodia, filipodia and rear end uropod which severely impairs migration and

chemotactic movements of T lymphocytes [485,486]. We, thereby, sought to explore the plausible aspect of Piezo1-mediated regulation of actin polarity in migrating T lymphocytes.

18.2 Methods

Isolation and transfection of $CD4^+$ $CD45RA^+$ naïve T lymphocytes

PBMCs were isolated from blood of healthy volunteers. $CD4^+$ $CD45RA^+$ T lymphocytes were isolated by using microbeads against CD4 and CD45RA through successive positive selection (Described in detail in section 16.2). Isolated cells were transfected with 150ng/ml of control EGFP siRNA or Piezo1-specific siRNA by nucleofection using Amaxa 4D-Nucleofector (Detailed protocol in section 16.2), program EO-115. Transfected cells were incubated at 37˚C for 3 days to allow Piezo1 downregulation.

Stimulation of actin polymerisation

13mm glass coverslips were washed thoroughly with 100% ethanol and allowed to dry at room temperature. 100µl of 15µg/ml of recombinant human fibronectin (Takara Bio.) were added and incubated at 4˚C overnight. Fibronectin was removed the following day and coverslips were washed thoroughly with 1X PBS. They were allowed to dry at room temperature.

Approximately 100,000 control or Piezo1 siRNA-transfected cells (on day 3 post-nucleofection) were seeded on coated coverslips and incubated at 37˚C for 2 hours. 0.5µg/ml of recombinant human CCL19 was added at one region of the coverslip and cells were stimulated for 40 minutes at 37˚C. After stimulation, cells were washed twice with 1X PBS. 100µl of 4% paraformaldehyde was added and fixation was performed for 30 minutes at room temperature. Cells were washed thrice with 1X PBS following which blocking and

permeabilization was performed with 3% Bovine-serum albumin (BSA) in 1X PBS + 0.2% Triton-X 100. Cells were washed again thrice with 1X PBS. 100µl of Alexa 532-conjugated phalloidin (1:100 dilution) was added and incubated at room temperature in a dark moist chamber for 30 minutes. Cells were washed thrice with 1X PBS and stained with 1µg/ml of DAPI for 1 minute. Excess stain was washed off by washing 4 times with 1X PBS. Coverslips were mounted on 4µl VECTASHIELD mounting media.

Image acquisition

Images were acquired on EVOS immunofluorescence microscope at a magnification of 40X using the RFP filter.

Image analysis

All images were analysed using Fiji ImageJ. Each cell was divided into 2 halves with the division axis perpendicular to the long axis of the cell. This divides the cell into two ROIs (region-of-interest) – front half/rear half. Fluorescent intensity of actin-bound phalloidin was then measured separately in the two halves. Polarity Index was calculated as ratio of the difference between the fluorescent intensities of the two halves divided by the average fluorescent intensity of the entire cell. Statistical significance was calculated using unpaired t-test in GraphPad Prism 5.0.

18.3 Results

Piezo1 knockdown abrogates actin polarisation response to chemokine stimulation.

Control and Piezo1-specific siRNA transfected $CD4^+$ $CD45RA^+$ T lymphocytes were stimulated with 0.5µg/ml of recombinant human CCL19. Post stimulation, degree of actin polarity was quantified through immunofluorescence microscopy. Any cell with actin signal mostly

concentrated on one half of the cell will yield a higher actin polarity index than a cell with uniformly distributed actin (Details in section 18.2). It was observed that Piezo1 downregulation resulted in significant loss of cytoskeletal actin polarity in response chemokine stimulation. Control $CD4^+$ naïve T lymphocytes on the other hand, showed distinct polarisation of the actin cytoskeleton on one pole of chemokine-stimulated cell (Fig. 18-A, B).

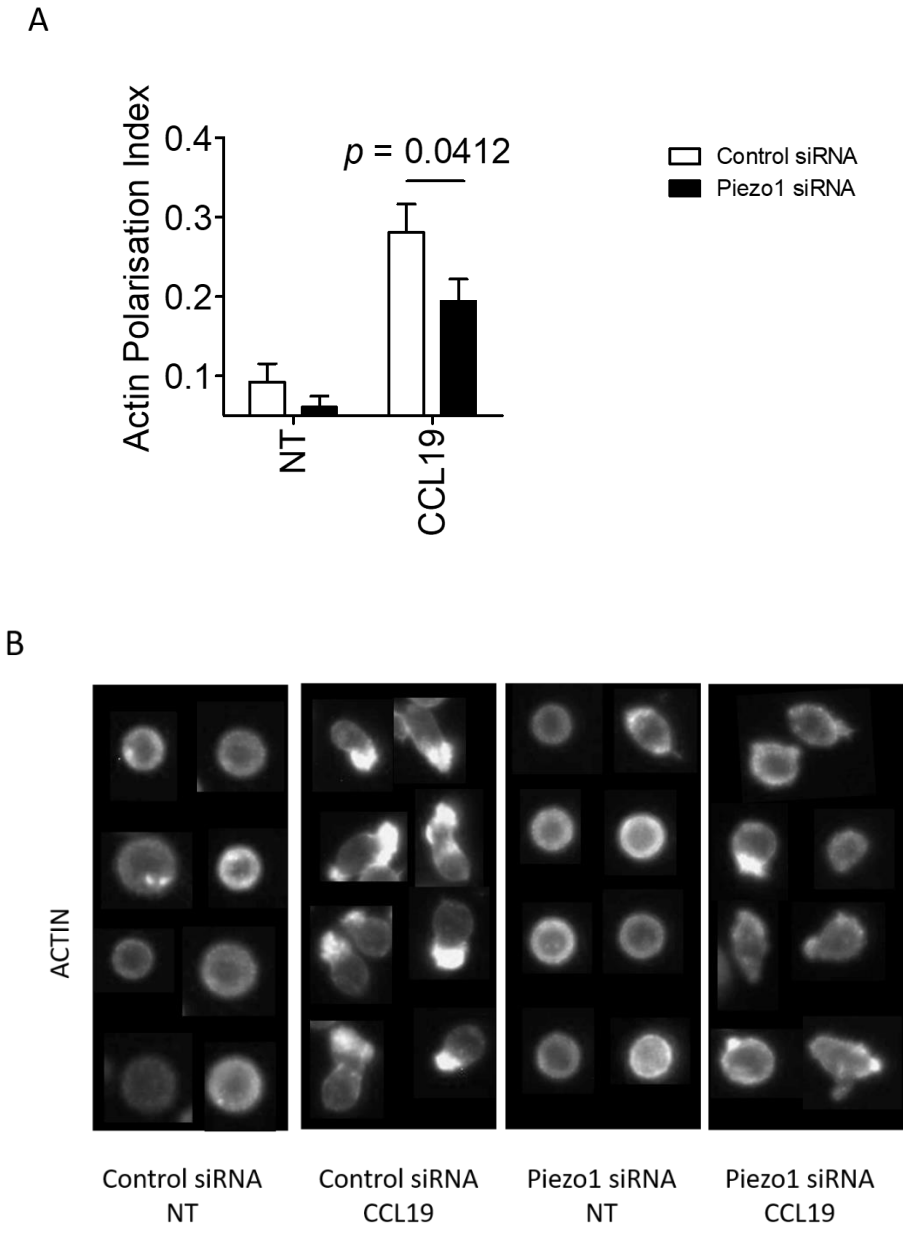

Figure 18-A-B. Piezo1 knockdown abolishes actin polarity in response to chemokine stimulation in $CD4^+$ naïve T lymphocytes. Transfected T lymphocytes were stimulated with

0.5µg/ml of recombinant human CCL19 for 40 minutes. Polarisation of the actin cytoskeleton in response to chemokine stimulation was calculated. Actin polarity index was significantly reduced on Piezo1 downregulation as compared to control cells (A). Representative fields of Alexa 532-phalloidin stained transfected $CD4^+$ $CD45RA^+$ T cells with or without chemokine stimulation (B). Data is representative of at least 3 independent experiments. (Control siRNA transfected cells, n > 50, Piezo1 siRNA transfected cells, n > 50)

18.4 Discussion

Generation of cell polarity is crucial for T lymphocytes to migrate along a chemokine gradient. A polarised T lymphocyte is characterised by having leading edge lamellipodia and a rear end uropod. Both these structures are actin cytoskeleton-based membrane extensions that are necessary for directional cell migration. Chemical abrogation of frontal-rear axis of a moving T lymphocyte completely abolishes T lymphocyte migration. Upon sensing of chemokine gradient, this frontal-rear polarity is established through polymerisation and remodelling of the cytosolic actin cytoskeletal network. It has been shown that migrating T lymphocytes show active actin polymerisation at the leading pole of the cell that undergoes retrograde flow to the back of the cell through myosin-driven contractions of the actin fibres. This process is necessary for the generation of traction forces that retracts the trailing uropod and propels the cell forward. In the above section., we decided to explore the potential role of Piezo1 regulation of generating and maintaining actin polarity in migrating $CD4^+$ T lymphocytes. Piezo1 knockdown resulted in loss of actin polarity in response to chemokine. Control $CD4^+$ T lymphocytes, on the other hand, showed distinct polarisation of F-actin towards one pole of the cell. Thus, Piezo1 plays a crucial role in generating F-actin polarity thus, facilitating directional movement towards a chemokine source.

Chapter 19. Piezo1 undergoes redistribution in during migration in response to chemokine stimulation

19.1 Introduction

As described in the previous chapter, during migration, T lymphocytes transition from an apolar state where cellular components are uniformly distributed to a polarised state where signalling components are preferentially localised to the leading and rear poles of the cell [(485)]. Reorganisation of signalling components within the cell is essential for establishing polarity which facilitates chemotactic migration. Cellular components that establish T cell polarity during migration include Phosphoinositide 3-kinases (PI3Ks), Phosphatase and tensin homolog (PTEN), chemokine receptors CCR7, CXCR4 and family of Rho-GTPases – RhoA, Rac1 and Cdc42 [(475)]. Activity of Rho-GTPases drive actin polymerisation and polarisation through the WAVE-Arp2/3 signalling pathway [(475)]. Cell polarity is generated in response to chemokine gradient which facilitate directed T cell migration. Since we observed that Piezo1 activity is essential to drive actin polarity in migrating $CD4^+$ T lymphocytes, we sought to explore if Piezo1 undergoes a similar form of cellular redistribution during $CD4^+$ T lymphocyte migration. Previous findings revealed that Piezo1 undergoes preferential peripheral distribution in $CD4^+$ T lymphocytes during antigen stimulation since localisation of Piezo1 towards the cell periphery will enhance sensing of mechanical force generated during interaction with cognate APCs. This finding led us to the plausible scenario of altered Piezo1 cellular distribution during migration of $CD4^+$ T lymphocytes.

19.2 Methods

Piezo1 overexpression construct

Piezo1 tagged RFP construct was provided by Dr. Charles D. Cox from Victor Chang Cardiac Research Institute, Australia. Briefly, Piezo1 overexpression construct was synthesised using a pIRES2-EGFP vector backbone. The GFP expression was silenced and DNA coding mcherry and Piezo1 were ligated. DNA encoding mcherry protein were introduced into amino acid positions 160, 724, 855, 1591 and 1851 through Age1/Spe1 restriction sites in Piezo1-encoded DNA. DNA encoding Piezo1 and fluorescent mcherry were then ligated on to the Age1/Spe1-inserted vector backbone [399].

Amplification of Piezo1-RFP construct

Piezo1-RFP construct amplification was performed by Dr. Dibyanti Mukherjee. Briefly, *E. coli* strain, DH5α bacterial (from Dr. Arun Bandopadhyay, IICB) glycerol stock was allowed to thaw at room temperature. Bacterial cells were streaked on LB-agar plate (Luria Bertini HiVeg Broth + 20% agar) without antibiotics. Plate was incubated at 37˚C overnight.

A single colony of DH5α *E. coli* added to 10ml of LB media without any antibiotic. Bacteria was allowed to grow overnight at 37˚C under shaking conditions (240 rpm).

The following day, 10µl of bacterial culture was then added to 10ml of fresh LB broth without antibiotics and incubated at 37˚C under shaking conditions. Optical density at 600nm ($O.D._{600nm}$) was measured every 15-30 minutes in a spectrophotometer to check cell growth and density. When cell density reached an $O.D._{600nm}$ of 0.3-0.35, the cells were immediately placed on ice for 30 minutes with occasional shaking. The following steps must all be performed on ice and centrifuge or tubes must be pre-chilled to 4˚C. Cells were then centrifuged for 15 minutes at 4000rpm for 15 minutes at 4˚C. Cells were then washed subsequently with 30ml of ice-cold $MgCl_2$ (80mM) and $CaCl_2$ (20mM) solution for 15 minutes at 4000rpm and 4˚C. Supernatant was discarded and cells were resuspended in 200µL of ice-

cold 100mM $CaCl_2$, and incubated on ice for 30 minutes. Cells were then centrifuged at 3000rpm for 15 minutes at 4˚C. Competent cells were then centrifuged at 3000rpm for 15 minutes at 4˚C.

200µl of competent cells in 100mM $CaCl_2$ were then mixed with 1-2µl of DNA encoding Piezo1 mcherry (corresponds to 50 – 100ng/µl of DNA). Mixing was performed by gently tapping the microfuge tube. The mixture was incubated on ice for 30 minutes. The tube was then placed in a pre-warmed 42˚C water bath for 90 seconds following which they were immediately placed on ice. 1ml off LB media without antibiotics was added to the transformed cells and allowed to grow at 37˚C for 1 hour under gentle shaking conditions. This allows transformed bacteria to express the antibiotic resistance protein. Transformed cells were then streaked on to LB-agar plates containing 10µg/ml of Kanamycin antibiotic. Cells were allowed to grow overnight at 37˚C.

Appearance of kanamycin-resistant colonies the following day, showed successful transformation. A single colony was then added to 10ml of LB media containing 10µg/ml of kanamycin and cells were allowed to grow overnight at 37˚C under shaking conditions.

Bacterial stock preparation

Piezo1-RFP expressing *E.coli* DH5α bacterial cells were collected. Equal volume of 50% glycerol was added to bacterial culture and aliquoted into cryovial, 1ml each. Stocks were stored at -80˚C.

For concentrating DNA amount, plasmid DNA was precipitated by adding one-tenth volume of 3M Sodium acetate, pH 5.2, and 2-3 times volume of absolute ethanol. The contents were mixed by inverting the tube 4-5 times following which they were incubated at -20˚C for 2

hours to allow precipitation. Contents were centrifuged at 13000rpm for 15 minutes at 4˚C. Supernatant was discarded and plasmid DNA pellet was washed thrice with 75% ethanol in nuclease-free water. Washing was done by adding 1ml of 75% ethanol to the pellet followed by inverting the tubes 4-5 times. This was incubated at room temperature for 5 minutes followed by centrifugation at 13000rpm or 15 minutes at 15˚C. DNA pellet was dried at room temperature in a laminar hood. Pellet was then dissolved in appropriated volume of 1X TE buffer.

Plasmid isolation

Piezo1-RFP expressing bacterial cells were collected the following day and centrifuged at 4000rpm for 10 minutes at 25˚C. Plasmid was isolated using QIAprep Spin Miniprep Kit (Qiagen). Pellet from 5ml bacterial culture was resuspended in 250µl of P1 buffer containing LyseBlue reagent at a dilution of 1:1000 and RNase A solution. 250µl of buffer P2 was added and mixed rigorously by inverting the tubes multiple times. Proper cell lysis is evident by solution turning uniformly blue. After 4-5 minutes of lysis, 350µl of neutralization buffer N3 was added. Tubes were then inverted multiple times so as to allow proper mixing. The solution turned colourless after addition of N3 buffer. Contents were centrifuged at 13000rpm for 15 minutes at 4˚C. 800µl of debris-free supernatant was then applied to QIAprep spin column 2.0. The columns were centrifuged at 13000rpm for 1 minute. Flow-through was discarded. The column was washed with 500µl of binding buffer PB. Centrifugation at 13000rpm for 1 minute was performed again. Flow-through was discarded again followed by addition of 750µl of ethanol-containing buffer PE. After centrifugation at 13000rpm for 1 minute, flow-through was discarded. The column was centrifuged again similarly to remove any residual wash buffer. The columns were then placed on fresh 1.5ml

microfuge tubes. 50µl of elution buffer EB (10mM Tris, pH 8.5) was added to the top of the column and allowed to incubate for 1 minute at room temperature. Centrifugation at 13000rpm for 1 minute was performed. The elution step was performed again similarly. Plasmid DNA-containing flow-through was collected.

Transient Piezo1 overexpression in Jurkat cell line

Jurkat EP6-1 was maintained in RPMI + 10% FBS. Cells were split at a density of 0.5 million per ml of media without antibiotics 1-2 days before transfection. On the day of transfection, cells were washed at 900 rpm at 4˚C for 5 minutes. Approximately 1.5 million cells were resuspended in nucleofection buffer (Lonza) consisting of 82µl of Cell Line SE buffer and 18µl of P1 supplement buffer. 10µg of RFP-tagged Piezo1 construct was added and mixed. Cells were nucleofected using Amaxa 4D Nucleofector, program CL-120. Cells were then cultured in a 24-well plate in 2ml RPMI + 20% FBS without antibiotics at 37˚C. Cells were washed after 24 hours at 900rpm, 4˚C for 5 minutes and plated in fresh RPMI + 20% FBS without antibiotics. Overexpression was measured using BD LSR II flow cytometer after 36-48 hours post-transfection. All transfections were performed within 10 passages after thawing of stock Jurkat.

Live cell imaging

Transfected Jurkat cells were seeded on ICAM-1-coated (4µg/ml) millicell µ-chamber. A SDF1-α chemokine gradient of 0.5µg/ml (final concentration) was applied to the top half of the chamber (Detailed protocol of millicell µ-chamber migration assay described in section 16.2). Cells were incubated for 15 minutes at 37˚C. Live cell imaging was performed using EVOS immunofluorescent microscope using the PE-Texas Red emission filter. Cells were allowed to

migrated for 15 mins at an interval of 1 minute per frame. Localisation of mcherry-labelled Piezo1 was tracked in moving cells.

Image Analysis

All images were analysed using Fiji ImageJ software. Polarity of mcherry-labelled Piezo1 in moving Jurkat cells was measured. Moving Jurkat cells were tracked and direction of their transient movement was identified. A line perpendicular to the transient direction of movement was used to divide a moving cell into two halves – front and rear halves. Mean fluorescent intensity of Piezo1-mcherry in each half of the cell was measured using Fiji ImageJ. Difference between the mean fluorescence intensity was calculated and divided by the average fluorescence intensity of the entire cell. This was used as the Piezo1 Polarity Index in moving Jurkat cells.

19.3 Results

Flow cytometric measurements revealed transfection efficiency to be around 30% to 40% approximately 36 hours post-transfection. Overexpression of mcherry-tagged Piezo1 in Jurkat cells was transient and was significantly reduced on day 3 post-transfection (Fig. 19-A). So, transfected Jurkat cells were collected on day 2 after transfection and seeded on ICAM-1-coated millicell μ-migration chamber where SDF1α chemokine gradient was established. mcherry-tagged Piezo1 showed a strong polarity in Jurkat cells in the presence of a chemokine gradient (Fig. 19-B). Piezo1 tended to accumulate in the front half of a moving cell subjected to SDF1α chemokine gradient (Fig. 19-C). Piezo1, however, showed no preferential localisation in the cell in the absence of any chemokine.

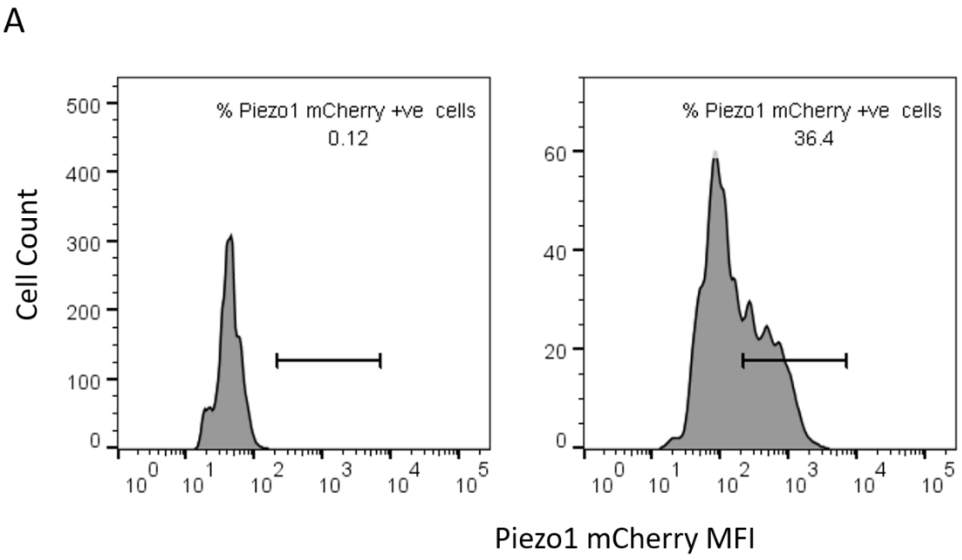

Figure 19-A. Representative flow cytometry plots depicting transfection efficiency of Jurkat cells overexpressing Piezo1-mcherry. Jurkat cells were nucleofected with Piezo1-mcherry expressing plasmid. Transfection efficiency was checked 36 hours after nucleofection through flow cytometry. Left panel: Un-transfected Jurkat cells, Right panel: Plasmid-transfected cells.

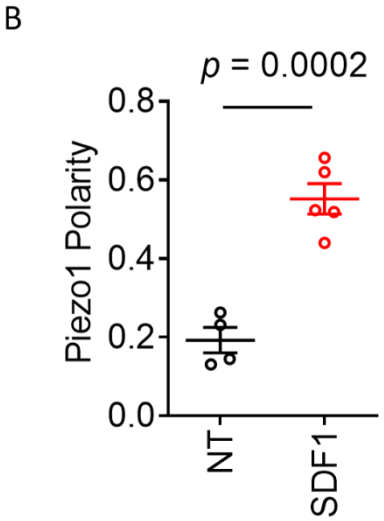

Figure 19-B. Polarity of Piezo1 proteins in Jurkat cells treated with chemokine. Jurkat cells overexpressing mCherry-tagged Piezo1 were subjected to 0.5µg/ml SDF-1α chemokine gradient in µ-millicell migration chambers. Piezo1 showed uniform cellular distribution in the

absence of chemokine gradient but tended to concentrate specifically in the frontal regions of the cells subjected to a chemokine gradient. Calculation of Piezo1 polarity is described in detail in section 18.2.

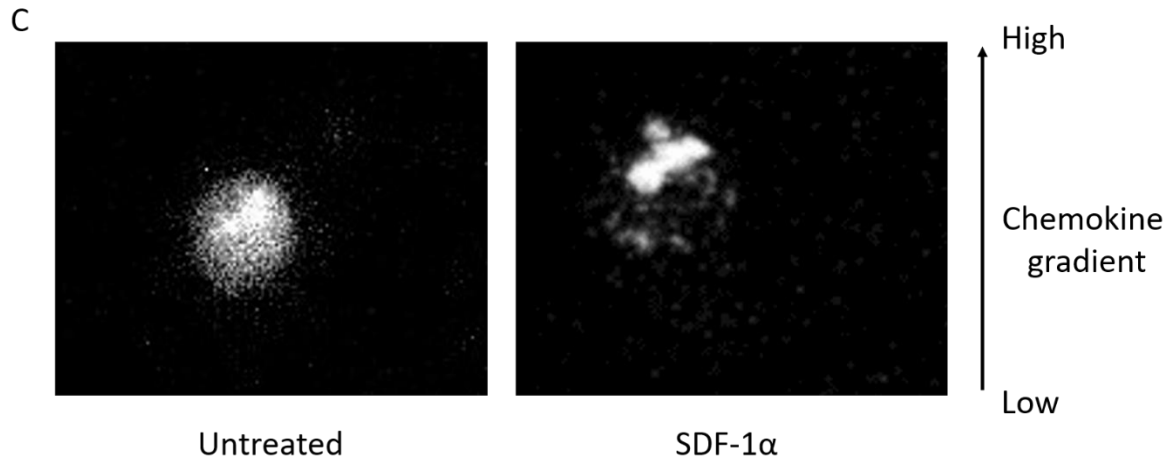

Figure 19-C. Representative images of Piezo1 distribution in moving Jurkat cells. Jurkat cells overexpressing mCherry-tagged Piezo1 were allowed to move in the presence of absence of SFF-1α chemokine gradient in a μ-millicell migration chamber. Piezo1 showed no preferential localisation in the absence of chemokine gradient (left panel) but tended to accumulate in the frontal regions of moving cells subjected to chemokine gradient (right panel). The frontal half of the cell was calculated on the basis of the cell's transient direction of movement (details in section 19.2).

19.4 Discussion

mcherry-tagged Piezo1 overexpression was used to determine intracellular Piezo1 dynamics in moving cells. It was observed that Piezo1 showed preferential accumulation in the front half of a moving Jurkat cell in the presence of chemokine. No specific enrichment of Piezo1 was seen in any region of a cell in the absence of chemokine, SDF1α. This observation makes an interesting finding that Piezo1 actively undergoes redistribution during chemokine-

triggered cell migration. Piezo1 tends to preferentially localise in cellular regions which are first exposed to mechanical cues like the leading edge of a moving cell. Active Piezo1 redistribution enables efficient sensing of mechanical cues during cell movement which may help to recruit and trigger downstream signalling adaptors that mediate directional migration. Rearrangement of cellular Piezo1 localisation depending on site of stimulus was also observed previously when Piezo1 preferentially accumulated in peripheral regions of $CD4^+$ T lymphocytes when stimulated with surface TCR-binding crosslinking antibodies.

Chapter 20. *In-vivo* validation of the role of Piezo1 in $CD4^+$ T lymphocyte migration in contact hypersensitivity mouse model

20.1 Introduction

The contact hypersensitivity (CHS) mouse model is an efficient system that is used to investigate host immune reaction in response to allergens [487]. The process consists of a primary stage of mouse exposure to contact allergens. This phase is known as the allergen sensitisation phase [487]. During this phase, antigen presenting cells (APCs) residing at the site of allergen application like skin-resident dendritic cells or Langerhans cells take up the allergen and carry them to site-draining lymph nodes. The contact allergen is typically a hapten which forms immunogenic complexes with host-intrinsic carrier proteins which are subsequently taken up by tissue-resident innate APCs. In the lymph nodes, they present the antigens to circulating naïve T cells where they get activated and differentiate to antigen-specific effector T lymphocytes. Antigen sensitisation and production of antigen-specific effector T lymphocytes usually takes about 5-6 days from the point of primary allergen exposure. Following sensitisation, the mouse is re-exposed to the same contact allergen at a site distinct but proximal to the primary exposure site. This will trigger an immediate and heightened immune reaction at the secondary site which can be studied in isolation from the rest of the system. During this phase, there is preferential and robust recruitment of allergen-specific T lymphocytes at the secondary site where their activity and function can be examined. The second phase of this contact hypersensitivity reaction is known as the elicitation phase [487]. The elicitation phase is characterised by an initial period consisting of inflammation driven by neutrophils, C5/C5a complement system, and inflammatory cytokines

like tumor necrosis factor alpha (TNF-α) and serotonin secreted by mast cells and platelets. This usually takes around 2 hours post stimulation to be triggered. The latter period of the elicitation phase occurs after 24 hours of allergen stimulation and consists of recruitment of effector T lymphocytes to stimulation site. The contact hypersensitivity (CHS) reaction is mediated by IFN-γ-producing Th1, IL-4 and IL-13-producing Th2 and IL-17-producing Th17 immune response. Apart from $CD4^+$ T lymphocytes, $CD8^+$ T lymphocytes, B lymphocytes and Natural Killer (NK) cells also drive the CHS reaction [487]. In mice, the site of allergen sensitisation is the dorsal or ventral abdominal skin while the usual site of elicitation is the ear. Ear swelling and redness act as indicators of inflammation through CHS reaction [487,488].

In the following sections, we used the technique of adoptive transfer to track the migration capacity of a population of $CD4^+$ T lymphocytes in a CHS mouse model. Adoptive transfer is a useful technique that involves isolating and labelling a particular population of cells and injecting them into the circulation of another mouse of the same strain, with the same genetic background [489]. This population of exogenously introduced cells, hereby referred to as adoptively transferred cells, can be tracked and analysed through flow cytometry or intra-vital microscopy. In our study we isolated $CD4^+$ T lymphocytes from peripheral lymph nodes and spleen of allergen-sensitised mice and transfected them with control or mouse-specific Piezo1 siRNA. After Piezo1 downregulation, these cells were fluorescently labelled and introduced into another mouse of the same genetic background. CHS reaction was then induced through topical application of the allergen at a distinct site and infiltration of labelled adoptively transferred $CD4^+$ T lymphocytes was measured through flow cytometry.

20.2 Methods

Contact Hypersensitivity (CHS) mouse model

8-12 weeks old, male, BALB/c mice were used for this study. The dorsal abdominal area was shaved and the skin was wiped with 75% ethanol one day prior to sensitisation.

Sensitisation: 4-Ethoxymethylene-2-phenyl-2-oxazolin-5-one or oxazolone (Sigma) was used as the contact allergen hapten to induce a CHS reaction. A stock of 3.75% oxazolone solution in acetone was used to create an emulsion of 3% oxazolone in olive oil (4:1, vol:vol) for topical application. 80µl of 3% oxazolone in olive oil was applied on shaved abdominal skin and 10µl of the same was applied on each paw of the mouse. The skin was allowed to dry before placing the mice back into their cages. Sensitisation was performed for 5 days after topical application of the allergen.

Transfection of mouse $CD4^+$ T lymphocytes

Oxazolone-sensitised mice were euthanised on day 6 post-sensitisation through cervical dislocation. Mouse peripheral lymph nodes (brachial, axillary and inguinal) and spleen were dissected and collected in RPMI + 10% FBS. These tissue sites will be enriched in oxazolone-sensitised effector $CD4^+$ T lymphocytes among other $CD4^+$ T lymphocytes. The spleen was processed through gently crushing it using a 5ml syringe-plunger. The dissociated cell and tissue contents were filtered through a 70µm strainer. Lymph nodes were incubated in digestion buffer containing RPMI + 10% FBS + 1mg/ml collagenase for 20 minutes at 37˚C. The lymph nodes were then crushed through a 70µm cell strainer. Cells were washed in excess RPMI media at 1000 rpm, 4˚C for 5 minutes. RBC lysis was performed for not more than 2 minutes at room temperature. Cells were washed with excess RPMI. Cells were then resuspended in MACS buffer and appropriate volume of mouse-specific $CD4^+$ microbeads were added (Miltenyi, according to manufacturer's protocol). Cells were incubated at 4˚C for 20 minutes under rotating conditions. Excess unbound microbeads were washed with excess

MACS buffer at 1000 rpm, 4˚C for 5 minutes. $CD4^+$ T lymphocytes were isolated passing the cells through magnetic large-sized columns (Miltenyi Biotec). Columns were washed with 9ml of ice-cold MACS buffer. $CD4^+$ T lymphocytes were isolated through plunging of the column-bound positive fraction with excess MACS buffer followed by centrifugation at 1000rpm for 5 minutes at 4˚C. Cells were incubated in RPMI + 10% FBS + 50µM β-mercaptoethanol for 20 minutes at 37˚C. Cells were washed with excess 1X PBS and media was completely removed from the cell pellet. Primary nucleofection buffer was prepared by adding 82µl of P3 primary buffer and 18µl of P1 supplement buffer. The buffer was diluted at a ratio of 1.5:1 with OPTI-MEM media (buffer: OPTI-MEM). Approximately 2-3 million $CD4^+$ T lymphocytes were resuspended in 100µl of final nucleofection buffer and transfected with 195ng/ml of control EGFP or mouse Piezo1-specific siRNA. A combination of 3 siRNA sequences were used for mouse Piezo1 downregulation:

a. 5’ CAGCUAUCGUCUUCACUGA dTdT 3’

b. 5’ GAAGCUGCUGAAGAAGCAA dTdT 3’

c. 5’ CUCCACCAACCUUAUCAGU dTdT 3’

Cells were pulsed using Amaxa 4D nucleofector using program,

Cells were then seeded in a 24-well plate containing 2ml of RPMI + 10% FBS + 50µM β-mercaptoethanol. Cells were seeded at a density of $1\text{-}2 \times 10^6$ per well. 1U/ml of recombinant IL-2 was added to each well.

Adoptive transfer

For each adoptive transfer in 1 mouse, $CD4^+$ T lymphocytes were isolated from spleen and lymph nodes from 5 mice. $CD4^+$ T lymphocytes were transfected with control and mouse

Piezo1-specific siRNAs. Transfected cells were collected on day 3 post nucleofection and washed at 1000rpm, 4˚C for 5 minutes. Control EGFP siRNA-transfected cells were labelled with CFSE dye (1:200 dilution in DMSO from 5mM stock) for 10 minutes at room temperature with intermittent shaking. Labelling was stopped with excess RPMI + 10% FBS + 50µM β-mercaptoethanol. Similarly, Piezo1 siRNA-transfected $CD4^+$ T cells were labelled with cell trace violet dye (1: 100 dilution in DMSO from 5mM stock). Cells were washed with excess media at 1000 rpm at 4˚C for 5 minutes. Control and Piezo1 siRNA-transfected cells were counted using Neubauer's Haemocytometer. Equal number of CFSE-labelled control siRNA and CTV-labelled Piezo1 siRNA-transfected $CD4^+$ T lymphocytes (approximately 8-10 million each, equal number) were mixed and introduced into oxazolone-pre-sensitised recipient BALB/c male mouse through intravenous (I.V.) injection in the tail vein.

CHS Elicitation phase: 2 hours after I.V. injection, 40µl of 3% oxazolone in olive oil (4:1, oxazolone : olive oil) was applied on the inner and outer skin surface of the right ear. 40µl of vehicle (4:1, acetone : olive oil) was similarly applied on the inner and outer skin surface of the left ear as control.

Flow cytometry staining

36 hours after application of application of vehicle or oxazolone on the mouse ear, mouse was euthanised by cervical dislocation. The left and right ear of the mouse was dissected and collected in media. Mouse spleen was also collected.

Ear digestion: The two layers of the ear were separated by pulling apart the upper and lower leaves at the base of the ear. The halves were then incubated in HEPES buffer containing 5% FBS and 5mM EDTA at 37˚C with intermittent vortexing. Tissue was washed with excess 1X PBS. The tissue was then cut into small pieces and transferred to 2ml RPMI + 10% FBS +

1mg/ml dispase + 1mg/ml collagenase. Digestion was performed for 15-20 minutes at 37˚C with shaking at 120rpm. Further digestion was stopped by adding excess RPMI + 10% FBS and contents were strained through 70µm strainer to collect single cells. Cells were washed with FACS buffer at 1000rpm, 4˚C for 5 minutes.

Spleen was crushed and passed through a 70µm strainer followed by centrifugation at 1000rpm, 4˚C, 5 minutes. RBC lysis was performed for 2 minutes at room temperature followed by washing with excess media and FACS buffer subsequently.

The following mouse -specific antibodies were used for staining – CD45 PerCP, TCRβ APCCy7 and CD4 APC (BD Bioscience). The percentage of infiltrating CFSE-labelled control siRNA and CTV-labelled Piezo1 siRNA-transfected $CD4^+$ T lymphocytes was measured using BD LSR II flow cytometer.

20.3 Results

We used the mouse contact hypersensitivity (CHS) model to validate Piezo1-mediated regulation of $CD4^+$ T lymphocyte migration. Primary $CD4^+$ T lymphocytes were isolated from spleen and peripheral lymph nodes (pLNs) from oxazolone-sensitised mice. Isolated cells were transfected with control or mouse Piezo1-specific siRNA. Transfected cells were differentially labelled with fluorescent dyes and introduced intravenously into a pre-sensitised recipient mouse. The mouse was then challenged on the ear with oxazolone or vehicle (Fig. 20-A). The proportion of CFSE-labelled control $CD4^+$ T lymphocytes and CTV-labelled Piezo1-downregulated $CD4^+$ T lymphocytes that were specifically recruited to the allergen-challenged site was then detected through flow cytometric measurements. Loss of Piezo1 expression negatively affected migration of $CD4^+$ T lymphocytes to the antigen-challenged site. There was significant reduction of ear-infiltrating Piezo- downregulated $CD4^+$ T

lymphocytes as compared to control $CD4^+$ T lymphocytes. Vehicle-treated ear did not show significant infiltration of $CD45^+$ immune cells including $CD4^+$ T lymphocytes as compared to oxazolone-challenged ear (Fig. 20-B, C).

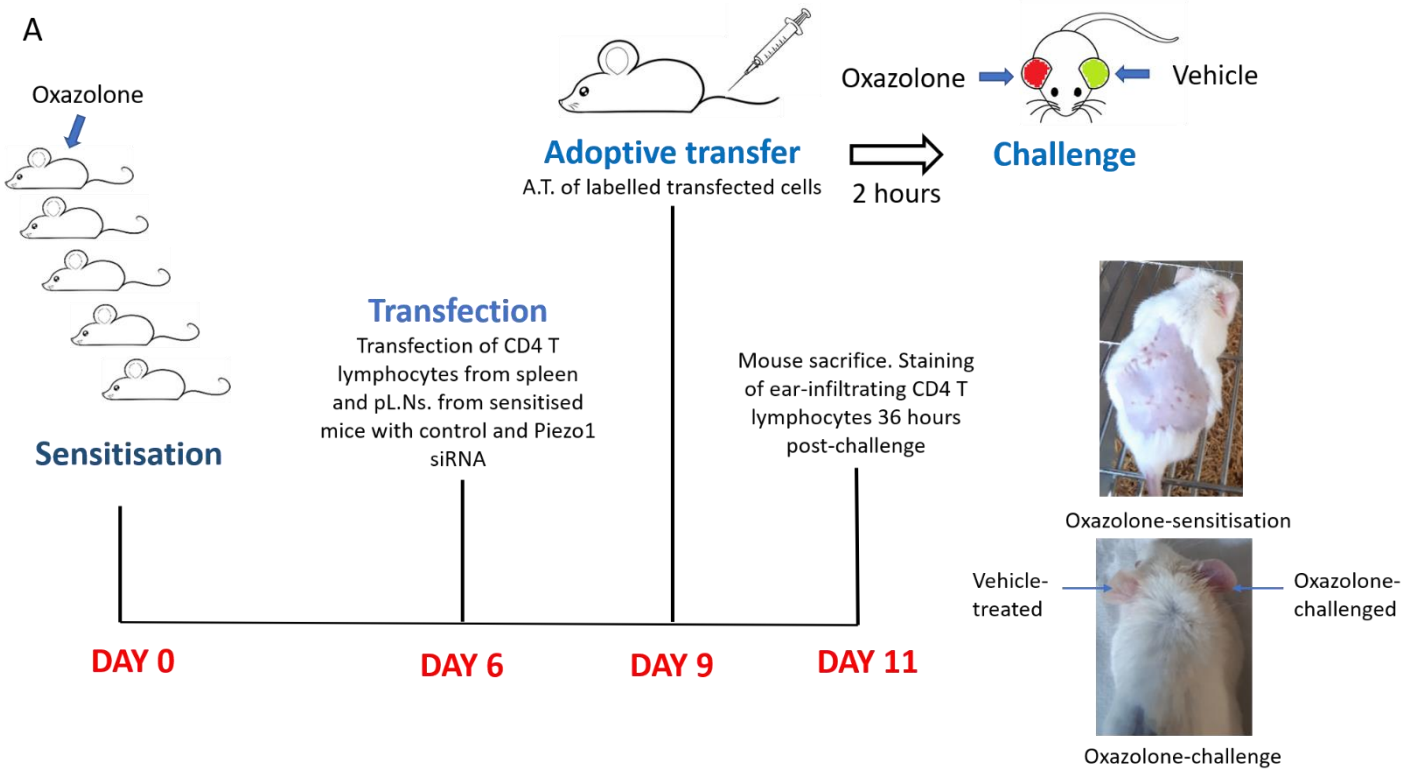

Figure 20-A. Contact Hypersensitivity (CHS) mouse model. In order to validate the role of Piezo1 in directional migration of $CD4^+$ T lymphocytes, we used the CHS mouse model. Adult BALB/c mice were sensitised with hapten, oxazolone by topical application. On day 6 after sensitisation, mice were sacrificed and primary $CD4^+$ T lymphocytes were isolated from peripheral lymph nodes (pLNs) and spleen. Isolated cells were transfected with control and Piezo1-specific siRNAs. Upon Piezo1 knockdown, cells were collected and labelled with fluorescent dyes (CFSE: control siRNA-transfected cells, CTV: Piezo1 siRNA-transfected cells) and equal number of cells were injected intravenously into a pre-sensitised mouse. 2 hours after adoptive transfer, the left and right ear of the recipient mouse was challenged with

vehicle and oxazolone respectively. Infiltration of labelled $CD4^+$ T lymphocytes into the mouse ear was measured through flow cytometry. Adoptively transferred Piezo1-deficient $CD4^+$ T lymphocytes showed significant reduction in recruitment to the oxazolone-challenged site as compared to control $CD4^+$ T lymphocytes (Fig. 20-D, E). Loss of Piezo1, thus impairs the ability of $CD4^+$ T lymphocytes to respond to inflammatory cues and migrate towards sites of inflammation. Homing of adoptively transferred control and Piezo1-deficient $CD4^+$ T cells to the spleen was however, did not show considerable difference (Fig. 20-F).

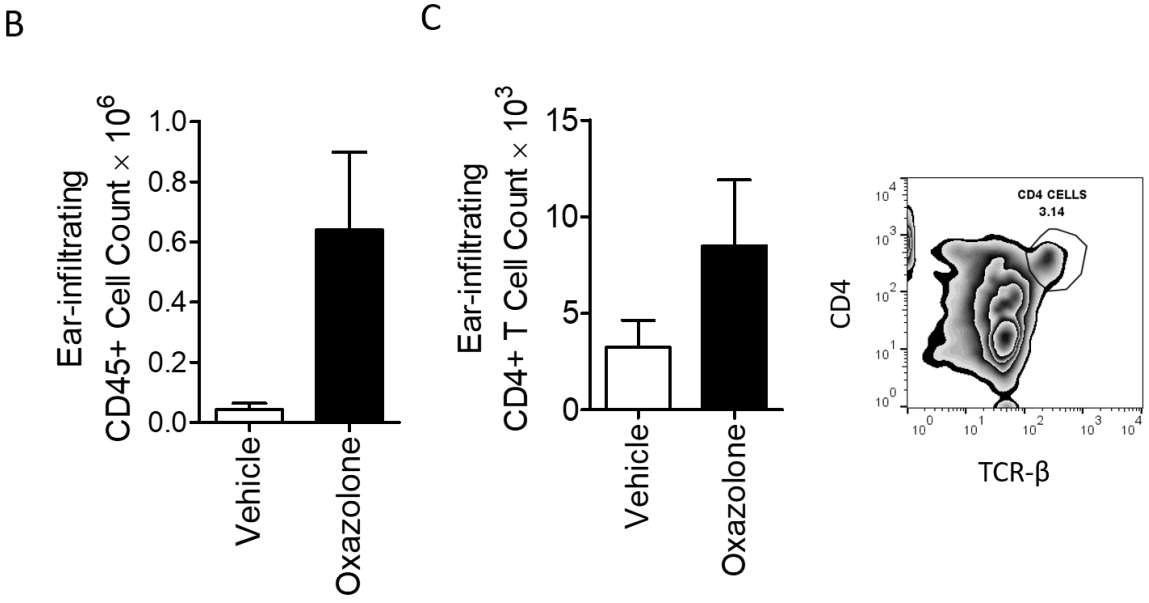

Figure 20-B, C. Infiltration of $CD45^+$ immune cells in oxazolone-challenged ear. Adoptive transfer of labelled transfected $CD4^+$ T lymphocytes was performed in mouse pre-sensitised with oxazolone. Post-transfer, the mouse was challenged with vehicle on the left ear and oxazolone on the right ear. Proportion of infiltrating $CD45^+$ immune cells (B) including whole $CD4^+$ T lymphocytes (C) in oxazolone-treated ear were much higher as compared to vehicle-treated ear, thus, accounting for inflammation due to CHS reaction upon oxazolone challenge. (Fig. C, Right panel – representative flow cytometry plot of $CD4^+$ T lymphocyte population in oxazolone treated ear.)

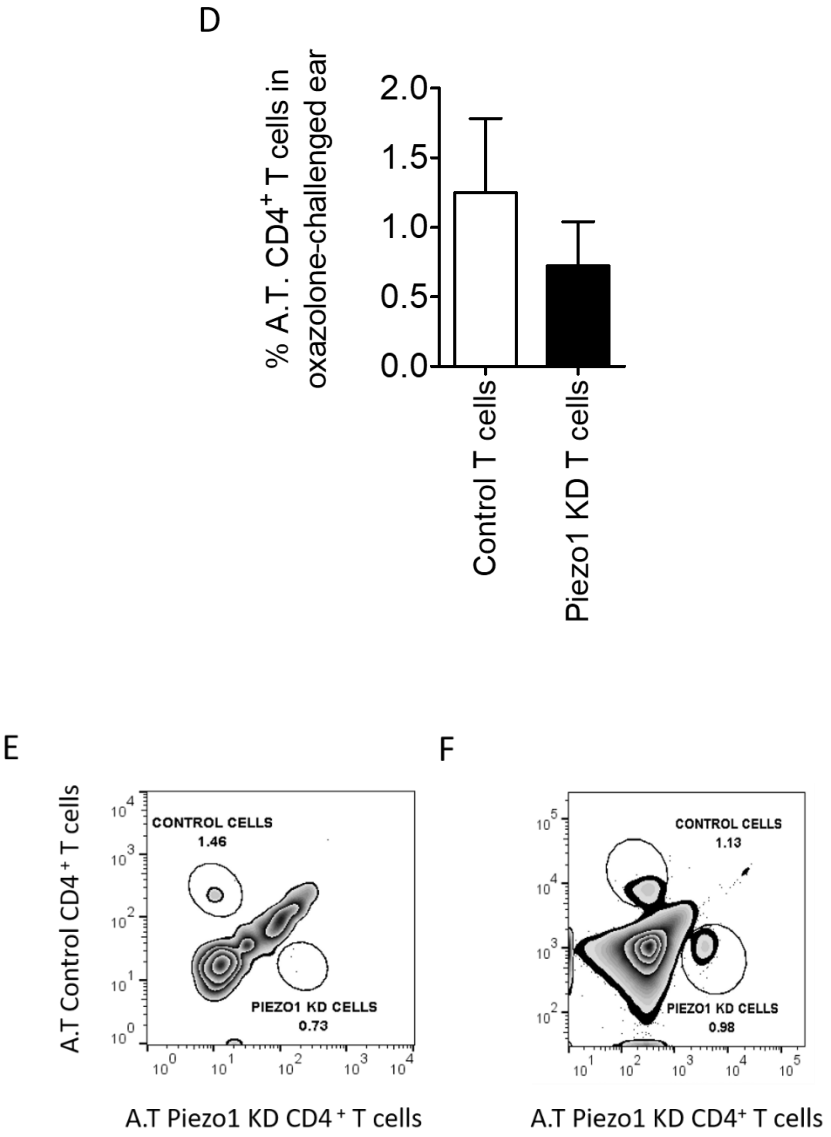

Figure 20-D-F. Piezo1 downregulation inhibits migration of CD4⁺ T lymphocytes to inflamed tissue sites. Infiltration of differentially labelled, adoptively transferred CD4⁺ T lymphocytes in oxazolone-challenged ear was measured by flow cytometry. Loss of Piezo1 expression reduced the ability of CD4⁺ T lymphocytes to migrate to inflamed, allergen-treated ear (D). Representative flow cytometry plot of percentage of control CD4⁺ T lymphocytes and Piezo1-deficient CD4⁺ T lymphocytes in oxazolone-challenged ear (E). Representative flow cytometry plot of percentage of control CD4⁺ T lymphocytes and Piezo1-deficient CD4⁺ T lymphocytes in spleen (F) (A.T.: Adoptively transferred)

20.4 Discussion

We used a CHS mouse model to validate our in-vitro findings of Piezo1-mediated regulation of $CD4^+$ T lymphocyte migration and chemotaxis. The CHS mouse model provides the advantage that one can study immune cell recruitment and inflammation in a specific tissue compartment. We sensitised mice to oxazolone, a contact allergen and allowed production of oxazolone-specific effector T lymphocytes. $CD4^+$ T lymphocytes were subsequently isolated from secondary lymphoid organs which will be enriched in allergen-specific $CD4^+$ T lymphocytes. Isolated cells were transfected with control or Piezo1 siRNAs and post-knockdown these cells were differentially labelled and adoptively transferred into a pre-sensitised mouse. The recipient mouse was subsequently challenged by a second dose of oxazolone at a distinct site – the ear. Proportion of ear-infiltrating labelled $CD4^+$ T lymphocytes was measured. Piezo1 downregulation resulted in dramatic reduction of ear-infiltrating $CD4^+$ T lymphocytes. As discussed in section 20.1, second application of oxazolone (challenge) in a pre-sensitised mouse results in exacerbated immune reaction that leads to production of inflammatory mediators that recruit effector immune cells including allergen-specific $CD4^+$ T lymphocytes to the challenged tissue site. Thus, this result confirms that Piezo1 expression is necessary for guided and directed migration of $CD4^+$ T lymphocytes to inflamed peripheral tissue sites. Loss of Piezo1 expression abrogates directional T cell movement and results in impaired immune response.

Chapter 21. *In-vivo* validation of the role of Piezo1 in $CD4^+$ T lymphocyte migration in air pouch mouse model

21.1 Introduction

The air pouch model was first devised by H. Selye in 1953 and it was known as the granuloma pouch technique [(490)]. This technique involves subcutaneous injection of sterile air in the intrascapular region of the dorsal skin of the mouse [(490)]. This creates a specific compartment where inflammation-triggering components can be introduced and immune reaction in terms of infiltrating immune cell populations, inflammatory mediators and efficacy of therapeutic drugs can be investigated. This technique is usually performed with injection of carrageenan solution into the air pouch which acts as an irritant and induces localised inflammation [(490)]. Inflammation is characterised by infiltration of immune cells, production of inflammatory mediators like prostaglandins, leukotrienes and proinflammatory cytokines like TNFα. Other inflammation inducers like lipopolysaccharides (LPS), mycobacteria, tumor cells have also been introduced into the air pouch to trigger local inflammation. The air pouch is formed through two subsequent subcutaneous injections of sterile air within a span of 6 days. Subcutaneous injection of air triggers skin-resident macrophages and fibroblasts that begin to proliferate and form a boundary around the air cavity [(490)]. Induced inflammatory response can be subsequently studied in this compartment by collecting the air pouch exudate and subjecting them to immunophenotyping for infiltrating cells and cytokine profiles. This system allows us to create a controlled local environment where induced inflammation and its elements can be studied in isolation from the rest of the system. This system has also been

used extensively in tumor models where efficacy of potential anti-cancer drugs was tested or exploration of the characteristics of the tumor microenvironment was performed [491].

In our study, we adopted this mouse model to examine recruitment of $CD4^+$ T lymphocytes to the air pouch upon filling the air pouch with tumor cell extract. $CD4^+$ T lymphocytes were isolated from healthy mice. Piezo1 expression was downregulated in these cells through siRNA-mediated knockdown. Control and Piezo1-deficient $CD4^+$ T lymphocytes were differentially labelled and injected into the circulation of mouse containing the air pouch. The air pouch was then filled with the inflammatory stimulus and recruitment of labelled adoptively transferred $CD4^+$ T lymphocytes was measured. It allowed us to gauge if Piezo1 regulates recruitment of $CD4^+$ T lymphocytes from peripheral circulation to local tissue compartments.

21.2 Methods

Air pouch mouse model

8-12 weeks old C57BL/6 mice were used for this model. The skin of the mouse was wiped with 75% ethanol. 5ml of sterile air was injected subcutaneously in the intrascapular region of the dorsal side of the mouse while passing the air through 0.22µm filter. Successful injection will result in formation of a dome-shaped pouch on the dorsal skin of the mouse. The mouse was allowed to rest for 2 days. On day 3, a second dose of 5ml sterile air was similarly injected subcutaneously in the same region. The mouse was allowed to rest and air pouch was allowed to settle for the next 3 days.

Transfection of mouse $CD4^+$ T lymphocytes

Peripheral lymph nodes (pLNs, auxiliary, brachial and inguinal) and spleen from age and sex-matched C57BL/6 mice were collected in RPMI + 10% FBS + 50µM β-mercaptoethanol. The spleen was crushed gently using a 5ml syringe-plunger in RPMI + 10% FBS + 50µM β-mercaptoethanol. Crushed contents were passed through a 70µm strainer. pLNs were incubated in media containing 1mg/ml collagenase for 20 mins at 37˚C. pLNs were then crushed in excess media through a 70µm cell strainer. Single cells thus, obtained were centrifuged at 1000 rpm, 4˚C for 5 minutes. RBC lysis was performed for not more than 2 minutes at room temperature. Further lysis was stopped with excess RPMI without FBS. Cells were centrifuged at 1000rpm, 4˚C for 5 minutes. Cells were incubated with appropriate volume of $CD4^+$ microbeads (Miltenyi Biotec) for 20 minutes at 4˚C under rotating conditions. $CD4^+$ T lymphocytes were isolated by passing the microbead-bound cells through magnetic large-sized columns (Miltenyi Biotec). The columns were washed with ice-cold MACS buffer and $CD4^+$ T lymphocytes were isolated by plunging the column-bound positive fraction with excess MACS buffer. Isolated $CD4^+$ T lymphocytes were allowed to recover in media at 37˚C for 20 minutes.

$CD4^+$ T lymphocytes were washed to completely remove residual media. Approximately 2-3 million cells were resuspended in 100µl of nucleofection buffer. 82µl of P3 primary buffer was mixed with 18µl of P1 supplement buffer. This mixture was diluted at a ratio 1.5:1 with OPTI-MEM and used for nucleofection. 195ng/ml of control EGFP siRNA and Piezo1 siRNA was used to transfect $CD4^+$ T lymphocytes. A pool of 3 siRNAs was used to downregulate Piezo1 expression (described in detail section 20.2). Cells were seeded in RPMI + 10% FBS + 50µM of β-mercaptoethanol for 3 days to allow Piezo1 knockdown. Cells were seeded at 1-2 × 10^6 per 2 ml of media. Recombinant IL-2 was added at a concentration of 1IU/ml.

Labelling of transfected CD4$^+$ T lymphocytes

On day 3 post-nucleofection, control and Piezo1 siRNA-transfected CD4$^+$ T lymphocytes were collected and washed in 1X PBS at 1000rpm, 4˚C for 5 minutes. Cells were resuspended in 1X PBS. Control CD4$^+$ T lymphocytes were stained with CFSE cell trace dye at a concentration of 75nM for 10 minutes at room temperature. Piezo1 siRNA-transfected CD4$^+$ T lymphocytes were stained with cell trace violet dye at a concentration of 75nM for 20 minutes at room temperature. Staining was performed in 1X PBS at a density of 2 million cells per ml of 1X PBS. Tubes were shaken intermittently to allow uniform dye uptake. After staining, cells were washed with excess RPMI + 10% FBS at 1000 rpm, 4˚C for 5 minutes. Cells were then counted on a Neubauer's Haemocytometer.

Adoptive transfer

Equal number of CFSE-labelled control siRNA and CTV-labelled Piezo1 siRNA-transfected CD4$^+$ T lymphocytes was mixed and injected intravenously (I.V.) into the tail of air pouch-containing C57BL/6 mouse. A total no. of 15 – 20 million cells were adoptively transferred. 2 hours after I.V. injection, EL4 lymphoma cell extract was injected into the air pouch. Proportion of adoptively transferred, labelled CD4$^+$ T lymphocytes that have infiltrated into the air pouch was detected 36 hours after I.V. injection.

Flow cytometry

36 hours after adoptive transfer, the mouse was sacrificed by cervical dislocation. The air pouch contents were harvested. 5ml 1X PBS was injected into the mouse and the air pouch was tapped slightly. The contents of the air pouch were subsequently withdrawn using a 5ml syringe. The air pouch was cut open and the remaining exudate was collected by pipetting.

The spleen of the mouse was also collected. The air pouch contents were strained through a 0.22µm cell strainer. The spleen was processed as described before. Cells were stained with the following antibodies – PerCP labelled anti-mouse CD45, APC-Cy7 conjugated anti-mouse TCRβ and APC conjugated anti-mouse CD4. Infiltrating immune cells were gated as $CD45^+$ cells. $TCR\beta^+$ $CD4^+$ were identified as $CD4^+$ T lymphocytes. Percentage of CFSE-labelled control and CTV-labelled Piezo1-deficient $CD4^+$ T cells were subsequently identified from parent $CD4^+$ T lymphocyte population.

EL4 tumor cell line

EL4 is a mouse lymphoma cell line established from C57BL/6 mice. It is cultured in RPMI + 10% FBS and passaged every 2-3 days. For tumor cell extract, approximately 6-8 million EL4 cells were washed in 1X PBS and resuspended in 1ml 1X PBS. Cells were then subjected to repeated snap freeze-thaw cycle (5-7 times). The contents were then centrifuged at 4000rpm, 4˚C for 10 minutes. Supernatant containing the cell extract was used for injection into the air pouch. Extract from 10 million cells was used per mouse.

21.3 Results

We used the mouse air pouch model to study the role of Piezo1 in site-specific migration of $CD4^+$ T lymphocytes. Piezo1 was downregulated through siRNA-mediated knockdown in $CD4^+$ T lymphocytes isolated from healthy, adult C57BL/6 mice. Control and Piezo1-deficient $CD4^+$ T lymphocytes were differentially labelled with CFSE and CTV dyes respectively. Equal number of both were then mixed and injected into the circulation of the mouse through tail vein. The air pouch was filled with EL4 tumor cell line extract. Air pouch exudates were harvested 36 hours after injection (21-A). There was significant infiltration of $CD45^+$ immune cells including $CD4^+$ T lymphocytes suggesting localised inflammation (21-B). Piezo1 downregulation

resulted in dramatic decrease of $CD4^+$ T lymphocyte migration into the air pouch. CTV-labelled Piezo1 siRNA transfected cells that were adoptively transferred failed to infiltrate the air pouch compartment in response to inflammatory stimulus when compared to CFSE labelled control $CD4^+$ T lymphocytes (Fig. 21-C, D). This confirms that Piezo1 activity is crucial for tissue-specific directed migration of $CD4^+$ T lymphocytes in response to stimulus.

A

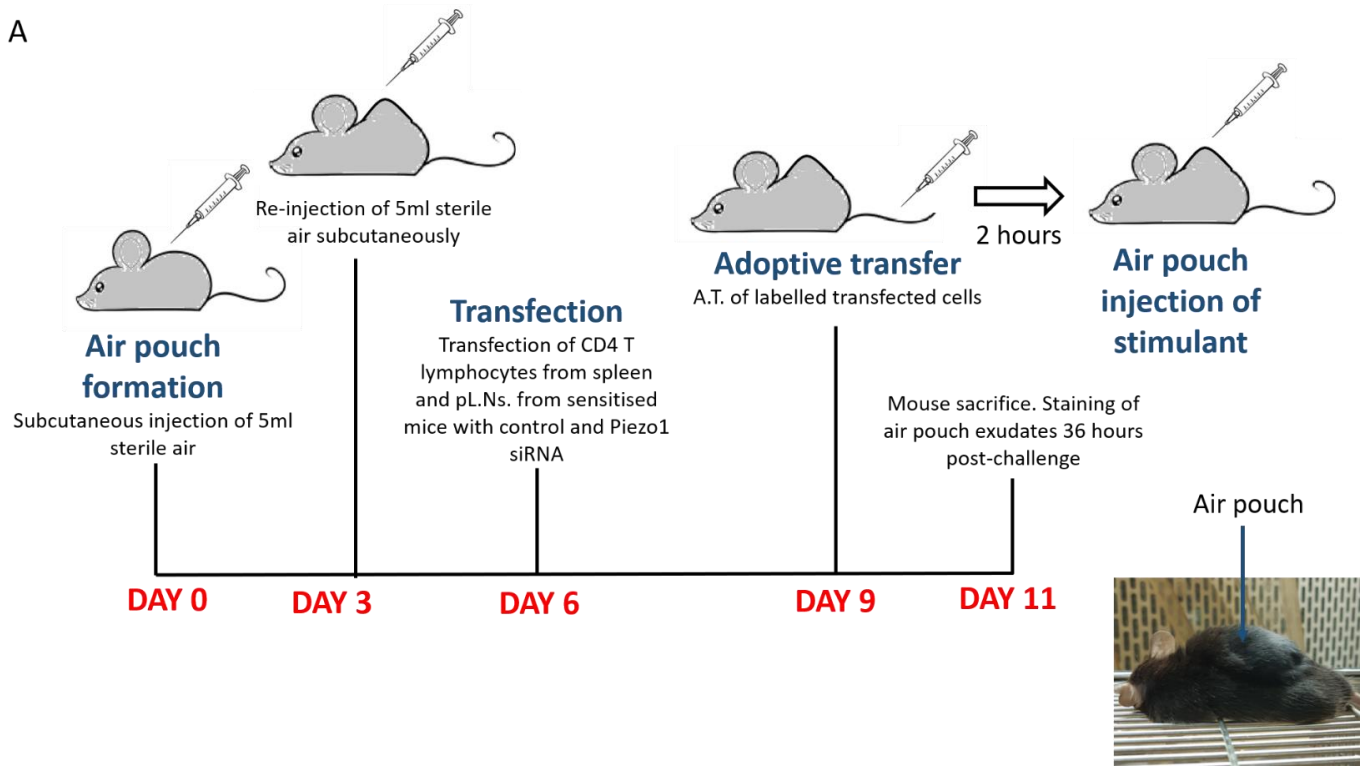

Figure 21-A. The mouse air pouch model of inflammation. This system can be used to study localised immune response. Briefly, sterile air is injected subcutaneously into the dorsal skin of the mouse. The air pouch is stabilised by reinjection of sterile air after a gap of 2 days. This creates a compartmentalised air cavity beneath the mouse epidermis that is lined by macrophages and fibroblast cells. Upon addition of appropriate stimulation in the air pouch which in this case is EL4 lymphoma cell line extract, localised inflammation will be induced that trigger immune cells including $CD4^+$ T lymphocyte recruitment. $CD4^+$ T lymphocytes that

were isolated from secondary lymphoid organs of healthy mice were transfected with control or mouse Piezo1-specific siRNA. Upon Piezo1 downregulation, control and knockdown cells were labelled with different fluorescent dyes and adoptively transferred into the circulation of air pouch-containing mouse. By adding appropriate stimulation in the air pouch, degree of adoptively transferred control and Piezo1 knockdown $CD4^+$ T lymphocyte migration into the air pouch was quantified.

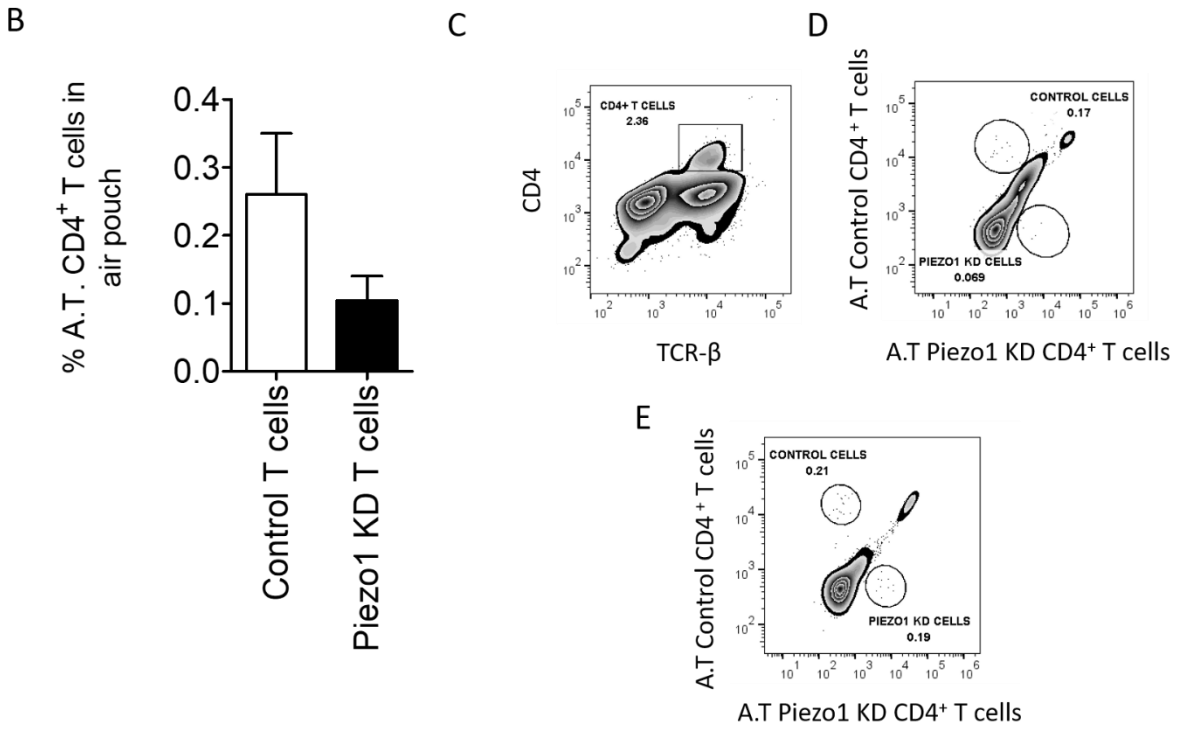

Figure 21-B-D. Loss of Piezo1 expression reduces $CD4^+$ T lymphocyte migration to the air pouch. $CD4^+$ T lymphocytes isolated from pLNs and spleen of age and sex-matched C57BL/6 mice were transfected with control or Piezo1 siRNA. Transfected cells were labelled with CFSE (control $CD4^+$ T lymphocytes) and CTV (Piezo1-knockdown $CD4^+$ T lymphocytes). Equal number of control and Piezo1 knockdown $CD4^+$ T cells were mixed and injected into the tail vein of the air pouch mouse. The air pouch was stimulated with mouse EL4 lymphoma cell line extract 2 hours after intravenous injection. Difference in adoptively transferred

transfected $CD4^+$ T lymphocytes that infiltrated the air pouch was measured by flow cytometry. There was significant $CD4^+$ T lymphocyte population in the air pouch. Representative flow cytometry plot of $TCR\beta^+$ $CD4^+$ T lymphocyte population in air pouch exudate (D). Piezo1 downregulation drastically reduced migration of adoptively transferred $CD4^+$ T lymphocytes in the air pouch upon stimulation (B). Representative flow cytometry plots of percentage of differentially labelled control and Piezo1 knockdown $CD4^+$ T cells that have infiltrated the air pouch (C). Representative flow cytometry plot of labelled adoptively transferred $CD4^+$ T lymphocytes in the spleen (E).

21.4 Discussion

The air pouch model is extensively used to study localised immune responses. By injecting sterile air subcutaneously into the mouse, we create a specialised compartmentalised cavity. Upon addition of inflammation-inducing stimulus, one can study immune response in this localised region. We used EL4 mouse lymphoma cell line extract as inducer of localised inflammation in the air pouch. We then measured degree of infiltration of adoptively transferred $CD4^+$ T lymphocytes into the air pouch. Differential labelling of control and Piezo1-deficient $CD4^+$ T lymphocytes that were adoptively transferred allowed us to quantify difference, if any, in the migratory capacity of these two cell types. As expected, $CD4^+$ T lymphocytes where Piezo1 expression was downregulated failed to migrate to the air pouch upon stimulation. This result further strengthens our confirmation that Piezo1 function is invaluable for site-specific migration of $CD4^+$ T lymphocytes upon stimulation. Loss of Piezo1 expression result in failure of $CD4^+$ T lymphocytes to populate inflamed peripheral tissue sites which leads to impaired immune response.

Chapter 22. Conclusion

In-vitro studies involving ICAM-1-dependent 2D migration or 2D confined migration in millicell μ-migration chambers and 3D chemotaxis across transwells have identified the significance of Piezo1 function in efficient $CD4^+$ T lymphocyte migration. Loss of Piezo1 activity resulted in dramatic inhibition of $CD4^+$ T lymphocyte chemotactic ability suggesting its importance in sensing chemokine gradient while facilitating directional migration. Migrating T lymphocytes adopt a polarised morphology that is crucial for movement. T cell polarity is characterised by leading edge lamellipodia and a trailing-end retracting uropod [343,485]. T cell polarity is generated when membrane and cytosolic components undergo reorganisation upon chemokine stimulation. These changes are mostly driven by remodelling of the actin cytoskeletal scaffold in migrating T lymphocytes. Active actin polymerisation at cell's leading edge and its myosin-driven retrograde flow to the uropod is responsible for generation of traction forces and forward propulsion of the cell [343,485]. Piezo1 downregulation through siRNA-mediated knockdown results in failure of actin to polymerise and accumulate at the cell poles in response to chemokine stimulation. Moreover, migrating $CD4^+$ T lymphocytes showed preferential Piezo1 enrichment at leading pole of the cell, thus suggesting that Piezo1 distribution undergoes constant rearrangement in the cell with preferable accumulation in areas which are exposed to mechanical cues. Our in-vitro results were further confirmed when we saw that Piezo1 downregulation also abrogated the ability of $CD4^+$ T lymphocytes to migrate *in-vivo*. The contact hypersensitivity (CHS) mouse model [488] and the air pouch inflammation [490] mouse model provide the advantage of studying site-specific immune cell migration and recruitment. Since inflammation-inducing agent is applied to a specific tissue site, one can study degree of immune cell infiltration in a localised region. This, in combination

with the technique of adoptive transfer, we could track the migration fate of a population of labelled cells introduced into the mouse. Loss of Piezo1 expression resulted in dramatic decrease in migration of $CD4^+$ T lymphocytes to peripheral inflamed sites. Thus, Piezo1 activity is essential for efficient and guided migration of $CD4^+$ T lymphocytes. Piezo1 deficiency results in severely impaired $CD4^+$ T lymphocytes migration to essential tissue sites thus, leading to a diminished and defective immune response.

Chapter 23. Implications and future perspective

As described before, mechanical forces are acutely associated with T lymphocyte activation, function and fate (Chapter 3.6). Mechanical aspects of tissue microenvironment or cellular interactions form an integral part of T lymphocyte biology, which play a critical role in determining T lymphocyte functional outcomes. The entire lifespan of T lymphocytes consists of encountering and trafficking through vastly different tissue sites, from the bone marrow and thymus during development, to peripheral circulation, and transmigration to tissue site. These mechanically diverse environmental cues regulate T cell resident function (Chapter 3.6.5 and Chapter 15.2). Mechanical interactions with the thymic stromal proteins affect T cell development and selection, thus, determining the peripheral antigen-specific T cell repertoire (Chapter 3.6.4). T lymphocytes encounter strong shear forces during circulation, which facilitate their trafficking through blood vessels. Shear stress and adhesion forces also regulate diapedesis across the endothelial wall to secondary lymphoid organs or peripheral tissue barriers where they can act against pathogens (Chapter 15). T lymphocyte activation upon interaction with cognate APCs is also characterised by generation of extrinsic and cell-intrinsic mechanical forces that are essential for optimal T cell activation. Abolishment of force generation through pharmacological or genetic interventions results in severe impairment of T lymphocyte activation and function (Chapter 3.6 and Chapter 5).

The identity of a committed T lymphocyte mechanosensor remained undefined until recently, when we showed that Piezo1 proteins, that belonged to a class of evolutionarily conserved mechanosensors, were highly expressed in the T lymphocyte subset [(470)]. We showed that optimal activation of T lymphocytes in response to TCR crosslinking requires functional Piezo1. Bead-immobilised TCR crosslinking antibodies were used to simulate mechanical

interactions between T cells and APCs and achieve optimal T lymphocyte activation. Piezo1 agonist, Yoda1 was used to accentuate TCR activation in response to soluble TCR crosslinking antibodies that do not exert mechanical stress and by itself, do not produce optimal T cell response. Downregulation of Piezo1 expression also abolished efficient T cell priming by APCs. Our model proposes that T cell interaction with APCs generates significant mechanical forces at the membrane interface, that is sensed by Piezo1 channels. Upon their activation, they allow influx of extracellular calcium that triggers activation of calpain-dependent actin polymerisation and stabilisation of the immunological synapse which is crucial for optimal activation [(470)]. We subsequently showed that Piezo1 also regulates T lymphocyte migration. Downregulation of Piezo1 impairs ICAM-1-dependent 2D migration and transmigration across membranes in response to chemokine gradients (Chapter 16 and 17). Weakened chemotactic ability of T lymphocytes could be attributed to abolishment of actin polymerisation and polarity in migrating T lymphocytes upon loss of Piezo1 (Chapter 18). We used two mouse models of contact hypersensitivity (CHS) (Chapter 20) and air pouch (Chapter 21), along with the technique of adoptive transfer to show that T lymphocyte migration to peripheral inflamed sites was significantly abolished on Piezo1 downregulation. Mounting an effective immune response is critically dependent on T lymphocytes' chemotactic ability that facilitates their guided migration to inflamed sites. Loss of Piezo1 thus, results in defective chemotactic capacity as well as weakened interactions with cognate APCs, which result in severely impaired immune response.

Mechanical aspects of immunotherapy

The highly dynamic mechanical nature of tissue sites and cellular interactions depend on diseased states and degree of inflammation. Tissue inflammation during infection,

autoimmunity or cancer is tightly associated with changes in ECM stiffness properties, as well as immune cell mechanical properties that provide altered cues for T lymphocyte activation and migration (Chapter 3.2 and 3.6). Immunotherapy involving adoptive transfer of activated T lymphocytes is a highly sought-after technique to treat infections, autoimmune conditions and cancer [(492)]. It involves isolating T lymphocytes from healthy individuals or patients, their ex-vivo stimulation and expansion followed by their therapeutic transfer to the affected individual. T lymphocytes are also designed to express receptors with higher affinity and specificity for target antigens, known as chimeric antigen receptors (CARs) [(493)]. A successful adoptive immunotherapy is dependent on the optimal ex-vivo stimulation and expansion of T lymphocytes, while maintaining their optimal activity post-transfer to affected individuals [(494)]. Former prevalent research focused on 3 aspects of TCR signalling: TCR-CD3 stimulation, TCR co-stimulation and the cytokine milieu for determination of T cell fate [(495)]. With the vast repository of mounting research confirming the imperative role of mechanical aspects of TCR signalling, the focus is being concentrated on regulating and manipulating the mechanical attributes of TCR signalling that will facilitate optimal T cell activation during immunotherapy. Substrate stiffness affects T lymphocyte expansion in-vitro. Techniques involving modulating substrate stiffness are being employed for optimal ex-vivo T lymphocyte expansion before adoptive transfer [(496)]. Polymeric microbeads coated with TCR stimulatory agents, liposomes and bio-scaffolds of appropriate stiffness and varying geometry that provide topographical and mechanical cues are being used to optimally activate T cells. Nanoparticles packed with T cell-specific antigens are also subjected to magnetic fields that facilitate TCR clustering in respond to antigen binding, thereby controlling magnitude of T cell response. Stimulatory cytokines like IL-2 are encapsulated in polymeric structures that facilitate stronger activation

of T lymphocytes, at much lower concentrations due to additional effects of mechanical cues [496].

The cancer microenvironment is characterised by stiffening of the ECM due to increased collagen deposition and crosslinking. This stiff environment seems to favour cancer cells survival and metastasis in an integrin-dependent fashion [497]. The cancer microenvironment can thus, present a range of mechanical cues which can be exploited in developing diagnostic and therapeutic tools in cancer. CAR T cells are being widely used in cancer immunotherapy. The mechanobiology of CAR T cells is becoming an area of intensive research directed towards improving their efficiency in the cancer microenvironment [496,497]. The success of CAR T cells have been limited by their inefficacy against solid tumors [498]. Specific activation of CAR T cells in solid tumors is challenging since the complex tumor microenvironment can easily result in their non-specific activation and subsequent killing of non-tumor, bystander cells that can be fatal. Prevailing techniques that allow activation of tumor-infiltrating CAR T cells, post-adoptive transfer involves use of chemical agents, radio waves, magnetic or optical stimulation [499]. The first three methods are limited by lack of spatial precision. Chemical agents diffuse non-specifically in the tumor microenvironment, while radio or magnetic waves require signal amplification and propagation through non-specific nanoparticles. While optical stimulation is characterised by spatial and temporal specificity, its efficacy is limited by its incapacity to penetrate the deeper regions of solid tumors [499]. In a novel and interesting approach by Pan et.al., mechanical stimulation by means of high frequency ultrasound (FUS) was used to achieve optimal CAR T cell stimulation with high spatial and temporal specificity in solid tumors [499]. HFU can reach deeper regions of the tumor, and at the same time could be focussed to activate a single cell. HFU was subsequently used to mechanically stimulate Piezo1-expressing T cells for immunotherapy. They engineered Jurkat

cells and primary $CD4^+$ T cells to express genetic transducing modues (GTMs) that consisted of T cell activation genes like NFAT placed under the control of Ca^{2+}-responsive promoter elements. CAR genes were placed under the control of NFAT-responsive promoter regions. This system allows remote, non-invasive and specific activation of CAR T cells in the tumor. CAR T lymphocytes infiltrating the tumor microenvironment are in the resting state where they do not express anti-CD19 CAR in the absence of HFU, thereby limiting off-target killing. Upon application of HFU and subsequent Piezo1 activation, Ca^{2+}-responsive NFAT is triggered and translocated to the nucleus where its triggers expression of anti-CD19 CAR, thereby stimulating killing activity of CAR T cells in the tumor environment. This system of remote-controlled mechanogenetics (ReCOM) exploited T cell-intrinsic Piezo1 mechanosensing property to achieve efficient immunotherapy against cancer [(499)]. Similar approach was used and validated in in-vivo tumor killing in mice. By applying short-pulsed FUS, CAR T lymphocytes were activated locally in tumor sites in mice bearing lymphomas and prostrate tumors [(500)].

An interesting study by Bandyopadhyay S et.al. (2016) showed that focussed ultrasound (FUS) can produce mechanical stress in the tumour cells in B16 melanoma mice [(501)]. Mechanical stimulation enhances the presentation of tumor antigens to T cells which supresses tumor-induced T cell tolerance and enhanced T cell-mediated tumor killing. Moreover, low frequency FUC in combination with radiation therapy reduces tumor metastases and frequency of cancer relapse [(501)]. Mechanical stimulation by means of FUS has shown beneficial effects against glioblastoma multiforme (GBM) [(502)]. Immunotherapy against GBM has been met with significant challenges because of poor penetrance of the blood-brain-barrier and limited tumor antigen repertoire. Application of low frequency FUS promoted

enhanced antigen presentation by dendritic cells, production of proinflammatory cytokines and potent killing capacity of cytotoxic T lymphocytes [502].

Nuclear mechanotransduction also regulate gene expression patterns that regulate cell function and fate. Mechanoresponsive transcriptional factors like YAP/TAZ signalling pathways have been implicated in a number of T cell-intrinsic signalling pathways that determine their fate and function [503]. Exploiting this aspect of T lymphocyte signalling can help engineer T lymphocytes that can adopt specific phenotype and function by altering mechanical cues depending on diseased conditions.

Since Piezo1-mediated mechanotransduction forms an integral aspect of T lymphocyte activation and homing to inflamed sites, manipulation of Piezo1-regulated activation threshold and migratory capacity in response to altered mechanical cues, can be active areas of future focus in improving adoptive immunotherapy.

Reference List

1. Parkin J, Cohen B. An overview of the immune system. Lancet. 2001 Jun 2; 357(9270):1777-89.
2. Zharkova MS, Orlov DS, Golubeva OY, Chakchir OB, Eliseev IE, Grinchuk TM, Shamova OV. Application of Antimicrobial Peptides of the Innate Immune System in Combination With Conventional Antibiotics-A Novel Way to Combat Antibiotic Resistance? Front Cell Infect Microbiol. 2019 Apr 30; 9:128.
3. Eyerich S, Eyerich K, Traidl-Hoffmann C, Biedermann T. Cutaneous Barriers and Skin Immunity: Differentiating A Connected Network. Trends Immunol. 2018 Apr; 39(4):315-327.
4. Kumar H, Kawai T, Akira S. Pathogen recognition by the innate immune system. Int Rev Immunol. 2011 Feb; 30(1):16-34.
5. O'Neill LA, Golenbock D, Bowie AG. The history of Toll-like receptors - redefining innate immunity. Nat Rev Immunol. 2013 Jun; 13(6):453-60.
6. Ganguly D, Haak S, Sisirak V, Reizis B. The role of dendritic cells in autoimmunity. Nat Rev Immunol. 2013 Aug; 13(8):566-77.
7. Motwani M, Pesiridis S, Fitzgerald KA. DNA sensing by the cGAS-STING pathway in health and disease. Nat Rev Genet. 2019 Nov; 20(11):657-674.
8. Broz P, Dixit VM. Inflammasomes: mechanism of assembly, regulation and signalling. Nat Rev Immunol. 2016 Jul; 16(7):407-20.
9. Netea MG, van der Meer JW. Immunodeficiency and genetic defects of pattern-recognition receptors. N Engl J Med. 2011 Jan 6; 364(1):60-70.

10. Dunkelberger JR, Song WC. Complement and its role in innate and adaptive immune responses. Cell Res. 2010 Jan; 20(1):34-50.

11. Medzhitov R, Janeway C Jr. Innate immune recognition: mechanisms and pathways. Immunol Rev. 2000 Feb; 173:89-97.

12. Vivier E, Tomasello E, Baratin M, Walzer T, Ugolini S. Functions of natural killer cells. Nat Immunol. 2008 May; 9(5):503-10.

13. Chaplin DD. Overview of the immune response. J Allergy Clin Immunol. 2010 Feb; 125(2 Suppl 2):S3-23.

14. Medzhitov R. Recognition of microorganisms and activation of the immune response. Nature. 2007 Oct 18; 449(7164):819-26.

15. Merad M, Sathe P, Helft J, Miller J, Mortha A. The dendritic cell lineage: ontogeny and function of dendritic cells and their subsets in the steady state and the inflamed setting. Annu Rev Immunol. 2013; 31:563-604.

16. den Haan JM, Arens R, van Zelm MC. The activation of the adaptive immune system: cross-talk between antigen-presenting cells, T cells and B cells. Immunol Lett. 2014 Dec; 162(2 Pt B):103-12.

17. Methot SP, Di Noia JM. Molecular Mechanisms of Somatic Hypermutation and Class Switch Recombination. Adv Immunol. 2017; 133:37-87.

18. Farber DL, Yudanin NA, Restifo NP. Human memory T cells: generation, compartmentalization and homeostasis. Nat Rev Immunol. 2014 Jan; 14(1):24-35.

19. Kurosaki T, Kometani K, Ise W. Memory B cells. Nat Rev Immunol. 2015 Mar; 15(3):149-59.

20. Sallusto F, Lanzavecchia A, Araki K, Ahmed R. From vaccines to memory and back. Immunity. 2010 Oct 29; 33(4):451-63.

21. Dennert G, Lennox E. Cell interactions in humoral and cell-mediated immunity. Nat New Biol. 1972 Jul 26; 238(82):114-6.

22. Marrack P, Kappler J. The T cell receptor. Science. 1987 Nov 20; 238(4830):1073-9.

23. von Boehmer H. The developmental biology of T lymphocytes. Annu Rev Immunol. 1988; 6:309-26.

24. Janeway CA Jr, Travers P, Walport M, et al. Immunobiology: The Immune System in Health and Disease. 5th edition. New York: Garland Science; 2001. The major histocompatibility complex and its functions. Available from: https://www.ncbi.nlm.nih.gov/books/NBK27156/

25. La Gruta NL, Gras S, Daley SR, Thomas PG, Rossjohn J. Understanding the drivers of MHC restriction of T cell receptors. Nat Rev Immunol. 2018 Jul; 18(7):467-478.

26. Zinkernagel RM, Doherty PC. The discovery of MHC restriction. Immunol Today. 1997 Jan; 18(1):14-7.

27. Kreslavsky T, Gleimer M, Garbe AI, von Boehmer H. αβ versus γδ fate choice: counting the T-cell lineages at the branch point. Immunol Rev. 2010 Nov; 238(1):169-81.

28. Wong WK, Leem J, Deane CM. Comparative Analysis of the CDR Loops of Antigen Receptors. Front Immunol. 2019 Oct 15; 10:2454.

29. Arden B, Clark SP, Kabelitz D, Mak TW. Human T-cell receptor variable gene segment families. Immunogenetics. 1995; 42(6):455-500.

30. Arstila TP, Casrouge A, Baron V, Even J, Kanellopoulos J, Kourilsky P. A direct estimate of the human alphabeta T cell receptor diversity. Science. 1999 Oct 29; 286(5441):958-61.

31. Krangel MS. Mechanics of T cell receptor gene rearrangement. Curr Opin Immunol. 2009 Apr; 21(2):133-9.

32. Kurd N, Robey EA. T-cell selection in the thymus: a spatial and temporal perspective. Immunol Rev. 2016 May; 271(1):114-26.

33. Turner SJ, Doherty PC, McCluskey J, Rossjohn J. Structural determinants of T-cell receptor bias in immunity. Nat Rev Immunol. 2006 Dec; 6(12):883-94.

34. Koch U, Radtke F. Mechanisms of T cell development and transformation. Annu Rev Cell Dev Biol. 2011; 27:539-62.

35. Kondo M. Lymphoid and myeloid lineage commitment in multipotent hematopoietic progenitors. Immunol Rev. 2010 Nov; 238(1):37-46.

36. Brandstadter JD, Maillard I. Notch signalling in T cell homeostasis and differentiation. Open Biol. 2019 Nov 29; 9(11):190187.

37. Deftos ML, Bevan MJ. Notch signaling in T cell development. Curr Opin Immunol. 2000 Apr; 12(2):166-72.

38. Kumar BV, Connors TJ, Farber DL. Human T Cell Development, Localization, and Function throughout Life. Immunity. 2018 Feb 20; 48(2):202-213.

39. Spits H. Development of alphabeta T cells in the human thymus. Nat Rev Immunol. 2002 Oct; 2(10):760-72.

40. Shah DK, Zúñiga-Pflücker JC. An overview of the intrathymic intricacies of T cell development. J Immunol. 2014 May 1; 192(9):4017-23.

41. Takaba H, Takayanagi H. The Mechanisms of T Cell Selection in the Thymus. Trends Immunol. 2017 Nov; 38(11):805-816.

42. Klein L, Kyewski B, Allen PM, Hogquist KA. Positive and negative selection of the T cell repertoire: what thymocytes see (and don't see). Nat Rev Immunol. 2014 Jun; 14(6):377-91. doi: 10.1038/nri3667.

43. Germain RN. T-cell development and the CD4-CD8 lineage decision. Nat Rev Immunol. 2002 May; 2(5):309-22.

44. Peterson P, Org T, Rebane A. Transcriptional regulation by AIRE: molecular mechanisms of central tolerance. Nat Rev Immunol. 2008 Dec; 8(12):948-57.

45. Anderson MS, Su MA. Aire and T cell development. Curr Opin Immunol. 2011 Apr; 23(2):198-206.

46. Akirav EM, Ruddle NH, Herold KC. The role of AIRE in human autoimmune disease. Nat Rev Endocrinol. 2011 Jan; 7(1):25-33.

47. Xing Y, Hogquist KA. T-cell tolerance: central and peripheral. Cold Spring Harb Perspect Biol. 2012 Jun 1; 4(6):a006957.

48. Thaxton JE, Li Z. To affinity and beyond: harnessing the T cell receptor for cancer immunotherapy. Hum Vaccin Immunother. 2014; 10(11):3313-21.

49. Pohar J, Simon Q, Fillatreau S. Antigen-Specificity in the Thymic Development and Peripheral Activity of $CD4^{+}FOXP3^{+}$ T Regulatory Cells. Front Immunol. 2018 Jul 23;9:1701. doi: 10.3389/fimmu.2018.01701. PMID: 30083162; PMCID: PMC6064734.

50. Boehncke WH, Brembilla NC. Autoreactive T-Lymphocytes in Inflammatory Skin Diseases. Front Immunol. 2019 May 29; 10:1198.

51. Guy CS, Vignali DA. Organization of proximal signal initiation at the TCR:CD3 complex. Immunol Rev. 2009 Nov; 232(1):7-21.

52. Gorentla BK, Zhong XP. T cell Receptor Signal Transduction in T lymphocytes. J Clin Cell Immunol. 2012 Oct 27; 2012(Suppl 12):5.

53. Courtney AH, Lo WL, Weiss A. TCR Signaling: Mechanisms of Initiation and Propagation. Trends Biochem Sci. 2018 Feb; 43(2):108-123.

54. Smith-Garvin JE, Koretzky GA, Jordan MS. T cell activation. Annu Rev Immunol. 2009; 27:591-619.

55. Chen L, Flies DB. Molecular mechanisms of T cell co-stimulation and co-inhibition. Nat Rev Immunol. 2013 Apr; 13(4):227-42. Erratum in: Nat Rev Immunol. 2013 Jul; 13(7):542.

56. Lucca LE, Dominguez-Villar M. Modulation of regulatory T cell function and stability by co-inhibitory receptors. Nat Rev Immunol. 2020 Nov; 20(11):680-693.

57. Waldman AD, Fritz JM, Lenardo MJ. A guide to cancer immunotherapy: from T cell basic science to clinical practice. Nat Rev Immunol. 2020 Nov; 20(11):651-668.

58. Hwang JR, Byeon Y, Kim D, Park SG. Recent insights of T cell receptor-mediated signaling pathways for T cell activation and development. Exp Mol Med. 2020 May; 52(5):750-761.

59. Taniuchi I. CD4 Helper and CD8 Cytotoxic T Cell Differentiation. Annu Rev Immunol. 2018 Apr 26; 36:579-601.

60. Zhang N, Bevan MJ. CD8(+) T cells: foot soldiers of the immune system. Immunity. 2011 Aug 26; 35(2):161-8.

61. Farhood B, Najafi M, Mortezaee K. $CD8^+$ cytotoxic T lymphocytes in cancer immunotherapy: A review. J Cell Physiol. 2019 Jun; 234(6):8509-8521.

62. Olsen Saraiva Camara N, Lepique AP, Basso AS. Lymphocyte differentiation and effector functions. Clin Dev Immunol. 2012; 2012:510603.

63. Roche PA, Furuta K. The ins and outs of MHC class II-mediated antigen processing and presentation. Nat Rev Immunol. 2015 Apr; 15(4):203-16.

64. Zhu J, Yamane H, Paul WE. Differentiation of effector CD4 T cell populations (*). Annu Rev Immunol. 2010; 28:445-89.

65. Geginat J, Paroni M, Maglie S, Alfen JS, Kastirr I, Gruarin P, De Simone M, Pagani M, Abrignani S. Plasticity of human CD4 T cell subsets. Front Immunol. 2014 Dec 16; 5:630.

66. Crotty S. T follicular helper cell differentiation, function, and roles in disease. Immunity. 2014 Oct 16; 41(4):529-42.

67. Leung S, Liu X, Fang L, Chen X, Guo T, Zhang J. The cytokine milieu in the interplay of pathogenic Th1/Th17 cells and regulatory T cells in autoimmune disease. Cell Mol Immunol. 2010 May; 7(3):182-9.

68. Gasper DJ, Tejera MM, Suresh M. CD4 T-cell memory generation and maintenance. Crit Rev Immunol. 2014; 34(2):121-46.

69. Berard M, Tough DF. Qualitative differences between naïve and memory T cells. Immunology. 2002 Jun; 106(2):127-38.

70. MacLeod MK, Kappler JW, Marrack P. Memory CD4 T cells: generation, reactivation and re-assignment. Immunology. 2010 May; 130(1):10-5.

71. Sallusto F, Geginat J, Lanzavecchia A. Central memory and effector memory T cell subsets: function, generation, and maintenance. Annu Rev Immunol. 2004; 22:745-63.

72. Gray JI, Westerhof LM, MacLeod MKL. The roles of resident, central and effector memory CD4 T-cells in protective immunity following infection or vaccination. Immunology. 2018 Mar 23; 154(4):574–81.

73. Griffiths PE. Genetic, epigenetic and exogenetic information in development and evolution. Interface Focus. 2017 Oct 6; 7(5):20160152.

74. Jansen KA, Donato DM, Balcioglu HE, Schmidt T, Danen EH, Koenderink GH. A guide to mechanobiology: Where biology and physics meet. Biochim Biophys Acta. 2015 Nov; 1853(11 Pt B):3043-52.

75. Pelham RJ Jr, Wang Yl. Cell locomotion and focal adhesions are regulated by substrate flexibility. Proc Natl Acad Sci U S A. 1997 Dec 9; 94(25):13661-5.

76. Shivashankar GV, Sheetz M, Matsudaira P. Mechanobiology. Integr Biol (Camb). 2015 Oct; 7(10):1091-2.

77. Paluch EK, Nelson CM, Biais N, Fabry B, Moeller J, Pruitt BL, Wollnik C, Kudryasheva G, Rehfeldt F, Federle W. Mechanotransduction: use the force(s). BMC Biol. 2015 Jul 4; 13:47.

78. Vogel, V. and Sheetz, M.P. (2010). Mechanical Forces Matter in Health and Disease: From Cancer to Tissue Engineering. In Nanotechnology, (Ed.). https://doi.org/10.1002/9783527628155.nanotech057

79. Chen J, Wang N. Tissue cell differentiation and multicellular evolution via cytoskeletal stiffening in mechanically stressed microenvironments. Acta Mech Sin. 2019; 35(2):270-274.

80. Chowdhury F, Na S, Li D, Poh YC, Tanaka TS, Wang F, Wang N. Material properties of the cell dictate stress-induced spreading and differentiation in embryonic stem cells. Nat Mater. 2010 Jan; 9(1):82-8.

81. Discher DE, Janmey P, Wang YL. Tissue cells feel and respond to the stiffness of their substrate. Science. 2005 Nov 18; 310(5751):1139-43.

82. Janmey PA, McCulloch CA. Cell mechanics: integrating cell responses to mechanical stimuli. Annu Rev Biomed Eng. 2007; 9:1-34.

83. Engler AJ, Griffin MA, Sen S, Bönnemann CG, Sweeney HL, Discher DE. Myotubes differentiate optimally on substrates with tissue-like stiffness: pathological implications for soft or stiff microenvironments. J Cell Biol. 2004 Sep 13; 166(6):877-87

84. Meshel AS, Wei Q, Adelstein RS, Sheetz MP. Basic mechanism of three-dimensional collagen fibre transport by fibroblasts. Nat Cell Biol. 2005 Feb; 7(2):157-64.

85. Iskratsch T, Wolfenson H, Sheetz MP. Appreciating force and shape—the rise of mechanotransduction in cell biology. Nat Rev Mol Cell Biol. 2014 Dec; 15(12):825-33.

86. Li H, Yang J, Chu TT, Naidu R, Lu L, Chandramohanadas R, Dao M, Karniadakis GE. Cytoskeleton Remodeling Induces Membrane Stiffness and Stability Changes of Maturing Reticulocytes. Biophys J. 2018 Apr 24; 114(8):2014-2023.

87. Vicente-Manzanares M, Webb DJ, Horwitz AR. Cell migration at a glance. J Cell Sci. 2005 Nov 1; 118(Pt 21):4917-9.

88. Gardel ML, Schneider IC, Aratyn-Schaus Y, Waterman CM. Mechanical integration of actin and adhesion dynamics in cell migration. Annu Rev Cell Dev Biol. 2010; 26:315-33.

89. Charras G, Sahai E. Physical influences of the extracellular environment on cell migration. Nat Rev Mol Cell Biol. 2014 Dec; 15(12):813-24.

90. van Helvert S, Storm C, Friedl P. Mechanoreciprocity in cell migration. Nat Cell Biol. 2018 Jan; 20(1):8-20.

91. Lange JR, Fabry B. Cell and tissue mechanics in cell migration. Exp Cell Res. 2013 Oct 1; 319(16):2418-23.

92. Northcott JM, Dean IS, Mouw JK, Weaver VM. Feeling Stress: The Mechanics of Cancer Progression and Aggression. Front Cell Dev Biol. 2018 Feb 28; 6:17.

93. Friedl P, Alexander S. Cancer invasion and the microenvironment: plasticity and reciprocity. Cell. 2011 Nov 23; 147(5):992-1009.

94. Butcher DT, Alliston T, Weaver VM. A tense situation: forcing tumour progression. Nat Rev Cancer. 2009 Feb; 9(2):108-22.

95. Broders-Bondon F, Nguyen Ho-Bouldoires TH, Fernandez-Sanchez ME, Farge E. Mechanotransduction in tumor progression: The dark side of the force. J Cell Biol. 2018 May 7; 217(5):1571-1587.

96. Wirtz D, Konstantopoulos K, Searson PC. The physics of cancer: the role of physical interactions and mechanical forces in metastasis. Nat Rev Cancer. 2011 Jun 24; 11(7):512-22.

97. Yu H, Mouw JK, Weaver VM. Forcing form and function: biomechanical regulation of tumor evolution. Trends Cell Biol. 2011 Jan; 21(1):47-56.

98. Laklai H, Miroshnikova YA, Pickup MW, Collisson EA, Kim GE, Barrett AS, Hill RC, Lakins JN, Schlaepfer DD, Mouw JK, LeBleu VS, Roy N, Novitskiy SV, Johansen JS, Poli V, Kalluri R, Iacobuzio-Donahue CA, Wood LD, Hebrok M, Hansen K, Moses HL, Weaver VM. Genotype tunes pancreatic ductal adenocarcinoma tissue tension to induce matricellular fibrosis and tumor progression. Nat Med. 2016 May; 22(5):497-505.

99. Santos FP, Verstovsek S. Therapy with JAK2 inhibitors for myeloproliferative neoplasms. Hematol Oncol Clin North Am. 2012 Oct; 26(5):1083-99.

100. Hurwitz HI, Uppal N, Wagner SA, Bendell JC, Beck JT, Wade SM 3rd, Nemunaitis JJ, Stella PJ, Pipas JM, Wainberg ZA, Manges R, Garrett WM, Hunter DS, Clark J, Leopold L, Sandor V, Levy RS. Randomized, Double-Blind, Phase II Study of Ruxolitinib or Placebo in Combination With Capecitabine in Patients With Metastatic Pancreatic Cancer for Whom Therapy With Gemcitabine Has Failed. J Clin Oncol. 2015 Dec 1; 33(34):4039-47.

101. Vennin C, Chin VT, Warren SC, Lucas MC, Herrmann D, Magenau A, Melenec P, Walters SN, Del Monte-Nieto G, Conway JR, Nobis M, Allam AH, McCloy RA, Currey N, Pinese M, Boulghourjian A, Zaratzian A, Adam AA, Heu C, Nagrial AM, Chou A, Steinmann A, Drury A, Froio D, Giry-Laterriere M, Harris NL, Phan T, Jain R, Weninger W, McGhee EJ, Whan R, Johns AL, Samra JS, Chantrill L, Gill AJ, Kohonen-Corish M, Harvey RP, Biankin AV; Australian Pancreatic Cancer Genome Initiative (APGI), Evans TR, Anderson KI, Grey ST, Ormandy CJ, Gallego-Ortega D, Wang Y, Samuel MS, Sansom OJ, Burgess A, Cox TR, Morton JP, Pajic M, Timpson P. Transient tissue priming via ROCK inhibition uncouples pancreatic cancer progression, sensitivity to chemotherapy, and metastasis. Sci Transl Med. 2017 Apr 5; 9(384): eaai8504.

102. Jiang H, Hegde S, Knolhoff BL, Zhu Y, Herndon JM, Meyer MA, Nywening TM, Hawkins WG, Shapiro IM, Weaver DT, Pachter JA, Wang-Gillam A, DeNardo DG. Targeting focal adhesion kinase renders pancreatic cancers responsive to checkpoint immunotherapy. Nat Med. 2016 Aug; 22(8):851-60.

103. Sun M, Chi G, Li P, Lv S, Xu J, Xu Z, Xia Y, Tan Y, Xu J, Li L, Li Y. Effects of Matrix Stiffness on the Morphology, Adhesion, Proliferation and Osteogenic Differentiation of Mesenchymal Stem Cells. Int J Med Sci. 2018 Jan 15; 15(3):257-268.

104. Miroshnikova YA, Le HQ, Schneider D, Thalheim T, Rübsam M, Bremicker N, Polleux J, Kamprad N, Tarantola M, Wang I, Balland M, Niessen CM, Galle J, Wickström SA. Adhesion forces and cortical tension couple cell proliferation and differentiation to drive epidermal stratification. Nat Cell Biol. 2018 Jan; 20(1):69-80.

105. Eisenhoffer GT, Rosenblatt J. Bringing balance by force: live cell extrusion controls epithelial cell numbers. Trends Cell Biol. 2013 Apr; 23(4):185-92.

106. Saw TB, Doostmohammadi A, Nier V, Kocgozlu L, Thampi S, Toyama Y, Marcq P, Lim CT, Yeomans JM, Ladoux B. Topological defects in epithelia govern cell death and extrusion. Nature. 2017 Apr 12; 544(7649):212-216.

107. Dupont S, Morsut L, Aragona M, Enzo E, Giulitti S, Cordenonsi M, Zanconato F, Le Digabel J, Forcato M, Bicciato S, Elvassore N, Piccolo S. Role of YAP/TAZ in mechanotransduction. Nature. 2011 Jun 8; 474(7350):179-83.

108. Nestor-Bergmann A, Goddard G, Woolner S. Force and the spindle: mechanical cues in mitotic spindle orientation. Semin Cell Dev Biol. 2014 Oct; 34:133-9.

109. Fink J, Carpi N, Betz T, Bétard A, Chebah M, Azioune A, Bornens M, Sykes C, Fetler L, Cuvelier D, Piel M. External forces control mitotic spindle positioning. Nat Cell Biol. 2011 Jun 12; 13(7):771-8.

110. Campinho P, Behrndt M, Ranft J, Risler T, Minc N, Heisenberg CP. Tension-oriented cell divisions limit anisotropic tissue tension in epithelial spreading during zebrafish epiboly. Nat Cell Biol. 2013 Dec; 15(12):1405-14.

111. Théry M, Jiménez-Dalmaroni A, Racine V, Bornens M, Jülicher F. Experimental and theoretical study of mitotic spindle orientation. Nature. 2007 May 24; 447(7143):493-6.

112. Mao Y, Tournier AL, Hoppe A, Kester L, Thompson BJ, Tapon N. Differential proliferation rates generate patterns of mechanical tension that orient tissue growth. EMBO J. 2013 Oct 30; 32(21):2790-803.

113. Legoff L, Rouault H, Lecuit T. A global pattern of mechanical stress polarizes cell divisions and cell shape in the growing Drosophila wing disc. Development. 2013 Oct; 140(19):4051-9.

114. Mao Y, Tournier AL, Bates PA, Gale JE, Tapon N, Thompson BJ. Planar polarization of the atypical myosin Dachs orients cell divisions in Drosophila. Genes Dev. 2011 Jan 15; 25(2):131-6.

115. Itabashi T, Terada Y, Kuwana K, Kan T, Shimoyama I, Ishiwata S. Mechanical impulses can control metaphase progression in a mammalian cell. Proc Natl Acad Sci U S A. 2012 May 8; 109(19):7320-5.

116. Pinheiro D, Hannezo E, Herszterg S, Bosveld F, Gaugue I, Balakireva M, Wang Z, Cristo I, Rigaud SU, Markova O, Bellaïche Y. Transmission of cytokinesis forces via E-cadherin dilution and actomyosin flows. Nature. 2017 May 4; 545(7652):103-107.

117. Matamoro-Vidal A, Levayer R. Multiple Influences of Mechanical Forces on Cell Competition. Curr Biol. 2019 Aug 5; 29(15):R762-R774.

118. Aragona M, Panciera T, Manfrin A, Giulitti S, Michielin F, Elvassore N, Dupont S, Piccolo S. A mechanical checkpoint controls multicellular growth through YAP/TAZ regulation by actin-processing factors. Cell. 2013 Aug 29; 154(5):1047-1059.

119. Butcher DT, Alliston T, Weaver VM. A tense situation: forcing tumour progression. Nat Rev Cancer. 2009 Feb; 9(2):108-22.

120. Mammoto A, Mammoto T, Ingber DE. Mechanosensitive mechanisms in transcriptional regulation. J Cell Sci. 2012 Jul 1; 125(Pt 13):3061-73.

121. Uhler C, Shivashankar GV. Regulation of genome organization and gene expression by nuclear mechanotransduction. Nat Rev Mol Cell Biol. 2017 Dec; 18(12):717-727.

122. Kirby TJ, Lammerding J. Emerging views of the nucleus as a cellular mechanosensor. Nat Cell Biol. 2018 Apr; 20(4):373-381.

123. Tajik A, Zhang Y, Wei F, Sun J, Jia Q, Zhou W, Singh R, Khanna N, Belmont AS, Wang N. Transcription upregulation via force-induced direct stretching of chromatin. Nat Mater. 2016 Dec; 15(12):1287-1296.

124. Alam SG, Zhang Q, Prasad N, Li Y, Chamala S, Kuchibhotla R, Kc B, Aggarwal V, Shrestha S, Jones AL, Levy SE, Roux KJ, Nickerson JA, Lele TP. The mammalian LINC complex regulates genome transcriptional responses to substrate rigidity. Sci Rep. 2016 Dec 1; 6:38063.

125. Arsenovic PT, Ramachandran I, Bathula K, Zhu R, Narang JD, Noll NA, Lemmon CA, Gundersen GG, Conway DE. Nesprin-2G, a Component of the Nuclear LINC Complex, Is Subject to Myosin-Dependent Tension. Biophys J. 2016 Jan 5; 110(1):34-43.

126. Miroshnikova YA, Nava MM, Wickström SA. Emerging roles of mechanical forces in chromatin regulation. J Cell Sci. 2017 Jul 15; 130(14):2243-2250.

127. Jain N, Iyer KV, Kumar A, Shivashankar GV. Cell geometric constraints induce modular gene-expression patterns via redistribution of HDAC3 regulated by actomyosin contractility. Proc Natl Acad Sci U S A. 2013 Jul 9; 110(28):11349-54.

128. Heo SJ, Driscoll TP, Thorpe SD, Nerurkar NL, Baker BM, Yang MT, Chen CS, Lee DA, Mauck RL. Differentiation alters stem cell nuclear architecture, mechanics, and mechano-sensitivity. Elife. 2016 Nov 30; 5:e18207.

129. Martins RP, Finan JD, Guilak F, Lee DA. Mechanical regulation of nuclear structure and function. Annu Rev Biomed Eng. 2012; 14:431-55.

130. Heo SJ, Han WM, Szczesny SE, Cosgrove BD, Elliott DM, Lee DA, Duncan RL, Mauck RL. Mechanically Induced Chromatin Condensation Requires Cellular Contractility in Mesenchymal Stem Cells. Biophys J. 2016 Aug 23; 111(4):864-874.

131. Miroshnikova YA, Cohen I, Ezhkova E, Wickström SA. Epigenetic gene regulation, chromatin structure, and force-induced chromatin remodelling in epidermal development and homeostasis. Curr Opin Genet Dev. 2019 Apr; 55:46-51.

132. Le HQ, Ghatak S, Yeung CY, Tellkamp F, Günschmann C, Dieterich C, Yeroslaviz A, Habermann B, Pombo A, Niessen CM, Wickström SA. Mechanical regulation of transcription controls Polycomb-mediated gene silencing during lineage commitment. Nat Cell Biol. 2016 Aug; 18(8):864-75.

133. Jin F, Li Y, Dixon JR, Selvaraj S, Ye Z, Lee AY, Yen CA, Schmitt AD, Espinoza CA, Ren B. A high-resolution map of the three-dimensional chromatin interactome in human cells. Nature. 2013 Nov 14; 503(7475):290-4.

134. Spichal M, Fabre E. The Emerging Role of the Cytoskeleton in Chromosome Dynamics. Front Genet. 2017 May 19; 8:60.

135. Przybyla L, Muncie JM, Weaver VM. Mechanical Control of Epithelial-to-Mesenchymal Transitions in Development and Cancer. Annu Rev Cell Dev Biol. 2016 Oct 6; 32:527-554.

136. Mohammadi H, Sahai E. Mechanisms and impact of altered tumour mechanics. Nat Cell Biol. 2018 Jul; 20(7):766-774.

137. Paul A. Janmey, R. Tyler Miller. Mechanisms of mechanical signaling in development and disease. Journal of Cell Science 2011 124: 9-18.

138. Kumar A, Placone JK, Engler AJ. Understanding the extracellular forces that determine cell fate and maintenance. Development. 2017 Dec 1; 144(23):4261-4270.

139. Engler AJ, Sen S, Sweeney HL, Discher DE. Matrix elasticity directs stem cell lineage specification. Cell. 2006 Aug 25; 126(4):677-89.

140. Lee DA, Knight MM, Campbell JJ, Bader DL. Stem cell mechanobiology. J Cell Biochem. 2011 Jan; 112(1):1-9.

141. Leipzig ND, Shoichet MS. The effect of substrate stiffness on adult neural stem cell behavior. Biomaterials. 2009 Dec; 30(36):6867-78.

142. Saha K, Keung AJ, Irwin EF, Li Y, Little L, Schaffer DV, Healy KE. Substrate modulus directs neural stem cell behavior. Biophys J. 2008 Nov 1; 95(9):4426-38.

143. Arulmoli J, Pathak MM, McDonnell LP, Nourse JL, Tombola F, Earthman JC, Flanagan LA. Static stretch affects neural stem cell differentiation in an extracellular matrix-dependent manner. Sci Rep. 2015 Feb 17; 5:8499.

144. Nishimura T, Honda H, Takeichi M. Planar cell polarity links axes of spatial dynamics in neural-tube closure. Cell. 2012 May 25; 149(5):1084-97.

145. Lourenço T, Paes de Faria J, Bippes CA, Maia J, Lopes-da-Silva JA, Relvas JB, Grãos M. Modulation of oligodendrocyte differentiation and maturation by combined biochemical and mechanical cues. Sci Rep. 2016 Feb 16; 6:21563.

146. Bonnans C, Chou J, Werb Z. Remodelling the extracellular matrix in development and disease. Nat Rev Mol Cell Biol. 2014 Dec; 15(12):786-801.

147. Furman D, Campisi J, Verdin E, Carrera-Bastos P, Targ S, Franceschi C, Ferrucci L, Gilroy DW, Fasano A, Miller GW, Miller AH, Mantovani A, Weyand CM, Barzilai N, Goronzy JJ, Rando TA, Effros RB, Lucia A, Kleinstreuer N, Slavich GM. Chronic

inflammation in the etiology of disease across the life span. Nat Med. 2019 Dec; 25(12):1822-1832.

148. Humphrey JD, Dufresne ER, Schwartz MA. Mechanotransduction and extracellular matrix homeostasis. Nat Rev Mol Cell Biol. 2014 Dec; 15(12):802-12.

149. Wynn TA, Ramalingam TR. Mechanisms of fibrosis: therapeutic translation for fibrotic disease. Nat Med. 2012 Jul 6; 18(7):1028-40.

150. Gieseck RL 3rd, Wilson MS, Wynn TA. Type 2 immunity in tissue repair and fibrosis. Nat Rev Immunol. 2018 Jan; 18(1):62-76.

151. Li S, Gallup M, Chen YT, McNamara NA. Molecular mechanism of proinflammatory cytokine-mediated squamous metaplasia in human corneal epithelial cells. Invest Ophthalmol Vis Sci. 2010 May; 51(5):2466-75.

152. Nowell CS, Odermatt PD, Azzolin L, Hohnel S, Wagner EF, Fantner GE, Lutolf MP, Barrandon Y, Piccolo S, Radtke F. Chronic inflammation imposes aberrant cell fate in regenerating epithelia through mechanotransduction. Nat Cell Biol. 2016 Feb; 18(2):168-80.

153. Vining KH, Mooney DJ. Mechanical forces direct stem cell behaviour in development and regeneration. Nat Rev Mol Cell Biol. 2017 Dec; 18(12):728-742.

154. Mihajlović AI, Bruce AW. The first cell-fate decision of mouse preimplantation embryo development: integrating cell position and polarity. Open Biol. 2017 Nov; 7(11):170210.

155. Maître JL, Turlier H, Illukkumbura R, Eismann B, Niwayama R, Nédélec F, Hiiragi T. Asymmetric division of contractile domains couples cell positioning and fate specification. Nature. 2016 Aug 18; 536(7616):344-348.

156. Krieg M, Arboleda-Estudillo Y, Puech PH, Käfer J, Graner F, Müller DJ, Heisenberg CP. Tensile forces govern germ-layer organization in zebrafish. Nat Cell Biol. 2008 Apr; 10(4):429-36.

157. Nonaka S, Shiratori H, Saijoh Y, Hamada H. Determination of left-right patterning of the mouse embryo by artificial nodal flow. Nature. 2002 Jul 4; 418(6893):96-9.

158. Galbraith CG, Yamada KM, Sheetz MP. The relationship between force and focal complex development. J Cell Biol. 2002 Nov 25; 159(4):695-705.

159. Adamo L, Naveiras O, Wenzel PL, McKinney-Freeman S, Mack PJ, Gracia-Sancho J, Suchy-Dicey A, Yoshimoto M, Lensch MW, Yoder MC, García-Cardeña G, Daley GQ. Biomechanical forces promote embryonic haematopoiesis. Nature. 2009 Jun 25; 459(7250):1131-5.

160. North TE, Goessling W, Peeters M, Li P, Ceol C, Lord AM, Weber GJ, Harris J, Cutting CC, Huang P, Dzierzak E, Zon LI. Hematopoietic stem cell development is dependent on blood flow. Cell. 2009 May 15; 137(4):736-48.

161. Hove JR, Köster RW, Forouhar AS, Acevedo-Bolton G, Fraser SE, Gharib M. Intracardiac fluid forces are an essential epigenetic factor for embryonic cardiogenesis. Nature. 2003 Jan 9; 421(6919):172-7.

162. Rubin J, Rubin C, Jacobs CR. Molecular pathways mediating mechanical signaling in bone. Gene. 2006 Feb 15; 367:1-16.

163. Stoltz JF, Magdalou J, George D, Chen Y, Li Y, Isla ND, He X, Remond Y. Influence of mechanical forces on bone: Introduction to mechanobiology and mechanical adaptation concept, Journal of Cellular Immunotherapy, Volume 4, Issue 1, 2018, Pages 10-12, ISSN 2352-1775. https://doi.org/10.1016/j.jocit.2018.09.003.

164. Wittkowske C, Reilly GC, Lacroix D, Perrault CM. *In Vitro* Bone Cell Models: Impact of Fluid Shear Stress on Bone Formation. Front Bioeng Biotechnol. 2016 Nov 15; 4:87.

165. Mammoto A, Connor KM, Mammoto T, Yung CW, Huh D, Aderman CM, Mostoslavsky G, Smith LE, Ingber DE. A mechanosensitive transcriptional mechanism that controls angiogenesis. Nature. 2009 Feb 26; 457(7233):1103-8.

166. Elliott H, Fischer RS, Myers KA, Desai RA, Gao L, Chen CS, Adelstein RS, Waterman CM, Danuser G. Myosin II controls cellular branching morphogenesis and migration in three dimensions by minimizing cell-surface curvature. Nat Cell Biol. 2015 Feb; 17(2):137-47.

167. Ermis M, Antmen E, Hasirci V. Micro and Nanofabrication methods to control cell-substrate interactions and cell behavior: A review from the tissue engineering perspective. Bioact Mater. 2018 May 18; 3(3):355-369. Erratum in: Bioact Mater. 2020 Dec 04; 6(6):1789-1790.

168. Yanagawa F, Sugiura S, Kanamori T. Hydrogel microfabrication technology toward three dimensional tissue engineering. Regen Ther. 2016 Mar 17; 3:45-57.

169. Jain RK, Martin JD, Stylianopoulos T. The role of mechanical forces in tumor growth and therapy. Annu Rev Biomed Eng. 2014 Jul 11; 16:321-46.

170. Nelson CM. From static to animated: Measuring mechanical forces in tissues. J Cell Biol. 2017 Jan 2; 216(1):29-30.

171. Roca-Cusachs P, Conte V, Trepat X. Quantifying forces in cell biology. Nat Cell Biol. 2017 Jul; 19(7):742-751.

172. Wang JH, Lin JS. Cell traction force and measurement methods. Biomech Model Mechanobiol. 2007 Nov; 6(6):361-71.

173. Hur SS, Jeong JH, Ban MJ, Park JH, Yoon JK, Hwang Y. Traction force microscopy for understanding cellular mechanotransduction. BMB Rep. 2020 Feb; 53(2):74-81.

174. Uroz M, Garcia-Puig A, Tekeli I, Elosegui-Artola A, Abenza JF, Marín-Llauradó A, Pujals S, Conte V, Albertazzi L, Roca-Cusachs P, Raya Á, Trepat X. Traction forces at the cytokinetic ring regulate cell division and polyploidy in the migrating zebrafish epicardium. Nat Mater. 2019 Sep; 18(9):1015-1023.

175. Itou J, Oishi I, Kawakami H, Glass TJ, Richter J, Johnson A, Lund TC, Kawakami Y. Migration of cardiomyocytes is essential for heart regeneration in zebrafish. Development. 2012 Nov; 139(22):4133-42.

176. Muiznieks LD, Keeley FW. Molecular assembly and mechanical properties of the extracellular matrix: A fibrous protein perspective. Biochim Biophys Acta. 2013 Jul; 1832(7):866-75.

177. Park D, Wershof E, Boeing S, Labernadie A, Jenkins RP, George S, Trepat X, Bates PA, Sahai E. Extracellular matrix anisotropy is determined by TFAP2C-dependent regulation of cell collisions. Nat Mater. 2020 Feb; 19(2):227-238.

178. Polacheck WJ, Chen CS. Measuring cell-generated forces: a guide to the available tools. Nat Methods. 2016 Apr 28; 13(5):415-23.

179. Steinwachs J, Metzner C, Skodzek K, Lang N, Thievessen I, Mark C, Münster S, Aifantis KE, Fabry B. Three-dimensional force microscopy of cells in biopolymer networks. Nat Methods. 2016 Feb; 13(2):171-6.

180. Maskarinec SA, Franck C, Tirrell DA, Ravichandran G. Quantifying cellular traction forces in three dimensions. Proc Natl Acad Sci U S A. 2009 Dec 29; 106(52):22108-13.

181. Sugimura K, Lenne PF, Graner F. Measuring forces and stresses in situ in living tissues. Development. 2016 Jan 15; 143(2):186-96.

182. Gavara N. A beginner's guide to atomic force microscopy probing for cell mechanics. Microsc Res Tech. 2017 Jan; 80(1):75-84.

183. Krieg, M., Fläschner, G., Alsteens, D. et al. Atomic force microscopy-based mechanobiology. Nat Rev Phys. 2019; 1:45-57. https://doi.org/10.1038/s42254-018-0001-7.

184. Luo Q, Kuang D, Zhang B, Song G. Cell stiffness determined by atomic force microscopy and its correlation with cell motility. Biochim Biophys Acta. 2016 Sep; 1860(9):1953-60.

185. Puchner EM, Gaub HE. Force and function: probing proteins with AFM-based force spectroscopy. Curr Opin Struct Biol. 2009 Oct; 19(5):605-14.

186. Cost AL, Ringer P, Chrostek-Grashoff A, Grashoff C. How to Measure Molecular Forces in Cells: A Guide to Evaluating Genetically-Encoded FRET-Based Tension Sensors. Cell Mol Bioeng. 2015; 8(1):96-105.

187. Yang C, Zhang X, Guo Y, Meng F, Sachs F, Guo J. Mechanical dynamics in live cells and fluorescence-based force/tension sensors. Biochim Biophys Acta. 2015 Aug; 1853(8):1889-904.

188. Murad Y, Li ITS. Quantifying Molecular Forces with Serially Connected Force Sensors. Biophys J. 2019 Apr 2; 116(7):1282-1291.

189. Wang X, Ha T. Defining single molecular forces required to activate integrin and notch signaling. Science. 2013 May 24; 340(6135):991-4.

190. Wang X, Sun J, Xu Q, Chowdhury F, Roein-Peikar M, Wang Y, Ha T. Integrin Molecular Tension within Motile Focal Adhesions. Biophys J. 2015 Dec 1; 109(11):2259-67.

191. Zhang Y, Ge C, Zhu C, Salaita K. DNA-based digital tension probes reveal integrin forces during early cell adhesion. Nat Commun. 2014 Oct 24; 5:5167.

192. Stabley DR, Jurchenko C, Marshall SS, Salaita KS. Visualizing mechanical tension across membrane receptors with a fluorescent sensor. Nat Methods. 2011 Oct 30; 9(1):64-7.

193. González-Bermúdez B, Guinea GV, Plaza GR. Advances in Micropipette Aspiration: Applications in Cell Biomechanics, Models, and Extended Studies. Biophys J. 2019 Feb 19; 116(4):587-594.

194. Hochmuth RM. Micropipette aspiration of living cells. J Biomech. 2000 Jan; 33(1):15-22.

195. Shchelokovskyy P, Tristram-Nagle S, Dimova R. Effect of the HIV-1 fusion peptide on the mechanical properties and leaflet coupling of lipid bilayers. New J Phys. 2011 Feb; 13:25004.

196. Kim JH, Ren Y, Ng WP, Li S, Son S, Kee YS, Zhang S, Zhang G, Fletcher DA, Robinson DN, Chen EH. Mechanical tension drives cell membrane fusion. Dev Cell. 2015 Mar 9; 32(5):561-73.

197. Lee LM, Liu AP. The Application of Micropipette Aspiration in Molecular Mechanics of Single Cells. J Nanotechnol Eng Med. 2014 Nov; 5(4):0408011-408016.

198. Guo MT, Rotem A, Heyman JA, Weitz DA. Droplet microfluidics for high-throughput biological assays. Lab Chip. 2012 Jun 21; 12(12):2146-55.

199. Davidson PM, Fedorchak GR, Mondésert-Deveraux S, Bell ES, Isermann P, Aubry D, Allena R, Lammerding J. High-throughput microfluidic micropipette aspiration device to probe time-scale dependent nuclear mechanics in intact cells. Lab Chip. 2019 Nov 7; 19(21):3652-3663.

200. Guillou L, Dahl JB, Lin JG, Barakat AI, Husson J, Muller SJ, Kumar S. Measuring Cell Viscoelastic Properties Using a Microfluidic Extensional Flow Device. Biophys J. 2016 Nov 1; 111(9):2039-2050.

201. Ashkin A. Optical trapping and manipulation of neutral particles using lasers. Proc Natl Acad Sci U S A. 1997 May 13; 94(10):4853-60.

202. Zhang H, Liu KK. Optical tweezers for single cells. J R Soc Interface. 2008 Jul 6; 5(24):671-90.

203. Arbore C, Perego L, Sergides M, Capitanio M. Probing force in living cells with optical tweezers: from single-molecule mechanics to cell mechanotransduction. Biophys Rev. 2019 Oct; 11(5):765-782.

204. Biswas A, Alex A, Sinha B. Mapping Cell Membrane Fluctuations Reveals Their Active Regulation and Transient Heterogeneities. Biophys J. 2017 Oct 17; 113(8):1768-1781.

205. Turlier H and Betz T. Unveiling the Active Nature of Living-Membrane Fluctuations and Mechanics. Annual Review of Condensed Matter Physics. 2019; 10:213-232.

206. Döbereiner HG, Gompper G, Haluska CK, Kroll DM, Petrov PG, and Riske KA. Advanced Flicker Spectroscopy of Fluid Membranes. Phys. Rev. Lett. 2003 July 23; 91, 048301.

207. Fricke K, Wirthensohn K, Laxhuber R, Sackmann E. Flicker spectroscopy of erythrocytes. A sensitive method to study subtle changes of membrane bending stiffness. Eur Biophys J. 1986; 14(2):67-81.

208. Monzel C & Schmidt D & Seifert U & Smith AS & Sengupta K & Merkel R. (2016). Dynamic Optical Displacement Spectroscopy to Quantify Biomembrane Bending Fluctuations. Biophys J. 110. 487a. 10.1016/j.bpj.2015.11.2603.

209. Ribezzi-Crivellari M, Ritort F. Force spectroscopy with dual-trap optical tweezers: molecular stiffness measurements and coupled fluctuations analysis. Biophys J. 2012 Nov 7; 103(9):1919-28.

210. Barr VA, Bunnell SC. Interference reflection microscopy. Curr Protoc Cell Biol. 2009 Dec; Chapter 4:Unit 4.23.

211. Kihm K.D. Reflection Interference Contrast Microscopy (RICM). In: Near-Field Characterization of Micro/Nano-Scaled Fluid Flows. Experimental Fluid Mechanics, 2011. Vol 0. Springer, Berlin, Heidelberg. https://doi.org/10.1007/978-3-642-20426-5_6

212. Contreras-Naranjo JC, Ugaz VM. A nanometre-scale resolution interference-based probe of interfacial phenomena between microscopic objects and surfaces. Nat Commun. 2013; 4:1919.

213. Ajo-Franklin CM, Ganesan PV, Boxer SG. Variable incidence angle fluorescence interference contrast microscopy for z-imaging single objects. Biophys J. 2005 Oct; 89(4):2759-69.

214. Yang Y, Wang K, Gu X, Leong KW. Biophysical Regulation of Cell Behavior-Cross Talk between Substrate Stiffness and Nanotopography. Engineering (Beijing). 2017 Feb; 3(1):36-54.

215. Gabriel Popescu, Takahiro Ikeda, Ramachandra R. Dasari, and Michael S. Feld. Diffraction phase microscopy for quantifying cell structure and dynamics. Optics Letters. 2006; 31(6): 775-777.

216. Loubet B, Seifert U, Lomholt MA. Effective tension and fluctuations in active membranes. Phys Rev E Stat Nonlin Soft Matter Phys. 2012 Mar; 85(3 Pt 1):031913.

217. Farago O. Mechanical surface tension governs membrane thermal fluctuations. Phys Rev E Stat Nonlin Soft Matter Phys. 2011 Nov; 84(5 Pt 1):051914.

218. Tuvia S, Levin S, Bitler A, Korenstein R. Mechanical fluctuations of the membrane-skeleton are dependent on F-actin ATPase in human erythrocytes. J Cell Biol. 1998 Jun 29; 141(7):1551-61.

219. Huse M. Mechanical forces in the immune system. Nat Rev Immunol. 2017 Nov; 17(11):679-690.

220. Pageon SV, Govendir MA, Kempe D, Biro M. Mechanoimmunology: molecular-scale forces govern immune cell functions. Mol Biol Cell. 2018 Aug 8; 29(16):1919-1926.

221. Mierke CT. The fundamental role of mechanical properties in the progression of cancer disease and inflammation. Rep Prog Phys. 2014 Jul; 77(7):076602.

222. Moazzam F, DeLano FA, Zweifach BW, Schmid-Schönbein GW. The leukocyte response to fluid stress. Proc Natl Acad Sci U S A. 1997 May 13; 94(10):5338-43.

223. Sundd P, Pospieszalska MK, Cheung LS, Konstantopoulos K, Ley K. Biomechanics of leukocyte rolling. Biorheology. 2011; 48(1):1-35.

224. Fritz J, Katopodis AG, Kolbinger F, Anselmetti D. Force-mediated kinetics of single P-selectin/ligand complexes observed by atomic force microscopy. Proc Natl Acad Sci U S A. 1998 Oct 13; 95(21):12283-8.

225. Ochoa CD, Stevens T. Studies on the cell biology of interendothelial cell gaps. Am J Physiol Lung Cell Mol Physiol. 2012 Feb 1; 302(3):L275-86.

226. Stroka KM, Aranda-Espinoza H. Endothelial cell substrate stiffness influences neutrophil transmigration via myosin light chain kinase-dependent cell contraction. Blood. 2011 Aug 11; 118(6):1632-40.

227. Yang L, Froio RM, Sciuto TE, Dvorak AM, Alon R, Luscinskas FW. ICAM-1 regulates neutrophil adhesion and transcellular migration of TNF-alpha-activated vascular endothelium under flow. Blood. 2005 Jul 15; 106(2):584-92.

228. Cinamon G, Shinder V, Alon R. Shear forces promote lymphocyte migration across vascular endothelium bearing apical chemokines. Nat Immunol. 2001 Jun; 2(6):515-22.

229. Yeh YT, Serrano R, François J, Chiu JJ, Li YJ, Del Álamo JC, Chien S, Lasheras JC. Three-dimensional forces exerted by leukocytes and vascular endothelial cells dynamically facilitate diapedesis. Proc Natl Acad Sci U S A. 2018 Jan 2; 115(1):133-138.

230. Vicente-Manzanares M, Choi CK, Horwitz AR. Integrins in cell migration--the actin connection. J Cell Sci. 2009 Jan 15;122(Pt 2):199-206. Erratum in: J Cell Sci. 2009 May 1;122(Pt 9):1473.

231. Moreau HD, Piel M, Voituriez R, Lennon-Duménil AM. Integrating Physical and Molecular Insights on Immune Cell Migration. Trends Immunol. 2018 Aug; 39(8):632-643.

232. Ladoux B, Mège RM, Trepat X. Front-Rear Polarization by Mechanical Cues: From Single Cells to Tissues. Trends Cell Biol. 2016 Jun; 26(6):420-433.

233. Basu R, Huse M. Mechanical Communication at the Immunological Synapse. Trends Cell Biol. 2017 Apr; 27(4):241-254.

234. Spillane KM, Tolar P. Mechanics of antigen extraction in the B cell synapse. Mol Immunol. 2018 Sep; 101:319-328.

235. Spillane KM, Tolar P. B cell antigen extraction is regulated by physical properties of antigen-presenting cells. J Cell Biol. 2017 Jan 2; 216(1):217-230.

236. Pierobon P, Lennon-Duménil AM. To use or not to use the force: How B lymphocytes extract surface-tethered antigens. J Cell Biol. 2017 Jan 2; 216(1):17-19.

237. Tolar P, Spillane KM. Force generation in B-cell synapses: mechanisms coupling B-cell receptor binding to antigen internalization and affinity discrimination. Adv Immunol. 2014; 123:69-100.

238. Natkanski E, Lee WY, Mistry B, Casal A, Molloy JE, Tolar P. B cells use mechanical energy to discriminate antigen affinities. Science. 2013 Jun 28; 340(6140):1587-90.

239. Hosseini BH, Louban I, Djandji D, Wabnitz GH, Deeg J, Bulbuc N, Samstag Y, Gunzer M, Spatz JP, Hämmerling GJ. Immune synapse formation determines interaction forces between T cells and antigen-presenting cells measured by atomic force microscopy. Proc Natl Acad Sci U S A. 2009 Oct 20; 106(42):17852-7. Erratum in: Proc Natl Acad Sci U S A. 2010 Feb 2; 107(5):2373.

240. Lim TS, Mortellaro A, Lim CT, Hämmerling GJ, Ricciardi-Castagnoli P. Mechanical interactions between dendritic cells and T cells correlate with T cell responsiveness. J Immunol. 2011 Jul 1; 187(1):258-65.

241. Lewis JS, Dolgova NV, Chancellor TJ, Acharya AP, Karpiak JV, Lele TP, Keselowsky BG. The effect of cyclic mechanical strain on activation of dendritic cells cultured on adhesive substrates. Biomaterials. 2013 Dec; 34(36):9063-70.

242. Chakraborty M, Chu K, Shrestha A, Revelo XS, Zhang X, Gold MJ, Khan S, Lee M, Huang C, Akbari M, Barrow F, Chan YT, Lei H, Kotoulas NK, Jovel J, Pastrello C, Kotlyar M, Goh C, Michelakis E, Clemente-Casares X, Ohashi PS, Engleman EG, Winer S, Jurisica I, Tsai S, Winer DA. Mechanical Stiffness Controls Dendritic Cell Metabolism and Function. Cell Rep. 2021 Jan 12; 34(2):108609.

243. Yang JH, Sakamoto H, Xu EC, Lee RT. Biomechanical regulation of human monocyte/macrophage molecular function. Am J Pathol. 2000 May; 156(5):1797-804.

244. Harwani SC. Macrophages under pressure: the role of macrophage polarization in hypertension. Transl Res. 2018 Jan; 191:45-63.

245. Fahy N, Menzel U, Alini M, Stoddart MJ. Shear and Dynamic Compression Modulates the Inflammatory Phenotype of Human Monocytes in vitro. Front Immunol. 2019 Mar 5; 10:383.

246. Solis AG, Bielecki P, Steach HR, Sharma L, Harman CCD, Yun S, de Zoete MR, Warnock JN, To SDF, York AG, Mack M, Schwartz MA, Dela Cruz CS, Palm NW, Jackson R, Flavell RA. Mechanosensation of cyclical force by PIEZO1 is essential for innate immunity. Nature. 2019 Sep; 573(7772):69-74.

247. Jain N, Moeller J, Vogel V. Mechanobiology of Macrophages: How Physical Factors Coregulate Macrophage Plasticity and Phagocytosis. Annu Rev Biomed Eng. 2019 Jun 4; 21:267-297.

248. Ekpenyong AE, Toepfner N, Chilvers ER, Guck J. Mechanotransduction in neutrophil activation and deactivation. Biochim Biophys Acta. 2015 Nov; 1853(11 Pt B):3105-16.

249. Wan Z, Chen X, Chen H, Ji Q, Chen Y, Wang J, Cao Y, Wang F, Lou J, Tang Z, Liu W. The activation of IgM- or isotype-switched IgG- and IgE-BCR exhibits distinct mechanical force sensitivity and threshold. Elife. 2015 Aug 10; 4:e06925.

250. Wan Z, Xu C, Chen X, Xie H, Li Z, Wang J, Ji X, Chen H, Ji Q, Shaheen S, Xu Y, Wang F, Tang Z, Zheng JS, Chen W, Lou J, Liu W. PI(4,5)P2 determines the threshold of mechanical force-induced B cell activation. J Cell Biol. 2018 Jul 2; 217(7):2565-2582.

251. Mennens SFB, Bolomini-Vittori M, Weiden J, Joosten B, Cambi A, van den Dries K. Substrate stiffness influences phenotype and function of human antigen-presenting dendritic cells. Sci Rep. 2017 Dec 13; 7(1):17511.

252. Friedman D, Hale A, White M, Davis DM. The impact of target stiffness on NK cell activation. 2018 May 1; J. Immunol. 200 (1 Supplement) 111.5.

253. Mordechay L, Le Saux G, Edri A, Hadad U, Porgador A, Schvartzman M. Mechanical Regulation of the Cytotoxic Activity of Natural Killer Cells. ACS Biomater Sci Eng. 2021 Jan 11; 7(1):122-132.

254. Choraghe RP, Kołodziej T, Buser A, Rajfur Z, Neumann AK. RHOA-mediated mechanical force generation through Dectin-1. J Cell Sci. 2020 Mar 2; 133(5):jcs236166.

255. Brown GD. Dectin-1: a signalling non-TLR pattern-recognition receptor. Nat Rev Immunol. 2006 Jan; 6(1):33-43.

256. Wu J, Yan Z, Schwartz DE, Yu J, Malik AB, Hu G. Activation of NLRP3 inflammasome in alveolar macrophages contributes to mechanical stretch-induced lung inflammation and injury. J Immunol. 2013 Apr 1; 190(7):3590-9.

257. Maruyama K, Nemoto E, Yamada S. Mechanical regulation of macrophage function - cyclic tensile force inhibits NLRP3 inflammasome-dependent IL-1β secretion in murine macrophages. Inflamm Regen. 2019 Feb 7; 39:3.

258. Chen W, Zhu C. Mechanical regulation of T-cell functions. Immunol Rev. 2013 Nov; 256(1):160-76.

259. George AJ, Stark J, Chan C. Understanding specificity and sensitivity of T-cell recognition. Trends Immunol. 2005 Dec; 26(12):653-9.

260. van der Merwe PA, Dushek O. Mechanisms for T cell receptor triggering. Nat Rev Immunol. 2011 Jan; 11(1):47-55.

261. Jameson SC. Maintaining the norm: T-cell homeostasis. Nat Rev Immunol. 2002 Aug; 2(8):547-56.

262. Stone JD, Chervin AS, Kranz DM. T-cell receptor binding affinities and kinetics: impact on T-cell activity and specificity. Immunology. 2009 Feb; 126(2):165-76.

263. Turner SJ, La Gruta NL, Kedzierska K, Thomas PG, Doherty PC. Functional implications of T cell receptor diversity. Curr Opin Immunol. 2009 Jun; 21(3):286-90.

264. Singh NK, Riley TP, Baker SCB, Borrman T, Weng Z, Baker BM. Emerging Concepts in TCR Specificity: Rationalizing and (Maybe) Predicting Outcomes. J Immunol. 2017 Oct 1; 199(7):2203-2213.

265. Matsui K, Boniface JJ, Reay PA, Schild H, Fazekas de St Groth B, Davis MM. Low affinity interaction of peptide-MHC complexes with T cell receptors. Science. 1991 Dec 20; 254(5039):1788-91.

266. Zhu C, Jiang N, Huang J, Zarnitsyna VI, Evavold BD. Insights from in situ analysis of TCR-pMHC recognition: response of an interaction network. Immunol Rev. 2013 Jan; 251(1):49-64.

267. Gálvez J, Gálvez JJ, García-Peñarrubia P. Is TCR/pMHC Affinity a Good Estimate of the T-cell Response? An Answer Based on Predictions From 12 Phenotypic Models. Front Immunol. 2019 Mar 4; 10:349.

268. Valitutti S, Müller S, Cella M, Padovan E, Lanzavecchia A. Serial triggering of many T-cell receptors by a few peptide-MHC complexes. Nature. 1995 May 11; 375(6527):148-51.

269. San José E, Borroto A, Niedergang F, Alcover A, Alarcón B. Triggering the TCR complex causes the downregulation of nonengaged receptors by a signal transduction-dependent mechanism. Immunity. 2000 Feb; 12(2):161-70.

270. Davis SJ, van der Merwe PA. The kinetic-segregation model: TCR triggering and beyond. Nat Immunol. 2006 Aug; 7(8):803-9.

271. Burroughs NJ, Lazic Z, van der Merwe PA. Ligand detection and discrimination by spatial relocalization: A kinase-phosphatase segregation model of TCR activation. Biophys J. 2006 Sep 1; 91(5):1619-29.

272. Smith-Garvin JE, Koretzky GA, Jordan MS. T cell activation. Annu Rev Immunol. 2009; 27:591-619.

273. Leupin O, Zaru R, Laroche T, Müller S, Valitutti S. Exclusion of CD45 from the T-cell receptor signaling area in antigen-stimulated T lymphocytes. Curr Biol. 2000 Mar 9; 10(5):277-80.

274. Leitenberg D, Novak TJ, Farber D, Smith BR, Bottomly K. The extracellular domain of CD45 controls association with the CD4-T cell receptor complex and the response to antigen-specific stimulation. J Exp Med. 1996 Jan 1; 183(1):249-59.

275. Sykulev Y. Changing separating distances between immune receptors as a sensitive mechanism regulating T-cell activation. Self Nonself. 2010 Jan; 1(1):67-68.

276. James JR, Vale RD. Biophysical mechanism of T-cell receptor triggering in a reconstituted system. Nature. 2012 Jul 5; 487(7405):64-9.

277. Chakraborty AK, Das J. Pairing computation with experimentation: a powerful coupling for understanding T cell signalling. Nat Rev Immunol. 2010 Jan; 10(1):59-71.

278. Davis SJ, van der Merwe PA. TCR triggering: co-receptor-dependent or -independent? Trends Immunol. 2003 Dec;24(12):624-6.

279. Krogsgaard M, Juang J, Davis MM. A role for "self" in T-cell activation. Semin Immunol. 2007 Aug; 19(4):236-44.

280. Gascoigne NR, Zal T, Yachi PP, Hoerter JA. Co-receptors and recognition of self at the immunological synapse. Curr Top Microbiol Immunol. 2010; 340:171-89.

281. Ma Z, Sharp KA, Janmey PA, Finkel TH. Surface-anchored monomeric agonist pMHCs alone trigger TCR with high sensitivity. PLoS Biol. 2008 Feb; 6(2):e43.

282. Wang JH, Reinherz EL. Revisiting the putative TCR Cα dimerization model through structural analysis. Front Immunol. 2013 Jan 30; 4:16.

283. Beck-García K, Beck-García E, Bohler S, Zorzin C, Sezgin E, Levental I, Alarcón B, Schamel WW. Nanoclusters of the resting T cell antigen receptor (TCR) localize to non-raft domains. Biochim Biophys Acta. 2015 Apr; 1853(4):802-9.

284. Crites TJ, Padhan K, Muller J, Krogsgaard M, Gudla PR, Lockett SJ, Varma R. TCR Microclusters pre-exist and contain molecules necessary for TCR signal transduction. J Immunol. 2014 Jul 1; 193(1):56-67.

285. Varma R, Campi G, Yokosuka T, Saito T, Dustin ML. T cell receptor-proximal signals are sustained in peripheral microclusters and terminated in the central supramolecular activation cluster. Immunity. 2006 Jul; 25(1):117-27.

286. Barr VA, Yi J, Samelson LE. Super-resolution Analysis of TCR-Dependent Signaling: Single-Molecule Localization Microscopy. Methods Mol Biol. 2017; 1584:183-206.

287. Rossboth B, Arnold AM, Ta H, Platzer R, Kellner F, Huppa JB, Brameshuber M, Baumgart F, Schütz GJ. TCRs are randomly distributed on the plasma membrane of resting antigen-experienced T cells. Nat Immunol. 2018 Aug; 19(8):821-827.

288. Brameshuber M, Kellner F, Rossboth BK, Ta H, Alge K, Sevcsik E, Göhring J, Axmann M, Baumgart F, Gascoigne NRJ, Davis SJ, Stockinger H, Schütz GJ, Huppa JB. Monomeric TCRs drive T cell antigen recognition. Nat Immunol. 2018 May; 19(5):487-496.

289. Armstrong KM, Piepenbrink KH, Baker BM. Conformational changes and flexibility in T-cell receptor recognition of peptide-MHC complexes. Biochem J. 2008 Oct 15; 415(2):183-96.

290. Sasmal DK, Feng W, Roy S, Leung P, He Y, Cai C, Cao G, Lian H, Qin J, Hui E, Schreiber H, Adams E, Huang J. TCR-pMHC bond length controls TCR ligand discrimination. bioRxiv 433938; doi: https://doi.org/10.1101/433938

291. Sasmal DK, Feng W, Roy S, Leung P, He Y, Cai C, Cao G, Lian H, Qin J, Hui E, Schreiber H, Adams EJ, Huang J. TCR-pMHC bond conformation controls TCR ligand discrimination. Cell Mol Immunol. 2020 Mar; 17(3):203-217.

292. Beddoe T, Chen Z, Clements CS, Ely LK, Bushell SR, Vivian JP, Kjer-Nielsen L, Pang SS, Dunstone MA, Liu YC, Macdonald WA, Perugini MA, Wilce MC, Burrows SR, Purcell AW, Tiganis T, Bottomley SP, McCluskey J, Rossjohn J. Antigen ligation triggers a conformational change within the constant domain of the alphabeta T cell receptor. Immunity. 2009 Jun 19; 30(6):777-88.

293. Birnbaum ME, Berry R, Hsiao YS, Chen Z, Shingu-Vazquez MA, Yu X, Waghray D, Fischer S, McCluskey J, Rossjohn J, Walz T, Garcia KC. Molecular architecture of the αβ T cell receptor-CD3 complex. Proc Natl Acad Sci U S A. 2014 Dec 9; 111(49):17576-81.

294. Mariuzza RA, Agnihotri P, Orban J. The structural basis of T-cell receptor (TCR) activation: An enduring enigma. J Biol Chem. 2020 Jan 24; 295(4):914-925.

295. Gil D, Schamel WW, Montoya M, Sánchez-Madrid F, Alarcón B. Recruitment of Nck by CD3 epsilon reveals a ligand-induced conformational change essential for T cell receptor signaling and synapse formation. Cell. 2002 Jun 28; 109(7):901-12.

296. Mingueneau M, Sansoni A, Grégoire C, Roncagalli R, Aguado E, Weiss A, Malissen M, Malissen B. The proline-rich sequence of CD3epsilon controls T cell antigen receptor expression on and signaling potency in preselection CD4+CD8+ thymocytes. Nat Immunol. 2008 May; 9(5):522-32.

297. Deford-Watts LM, Tassin TC, Becker AM, Medeiros JJ, Albanesi JP, Love PE, Wülfing C, van Oers NS. The cytoplasmic tail of the T cell receptor CD3 epsilon subunit contains a phospholipid-binding motif that regulates T cell functions. J Immunol. 2009 Jul 15; 183(2):1055-64.

298. Xu C, Gagnon E, Call ME, Schnell JR, Schwieters CD, Carman CV, Chou JJ, Wucherpfennig KW. Regulation of T cell receptor activation by dynamic membrane binding of the CD3epsilon cytoplasmic tyrosine-based motif. Cell. 2008 Nov 14; 135(4):702-13.

299. Kuhns MS, Davis MM. The safety on the TCR trigger. Cell. 2008 Nov 14; 135(4):594-6.

300. Aivazian D, Stern LJ. Phosphorylation of T cell receptor zeta is regulated by a lipid dependent folding transition. Nat Struct Biol. 2000 Nov; 7(11):1023-6.

301. Fernandes RA, Huo J, Lui Y, Felce JH, Davis SJ. On the Control of TCR Phosphorylation. Front Immunol. 2012 May 7; 3:92.

302. Imbert V, Peyron JF, Farahi Far D, Mari B, Auberger P, Rossi B. Induction of tyrosine phosphorylation and T-cell activation by vanadate peroxide, an inhibitor of protein tyrosine phosphatases. Biochem J. 1994 Jan 1; 297 (Pt 1)(Pt 1):163-73.

303. Fernandes RA, Shore DA, Vuong MT, Yu C, Zhu X, Pereira-Lopes S, Brouwer H, Fennelly JA, Jessup CM, Evans EJ, Wilson IA, Davis SJ. T cell receptors are structures capable of initiating signaling in the absence of large conformational rearrangements. J Biol Chem. 2012 Apr 13; 287(16):13324-35.

304. Sun ZJ, Kim KS, Wagner G, Reinherz EL. Mechanisms contributing to T cell receptor signaling and assembly revealed by the solution structure of an ectodomain fragment of the CD3 epsilon gamma heterodimer. Cell. 2001 Jun 29; 105(7):913-23.

305. Wang Y, Becker D, Vass T, White J, Marrack P, Kappler JW. A conserved CXXC motif in CD3epsilon is critical for T cell development and TCR signaling. PLoS Biol. 2009 Dec; 7(12):e1000253.

306. Martínez-Martín N, Risueño RM, Morreale A, Zaldívar I, Fernández-Arenas E, Herranz F, Ortiz AR, Alarcón B. Cooperativity between T cell receptor complexes revealed by conformational mutants of CD3epsilon. Sci Signal. 2009 Aug 11; 2(83):ra43.

307. Natarajan K, Jiang J, May NA, Mage MG, Boyd LF, McShan AC, Sgourakis NG, Bax A, Margulies DH. The Role of Molecular Flexibility in Antigen Presentation and T Cell Receptor-Mediated Signaling. Front Immunol. 2018 Jul 17; 9:1657.

308. Ma, Z., Janmey, P.A. and Finkel, T.H. The receptor deformation model of TCR triggering. The Faseb J. 2008; 22:1002-1008.

309. Krogsgaard M, Prado N, Adams EJ, He XL, Chow DC, Wilson DB, Garcia KC, Davis MM. Evidence that structural rearrangements and/or flexibility during TCR binding can contribute to T cell activation. Mol Cell. 2003 Dec; 12(6):1367-78.

310. Matsui K, Boniface JJ, Steffner P, Reay PA, Davis MM. Kinetics of T-cell receptor binding to peptide/I-Ek complexes: correlation of the dissociation rate with T-cell responsiveness. Proc Natl Acad Sci U S A. 1994 Dec 20; 91(26):12862-6.

311. Liu CSC, Ganguly D. Mechanical Cues for T Cell Activation: Role of Piezo1 Mechanosensors. Crit Rev Immunol. 2019; 39(1):15-38.

312. Li YC, Chen BM, Wu PC, Cheng TL, Kao LS, Tao MH, Lieber A, Roffler SR. Cutting Edge: mechanical forces acting on T cells immobilized via the TCR complex can trigger TCR signaling. J Immunol. 2010 Jun 1; 184(11):5959-63.

313. O'Connor RS, Hao X, Shen K, Bashour K, Akimova T, Hancock WW, Kam LC, Milone MC. Substrate rigidity regulates human T cell activation and proliferation. J Immunol. 2012 Aug 1; 189(3):1330-9.

314. Judokusumo E, Tabdanov E, Kumari S, Dustin ML, Kam LC. Mechanosensing in T lymphocyte activation. Biophys J. 2012 Jan 18;102(2):L5-7.

315. Harrison DL, Fang Y, Huang J. T-Cell Mechanobiology: Force Sensation, Potentiation, and Translation. Front Phys. 2019 Apr; 7:45.

316. Husson J, Chemin K, Bohineust A, Hivroz C, Henry N. Force generation upon T cell receptor engagement. PLoS One. 2011 May 10; 6(5):e19680.

317. Hivroz C, Saitakis M. Biophysical Aspects of T Lymphocyte Activation at the Immune Synapse. Front Immunol. 2016 Feb 15; 7:46.

318. Hu KH, Butte MJ. T cell activation requires force generation. J Cell Biol. 2016 Jun 6; 213(5):535-42.

319. Lim TS, Mortellaro A, Lim CT, Hämmerling GJ, Ricciardi-Castagnoli P. Mechanical interactions between dendritic cells and T cells correlate with T cell responsiveness. J Immunol. 2011 Jul 1; 187(1):258-65.

320. Kim ST, Takeuchi K, Sun ZY, Touma M, Castro CE, Fahmy A, Lang MJ, Wagner G, Reinherz EL. The alphabeta T cell receptor is an anisotropic mechanosensor. J Biol Chem. 2009 Nov 6; 284(45):31028-37.

321. Brockman JM, Salaita K. Mechanical Proofreading: A General Mechanism to Enhance the Fidelity of Information Transfer Between Cells. Front Phys. 2019 Feb; 7:14.

322. Liu B, Chen W, Evavold BD, Zhu C. Accumulation of dynamic catch bonds between TCR and agonist peptide-MHC triggers T cell signaling. Cell. 2014 Apr 10; 157(2):357-368.

323. Kolawole EM, Andargachew R, Liu B, Jacobs JR, Evavold BD. 2D Kinetic Analysis of TCR and CD8 Coreceptor for LCMV GP33 Epitopes. Front Immunol. 2018 Oct 15; 9:2348.

324. Liu Y, Blanchfield L, Ma VP, Andargachew R, Galior K, Liu Z, Evavold B, Salaita K. DNA-based nanoparticle tension sensors reveal that T-cell receptors transmit defined pN forces to their antigens for enhanced fidelity. Proc Natl Acad Sci U S A. 2016 May 17; 113(20):5610-5.

325. Das DK, Feng Y, Mallis RJ, Li X, Keskin DB, Hussey RE, Brady SK, Wang JH, Wagner G, Reinherz EL, Lang MJ. Force-dependent transition in the T-cell receptor β-

subunit allosterically regulates peptide discrimination and pMHC bond lifetime. Proc Natl Acad Sci U S A. 2015 Feb 3; 112(5):1517-22.

326. Palmer E, Naeher D. Affinity threshold for thymic selection through a T-cell receptor-co-receptor zipper. Nat Rev Immunol. 2009 Mar; 9(3):207-13.

327. Hong J, Ge C, Jothikumar P, Yuan Z, Liu B, Bai K, Li K, Rittase W, Shinzawa M, Zhang Y, Palin A, Love P, Yu X, Salaita K, Evavold BD, Singer A, Zhu C. A TCR mechanotransduction signaling loop induces negative selection in the thymus. Nat Immunol. 2018 Dec; 19(12):1379-1390.

328. Rushdi M, Li K, Yuan Z, Travaglino S, Grakoui A, Zhu C. Mechanotransduction in T Cell Development, Differentiation and Function. Cells. 2020 Feb 5; 9(2):364.

329. Saitakis M, Dogniaux S, Goudot C, Bufi N, Asnacios S, Maurin M, Randriamampita C, Asnacios A, Hivroz C. Different TCR-induced T lymphocyte responses are potentiated by stiffness with variable sensitivity. Elife 2017 Jun 8; 6: e23190.

330. Bufi N, Saitakis M, Dogniaux S, Buschinger O, Bohineust A, Richert A, Maurin M, Hivroz C, Asnacios A. Human Primary Immune Cells Exhibit Distinct Mechanical Properties that Are Modified by Inflammation. Biophys J. 2015 May 5; 108(9):2181-90.

331. Ekpenyong AE, Whyte G, Chalut K, Pagliara S, Lautenschläger F, Fiddler C, Paschke S, Keyser UF, Chilvers ER, Guck J. Viscoelastic properties of differentiating blood cells are fate- and function-dependent. PLoS One. 2012; 7(9):e45237.

332. Ekpenyong AE, Whyte G, Chalut K, Pagliara S, Lautenschläger F, Fiddler C, Paschke S, Keyser UF, Chilvers ER, Guck J. Viscoelastic properties of differentiating blood cells are fate- and function-dependent. PLoS One. 2012; 7(9):e45237.

333. Wong VW, Paterno J, Sorkin M, Glotzbach JP, Levi K, Januszyk M, Rustad KC, Longaker MT, Gurtner GC. Mechanical force prolongs acute inflammation via T-cell-dependent pathways during scar formation. FASEB J. 2011 Dec; 25(12):4498-510.

334. Basu R, Whitlock BM, Husson J, Le Floc'h A, Jin W, Oyler-Yaniv A, Dotiwala F, Giannone G, Hivroz C, Biais N, Lieberman J, Kam LC, Huse M. Cytotoxic T Cells Use Mechanical Force to Potentiate Target Cell Killing. Cell. 2016 Mar 24; 165(1):100-110.

335. Kabanova A, Zurli V, Baldari CT. Signals Controlling Lytic Granule Polarization at the Cytotoxic Immune Synapse. Front Immunol. 2018 Feb 20; 9:307.

336. Tamzalit F, Wang MS, Jin W, Tello-Lafoz M, Boyko V, Heddleston JM, Black CT, Kam LC, Huse M. Interfacial actin protrusions mechanically enhance killing by cytotoxic T cells. Sci Immunol. 2019 Mar 22; 4(33): eaav5445.

337. Luscinskas FW, Lim YC, Lichtman AH. Wall shear stress: the missing step for T cell transmigration? Nat Immunol. 2001 Jun; 2(6):478-80.

338. Strazza M, Azoulay-Alfaguter I, Peled M, Mor A. Assay of Adhesion Under Shear Stress for the Study of T Lymphocyte-Adhesion Molecule Interactions. J Vis Exp. 2016 Jun 29; (112):54203.

339. Roy NH, MacKay JL, Robertson TF, Hammer DA, Burkhardt JK. Crk adaptor proteins mediate actin-dependent T cell migration and mechanosensing induced by the integrin LFA-1. Sci Signal. 2018 Dec 11; 11(560): eaat3178.

340. Rossy J, Laufer JM, Legler DF. Role of Mechanotransduction and Tension in T Cell Function. Front Immunol. 2018 Nov 15; 9:2638.

341. Kumari S, Mak M, Poh YC, Tohme M, Watson N, Melo M, Janssen E, Dustin M, Geha R, Irvine DJ. Cytoskeletal tension actively sustains the migratory T-cell synaptic contact. EMBO J. 2020 Mar 2;39(5): e102783.

342. Russell S. How polarity shapes the destiny of T cells. J Cell Sci. 2008 Jan 15; 121(Pt 2):131-6.

343. Krummel MF, Macara I. Maintenance and modulation of T cell polarity. Nat Immunol. 2006 Nov; 7(11):1143-9.

344. Renkawitz J, Kopf A, Stopp J, de Vries I, Driscoll MK, Merrin J, Hauschild R, Welf ES, Danuser G, Fiolka R, Sixt M. Nuclear positioning facilitates amoeboid migration along the path of least resistance. Nature. 2019 Apr; 568(7753):546-550.

345. Houot R, Schultz LM, Marabelle A, Kohrt H. T-cell-based Immunotherapy: Adoptive Cell Transfer and Checkpoint Inhibition. Cancer Immunol Res. 2015 Oct; 3(10):1115-22.

346. Li D, Li X, Zhou WL, Huang Y, Liang X, Jiang L, Yang X, Sun J, Li Z, Han WD, Wang W. Genetically engineered T cells for cancer immunotherapy. Signal Transduct Target Ther. 2019 Sep 20; 4:35.

347. Li R, Ma C, Cai H, Chen W. The CAR T-Cell Mechanoimmunology at a Glance. Adv Sci (Weinh). 2020 Nov 3; 7(24):2002628.

348. Chang ZL, Lorenzini MH, Chen X, Tran U, Bangayan NJ, Chen YY. Rewiring T-cell responses to soluble factors with chimeric antigen receptors. Nat Chem Biol. 2018 Mar; 14(3):317-324.

349. Chen Y, Ju L, Rushdi M, Ge C, Zhu C. Receptor-mediated cell mechanosensing. Mol Biol Cell. 2017 Nov 7; 28(23):3134-3155.

350. Martino F, Perestrelo AR, Vinarský V, Pagliari S, Forte G. Cellular Mechanotransduction: From Tension to Function. Front Physiol. 2018 Jul 5; 9:824.

351. Zhou J, Aponte-Santamaría C, Sturm S, Bullerjahn JT, Bronowska A, Gräter F. Mechanism of Focal Adhesion Kinase Mechanosensing. PLoS Comput Biol. 2015 Nov 6;11(11): e1004593.

352. Sun Z, Guo SS, Fässler R. Integrin-mediated mechanotransduction. J Cell Biol. 2016 Nov 21; 215(4):445-456.

353. Stutchbury B, Atherton P, Tsang R, Wang DY, Ballestrem C. Distinct focal adhesion protein modules control different aspects of mechanotransduction. J Cell Sci. 2017 May 1; 130(9):1612-1624.

354. Andrew R. Harris, Pamela Jreij, and Daniel A. Fletcher. Mechanotransduction by the Actin Cytoskeleton: Converting Mechanical Stimuli into Biochemical Signals. Annual Review of Biophysics. 2018 May; 47:617-631

355. Janota CS, Calero-Cuenca FJ, Gomes ER. The role of the cell nucleus in mechanotransduction. Curr Opin Cell Biol. 2020 Apr; 63:204-211.

356. Kirby TJ, Lammerding J. Emerging views of the nucleus as a cellular mechanosensor. Nat Cell Biol. 2018 Apr; 20(4):373-381.

357. Fredrickson BJ, Dong JF, McIntire LV, López JA. Shear-dependent rolling on von Willebrand factor of mammalian cells expressing the platelet glycoprotein Ib-IX-V complex. Blood. 1998 Nov 15; 92(10):3684-93.

358. Tarbell JM, Simon SI, Curry FR. Mechanosensing at the vascular interface. Annu Rev Biomed Eng. 2014 Jul 11; 16:505-32.

359. Liu C, Montell C. Forcing open TRP channels: Mechanical gating as a unifying activation mechanism. Biochem Biophys Res Commun. 2015 Apr 24; 460(1):22-5.

360. Jin M, Berrout J, O'Neil RG. Regulation of TRP Channels by Osmomechanical Stress. In: Zhu MX, editor. TRP Channels. Boca Raton (FL): CRC Press/Taylor & Francis; 2011. Chapter 16. Available from: https://www.ncbi.nlm.nih.gov/books/NBK92821/

361. Reinherz EL. The structure of a T-cell mechanosensor. Nature. 2019 Sep; 573(7775):502-504.

362. Ma Z, Discher DE, Finkel TH. Mechanical force in T cell receptor signal initiation. Front Immunol. 2012 Jul 20; 3:217.

363. Sun Z, Guo SS, Fässler R. Integrin-mediated mechanotransduction. J Cell Biol. 2016 Nov 21; 215(4):445-456.

364. Jankowska KI, Williamson EK, Roy NH, Blumenthal D, Chandra V, Baumgart T, Burkhardt JK. Integrins Modulate T Cell Receptor Signaling by Constraining Actin Flow at the Immunological Synapse. Front Immunol. 2018 Jan 18; 9:25.

365. Wahl A, Dinet C, Dillard P, Nassereddine A, Puech PH, Limozin L, Sengupta K. Biphasic mechanosensitivity of T cell receptor-mediated spreading of lymphocytes. Proc Natl Acad Sci U S A. 2019 Mar 26; 116(13):5908-5913.

366. Hashimoto-Tane A, Saito T. Dynamic Regulation of TCR-Microclusters and the Microsynapse for T Cell Activation. Front Immunol. 2016 Jun 28; 7:255.

367. Braiman A, Isakov N. The Role of Crk Adaptor Proteins in T-Cell Adhesion and Migration. Front Immunol. 2015 Oct 5; 6:509.

368. Santos LC, Blair DA, Kumari S, Cammer M, Iskratsch T, Herbin O, Alexandropoulos K, Dustin ML, Sheetz MP. Actin polymerization-dependent activation of Cas-L promotes immunological synapse stability. Immunol Cell Biol. 2016 Nov; 94(10):981-993.

369. Yu Y, Fay NC, Smoligovets AA, Wu HJ, Groves JT. Myosin IIA modulates T cell receptor transport and CasL phosphorylation during early immunological synapse formation. PLoS One. 2012; 7(2):e30704.

370. Janoštiak R, Pataki AC, Brábek J, Rösel D. Mechanosensors in integrin signaling: the emerging role of p130Cas. Eur J Cell Biol. 2014 Oct; 93(10-12):445-54.

371. Roy NH, MacKay JL, Robertson TF, Hammer DA, Burkhardt JK. Crk adaptor proteins mediate actin-dependent T cell migration and mechanosensing induced by the integrin LFA-1. Sci Signal. 2018 Dec 11; 11(560):eaat3178.

372. Chesler AT, Szczot M. Portraits of a pressure sensor. Elife. 2018 Jan 29; 7:e34396.

373. Coste B, Mathur J, Schmidt M, Earley TJ, Ranade S, Petrus MJ, Dubin AE, Patapoutian A. Piezo1 and Piezo2 are essential components of distinct mechanically activated cation channels. Science. 2010 Oct 1; 330(6000):55-60.

374. Wu J, Lewis AH, Grandl J. Touch, Tension, and Transduction - The Function and Regulation of Piezo Ion Channels. Trends Biochem Sci. 2017 Jan; 42(1):57-71.

375. Ge J, Li W, Zhao Q, Li N, Chen M, Zhi P, Li R, Gao N, Xiao B, Yang M. Architecture of the mammalian mechanosensitive Piezo1 channel. Nature. 2015 Nov 5; 527(7576):64-9.

376. Fang XZ, Zhou T, Xu JQ, Wang YX, Sun MM, He YJ, Pan SW, Xiong W, Peng ZK, Gao XH, Shang Y. Structure, kinetic properties and biological function of mechanosensitive Piezo channels. Cell Biosci. 2021 Jan 9; 11(1):13.

377. Coste B, Murthy SE, Mathur J, Schmidt M, Mechioukhi Y, Delmas P, Patapoutian A. Piezo1 ion channel pore properties are dictated by C-terminal region. Nat Commun. 2015 May 26; 6:7223.

378. Saotome K, Murthy SE, Kefauver JM, Whitwam T, Patapoutian A, Ward AB. Structure of the mechanically activated ion channel Piezo1. Nature. 2018 Feb 22; 554(7693):481-486.

379. Haselwandter CA, MacKinnon R. Piezo's membrane footprint and its contribution to mechanosensitivity. Elife. 2018 Nov 27; 7:e41968.

380. Zhao Q, Zhou H, Chi S, Wang Y, Wang J, Geng J, Wu K, Liu W, Zhang T, Dong MQ, Wang J, Li X, Xiao B. Structure and mechanogating mechanism of the Piezo1 channel. Nature. 2018 Feb 22; 554(7693):487-492.

381. Lewis AH, Grandl J. Inactivation Kinetics and Mechanical Gating of Piezo1 Ion Channels Depend on Subdomains within the Cap. Cell Rep. 2020 Jan 21; 30(3):870-880.e2.

382. Zhao Q, Zhou H, Li X, Xiao B. The mechanosensitive Piezo1 channel: a three-bladed propeller-like structure and a lever-like mechanogating mechanism. FEBS J. 2019 Jul; 286(13):2461-2470

383. Wang L, Zhou H, Zhang M, Liu W, Deng T, Zhao Q, Li Y, Lei J, Li X, Xiao B. Structure and mechanogating of the mammalian tactile channel PIEZO2. Nature. 2019 Sep; 573(7773):225-229.

384. Taberner FJ, Prato V, Schaefer I, Schrenk-Siemens K, Heppenstall PA, Lechner SG. Structure-guided examination of the mechanogating mechanism of PIEZO2. Proc Natl Acad Sci U S A. 2019 Jul 9; 116(28):14260-14269.

385. Szczot M, Pogorzala LA, Solinski HJ, Young L, Yee P, Le Pichon CE, Chesler AT, Hoon MA. Cell-Type-Specific Splicing of Piezo2 Regulates Mechanotransduction. Cell Rep. 2017 Dec 5; 21(10):2760-2771.

386. Teng J, Loukin S, Anishkin A, Kung C. The force-from-lipid (FFL) principle of mechanosensitivity, at large and in elements. Pflugers Arch. 2015 Jan; 467(1):27-37.

387. Ridone P, Grage SL, Patkunarajah A, Battle AR, Ulrich AS, Martinac B. "Force-from-lipids" gating of mechanosensitive channels modulated by PUFAs. J Mech Behav Biomed Mater. 2018 Mar; 79:158-167.

388. Brohawn SG, Su Z, MacKinnon R. Mechanosensitivity is mediated directly by the lipid membrane in TRAAK and TREK1 K+ channels. Proc Natl Acad Sci U S A. 2014 Mar 4; 111(9):3614-9.

389. Zanini D, Göpfert MC. Mechanosensation: tethered ion channels. Curr Biol. 2013 May 6; 23(9):R349-51.

390. Zhang W, Cheng LE, Kittelmann M, Li J, Petkovic M, Cheng T, Jin P, Guo Z, Göpfert MC, Jan LY, Jan YN. Ankyrin Repeats Convey Force to Gate the NOMPC Mechanotransduction Channel. Cell. 2015 Sep 10; 162(6):1391-403.

391. Syeda R, Florendo MN, Cox CD, Kefauver JM, Santos JS, Martinac B, Patapoutian A. Piezo1 Channels Are Inherently Mechanosensitive. Cell Rep. 2016 Nov 8; 17(7):1739-1746.

392. Liang X, Howard J. Structural Biology: Piezo Senses Tension through Curvature. Curr Biol. 2018 Apr 23; 28(8):R357-R359.

393. Buyan A, Cox CD, Rae J, Barnoud J, Li J, Cvetovska J, Bastiani M, Chan HSM, Hodson MP, Martinac B, Parton RG, Marrink SJ, Corry B. Piezo1 Induces Local Curvature in a Mammalian Membrane and Forms Specific Protein-Lipid Interactions. bioRxiv 787531; doi: https://doi.org/10.1101/787531

394. Lewis AH, Grandl J. Mechanical sensitivity of Piezo1 ion channels can be tuned by cellular membrane tension. Elife. 2015 Dec 8; 4: e12088.

395. Perozo E, Cortes DM, Sompornpisut P, Kloda A, Martinac B. Open channel structure of MscL and the gating mechanism of mechanosensitive channels. Nature. 2002 Aug 29; 418(6901):942-8.

396. Gnanasambandam R, Bae C, Gottlieb PA, Sachs F. Ionic Selectivity and Permeation Properties of Human PIEZO1 Channels. PLoS One. 2015 May 8; 10(5): e0125503.

397. Lin YC, Guo YR, Miyagi A, Levring J, MacKinnon R, Scheuring S. Force-induced conformational changes in PIEZO1. Nature. 2019 Sep; 573(7773):230-234.

398. Nourse JL, Pathak MM. How cells channel their stress: Interplay between Piezo1 and the cytoskeleton. Semin Cell Dev Biol. 2017 Nov; 71:3-12.

399. Cox CD, Bae C, Ziegler L, Hartley S, Nikolova-Krstevski V, Rohde PR, Ng CA, Sachs F, Gottlieb PA, Martinac B. Removal of the mechanoprotective influence of the cytoskeleton reveals PIEZO1 is gated by bilayer tension. Nat Commun. 2016 Jan 20; 7:10366.

400. Ko KS, McCulloch CA. Partners in protection: interdependence of cytoskeleton and plasma membrane in adaptations to applied forces. J Membr Biol. 2000 Mar 15; 174(2):85-95.

401. Wang J, Jiang J, Yang X, Wang L, Xiao B. Tethering Piezo channels to the actin cytoskeleton for mechanogating via the E-cadherin-β-catenin mechanotransduction complex. bioRxiv 2020.05.12.092148.

402. Ridone P, Vassalli M, Martinac B. Piezo1 mechanosensitive channels: what are they and why are they important. Biophys Rev. 2019 Oct; 11(5):795-805.

403. Wang Y, Chi S, Guo H, Li G, Wang L, Zhao Q, Rao Y, Zu L, He W, Xiao B. A lever-like transduction pathway for long-distance chemical- and mechano-gating of the mechanosensitive Piezo1 channel. Nat Commun. 2018 Apr 3; 9(1):1300.

404. Gaub BM, Müller DJ. Mechanical Stimulation of Piezo1 Receptors Depends on Extracellular Matrix Proteins and Directionality of Force. Nano Lett. 2017 Mar 8; 17(3):2064-2072.

405. Chen X, Wanggou S, Bodalia A, Zhu M, Dong W, Fan JJ, Yin WC, Min HK, Hu M, Draghici D, Dou W, Li F, Coutinho FJ, Whetstone H, Kushida MM, Dirks PB, Song Y, Hui CC, Sun Y, Wang LY, Li X, Huang X. A Feedforward Mechanism Mediated by Mechanosensitive Ion Channel PIEZO1 and Tissue Mechanics Promotes Glioma Aggression. Neuron. 2018 Nov 21; 100(4):799-815.e7.

406. Qi Y, Andolfi L, Frattini F, Mayer F, Lazzarino M, Hu J. Membrane stiffening by STOML3 facilitates mechanosensation in sensory neurons. Nat Commun. 2015 Oct 7; 6:8512.

407. Borbiro I, Badheka D, Rohacs T. Activation of TRPV1 channels inhibits mechanosensitive Piezo channel activity by depleting membrane phosphoinositides. Sci Signal. 2015 Feb 10; 8(363):ra15.

408. Romero LO, Massey AE, Mata-Daboin AD, Sierra-Valdez FJ, Chauhan SC, Cordero-Morales JF, Vásquez V. Dietary fatty acids fine-tune Piezo1 mechanical response. Nat Commun. 2019 Mar 13; 10(1):1200.

409. Ridone P, Pandzic E, Vassalli M, Cox CD, Macmillan A, Gottlieb PA, Martinac B. Disruption of membrane cholesterol organization impairs the activity of PIEZO1 channel clusters. J Gen Physiol. 2020 Aug 3; 152(8):e201912515.

410. Morrison SJ, Spradling AC. Stem cells and niches: mechanisms that promote stem cell maintenance throughout life. Cell. 2008 Feb 22; 132(4):598-611.

411. Sun Y, Chen CS, Fu J. Forcing stem cells to behave: a biophysical perspective of the cellular microenvironment. Annu Rev Biophys. 2012; 41:519-42.

412. Pathak MM, Nourse JL, Tran T, Hwe J, Arulmoli J, Le DT, Bernardis E, Flanagan LA, Tombola F. Stretch-activated ion channel Piezo1 directs lineage choice in human neural stem cells. Proc Natl Acad Sci U S A. 2014 Nov 11; 111(45):16148-53.

413. Sugimoto A, Miyazaki A, Kawarabayashi K, Shono M, Akazawa Y, Hasegawa T, Ueda-Yamaguchi K, Kitamura T, Yoshizaki K, Fukumoto S, Iwamoto T. Piezo type mechanosensitive ion channel component 1 functions as a regulator of the cell fate determination of mesenchymal stem cells. Sci Rep. 2017 Dec 18; 7(1):17696.

414. Benedetti MG, Furlini G, Zati A, Letizia Mauro G. The Effectiveness of Physical Exercise on Bone Density in Osteoporotic Patients. Biomed Res Int. 2018 Dec 23; 2018:4840531.

415. He L, Si G, Huang J, Samuel ADT, Perrimon N. Mechanical regulation of stem-cell differentiation by the stretch-activated Piezo channel. Nature. 2018 Mar 1; 555(7694):103-106.

416. Li J, Hou B, Tumova S, Muraki K, Bruns A, Ludlow MJ, Sedo A, Hyman AJ, McKeown L, Young RS, Yuldasheva NY, Majeed Y, Wilson LA, Rode B, Bailey MA, Kim HR, Fu Z, Carter DA, Bilton J, Imrie H, Ajuh P, Dear TN, Cubbon RM, Kearney MT, Prasad RK, Evans PC, Ainscough JF, Beech DJ. Piezo1 integration of vascular architecture with physiological force. Nature. 2014 Nov 13; 515(7526):279-282.

417. Lu D, Kassab GS. Role of shear stress and stretch in vascular mechanobiology. J R Soc Interface. 2011 Oct 7; 8(63):1379-85.

418. Wang S, Chennupati R, Kaur H, Iring A, Wettschureck N, Offermanns S. Endothelial cation channel PIEZO1 controls blood pressure by mediating flow-induced ATP release. J Clin Invest. 2016 Dec 1; 126(12):4527-4536.

419. Retailleau K, Duprat F, Arhatte M, Ranade SS, Peyronnet R, Martins JR, Jodar M, Moro C, Offermanns S, Feng Y, Demolombe S, Patel A, Honoré E. Piezo1 in Smooth Muscle Cells Is Involved in Hypertension-Dependent Arterial Remodeling. Cell Rep. 2015 Nov 10; 13(6):1161-1171.

420. Brown IAM, Diederich L, Good ME, DeLalio LJ, Murphy SA, Cortese-Krott MM, Hall JL, Le TH, Isakson BE. Vascular Smooth Muscle Remodeling in Conductive and Resistance Arteries in Hypertension. Arterioscler Thromb Vasc Biol. 2018 Sep; 38(9):1969-1985.

421. Lee W, Leddy HA, Chen Y, Lee SH, Zelenski NA, McNulty AL, Wu J, Beicker KN, Coles J, Zauscher S, Grandl J, Sachs F, Guilak F, Liedtke WB. Synergy between Piezo1 and Piezo2 channels confers high-strain mechanosensitivity to articular cartilage. Proc Natl Acad Sci U S A. 2014 Nov 25; 111(47): E5114-22.

422. Stewart TA, Davis FM. Formation and Function of Mammalian Epithelia: Roles for Mechanosensitive PIEZO1 Ion Channels. Front Cell Dev Biol. 2019 Oct 31; 7:260.

423. Gudipaty SA, Lindblom J, Loftus PD, Redd MJ, Edes K, Davey CF, Krishnegowda V, Rosenblatt J. Mechanical stretch triggers rapid epithelial cell division through Piezo1. Nature. 2017 Mar 2; 543(7643):118-121.

424. Albuisson J, Murthy SE, Bandell M, Coste B, Louis-Dit-Picard H, Mathur J, Fénéant-Thibault M, Tertian G, de Jaureguiberry JP, Syfuss PY, Cahalan S, Garçon L, Toutain F, Simon Rohrlich P, Delaunay J, Picard V, Jeunemaitre X, Patapoutian A. Dehydrated hereditary stomatocytosis linked to gain-of-function mutations in

mechanically activated PIEZO1 ion channels. Nat Commun. 2013;4:1884. Erratum in: Nat Commun. 2013; 4:2440.

425. Cahalan SM, Lukacs V, Ranade SS, Chien S, Bandell M, Patapoutian A. Piezo1 links mechanical forces to red blood cell volume. Elife. 2015 May 22; 4:e07370.

426. Ma S, Cahalan S, LaMonte G, Grubaugh ND, Zeng W, Murthy SE, Paytas E, Gamini R, Lukacs V, Whitwam T, Loud M, Lohia R, Berry L, Khan SM, Janse CJ, Bandell M, Schmedt C, Wengelnik K, Su AI, Honore E, Winzeler EA, Andersen KG, Patapoutian A. Common PIEZO1 Allele in African Populations Causes RBC Dehydration and Attenuates Plasmodium Infection. Cell. 2018 Apr 5; 173(2):443-455.e12.

427. Ranade SS, Woo SH, Dubin AE, Moshourab RA, Wetzel C, Petrus M, Mathur J, Bégay V, Coste B, Mainquist J, Wilson AJ, Francisco AG, Reddy K, Qiu Z, Wood JN, Lewin GR, Patapoutian A. Piezo2 is the major transducer of mechanical forces for touch sensation in mice. Nature. 2014 Dec 4; 516(7529):121-5.

428. Woo SH, Lumpkin EA, Patapoutian A. Merkel cells and neurons keep in touch. Trends Cell Biol. 2015 Feb; 25(2):74-81.

429. Woo SH, Ranade S, Weyer AD, Dubin AE, Baba Y, Qiu Z, Petrus M, Miyamoto T, Reddy K, Lumpkin EA, Stucky CL, Patapoutian A. Piezo2 is required for Merkel-cell mechanotransduction. Nature. 2014 May 29; 509(7502):622-6.

430. Jia Z, Ikeda R, Ling J, Viatchenko-Karpinski V, Gu JG. Regulation of Piezo2 Mechanotransduction by Static Plasma Membrane Tension in Primary Afferent Neurons. J Biol Chem. 2016 Apr 22; 291(17):9087-104.

431. Abraira VE, Ginty DD. The sensory neurons of touch. Neuron. 2013 Aug 21; 79(4):618-39.

432. Schrenk-Siemens K, Wende H, Prato V, Song K, Rostock C, Loewer A, Utikal J, Lewin GR, Lechner SG, Siemens J. PIEZO2 is required for mechanotransduction in human stem cell-derived touch receptors. Nat Neurosci. 2015 Jan; 18(1):10-6.

433. Eijkelkamp N, Linley JE, Torres JM, Bee L, Dickenson AH, Gringhuis M, Minett MS, Hong GS, Lee E, Oh U, Ishikawa Y, Zwartkuis FJ, Cox JJ, Wood JN. A role for Piezo2 in EPAC1-dependent mechanical allodynia. Nat Commun. 2013; 4:1682.

434. Borbiro I, Badheka D, Rohacs T. Activation of TRPV1 channels inhibits mechanosensitive Piezo channel activity by depleting membrane phosphoinositides. Sci Signal. 2015 Feb 10; 8(363):ra15.

435. Murthy SE, Loud MC, Daou I, Marshall KL, Schwaller F, Kühnemund J, Francisco AG, Keenan WT, Dubin AE, Lewin GR, Patapoutian A. The mechanosensitive ion channel Piezo2 mediates sensitivity to mechanical pain in mice. Sci Transl Med. 2018 Oct 10; 10(462): eaat9897.

436. Proske U, Gandevia SC. The proprioceptive senses: their roles in signaling body shape, body position and movement, and muscle force. Physiol Rev. 2012 Oct; 92(4):1651-97.

437. Woo SH, Lukacs V, de Nooij JC, Zaytseva D, Criddle CR, Francisco A, Jessell TM, Wilkinson KA, Patapoutian A. Piezo2 is the principal mechanotransduction channel for proprioception. Nat Neurosci. 2015 Dec; 18(12):1756-62.

438. Florez-Paz D, Bali KK, Kuner R, Gomis A. A critical role for Piezo2 channels in the mechanotransduction of mouse proprioceptive neurons. Sci Rep. 2016 May 17; 6:25923.

439. Okubo M, Fujita A, Saito Y, Komaki H, Ishiyama A, Takeshita E, Kojima E, Koichihara R, Saito T, Nakagawa E, Sugai K, Yamazaki H, Kusaka K, Tanaka H, Miyake

N, Matsumoto N, Sasaki M. A family of distal arthrogryposis type 5 due to a novel PIEZO2 mutation. Am J Med Genet A. 2015 May; 167A(5):1100-6.

440. McMillin MJ, Beck AE, Chong JX, Shively KM, Buckingham KJ, Gildersleeve HI, Aracena MI, Aylsworth AS, Bitoun P, Carey JC, Clericuzio CL, Crow YJ, Curry CJ, Devriendt K, Everman DB, Fryer A, Gibson K, Giovannucci Uzielli ML, Graham JM Jr, Hall JG, Hecht JT, Heidenreich RA, Hurst JA, Irani S, Krapels IP, Leroy JG, Mowat D, Plant GT, Robertson SP, Schorry EK, Scott RH, Seaver LH, Sherr E, Splitt M, Stewart H, Stumpel C, Temel SG, Weaver DD, Whiteford M, Williams MS, Tabor HK, Smith JD, Shendure J, Nickerson DA; University of Washington Center for Mendelian Genomics, Bamshad MJ. Mutations in PIEZO2 cause Gordon syndrome, Marden-Walker syndrome, and distal arthrogryposis type 5. Am J Hum Genet. 2014 May 1; 94(5):734-44.

441. Murthy SE, Dubin AE, Patapoutian A. Piezos thrive under pressure: mechanically activated ion channels in health and disease. Nat Rev Mol Cell Biol. 2017 Dec; 18(12):771-783.

442. Zhao C, Sun Q, Tang L, Cao Y, Nourse JL, Pathak MM, Lu X, Yang Q. Mechanosensitive Ion Channel Piezo1 Regulates Diet-Induced Adipose Inflammation and Systemic Insulin Resistance. Front Endocrinol (Lausanne). 2019 Jun 13; 10:373.

443. Huang Z, Sun Z, Zhang X, Niu K, Wang Y, Zheng J, Li H, Liu Y. Loss of stretch-activated channels, PIEZOs, accelerates non-small cell lung cancer progression and cell migration. Biosci Rep. 2019 Mar 22; 39(3): BSR20181679.

444. Tijore A, Yao M, Wang YH, Nematbakhsh Y, Hariharan A, Lim CT, Sheetz M. Mechanical Stretch Kills Transformed Cancer Cells. bioRxiv 491746.

445. De Felice D, Alaimo A. Mechanosensitive Piezo Channels in Cancer: Focus on altered Calcium Signaling in Cancer Cells and in Tumor Progression. Cancers (Basel). 2020 Jul 3; 12(7):1780.

446. Nguetse CN, Purington N, Ebel ER, Shakya B, Tetard M, Kremsner PG, Velavan TP, Egan ES. A common polymorphism in the mechanosensitive ion channel PIEZO1 is associated with protection from severe malaria in humans. Proc Natl Acad Sci U S A. 2020 Apr 21; 117(16):9074-9081.

447. Dustin ML. The immunological synapse. Cancer Immunol Res. 2014 Nov;2(11):1023-33.

448. Kumari S, Curado S, Mayya V, Dustin ML. T cell antigen receptor activation and actin cytoskeleton remodeling. Biochim Biophys Acta. 2014 Feb; 1838(2):546-56.

449. Gérard A, Patino-Lopez G, Beemiller P, Nambiar R, Ben-Aissa K, Liu Y, Totah FJ, Tyska MJ, Shaw S, Krummel MF. Detection of rare antigen-presenting cells through T cell-intrinsic meandering motility, mediated by Myo1g. Cell. 2014 Jul 31; 158(3):492-505.

450. Dong D, Zheng L, Lin J, Zhang B, Zhu Y, Li N, Xie S, Wang Y, Gao N, Huang Z. Structural basis of assembly of the human T cell receptor-CD3 complex. Nature. 2019 Sep; 573(7775):546-552.

451. Brownlie RJ, Zamoyska R. T cell receptor signalling networks: branched, diversified and bounded. Nat Rev Immunol. 2013 Apr; 13(4):257-69.

452. Wang H, Kadlecek TA, Au-Yeung BB, Goodfellow HE, Hsu LY, Freedman TS, Weiss A. ZAP-70: an essential kinase in T-cell signaling. Cold Spring Harb Perspect Biol. 2010 May; 2(5):a002279.

453. Cibrián D, Sánchez-Madrid F. CD69: from activation marker to metabolic gatekeeper. Eur J Immunol. 2017 Jun; 47(6):946-953.

454. Nelson BH, Willerford DM. Biology of the interleukin-2 receptor. Adv Immunol. 1998; 70:1-81.

455. Ge Q, Palliser D, Eisen HN, Chen J. Homeostatic T cell proliferation in a T cell-dendritic cell coculture system. Proc Natl Acad Sci U S A. 2002 Mar 5; 99(5):2983-8.

456. Lakkis FG, Lechler RI. Origin and biology of the allogeneic response. Cold Spring Harb Perspect Med. 2013 Aug 1; 3(8):a014993.

457. Marino J, Paster J, Benichou G. Allorecognition by T Lymphocytes and Allograft Rejection. Front Immunol. 2016 Dec 14; 7:582.

458. Harrison BD, Adams JA, Briggs M, Brereton ML, Yin JA. Stimulation of autologous proliferative and cytotoxic T-cell responses by "leukemic dendritic cells" derived from blast cells in acute myeloid leukemia. Blood. 2001 May 1; 97(9):2764-71.

459. Syeda R, Xu J, Dubin AE, Coste B, Mathur J, Huynh T, Matzen J, Lao J, Tully DC, Engels IH, Petrassi HM, Schumacher AM, Montal M, Bandell M, Patapoutian A. Chemical activation of the mechanotransduction channel Piezo1. Elife. 2015 May 22; 4:e07369.

460. Evans EL, Cuthbertson K, Endesh N, Rode B, Blythe NM, Hyman AJ, Hall SJ, Gaunt HJ, Ludlow MJ, Foster R, Beech DJ. Yoda1 analogue (Dooku1) which antagonizes Yoda1-evoked activation of Piezo1 and aortic relaxation. Br J Pharmacol. 2018 May; 175(10):1744-1759.

461. Lacroix JJ, Botello-Smith WM, Luo Y. Probing the gating mechanism of the mechanosensitive channel Piezo1 with the small molecule Yoda1. Nat Commun. 2018 May 23; 9(1):2029.

462. Botello-Smith WM, Jiang W, Zhang H, Ozkan AD, Lin YC, Pham CN, Lacroix JJ, Luo Y. A mechanism for the activation of the mechanosensitive Piezo1 channel by the small molecule Yoda1. Nat Commun. 2019 Oct 3; 10(1):4503.

463. Trebak M, Kinet JP. Calcium signalling in T cells. Nat Rev Immunol. 2019 Mar; 19(3):154-169.

464. Quintana A, Pasche M, Junker C, Al-Ansary D, Rieger H, Kummerow C, Nuñez L, Villalobos C, Meraner P, Becherer U, Rettig J, Niemeyer BA, Hoth M. Calcium microdomains at the immunological synapse: how ORAI channels, mitochondria and calcium pumps generate local calcium signals for efficient T-cell activation. EMBO J. 2011 Aug 16; 30(19):3895-912.

465. Roy NH, Burkhardt JK. The Actin Cytoskeleton: A Mechanical Intermediate for Signal Integration at the Immunological Synapse. Front Cell Dev Biol. 2018 Sep 19; 6:116.

466. Potter DA, Tirnauer JS, Janssen R, Croall DE, Hughes CN, Fiacco KA, Mier JW, Maki M, Herman IM. Calpain regulates actin remodeling during cell spreading. J Cell Biol. 1998 May 4; 141(3):647-62.

467. Suzuki K, Hata S, Kawabata Y, Sorimachi H. Structure, activation, and biology of calpain. Diabetes. 2004 Feb;53 Suppl 1:S12-8.

468. Lebart MC, Benyamin Y. Calpain involvement in the remodeling of cytoskeletal anchorage complexes. FEBS J. 2006 Aug; 273(15):3415-26.

469. M L Dustin, J A Cooper. The Immunological Synapse and the Actin Cytoskeleton: Molecular Hardware for T Cell Signaling. Nat Immunol. 2000 Jul;1(1):23-9.

470. Liu CSC, Raychaudhuri D, Paul B, Chakrabarty Y, Ghosh AR, Rahaman O, Talukdar A, Ganguly D. Cutting Edge: Piezo1 Mechanosensors Optimize Human T Cell Activation. J Immunol. 2018 Feb 15; 200(4):1255-1260.

471. Luster AD, Alon R, von Andrian UH. Immune cell migration in inflammation: present and future therapeutic targets. Nat Immunol. 2005 Dec; 6(12):1182-90.

472. Kameritsch P, Renkawitz J. Principles of Leukocyte Migration Strategies. Trends Cell Biol. 2020 Oct; 30(10):818-832.

473. Lämmermann T, Sixt M. Mechanical modes of 'amoeboid' cell migration. Curr Opin Cell Biol. 2009 Oct; 21(5):636-44.

474. O'Neill PR, Castillo-Badillo JA, Meshik X, Kalyanaraman V, Melgarejo K, Gautam N. Membrane Flow Drives an Adhesion-Independent Amoeboid Cell Migration Mode. Dev Cell. 2018 Jul 2; 46(1):9-22.e4.

475. Gómez-Moutón C, Mañes S. Establishment and maintenance of cell polarity during leukocyte chemotaxis. Cell Adh Migr. 2007 Apr-Jun; 1(2):69-76.

476. Asnacios A, Hamant O. The mechanics behind cell polarity. Trends Cell Biol. 2012 Nov; 22(11):584-91.

477. Houk AR, Jilkine A, Mejean CO, Boltyanskiy R, Dufresne ER, Angenent SB, Altschuler SJ, Wu LF, Weiner OD. Membrane tension maintains cell polarity by confining signals to the leading edge during neutrophil migration. Cell. 2012 Jan 20; 148(1-2):175-88.

478. Emon B, Bauer J, Jain Y, Jung B, Saif T. Biophysics of Tumor Microenvironment and Cancer Metastasis - A Mini Review. Comput Struct Biotechnol J. 2018 Jul 27; 16:279-287.

479. Hui KL, Balagopalan L, Samelson LE, Upadhyaya A. Cytoskeletal forces during signaling activation in Jurkat T-cells. Mol Biol Cell. 2015 Feb 15; 26(4):685-95.

480. Tabdanov ED, Rodríguez-Merced NJ, Cartagena-Rivera AX, Puram VV, Callaway MK, Ensminger EA, Pomeroy EJ, Yamamoto K, Lahr WS, Webber BR, Moriarity BS, Zhovmer AS, Provenzano PP. Engineering T cells to enhance 3D migration through structurally and mechanically complex tumor microenvironments. bioRxiv 2020.04.21.051615.

481. Dupré L, Houmadi R, Tang C, Rey-Barroso J. T Lymphocyte Migration: An Action Movie Starring the Actin and Associated Actors. Front Immunol. 2015 Nov 18; 6:586.

482. Gaylo A, Schrock DC, Fernandes NR, Fowell DJ. T Cell Interstitial Migration: Motility Cues from the Inflamed Tissue for Micro- and Macro-Positioning. Front Immunol. 2016 Oct 14; 7:428.

483. Mackay CR. Chemokine receptors and T cell chemotaxis. J Exp Med. 1996 Sep 1; 184(3):799-802.

484. Stein JV, Nombela-Arrieta C. Chemokine control of lymphocyte trafficking: a general overview. Immunology. 2005 Sep; 116(1):1-12.

485. Niggli V. Insights into the mechanism for dictating polarity in migrating T-cells. Int Rev Cell Mol Biol. 2014; 312:201-70.

486. Ridley AJ. Rho GTPase signalling in cell migration. Curr Opin Cell Biol. 2015 Oct; 36:103-12.

487. Christensen AD, Haase C. Immunological mechanisms of contact hypersensitivity in mice. APMIS. 2012 Jan; 120(1):1-27.

488. Gaspari AA, Katz SI, Martin SF. Contact Hypersensitivity. Curr Protoc Immunol. 2016 Apr 1; 113:4.2.1-4.2.7.

489. Matheu MP, Cahalan MD, Parker I. General approach to adoptive transfer and cell labeling for immunoimaging. Cold Spring Harb Protoc. 2011 Feb 1; 2011(2):pdb.prot5565.

490. Duarte DB, Vasko MR, Fehrenbacher JC. Models of inflammation: carrageenan air pouch. Curr Protoc Pharmacol. 2012 Mar; Chapter 5:Unit5.6.

491. Armides M, Molina F, Elena S, Krímskaya S and Rodríguez-Padilla C, Mehanna RW. Air Pouch Model: An Alternative Method for Cancer Drug Discovery, Cell Culture. IntechOpen; 2018. Nov 5. DOI: 10.5772/intechopen.79503. Available from: https://www.intechopen.com/books/cell-culture/air-pouch-model-an-alternative-method-for-cancer-drug-discovery

492. Corrigan-Curay J, Kiem HP, Baltimore D, O'Reilly M, Brentjens RJ, Cooper L, Forman S, Gottschalk S, Greenberg P, Junghans R, Heslop H, Jensen M, Mackall C, June C, Press O, Powell D, Ribas A, Rosenberg S, Sadelain M, Till B, Patterson AP, Jambou RC, Rosenthal E, Gargiulo L, Montgomery M, Kohn DB. T-cell immunotherapy: looking forward. Mol Ther. 2014 Sep; 22(9):1564-74.

493. Rafiq S, Hackett CS, Brentjens RJ. Engineering strategies to overcome the current roadblocks in CAR T cell therapy. Nat Rev Clin Oncol. 2020 Mar; 17(3):147-167.

494. Maus MV, Fraietta JA, Levine BL, Kalos M, Zhao Y, June CH. Adoptive immunotherapy for cancer or viruses. Annu Rev Immunol. 2014; 32:189-225.

495. Li R, Ma C, Cai H, Chen W. The CAR T-Cell Mechanoimmunology at a Glance. Adv Sci (Weinh). 2020 Nov 3; 7(24):2002628.

496. Lei K, Kurum A, Tang L. Mechanical Immunoengineering of T cells for Therapeutic Applications. Acc Chem Res. 2020 Dec 15; 53(12):2777-2790.

497. Levental KR, Yu H, Kass L, Lakins JN, Egeblad M, Erler JT, Fong SF, Csiszar K, Giaccia A, Weninger W, Yamauchi M, Gasser DL, Weaver VM. Matrix crosslinking forces tumor progression by enhancing integrin signaling. Cell. 2009 Nov 25; 139(5):891-906.

498. Kakarla S, Gottschalk S. CAR T cells for solid tumors: armed and ready to go? Cancer J. 2014 Mar-Apr; 20(2):151-5.

499. Pan Y, Yoon S, Sun J, Huang Z, Lee C, Allen M, Wu Y, Chang YJ, Sadelain M, Shung KK, Chien S, Wang Y. Mechanogenetics for the remote and noninvasive control of cancer immunotherapy. Proc Natl Acad Sci U S A. 2018 Jan 30; 115(5):992-997.

500. Wu Y, Liu Y, Huang Z, Wang X, Jin Z, Li J, Limsakul P, Zhu L, Allen M, Pan Y, Bussell R, Jacobson A, Liu T, Chien S, Wang Y. Acoustogenetic Control of CAR T Cells via Focused Ultrasound. bioRxiv 2020.02.18.955005.

501. Bandyopadhyay S, Quinn TJ, Scandiuzzi L, Basu I, Partanen A, Tomé WA, Macian F, Guha C. Low-Intensity Focused Ultrasound Induces Reversal of Tumor-Induced T Cell Tolerance and Prevents Immune Escape. J Immunol. 2016 Feb 15; 196(4):1964-76.

502. Cohen-Inbar O, Xu Z, Sheehan JP. Focused ultrasound-aided immunomodulation in glioblastoma multiforme: a therapeutic concept. J Ther Ultrasound. 2016 Jan 22; 4:2.

503. Aramesh M. Stoycheva D. Raaz L. Klotzsch E. Engineering T-cell activation for immunotherapy by mechanical forces. Current Opinion in Biomedical Engineering. 2019 June; 10: 134-141.

List of Publications

1. **Liu C.S.C**., Raychaudhuri D., Paul. B, Chakrabarty Y., Ghosh A.R., Rahaman O., Talukdar A., Ganguly D. Piezo1 Mechanosensors Optimize Human T Cell Activation. Cutting Edge-J. Immunology, 200**,** (2018).
2. **Liu CSC**, Ganguly D. Mechanical Cues for T Cell Activation: Role of Piezo1 Mechanosensors. Crit Rev Immunol. 2019; 39(1):15-38.
3. Rahaman O., Bhattacharya R., **Liu C.S.C**., Raychaudhuri D., Ghosh A.R., Bandopadhyay P., Pal S., Goswami R.P., Sircar G., Ghosh P. & Ganguly D. Dysregulated Endocannabinoid-Rheostat for Plasmacytoid Dendritic Cell Activation in a Systemic Lupus Endophenotype. Cutting edge-J Immunology, 202, (2019)
4. Raychaudhuri D., Bhattacharya B., Sinha B.P., **Liu C.S.C**., Ghosh A.R., Rahaman O., Bandopadhyay P., Sarif J., D'Rozario R, Paul S., Das A., Sarkar D.K., Chattopadhyay S. and Ganguly D. Lactate Induces Pro-tumor Reprogramming in Intratumoral Plasmacytoid Dendritic Cells. Frontiers in Immunology, 10, (2019)
5. Raychaudhuri D., Duttagupta P., **Liu C.S.C**., Sarif J., Ghosh A.R., Rahaman O., Ganguly D. Role of Ca2+ in toll-like receptor 9 activation in human plasmacytoid dendritic cells. Cytokine (2020).
6. Ghosh A.R., Bhattacharya R., Bhattacharya S., Nargis T., Rahaman O., Duttagupta P., Raychaudhuri D., **Liu C.S.C**., Roy S., Ghosh P., Khanna S., Chaudhuri T., Tantia O., Haak S., Bandyopadhyay S., Mukhopadhyay S., Chakrabarti C. & Ganguly D.; Adipose recruitment and activation of plasmacytoid dendritic cells fuel metaflammation. 65**,** ADA Diabetes, (2016)